NATIONAL CENTER FOR EARTHQUAKE ENGINEERING RESEARCH

ISSN 1088-3800

The Hanshin-Awaji Earthquake of January 17, 1995: Performance of Lifelines

Edited by M. Shinozuka

Technical Report NCEER-95-0015

November 3, 1995

This research was conducted at the National Center for Earthquake Engineering Research and was supported in whole or in part by the National Science Foundation under grant number BCS 90-25010and the New York State Science and Technology Foundation under Grant No. NEC-91029.

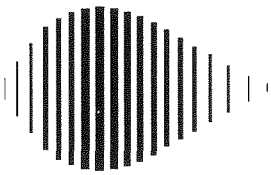
NOTICE

This report was prepared by the National Center for Earthquake Engineering Research as a result of research sponsored by the National Center for Earthquake Engineering Research (NCEER) through a grant from the National Science Foundation, and other sponsors. Neither NCEER, associates of NCEER, its sponsors, the National Center for Earthquake Engineering Research nor any person acting on their behalf:

a. makes any warranty, express or implied, with respect to the use of any information, apparatus, method, or process disclosed in this report or that such use may not infringe upon privately owned rights; or

b. assumes any liabilities of whatsoever kind with respect to the use of, or the damage resulting from the use of, any information, apparatus, method, or process disclosed in this report.

Any opinions, findings, and conclusions or recommendations expressed in this publication are those of the author(s) and do not necessarily reflect the views of NCEER, the National Science Foundation, or other sponsors.



The Hanshin-Awaji Earthquake of January 17, 1995: Performance of Lifelines

Edited by

M. Shinozuka[1]

Major Contributors: Donald Ballantyne, Roger Borcherdt,
Ian Buckle, Thomas O'Rourke and Anshel Schiff

November 3, 1995

Technical Report NCEER-95-0015

NCEER Task Number 94-9001

NSF Master Contract Number BCS 90-25010
and
NYSSTF Grant Number NEC-91029

1 Fred Champion Chair in Civil Engineering, Department of Civil Engineering, University of Southern California

NATIONAL CENTER FOR EARTHQUAKE ENGINEERING RESEARCH
State University of New York at Buffalo
Red Jacket Quadrangle, Buffalo, NY 14261

ABSTRACT

This reconnaissance report describes the seismic performance of electric power, gas delivery, hospital, telecommunications, transportation, and water/wastewater systems in the regions affected by the Hanshin-Awaji earthquake of January 17, 1995. Following an introductory section, significant reconnaissance information, together with collected data, forms a section on the ground motion characteristics of this earthquake. Each of the six sections that follow deal with one of the six lifeline systems mentioned above. The authors provide an overview of the lifeline system, indicating the owner/operator, the location and extent of the service area, the municipalities and communities in the service area, the number of households as well as industrial and business customers served (as appropriate), and other vital statistics. The system description is then given delineating the physical components and showing how these components are integrated to provide expected function and service. Design criteria of these components are also listed, reflecting as much information as the reconnaissance team was able to collect during the relatively short period of time made available. The difference in the operational and physical characteristics, including design concept and criteria between U.S. and Japanese systems, is also discussed to the extent possible.

Preliminary descriptions of the seismic performance of the various lifeline systems in terms of seismic damage, emergency response, seismic interruption and restoration, constitute the major ingredient of this reconnaissance report. The seismic performance of lifeline systems under the Hanshin-Awaji earthquake is compared to the performance of those subjected to earthquakes in the U.S., particularly during the Northridge earthquake. Each section ends with suggested lessons for the United States.

ACKNOWLEDGMENTS

Except where otherwise acknowledged, the material presented in this report was obtained during the U.S.-Japan reconnaissance visit to the Kobe, Japan area, which occurred on February 12-17, 1995 and was conducted under the auspices of the Wind and Seismic Effects Panel of the UJNR program. The U.S. organizer for the visit was the National Institute of Standards and Technology; the Japan host was the Ministry of Construction through the Public Works Research Institute and the Building Research Institute. The U.S. party consisted of 20 experts selected from various government agencies and the private sector. The National Center for Earthquake Engineering Research sponsored several of the private sector participants and, in particular, lifeline researchers and practitioners. Center funds for this purpose were provided by the National Science Foundation, the Federal Highway Administration and the State of New York.

In general, this report presents the findings of the Center-sponsored experts and thus focuses on lifelines and their performance in the earthquake. Some supplemental material has been added for completeness, such as the section on seismology. Additional reports have been prepared and published elsewhere by other team members which describe building performance and fire-related impacts.

The authors of this report wish to acknowledge the generous assistance of many organizations and agencies in Japan who made this visit possible and whose employees gave freely of their time and expertise. Their untiring efforts on behalf of the U.S. team not only provided dedicated transportation and access into and through the damaged areas but also provided opportunities to meet with technical experts and obtain valuable engineering data. Some of these organizations are listed below and others are identified in the body of this report. They include:

Architectural Institute of Japan
Building Research Institute
Chiyoda - Dames and Moore (Tokyo)
Committee on Earthquake Observation and Research in the Kansai Area
Disaster Prevention Research Institute, Kyoto University
Earthquake Research Institute, University of Tokyo
Geological Society of Japan
Gifu University, Department of Civil Engineering
Hanshin Expressway Public Corporation
Japan Highway Public Corporation
Japan Meteorological Agency
Japan Railway
Kansai Electric Power Co.
Kobe Rapid Transit Railway Company, Ltd.
Kobe Water Department
Kobe University
Ministry of Construction - Naniwa National Highway District Office
Ministry of Construction - Public Works Research Institute

National Research Institute for Earth Science and Disaster Prevention, Science and Technology Agency
Nippon Telegraph and Telephone
Osaka Gas Co.
Port and Harbor Research Institute
Waseda University

The authors also acknowledge various U.S. organizations who either directly facilitated the UJNR visit or provided field assistance and performed follow-up studies. These include:

ASCE Technical Council on Lifeline Earthquake Engineering
Earthquake Engineering Research Institute
National Institute of Standards and Technology

The technical editor for this report was Masanobu Shinozuka and the authors are grateful for Professor Shinozuka's guidance and oversight.

Members of the UJNR team who contributed to this report are:

Donald Ballantyne, formerly Dames and Moore, now EQE International, Inc., Seattle
Roger Borcherdt, U.S. Geological Survey, Menlo Park
Ian Buckle, NCEER/State University of New York at Buffalo
James Cooper, Federal Highway Administration
Thomas O'Rourke, Cornell University
Anshel Schiff, Stanford University/Precision Measurements, Inc.
Li-Hong Sheng, California Department of Transportation
Andrew Taylor, National Institute of Standards and Technology
Michael Whitney, Federal Highway Administration

TABLE OF CONTENTS

SECTON	TITLE	PAGE
1	**INTRODUCTION** *M. Shinozuka*	**1-1**
2	**SEISMOLOGY** *R.D. Borcherdt*	**2-1**
2.1	Source Characteristics	2-1
2.2	Strong-Ground Shaking	2-5
2.2.1	Strong Motion Recordings	2-5
2.2.2	Attenuation	2-21
2.2.3	Amplification Effects of Soft-Soil Deposits	2-26
2.3	Summary	2-26
2.4	Acknowledgments	2-28
2.5	References	2-29
3	**ELECTRIC POWER FACILITIES** *A. Schiff*	**3-1**
3.1	Overview of the Kansai Electric Company	3-1
3.1.1	System Description	3-1
3.1.2	Differences in Equipment, Facilities, and Practices Between Kobe and the U.S.	3-3
3.1.3	Seismic Design Criteria	3-5
3.2	Description of Damage to Kansai Electric Power Company	3-12
3.2.1	Seismic Environment at Power Facilities	3-12
3.2.2	Restoration of Service	3-13
3.2.3	Overview of Damage to Kansai Electric Company	3-15
3.2.4	Itami Control Center and Substation	3-21
3.2.5	Shin-Kobe Substation	3-40
3.2.6	Fukiai Control Center and Substation	3-45
3.2.7	Performance of Generating Facilities	3-50
3.2.8	Performance of High Voltage Transmission Lines	3-52
3.2.9	Performance of the Distribution System	3-52
3.3	Lessons from Damage to Electric Power Facilities	3-54
3.4	Summary	3-58
3.5	Acknowledgments	3-58
3.6	References	3-58
4	**GAS DELIVERY SYSTEM** *T.D. O'Rourke*	**4-1**
4.1	Overview of the Gas Delivery System	4-1
4.2	Description of the Gas Delivery System	4-3
4.3	Gas Pipeline Damage	4-3

TABLE OF CONTENTS (Cont'd)

SECTON	TITLE	PAGE
4.4	Emergency Response and System Restoration	4-6
4.5	Seismic Gas Shut-Off Valves	4-7
4.6	Lessons from Damage to the Gas Delivery System	4-7
4.7	References	4-10
5	**HOSPITALS**	**5-1**
	A. Schiff	
5.1	Overview of Hospitals	5-1
5.2	Description of Damage to Hospitals	5-1
5.3	Lessons from Damage to Hospitals	5-12
5.4	Summary	5-13
5.5	References	5-13
6	**TELECOMMUNICATIONS FACILITIES**	**6-1**
	A. Schiff	
6.1	Overview of Nippon Telegraph and Telephone (NTT) Corporation	6-1
6.2	Description of Damage to NTT	6-1
6.2.1	Central Offices	6-3
6.2.2	Outside Plant	6-3
6.2.3	Network Operations	6-4
6.2.4	Restoration	6-12
6.2.5	Special Post-Earthquake Services	6-12
6.3	Lessons from Damage to Telecommunications Facilities	6-12
6.4	Summary	6-13
6.5	Acknowledgments	6-13
6.6	References	6-13
7	**TRANSPORTATION SYSTEMS**	**7-1**
7.1	Airport Facilities	7-1
	A. Schiff	
7.1.1	Overview of Airport Facilities	7-1
7.1.1.1	Kansai Airport	7-1
7.1.1.2	Osaka Airport	7-15
7.1.2	Description of Damage to Airport Facilities	7-15
7.1.2.1	Kansai Airport	7-15
7.1.2.2	Osaka Airport	7-21
7.1.3	Lessons from Damage to Airport Facilities	7-21
7.1.4	Summary	7-22
7.1.5	References	7-22
7.2	Highways and Bridges	7-22
	I.G. Buckle	

TABLE OF CONTENTS (Cont'd)

SECTON	TITLE	PAGE
7.2.1	Overview of Highways and Bridges	7-22
7.2.2	Description of Damage to Highways and Bridges	7-24
7.2.2.1	Damage to Superstructures Due to Bearing Failures	7-28
7.2.2.2	Damage to Concrete Substructures	7-38
7.2.2.3	Damage to Steel Substructures	7-56
7.2.2.4	Damage to Structures Due to Special Conditions (Liquefaction, Skew, Protective Systems)	7-62
7.2.2.5	Performance of Other Highway Bridge Structures	7-68
7.2.3	Lessons from Damage to Highways and Bridges	7-71
7.2.4	Summary	7-72
7.2.5	References	7-73
7.3	Underground Rapid Transit Systems *T.D. O'Rourke*	7-73
7.3.1	Overview of Underground Rapid Transit Systems	7-73
7.3.2	Description of Damage to Underground Rapid Transit Systems	7-76
7.3.3	Lessons from Damage to Underground Rapid Transit Systems	7-84
7.3.4	References	7-85
8	**WATER AND WASTEWATER SYSTEMS** *D. Ballantyne*	**8-1**
8.1	Overview of the Water System	8-1
8.1.1	Supplies	8-4
8.1.2	Water Treatment Plants	8-6
8.1.3	Distribution	8-6
8.1.4	Distribution Reservoirs and Pump Stations	8-10
8.1.5	Control System	8-11
8.1.6	Earthquake Monitoring and Control	8-14
8.2	Description of Damage to the Water System	8-17
8.2.1	Conditions Following the Earthquake	8-17
8.2.2	Damage to Water Facilities	8-21
8.2.2.1	Supply Reservoirs	8-21
8.2.2.2	Water Purification Plants	8-21
8.2.2.3	Intake, Pump Stations, and Transmission Pipelines	8-28
8.2.2.4	Distribution Reservoirs (Tanks)	8-28
8.2.2.5	Distribution Pipes	8-28
8.2.2.6	Water Department Buildings	8-34
8.2.2.7	Monitoring and Control System	8-34
8.3	Description of Damage to the Wastewater System	8-34
8.4	Lessons from Damage to Water and Wastewater Systems	8-43
8.4.1	Overwhelming Conditions	8-53
8.4.2	Fire Following Earthquake	8-54

TABLE OF CONTENTS (Cont'd)

SECTON	TITLE	PAGE
8.4.3	Geotechnical Issues	8-54
8.4.4	Design	8-54
8.4.5	Recovery	8-55
8.5	Summary	8-55
8.6	Acknowledgments	8-56

LIST OF ILLUSTRATIONS

FIGURE	TITLE	PAGE
1-1	Rate of Restoration for Gas Delivery System	1-3
2-1	Map Showing Seismicity for Japan for Time Period 1961-1994, Plate Margins and Approximate Rupture Zones for the Large 1944 and 1946 Earthquakes	2-2
2-2	Map Showing Quaternary Faults and Seismicity for a Two Day Time Period Including the Occurrence Time of the Hanshin-Awaji Earthquake	2-3
2-3	(a) Map Showing Aftershock Distribution in Plan and Cross Section Views and (b) Source Mechanism for Inferred Subevents	2-4
2-4	Preliminary Map Showing Geologic Units, Strong-Motion Stations, Peak Horizontal Acceleration, and Approximate Contours of Acceleration	2-6
2-5	Record Section Showing Ground Velocity in the (a) NS, (b) EW and (c) UD Directions	2-11
2-6	Three-Component (1) Acceleration, (2) Velocity, (3) Displacement, and (4) Displacement Loci Inferred by Nakamura (1995) from Strong-Motion Recordings at Site (a) Kobe Marine (JM-KBM), (b) Takatori (JR-TKT), (c) Takarazuka (JR-TKD), and (d) Nishi-Akashi (JR-NSA)	2-12
2-7	Pseudo Velocity Response Spectra for Recent Devastating Earthquakes for (a) the Horizontal Components, (b) the UD Component and (c) Design Spectra for Tall Buildings	2-20
2-8	Geologic and Seismic Logs for the Port Island Vertical Array Site	2-22
2-9	Strong Motion Recordings Obtained on the Port Island Vertical Array at the Surface and at Approximate Depths of 12, 27, and 79 m for the (a) NS, (b) EW and (c) UD Components	2-23
2-10	Preliminary Compilation of Peak Horizontal Acceleration as a Function of Closest Distance to Seismogenic Rupture for the Northridge and Hanshin-Awaji Earthquakes	2-25
2-11	Preliminary Compilation of Peak Horizontal Acceleration Compiled Along Strike ($\pm$ 22.5 Degree) and Perpendicular to Strike ($\pm$ 67.5 Degrees)	2-25
2-12	Preliminary Compilation of Peak Vertical and Peak Horizontal Acceleration	2-27
2-13	Amplification of Peak Horizontal Acceleration With Respect to Corresponding Value at Shin-Kobe Station (0.57g) as Normalized by the Reciprocal Ratio of Respective Distances to Seismogenic Rupture for Sites Within a $\pm$ 22.5 Degree Azimuthal Window of Fault Strike (51^0)	2-27

LIST OF ILLUSTRATIONS (Cont'd)

FIGURE	TITLE	PAGE
3-1	Schematic Diagram of Kansai Service Area and Peak Acceleration at Utility Instruments	3-2
3-2	Transmission Tower Carrying Two 275 kV and Two 154 kV Circuits	3-4
3-3	Spun-concrete Distribution Pole Used in Kobe	3-4
3-4	Distribution Transformers (77 kV to 6.6 kV) Have Radiators with Structural Supports Independent of the Piping System and Flexible Couplings in Connections	3-6
3-5	Box with Porcelain Support is a Design Feature on a Distribution Transformer Not Seen in the U.S.	3-6
3-6	The 275 kV Potential Transformers are Much Larger than Their Counterpart in the U.S.	3-7
3-7	A 275 kV Bulk-oil Circuit Breaker which is Very Large Compared to 230 kV Units in the U.S.	3-7
3-8	Typical 230 kV Bulk-oil Circuit Breaker in the U.S.	3-8
3-9	Capacitors Observed in Japan are in Large Tanks and have Small Transformers on Isolated Rack, a Different Configuration than in the U.S.	3-8
3-10	Typical Capacitor Rack in the U.S.	3-9
3-11	Very Stiff Support Structure for a Potential Transformer Installed After the More Stringent Seismic Design Practices were Adopted in 1980	3-9
3-12	A 275 kV Circuit Breaker, Disconnect Switch, Pot Head and Lightning Arrester. Lightning Arrester Installed on Short Pedestal Reduces Cost and Amplification of a Taller Support Structure.	3-10
3-13	Current-Voltage Transformer is Used as the Lower Restraint for a Suspended Wave Trap	3-10
3-14	In the U.S., Suspended Wave Traps Usually have Independent Lower Restraints	3-11
3-15	Kawasumi Map Shows the Distribution of Horizontal Accelerations on the Ground Surface Expected at the Interval of 75 Years	3-14
3-16	Number of Customers and Loss of Power vs. Time	3-16
3-17	Sources and Types of Mutual Aid from Other Utilities	3-17
3-18	Damage to the Distribution System was Massive, but a Traffic Light in the Background is the Result of Special Restoration of the Traffic Control System	3-18
3-19	Schematic Diagram Showing the Damage to Substations and Transmission Lines	3-20
3-20	A Modified One-line Diagram for the 275 kV and 154 kV Switchyard	3-22
3-21	Failure of a Current-voltage Transformer Base Flange	3-24

LIST OF ILLUSTRATIONS (Cont'd)

FIGURE	TITLE	PAGE
3-22	A Cracked Cast Iron Anchor Tab on a Current-Voltage Transformer Remained in Service	3-24
3-23	Porcelain Failed at the Base Plate of this Current-Voltage Transformer	3-25
3-24	Bulk-oil Circuit Breaker and Pot Head on a 275 kV Circuit	3-25
3-25	Porcelain Slipped on its Lower Flange on a 275 kV Bulk-oil Circuit Breaker	3-26
3-26	Bulk-oil Circuit Breakers with the Bushings Removed to Replace Damaged Units at Other Sites	3-26
3-27	Very Strong and Stiff Anchorage Detailed Used on a Large Potential Transformer to Meet More Stringent 1980 Seismic Design Criteria	3-27
3-28	Isolated Failure of Disconnect Switch May be Due to Interaction with the Bus Drop and Insulator String	3-27
3-29	Damaged Post Insulators in the Graveyard Exhibit Unusual Longitudinal Cracks	3-29
3-30	Standoff Incorporated into the Design of the Base of the Lightning Arrester Failed	3-29
3-31	Damaged 275 kV Lightning Arrester in the Graveyard	3-30
3-32	Silicon Rubber Used to Improve Contamination Problems has Peels from this Damaged Equipment in the Graveyard	3-30
3-33	Bolts Anchoring a Transformer Failed Allowing the Unit to Slide 45 cm and Causing Damage to Bushings	3-31
3-34	Offset in Bus Covers Caused by the Failure of Transformer Anchorage and its Movement	3-31
3-35	Transformer Control Cables were Almost Sheared Off Due to Movement of the Transformer	3-32
3-36	Movement of Transformer Shorted Transformer Case to Cabinet Containing Tertiary Output	3-32
3-37	Transformer Acoustical Enclosure Support was Damaged and the Enclosure Shifted	3-33
3-38	Small Transformer Sheared its Anchor Bolts and Moved 25 cm Increasing the Load on Bushings	3-33
3-39	Batteries are Secured to a Well Braced and Anchored Battery Rack	3-35
3-40	Low Slung Battery Rack Configuration Not Found in the U.S. Reduces Bracing Requirements of the Rack	3-35
3-41	Different Approach Using Rubber Spacers in Japan to Restraining Cells to Battery Racks	3-36
3-42	Cable Tray Sections are Bolted Together and Cables Restrained with Ties to the Tray	3-36
3-43	Long Crack in the Ground Surface Opened About 25 cm and Damaged Cable Trenches	3-37

LIST OF ILLUSTRATIONS (Cont'd)

FIGURE	TITLE	PAGE
3-44	Cable Trenches Were Deformed with the Ground Fracturing an Air Line but Leaving Control Cables Undamaged	3-37
3-45	Large Soil Deformations at Equipment and Pedestal Foundations Did Not Damage Control Cables	3-38
3-46	Foundations of Conductor Support Structures were Disturbed and Individual Footings Rotated as Much as 25 Degrees	3-38
3-47	Lightning Arrester Support Structure Tipped About 2-1/2 Degrees and Probably Contributed to the Failure of the Lighting Arrester	3-39
3-48	New Monolithic Disconnect Switch Pad Replaced Individual Footings that were Disturbed by a Surface Crack in the Soil	3-39
3-49	Asphalt Surface Between the Tank and the Concrete Ring was Broken and the Bolts Stretched or were Pulled Out Due to Rocking of the Tank	3-41
3-50	While These were Old Installations, the Tanks were Provided with Flexible Coupling at Pipe Connections	3-41
3-51	Soil Around Footing Subsided About 15 cm	3-42
3-52	Conduit Attached to the Tower and Buried in the Ground was Displaced About 8 cm and has the Potential of Damaging Internal Signal Cables as They are Not Provided with Adequate Slack	3-42
3-53	Post Insulators that Restrain the Lines as They Pass Under the Support Arm Failed on Several Towers, but Did Not Cause Disruption	3-43
3-54	Bent Member in a Microwave Tower is very Unusual, but it Did Not Effect Operations	3-43
3-55	Lightning Arresters Failed and Probably Pulled Down Adjacent Disconnect Switches	3-44
3-56	All Three Bushings Shifted on this 275 kV Bulk-oil Circuit Breaker	3-44
3-57	Failure Pattern of Splits in the Post Insulators of These Disconnect Switches is Unusual	3-46
3-58	Neutral Resistors Failed, a Device Not Used in this Configuration in the U.S.	3-46
3-59	A 77 kV Three-phase, Dead-Tank Gas Insulated Circuit Breaker Failed at its Bushings, Probably Due to Inadequate Slack to Accommodate Soil Settlement at the Site	3-47
3-60	Water Spray Heads Near the Fence are Used to Reduce Salt Concentration and the Potential of Flash-Over Under Certain Atmospheric Conditions	3-47
3-61	Transformer Pushed Over the Fire Wall After it Failed at its Anchorage	3-48
3-62	Pot Head Connected to the Bushing Failed, Probably When it was Hit by the Bushing	3-48

LIST OF ILLUSTRATIONS (Cont'd)

FIGURE	TITLE	PAGE
3-63	Radiator on This Distribution Transformer has a Structural Support and the Piping Connections have Flexible Couplings	3-49
3-64	Movement of the Transformer After its Anchorage Failed Allowing the Radiators to Hit a Nearby Structural Support Causing a Leak	3-49
3-65	A 77 kV and 6.6 kV Gas Insulated Distribution Substation	3-51
3-66	Location of Generating Stations in the Earthquake Impacted Area	3-51
3-67	Damage to the Aerial Distribution System was Severe in Many Regions	3-53
3-68	Fallen Houses Pushed Over Some Distribution Poles	3-53
3-69	Some Poles Failed Due to Inertial Loads or were Pulled Down by Other Fallen Poles	3-55
3-70	Fallen Poles Contributed to the Disruption of Traffic	3-55
3-71	This Pole Settled About 1-1/2 m Due to Liquefaction at the Site	3-56
3-72	Conduit and Foundation Pad Under this Transformer Pad was Disrupted in Downtown Kobe Due to Soil Liquefaction	3-56
3-73	A Primary Distribution Line of 6.6 kV was Temporarily Installed to Restore Power to a Building	3-57
4-1	Map of Principal Facilities, Trunklines, and Major Pipelines Operated by the Osaka Gas Company	4-2
4-2	Map of Super Blocks and Middle Blocks in the Osaka Gas System Showing Areas Where Gas Flow Was Shut Off After the Earthquake	4-8
4-3	Three-Dimensional View of the Osaka Gas Intelligent Meter	4-9
5-1	Column on First Floor of Old Hospital Being Repaired with Epoxy Injection	5-2
5-2	Beam Shattered Due to Interaction Between the Two Wings of the Hospital at Crosswalks Connecting the Buildings	5-2
5-3	Engine-Generator in the New Hospital Wing, which has Vibration Isolators and Flexible Connections on Utilities	5-4
5-4	Detailed View of Vibration Isolators Used on Emergency Power Engines	5-4
5-5	Compressor and Air Storage Tanks Used to Start the Diesel Engine	5-5
5-6	Day Tank and Pump for the Fuel Supply to the Diesel Engine	5-5
5-7	Diesel Engine Used for Emergency Power in the Old Wing of the Hospital	5-6
5-8	Schematic Diagram for the Kobe Medical College Water System	5-6
5-9	Main Distribution Frame for the Hospital Communication System	5-8
5-10	Part of the Private Branch Exchange (PBX) Switch Used by the Hospital	5-8
5-11	Battery within UPS Used by the PBX	5-9
5-12	Cable Trays Used by the Telecommunication System Use Bolted Connections	5-9

LIST OF ILLUSTRATIONS (Cont'd)

FIGURE	TITLE	PAGE
5-13	Typical, Low Tensile Strength, Friction-Clip Type Communication Cable Tray Hardware Used to Join Tray Sections in the U.S.	5-10
5-14	Bolted Connections are Used to Anchor Cable Trays to Structural Walls	5-10
5-15	J Bolts are Often Used to Secure Cable Trays to Walls; These Type of Connections have not Been Reliable	5-11
5-16	Main Distribution Frame is Bolted to Cable Tray to Provide Bracing at the Top of the Frame	5-11
6-1	Microwave Tower on Top of a Central Office which was Damaged and Later Removed	6-5
6-2	Schematic Diagram of Tunnel-Building Connection Detail and Post-Earthquake Repair	6-5
6-3	Slight Movement at a Construction Joint Caused a Small Water Leak in a Joint Utility Tunnel	6-6
6-4	Trunk Lines in the Joint Utility Tunnel had Fire Retardent Covers Near Entrances and Stairways	6-6
6-5	Cables were Pushed into Manhole Box Breaking Water Seals and in Some Cases Damaging Cables	6-7
6-6	Movement of Manhole Box can Damage Conduits and Trunk Lines	6-7
6-7	Entry of a Manhole Built by Stacking Rings was Offset by 4 cm Due to Soil Failure	6-8
6-8	Subsidence Around Manhole can Damage Conduit and Trunk Lines	6-8
6-9	Conduits Carried on Bridges were Damaged when Bridge Deck Moved	6-9
6-10	Large Differential Settlements in Roadways can Damage Conduit and Trunk Lines	6-9
6-11	Settlement of a Walkway Adjacent to a Building Shears Conduit and Cables	6-10
6-12	Soil Instability Damaged Telephone Booths	6-10
6-13	Walls of a Canal Moved Causing Conduit Bridge and Conduit to Buckle	6-11
6-14	Fire Damaged Aerial Lines and Cables Along the Pole	6-11
7-1	Overview of Airport Looking East from Control Tower	7-2
7-2	Overview of Airport Looking West from Control Tower	7-2
7-3	Schematic Diagram of Airport, Access Bridge and Strong-Motion Instrument Locations	7-3
7-4	Kansai Airport Air Traffic Control Tower	7-5
7-5	Connection Between an Interior Pipe Column and a Vertical Truss in the Shaft of the Tower	7-5
7-6	Beam/Column Connection in the Penthouse Above the Cab	7-6
7-7	Active Control System to Reduce Wind Induced Vibration	7-6

LIST OF ILLUSTRATIONS (Cont'd)

FIGURE	TITLE	PAGE
7-8	Hydraulic Rams on Either Side of a Column	7-7
7-9	Basement of the Tower Showing System for Leveling the Building and Shear Keys	7-7
7-10	One of Two Shear Keys Parallel to Each Side of the Control Tower	7-8
7-11	Deep Girders of the Rigid Diaphragm Above a Column	7-8
7-12	Column Supporting the Cab Roof in Kansai Control Tower	7-10
7-13	Cab of the Osaka Airport Control Tower	7-10
7-14	Supervisor Control Position Located in Center of Control Tower Cab	7-11
7-15	Supervisor Control Position Communication Council	7-11
7-16	Communications Cable Tray with Bolted Connections Above Cab	7-12
7-17	Communications Cable Tray Secured with Friction Clips	7-12
7-18	Roof-Mounted Heat Exchanger Braced with Cables	7-13
7-19	Very Long Battery String on Low Slung Battery Racks Provides Emergency Power	7-13
7-20	Large Diesel Engine-Generator on Vibration Isolators Typically Found in Japan	7-14
7-21	Flexible Coupling in Water Cooling Line to Diesel Engine-Generator	7-14
7-22	Cooling Tower and Water Tank for Emergency Engine-Generator	7-16
7-23	Heat Exchanger on Roof Near Control Tower Cab is Rare Example of Poorly Anchored Equipment	7-16
7-24	Strong-Motion Instrument Locations at Kansai Airport	7-17
7-25	Strong-Motion Record from Kansai Airport Runway - Position W	7-18
7-26	Subsidence in Sidewalk and Repaired Sidewalk Outside the Kansai Terminal Building	7-20
7-27	Cracks in the Stairwell Shear Walls of the Osaka Airport Administration Building	7-20
7-28	Bridge Sites Visited by UJNR Reconnaissance Team, February 12-17, 1995	7-27
7-29a	General View of Nishinomiya-ko Bridge, Route 5	7-30
7-29b	Collapsed Approach Span Between Piers 111 and 112, Nishinomiya-ko Bridge	7-30
7-30	Damaged Expansion Bearings from Under Approach Spans, Nishinomiya-ko Bridge, Showing Nested Rollers and Guide Rails	7-31
7-31	Cap Beam of Pier 111, Nishinomiya-ko Bridge, Showing Cross-Girder of Arch and Failed Restrainers	7-31
7-32	General View of Rokko Island Bridge, Route 5	7-33
7-33	Damaged Expansion Bearing and Lateral Offset at West Face of South Pier, Rokko Island Bridge	7-33
7-34	Lateral Offset at East Face of South Pier, Rokko Island Bridge	7-34
7-35	Buckled Cross-Members in Upper Chord, Rokko Island Bridge	7-34

LIST OF ILLUSTRATIONS (Cont'd)

FIGURE	TITLE	PAGE
7-36	General View of Mukogawa Bridge, Meishin Expressway	7-35
7-37	Bearing and Restrainer Damage at Abutment A1, Mukogawa Bridge, Showing Distorted Guide Rails and Uncoupled Restrainer from Abutment Backwall	7-35
7-38	Damaged Restrainer at Abutment A1, Mukogawa Bridge Showing Failure of Anchor Bolts and Distortion of Web of Main Girder	7-37
7-39	Failure at Top of Buried Column, Pier P1, Mukogawa Bridge	7-37
7-40	Lateral Offset at Pier 36 in Upper Level of Hamate By-Pass Due to Bearing Failures at Piers 34 Through 38	7-40
7-41	View of the Collapsed Higashi-Nada Viaduct Looking West from Pier 125	7-40
7-42	Higashi-Nada Viaduct, Pier 126	7-41
7-43	Higashi-Nada Viaduct, Pier 134	7-41
7-44	General View of Hanshin Expressway (Route 3) Near Uozaki Showing Collapse of Section Over Pier 240 in Middle Distance	7-42
7-45	Pier 240 of Hanshin Expressway Showing Temporary Repair to This Single Column Bent	7-42
7-46	Shear Failure in Pier 240 of Hanshin Expressway Showing Temporary Repair to Column to Prevent Total Collapse	7-43
7-47	Compressive Failure in Lower Flange of Steel Box Girder Between Piers 238 and 239 of Hanshin Expressway	7-43
7-48	General View of Takarazuka Viaduct, Chugoku Expressway	7-46
7-49	Shear Failures in 3-Column Bent at Pier 3, Takarazuka Viaduct	7-46
7-50	Shear Failure in Wall Pier (West Face), Moribe Viaduct	7-48
7-51	Shear Failure in Wall Pier (East Face), Moribe Viaduct	7-48
7-52	General View of Kobe-Ohashi Connector Near Port Island Showing Formation of Flexural Hinges in Lower Level Columns	7-50
7-53	Hinge Formation in East Column of Pier 23, Kobe-Ohashi	7-50
7-54	Collapse of Southeast Ramp at the Minatogawa Interchange	7-52
7-55	Collapse of Northeast Ramp at the Minatogawa Interchange	7-52
7-56	Girder Web Failure Due to Unseating of the Southeast Ramp at Minatogawa Interchange	7-53
7-57	Column Failure in Southwest Ramp at Minatogawa Interchange	7-53
7-58	General View of Route 3 Crossing JR Sanyo Line Near Takatori	7-55
7-59	Side View of Shear Failure in Pier 688 of Route 3 Near JR Sanyo Line	7-55
7-60	Pier 55, Route 3 Near Tateishi	7-57
7-61	Pier 55, Route 3 Near Tateishi Showing Buckled Steel Plate on Ground	7-57
7-62	General View of Westbound Elevated Section of Route 3 Near Meiji Looking from Pier 586 Towards Pier 585	7-60
7-63	Pier 584 of Westbound Route 3 Near Meiji	7-60
7-64	Fracture at Mid-Height of Pier 584 of Westbound Route 3	7-61

LIST OF ILLUSTRATIONS (Cont'd)

FIGURE	TITLE	PAGE
7-65	Failed Bearings and Lateral Offset at Top of Pier 586 of Westbound Route 3	7-61
7-66	Local Buckling in Steel Box Columns at Pier 41 of the Hamate Bypass Viaduct	7-63
7-67	Buckling in Steel Column at Pier 49 of the Hamate Bypass Viaduct	7-63
7-68	General View of the Shukugawa Bridge on Route 5	7-65
7-69	Distant View of the Shukugawa Bridge Showing Lateral Deformation of the Foundation Soils and Spreading to the Right (to the center of the channel)	7-65
7-70	Vertical Offset in the Expansion Joints Above Pier 134 of the Shukugawa Bridge Due to Bearing Failure on the Bent Cap Below	7-66
7-71	Approach Span at Edge of Seat at Pier 134 of Shukugawa Bridge Due to Lateral Movement of the Pier Towards the Center of the Channel by About 1 m	7-66
7-72	General View of Kawaraginishi Bridge After Removal of Collapsed Eastbound Bridge Showing Skew and Pin-Ended Columns Under Westbound Bridge	7-67
7-73	Pier 27 of the Westbound Kawaraginishi Bridge Showing Shear Cracking and Repair by Injection Grouting	7-67
7-74	General View of the Higashi-Kobe Bridge on Route 5	7-69
7-75	Failed Wind Shoe at Pier 187 of the Higashi-Kobe Bridge	7-69
7-76	Failed Connection of Vane-Type Energy Dissipator and (at upper right) Part of Failed Dead Load Tie-down at Pier 187 of the Higashi-Kobe Bridge	7-70
7-77	Uplift at the West End (Pier 187) of the Main Girder of the Higashi-Kobe Bridge Due to Failure of the Dead Load	7-70
7-78	Map of Kobe Underground Rapid Transit Systems Showing Locations of Earthquake Damaged Stations	7-74
7-79	Schematic of the Kobe Rapid Transit Railway Showing Locations of Earthquake Damage	7-75
7-80	Cracked Reinforced Concrete Column at Underground Shopping Mall Near Shin Kaichi Station	7-78
7-81	Cracked Reinforced Concrete Column and Concrete Panel Wall at Underground Shopping Mall Near Shin Kaichi Station	7-78
7-82	Soil Boring Records Near Daikai Station	7-79
7-83	Plan and Profile Views of Daikai Station Collapse	7-80
7-84	Cross-Sections of Reinforced Concrete Station and Running Tunnel Structures at Daikai Station	7-81
7-85	Roof Collapse Viewed From the Station Platform at Daikai Station	7-82
7-86	Compressive Failure of Center Columns at Daikai Station	7-82
7-87	Subsidence of Street Surface Over the Collapsed Daikai Station	7-83

LIST OF ILLUSTRATIONS (Cont'd)

FIGURE	TITLE	PAGE
7-88	Earthquake Deformation of Running Tunnel at an Exaggerated Scale as Inferred from Reconnaissance Observations	7-83
8-1	Schematic of Kobe Water System	8-2
8-2	Kobe Water System, Urban Area	8-3
8-3	Schematic Profile of Kobe Water Delivery System	8-5
8-4	Cistern for Water for Fire Protection in Kobe	8-5
8-5	Schematic of Uegahara Water Purification Plant	8-8
8-6	Schematic of Motoyama Water Treatment Plant	8-8
8-7	Type SII (Seismic) Joint	8-9
8-8	Seismic Joints (S and SII)	8-9
8-9	Steel Tank Section of Okuhirano Purification Plant	8-12
8-10	(Top) Steel and (Bottom) Concrete Water Storage Tanks at Okuhirano Purification Plant	8-13
8-11	Schematic of Communication/Repeater System	8-15
8-12	Seismograph at Okuhirano Control Center Used for Control of Earthquake Valves on Reservoirs	8-15
8-13	Control Panel for Earthquake Valves to Provide Flexibility to Control Automatically or by Operations Staff in Okuhirano Control Center	8-16
8-14	Schematic of Typical Communication from Ground Motion Instrument, Through Radio Communication, to the Earthquake Valve	8-16
8-15	Map of Kobe Water Service Area Showing Reservoirs with Earthquake Valves and Their Respective Service Area	8-18
8-16	Schematic of Water Distribution from Tank with Earthquake Valve	8-18
8-17	Water Loss From Reservoirs After Kobe Earthquake	8-19
8-18	Person Collecting Water from Central Water Distribution Point Near the Collapsed Daikai Subway Station	8-19
8-19	Emergency Water Supply Delivered in Tank Trailer	8-20
8-20	Status of Emergency Water Supply	8-20
8-21	Mutual Aid from Other Cities Repairing the Water Distribution System	8-22
8-22	Mutual Aid from Other Cities Repairing the Water Supply Equipment (Purification Plants, Pump Stations, and Tanks)	8-22
8-23	Percent of People in Kobe Without Water Following Earthquake	8-23
8-24	Restoration of Distribution Reservoirs and Water Mains	8-23
8-25	Aerial View of Kobe's Uegahara Water Purification Plant (lower left) with the Hanshin Water Purification Plant Immediately Adjacent (upper right)	8-25

LIST OF ILLUSTRATIONS (Cont'd)

FIGURE	TITLE	PAGE
8-26	Repair of One of Three 1.2 Meter Treated Water Lines Leaving the Uegahara/Hanshin Plants Site	8-25
8-27	Subsidence (approximately 30 cm) Around Pile-Supported Sludge Hoppers at Uegahara Plant	8-26
8-28	Landslide; Undermined Solids Handling Building	8-26
8-29	Broken Lines to/from Backwash Tank at the Motoyama Water Purification Plant	8-27
8-30	The Retaining Wall (on the left) Cracked, Damaging the Overflow Line from the Motoyama Plant's Intake Box	8-27
8-31	Pipe Hanging from Bridge to Rokko Island (just to the right of crane cab)	8-31
8-32	Repair of 700-mm Welded Steel Pipeline	8-31
8-33	Ground Cracking from Lateral Spread in Fill Area Along a Water Way	8-32
8-34	Pipe Joint in Bottom of Crack, Where the Bell (to the right) was Separated from the Spigot (under foot)	8-32
8-35	Pipe Repair on Approach to Bridge to Island Where the Wastewater Plant is Located	8-33
8-36	Kyoto Water Department Crew Making Repairs to Pipe Shown in Figure 8-35	8-33
8-37	Differential Settlement of Building on Mid-Rokko Island	8-35
8-38	Utility Connections Required Repair Due to Differential Settlement	8-35
8-39	Utility Connections are Hanging Due to Differential Settlement Along Front of Pile Supported Ferry Terminal on Port Island	8-36
8-40	Pancaked 6th Floor of City Hall Annex	8-36
8-41	Manhole Floated as a Result of Liquefaction Near the Wastewater Treatment Plant	8-39
8-42	A 500 mm Diameter Sewer Floated Upward on Port Island, Resulting in the Upheaval of Ground	8-40
8-43	Aerial View of Higashinada Wastewater Treatment Plant	8-40
8-44	Location Map for Higashinada Wastewater Plant	8-41
8-45	Retaining Wall Along the Inlet Between the Island and Mainland Moved Towards the Water (North) 2 to 3 Meters	8-41
8-46	Ground Cracking Behind the Retaining Wall (which is off to the right)	8-42
8-47	Soil Profile at Higashinada Wastewater Treatment Plant	8-42
8-48	Higashinada Wastewater Treatment Plant Site Plan Showing Damage Locations	8-44
8-49	Effluent Channel, Approximately 2 Meters Square, Offset Nearly 1 Meter from Lateral Spreading	8-45

LIST OF ILLUSTRATIONS (Cont'd)

FIGURE	TITLE	PAGE
8-50	Pipe Rack Foundations Adjacent to Channel Settled Approximately 1 Meter, Distorting Piping	8-45
8-51	Aeration Tanks Construction Joint Separated Down the Entire Bank of Tankage as a Result of Settlement	8-46
8-52	Close Up of Torn Dumbbell Rubber Water Stop in Aeration Tank	8-46
8-53	Sludge Scraper Chain Came off Sprockets in Sedimentation Tanks	8-47
8-54	Differential Movement from Settlement Between Pile Supported Tanks and Non-pile Supported Pipe Caused Flexible Joint to Distort	8-47
8-55	Differential Settlement Between Pipe and Non-pile Supported Structures Damaged Piping Throughout the Plant	8-48
8-56	(Top) Filter Building Support Pipes Failed Allowing the Building to Move and Settle Differentially; (Bottom) Piping Distorted as a Result of the Building Movement	8-49
8-57	(Top) Control Building (upper right) Pile Supported Building Moved Towards Inlet Approximately 30 cm, Moving Away from Adjacent Building that Had a Basement; (Bottom) Gap Between the Buildings	8-50
8-58	Damage to Equipment on Mat Foundations; (Top) Piping Distorted as a Result of the Movement; (Bottom), (Top) Piping and Equipment Distorted as a Result of Subsidence at Foundation; (Bottom) Welded Steel Tee, Approximately 300 mm in Diameter, Cracked at Weld Between the Leg and Run	8-51
8-59	Welded Steel Pipe; Approximately 200 mm in Diameter Folded When the Foot/Pipe Bridge Support was Distorted from Lateral Spread	8-53

LIST OF TABLES

TABLE	TITLE	PAGE
2-I	Source Parameters Inferred for the Hanshin-Awaji Earthquake	2-5
2-II	Preliminary List of Strong Motion Stations for the Hanshin-Awaji Earthquake	2-8
3-I	Summary of Vital Statistics of the Kansai Electric Company	3-1
3-II	Breakdown of Kansai Power Electricity Sales	3-3
3-III	Specifications of Kansai Power Strong-Motion Instruments	3-13
3-IV	Distribution of Workers During Restoration	3-15
3-V	Summary of Damage to Power Facilities	3-19
3-VI	Power Stations Sustaining Damage to Main Facilities and Experiencing Trouble in Power Generation	3-50
3-VII	Power Stations Sustaining Damage to Facilities	3-52
4-I	Summary of Repairs of Medium-Pressure Gas Pipelines	4-4
4-II	Summary of Repairs of Low-Pressure Gas Distribution Pipelines	4-5
6-I	Current Measures Used to Improve Earthquake Resistance of Conduit Joints	6-2
7-I	Instrument Locations at Kansai Airport	7-18
7-II	Peak Accelerations Recorded at Kansai Airport	7-19
7-III	Location of Bridges with Major Damage	7-25
7-IV	List of Highway Bridges with Major Damage	7-26
7-V	Support Fixity Conditions for the Nishinomiya-ko Bridge	7-29
7-VI	Support Fixity Conditions for the Mukogawa Bridge	7-36
7-VII	Substructure Details for Piers 238 to 241, Route 3 near Uozaki	7-44
7-VIII	Support Fixity Conditions for the Takarazuka Viaduct	7-44
7-IX	Support Fixity Conditions for Piers 26 to 31, Moribe Viaduct	7-49
7-X	Support Fixity Conditions for Piers 23 to 26, Kobe-ohashi	7-49
7-XI	Structure Data for the Minatogawa Ramps, Route 3	7-51
7-XII	Substructure Details for Piers 687 to 690, Route 3 near Takatori	7-54
7-XIII	Substructure Details for Piers 54 to 56, Route 3 near Tateshi	7-58
7-XIV	Substructure Details for Piers 581 to 586, Westbound Route 3, Meiji	7-58
8-I	Kobe Water Supplies	8-4
8-II	Water Treatment Plants Serving Kobe	8-6
8-III	Pipe in Place as of April, 1994	8-7
8-IV	Rehabilitation and Renewal Project - 1978	8-7
8-V	Strengthening/Earthquake Proofing Pipelines - 1991	8-7
8-VI	Summary of Service Reservoirs by Elevation	8-10
8-VII	Reservoir Distribution by Area	8-11

LIST OF TABLES (Cont'd)

TABLE	TITLE	PAGE
8-VIII	Kobe Water Pipeline Damage as of March 29, 1995	8-29
8-IX	Kobe Wastewater Treatment Plants	8-37
8-X	Kobe Wastewater System Pipe	8-37

SECTION 1
INTRODUCTION

The January 17, 1995 Hanshin-Awaji earthquake, registered at a magnitude of 7.2 (JMA), delivered a totally unexpected and devastating shock to the densely populated Kobe-Osaka corridor squeezed between the Osaka Bay and the Rokko Mountains. This narrow corridor is about 3 km wide and 40 km long. Significant seismic damage was also observed in many communities much beyond this corridor, for example, in the epicentral area of Awaji Island, 20 km southwest of downtown Kobe (Sannomiya) and in the city of Takarazuka, 20 km north of downtown Osaka.

Human casualty turned out to be extremely high in the Hanshin-Awaji earthquake disaster (also known as the Hyogo-ken Nanbu and the Great Hanshin earthquake). It is particularly high for a nation perceived to be technologically well advanced and readily fortified for the impact of future earthquakes. In fact, a toll of approximately 5,500 deaths reported in this disaster is not acceptable by any standard. There is definitely a lesson to be learned from this disaster, particularly in this respect. The lesson is to recognize the utmost importance of retrofitting the unengineered and underdesigned houses, buildings and other constructed facilities. However, this report concentrates on the performance of the regional lifeline systems subjected to this earthquake.

Section 2 of this report describes the seismological characteristics of the Hanshin-Awaji earthquake and the nature of the resulting ground shaking. This strong ground shaking was responsible for inflicting the severe damage to the region's built environment including buildings, bridges, highways, railways, port facilities, utility and communication lifelines, and critical facilities such as hospitals.

Following the basic description of the ground motion in Section 2, the report proceeds to focus on the seismic performance of the lifelines that serve not only the city of Kobe but also many other municipalities located between and surrounding the cities of Kobe and Osaka. This report examines and analyzes, as much as an earthquake disaster reconnaissance report could, the seismic performance of (in the order of appearance in Sections 3 through 8) electric power, gas delivery, hospitals, telecommunications, transportation, and water and wastewater systems. The transportation section consists of three subsections: airport facilities, highways and bridges, and underground rapid transit systems. A hospital is considered here as a system, recognizing that it consists not only of building structures and architectural components, but also of in-house utility, communication and transportation (e.g., elevators) networks, which are vital to the medical (including acute care) services it provides. In addition, the report also recognizes that the hospital's emergency equipment and facilities, such as diesel generators and roof-top water tanks, are equally vital to its operation under earthquake induced stress and add to its complexity as a system.

In each of these sections, an overview of the system is given, indicating the owner/operator, the location and extent of the service area, the municipalities and communities in the service area, the number of households as well as industrial and business customers served (as appropriate),

and other vital statistics. The system description is then given, delineating the physical components and showing how these components are integrated to provide expected function and service. Design criteria of these components are also listed, reflecting as much information as the reconnaissance team was able to collect during the relatively short period of time made available. The difference in the operational and physical characteristics, including design concept and criteria between the U.S. and Japanese systems, is also discussed to the extent possible. Preliminary descriptions of the seismic performance of the various lifeline systems, in terms of seismic damage, emergency response, seismic interruption and restoration, constitute the major ingredient of this reconnaissance report. The seismic performance of lifeline systems under the Hanshin-Awaji earthquake is compared to the performance of those subjected to earthquakes in the U.S., particularly during the Northridge earthquake. Each section ends with suggested lessons for the United States.

Service restoration is a particularly important measure of the seismic performance of a lifeline system; particularly since it is most meaningful to the customers. As a matter of fact, it was generally understood in Japan from past damaging earthquakes such as Niigata (1964, M=7.5), Tokachi Oki (1968, M=7.9) and Miyagi-ken Oki (1978, M=7.4) earthquakes that it would take about one day, one week and one month to restore electric power, water and gas supplies, respectively, to most affected customers by similarly damaging earthquakes. Obviously, this rule did not apply in the case of the Hanshin-Awaji earthquake because of its truly near-field impact on a large urban area with a population density estimated to be 4,000/km^2. Indeed, it took about one week to complete emergency repairs in order to provide electric power to nearly all customers, while it took about three months to restore gas and water supplies. Figure 1-1 depicts the progress of emergency repair to the gas supply, as time proceeds following the earthquake. This figure reflects more updated information than obtained at the time the actual reconnaissance was carried out. Future study should pay more attention to restoration aspects of lifeline systems subjected to damaging earthquakes. This is important particularly because the extent of socio-economic impact of damaging earthquakes often depends significantly on the duration of lifeline system interruptions.

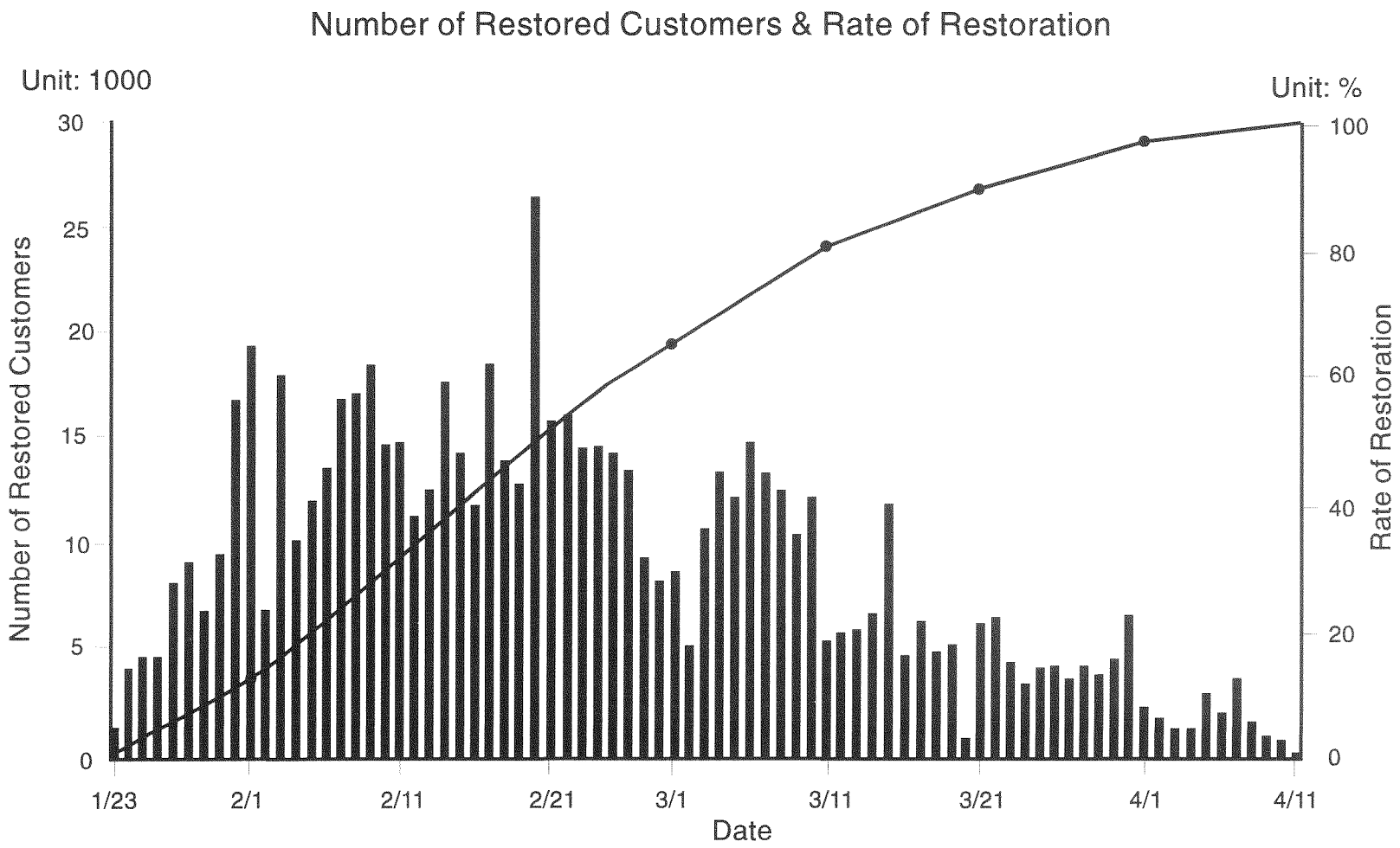


Figure 1-1 Rate of Restoration for Gas Delivery System

SECTION 2
SEISMOLOGY

The Hanshin-Awaji earthquake (also known as the Hyogo-ken Nanbu and the Great Hanshin earthquake) of January 17, 1995 was associated with crustal rupture and resultant strong ground shaking which caused at least 5,378 casualties and economic losses exceeding 96 billion U.S. dollars (Asahi Evening News, February 17,1995). Essentially all of the life loss and about 75 to 80 percent of the direct economic losses were caused by shaking-induced failure of residential and commercial structures. About 20 to 25 percent of the remaining direct economic losses are attributed to the failure of port, river and agricultural facilities caused by ground shaking either indirectly through shaking-induced ground failures associated with liquefaction and landsliding or directly through shaking-induced structural failures. Consequently, understanding the nature of the source rupture characteristics and resultant strong ground shaking is fundamental to understanding the damaging effects of this earthquake and the effects of similar earthquakes in other densely urbanized areas.

This section provides a preliminary summary of the source rupture characteristics and strong-motion data set reported to the author within the first two months after the earthquake. Preliminary analyses of the peak acceleration data regarding attenuation and the effects of local geologic deposits are provided. These results are reproduced from Borcherdt (1995) and Borcherdt and Wentworth (1995).

2.1 Source Characteristics

The Hanshin-Awaji earthquake of January 17, 1995 (5:46:52 JST) occurred in an area of complex faulting located near Awaji Island and the Hanshin area of Japan (34.607 N, 135.043 E, depth 14.3 km; Japan Meteorological Agency, JMA). The area which includes the major urban centers such as the cities of Kobe and Osaka is located about 200 km from the Nankai trough, which forms the boundary between the Philippine Sea and Eurasian plates (Figure 2-1). The earthquake of magnitude of 7.2 (JMA) is the largest and most severe earthquake to affect the region this century. The largest previous earthquake near Kobe City of magnitude 6.1 occurred in 1916 on or near the same fault. Other large, but distant earthquakes (M 7.9, 8.0) occurred in 1944 and 1946 along the plate boundary (Figure 2-1). Numerous faults known to be active in the Quaternary extend throughout the affected region (Figure 2-2). However, prior to January 17, 1995 the area was characterized by relatively low seismicity compared with areas near the plate boundaries (Figure 2-1). The earthquake, having occurred at considerable distance from the plate margin, can be considered as an intraplate event.

Coseismic crustal rupture associated with the earthquake initiated on the Nojima fault located on Awaji island. The rupture extended to the ground surface along a 9 km segment of the fault on Awaji Island. Maximum surface displacements of 1.7 m right-lateral, horizontal and 1.0 m vertical were observed (T. Masaharu, pers. commun., 1995). No surface rupture associated with the fault system had been confirmed in Kobe City as of this writing.

Aftershocks during the first two days and the first 10 days (Figures 2-3a and 2-3b) suggest a rupture surface extending between 35 and 50 km. Comparison of the seismicity pattern with mapped surface faults suggests that the rupture zone extends about 46 km from about 19 km southwest of the epicenter to about 27 km northwest of the epicenter. The aftershock locations suggest the rupture zone slightly increases in average depth to the northeast. The shallowest seismicity occurs beneath Awaji Island and downtown Kobe City.

Source rupture characteristics inferred from teleseismic and regional data by Kikuchi (1995) suggest three subevents (Figure 2-3, Table 2-I). The subevents are inferred to have moment magnitudes of 6.8, 6.3, and 6.4 and predominantly strike-slip source mechanisms. Relative locations of the subevents (Figure 2-3) suggest the third subevent is located beneath Kobe City near the region of shallow seismicity apparent in the aftershock distribution. The source mechanism inferred by Kikuchi suggests that rupture for the first subevent was bilateral, then it proceeded unilaterally with the two subsequent events in a northeasterly direction beneath Kobe City. Duration of total rupture is about 11 seconds with average depth inferred at 8 km. Hypocenter depth or depth of rupture initiation is 14.3 km (Figure 2-3b).

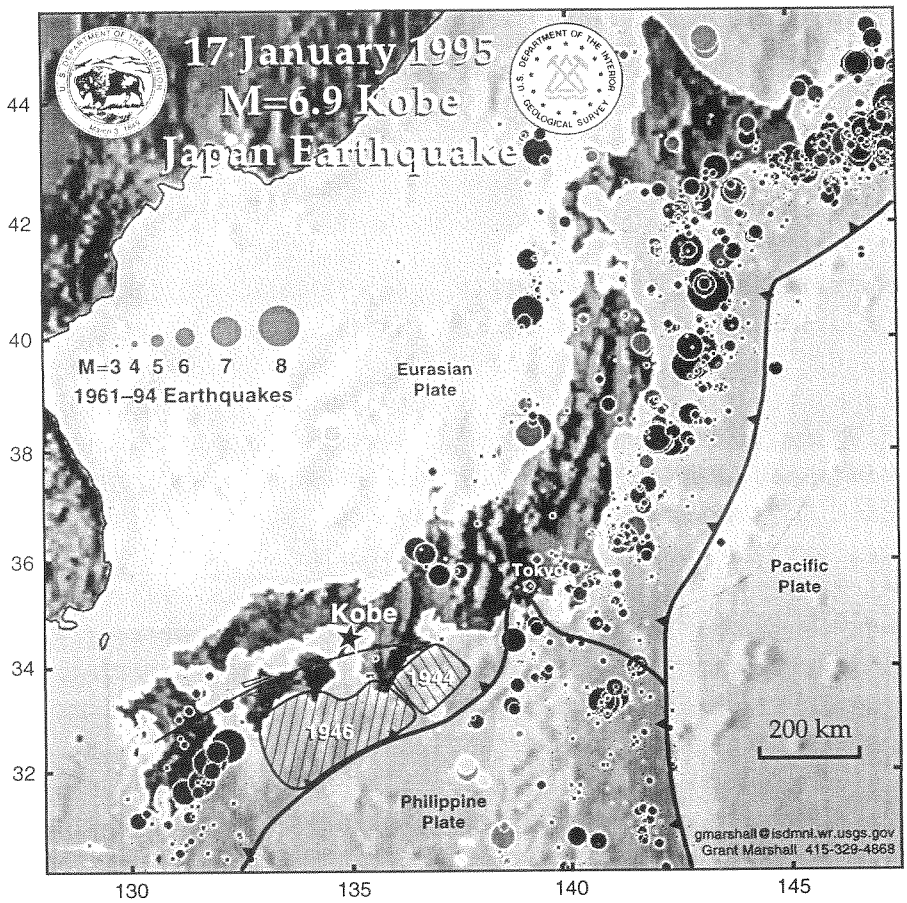


Figure 2-1 Map Showing Seismicity for Japan for Time Period 1961-1994, Plate Margins and Approximate Rupture Zones for the Large 1944 and 1946 Earthquakes (compiled by G. Marshall)

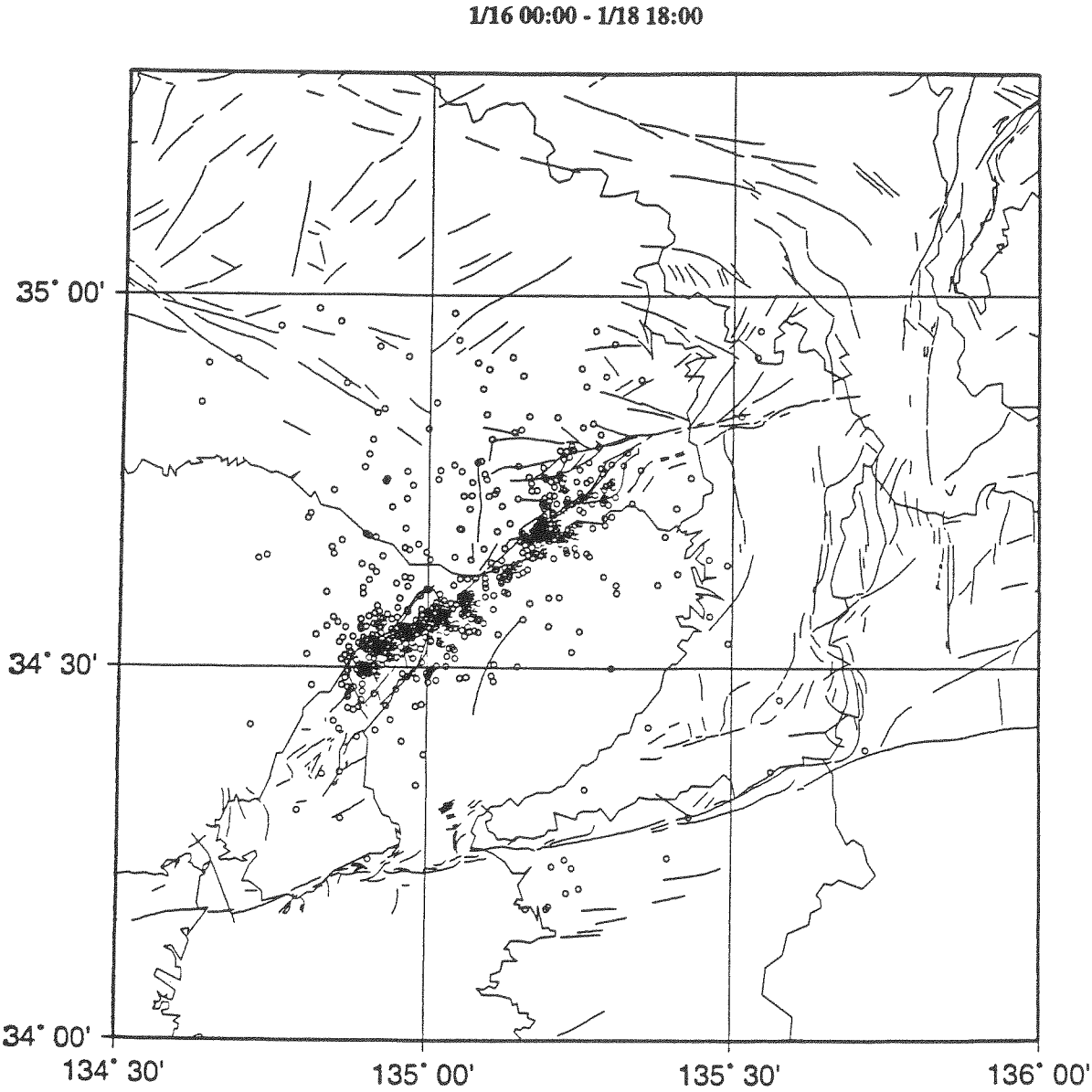
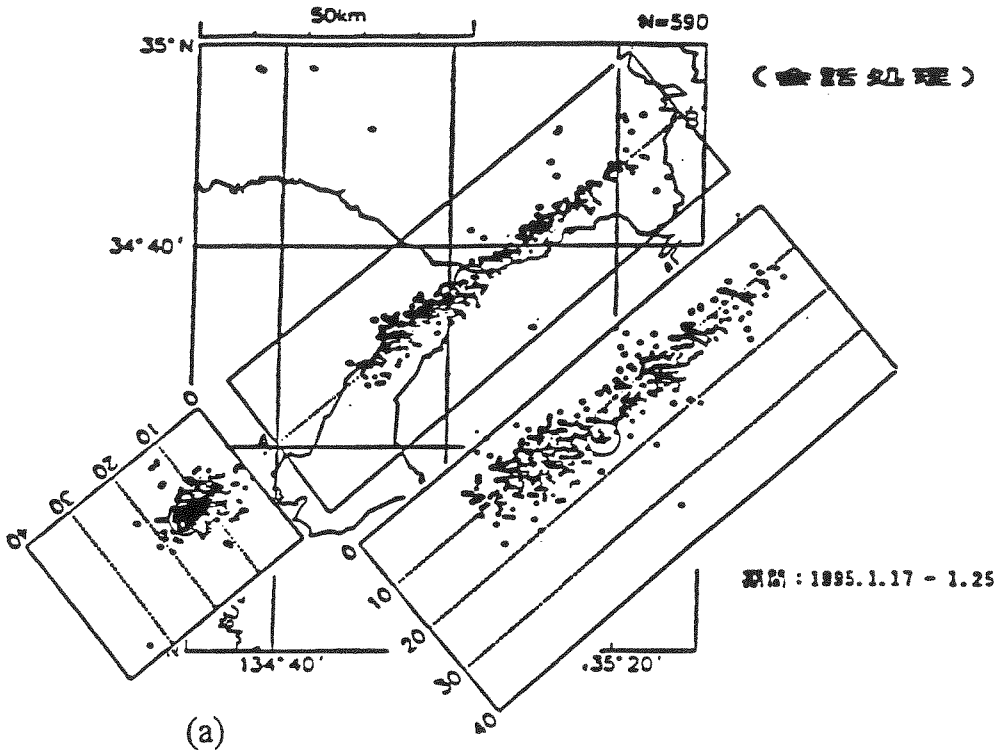


Figure 2-2 Map Showing Quaternary Faults and Seismicity for a Two Day Time Period Including the Occurrence Time of the Hanshin-Awaji Earthquake (from Earthquake Research Institute, University of Tokyo via ftp, Observation Networks of Disaster Prevention Research Institute, Kyoto University, and Faculty of Science, Kochi University)



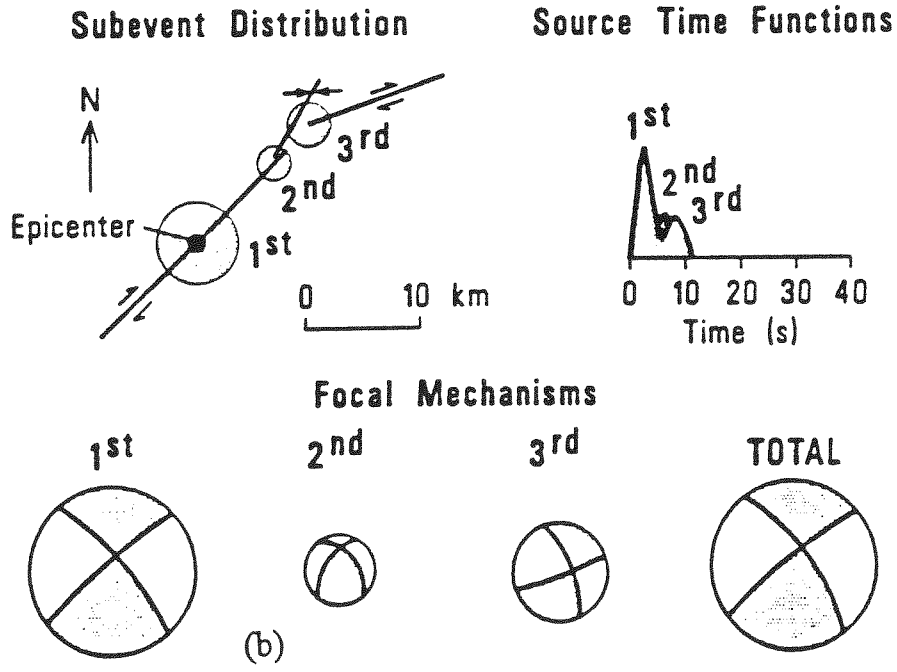


Figure 2-3 **(a) Map Showing Aftershock Distribution in Plan and Cross Section Views** (from Disaster Prevention Research Institute, Kyoto University) **and (b) Source Mechanism for Inferred Subevents** (from Kikuchi, 1995)

Table 2-I Source Parameters Inferred for the Hanshin-Awaji Earthquake (by Kikuchi, 1995)

Parameter	Subevent			Total
	1	2	3	
M_w	6.8	6.3	6.4	6.9
Area (km^2)	24x12	9x5	12x6	40x10
Slip (m)	2.1	2.5	2.7	2.1
Stress Drop (bar)	93	130	242	100-200
M_o (dyne-cm)				$2.5x10^{26}$

Comparison of source characteristics for the Loma Prieta (M_s 7.1, M_w 7.0) and Northridge (M_s 6.8, M_w 6.7) earthquakes suggests the Hanshin-Awaji earthquake (M_s 7.2, M_w 6.9) is about the same magnitude, but slightly longer rupture duration (11 seconds as opposed to six to eight or nine seconds for the other events). The rupture mechanism is predominantly strike slip or horizontal for the Hanshin-Awaji earthquake compared to relatively larger vertical components of motion associated with reverse and thrust faulting for the Loma Prieta and Northridge earthquakes. The average depth of rupture and hypocentral depth for the Hanshin-Awaji earthquake are less than those for Loma Prieta and Northridge earthquakes. Rupture for the Hanshin-Awaji earthquake reached the surface on Awaji Island and may have come within 4 km of the surface beneath Kobe City. Rupture was inferred not to extend closer than 6 to 8 km of the surface for the Loma Prieta and Northridge events.

2.2 Strong-Ground Shaking

The strong-motion recordings were obtained with instrumentation installed and maintained by a variety of private, government, and university-affiliated agencies in Japan. Data assimilation and distribution is provided by each agency with coordination provided for some agencies by The National Research Institute for Earth Science and Disaster Prevention of the Science and Technology Agency, Japan. All of the data and results reported here have been derived from preliminary information supplied by the various agencies, the **Prompt Report on Strong Motion Accelerograms No. 46** (1995), and principal investigators and colleagues in Japan. A conscious effort has been made to report the results accurately with appropriate credit to the agencies, which made this outstanding data set possible. Any omissions or inaccuracies are not intentional, but some are sure to exist due to language translation difficulties.

2.2.1 Strong Motion Recordings

Locations for the strong-motion stations, superimposed upon the geologic map for Japan and the seismicity for a two day interval are shown in Figure 2-4 as reproduced from Wentworth, et al. (1995). A detailed description of the map layers shown in Figure 2-4 is provided by Borcherdt and Wentworth (1995). The geologic map was derived from the digital version of the Geologic Map of Japan (Geological Survey of Japan, 1992). The geologic units shown in the figure differentiate the Holocene and Pleistocene "soil" units, the Pliocene, Miocene, and Pre-Miocene

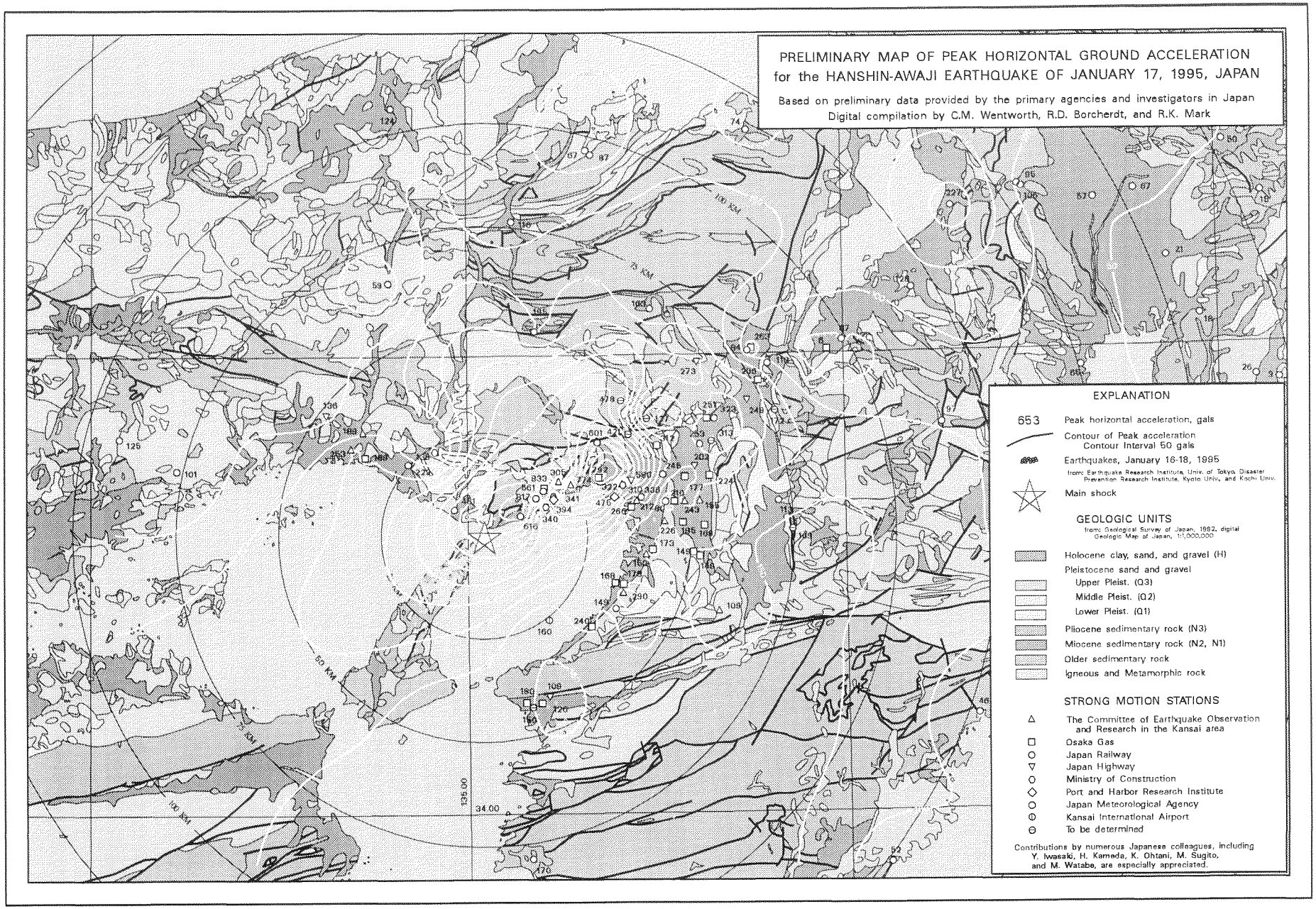


Figure 2-4 **Preliminary Map Showing Geologic Units, Strong-Motion Stations, Peak Horizontal Acceleration and Approximate Contours of Acceleration** (from Geologic Map of Japan, Scale 1:1,000,000, CD-ROM; strong motion information courtesy of agencies and colleagues indicated). A full color version of this map is available on the Internet by typing *http://quake.usgs.gov/QUAKES/shake/kobe/kobeshake.html*

sedimentary "rock" units, and one generalized unit of igneous and metamorphic "rocks". The boundaries for these units include those that approximately coincide with the boundaries for the site classes with distinct seismic response characteristics proposed for NEHRP code changes.

Seismicity for a two-day time period including the occurrence time of the main shock also is shown in Figure 2-4. The location of the main-shock epicenter is that reported in the **Prompt Report on Strong Motion Accelerograms No. 46** (1995). The seismicity distribution was derived from aftershock locations reported via ftp by the Earthquake Research Institute, University of Tokyo, Observation Networks of Disaster Prevention Research Institute, Kyoto University, and Faculty of Science, Kochi University. The seismicity suggests a rupture surface about 46 km long extending from about 19 km southwest of the epicenter to about 27 km northeast of the epicenter. The seismicity suggests the rupture zone increases slightly in average depth to the northeast beneath downtown Kobe City. No surface rupture associated with the fault system had been confirmed in Kobe City as of this writing.

Coordinates for the strong-motion stations are tabulated in Table 2-II. Coordinates for some stations were provided by the agencies and coordinates for others were inferred from page-sized maps projected to a common scale. The locations inferred from these maps (shown in italics in Table 2-II) are considered least accurate and should be updated, when additional information becomes available. Projection of available maps is expected to have introduced location errors in general less than 100 m; however, other sources of error may have contributed to larger uncertainties for some sites whose coordinates are shown in italics.

The peak amplitudes shown in Figure 2-4 were measured using different types of instrumentation and reported in different ways by some agencies. Measurements reported by the Committee on Earthquake Research and Observation in the Kansai region were detected with velocity transducers. Peak accelerations reported by the Railway Technical Research Institute (JR publication No. 23a) and Osaka Gas represent the maximum value of the vectorial sum of the two perpendicular horizontal components. Other agencies report the maximum value of the three orthogonal components, while others report the maximum value of only the horizontal components. An effort has been made to tabulate peak horizontal values (PGA in Table 2-II) as reported by the individual agencies. It is not possible at this writing to resolve all of the differences in reported values; however, resolution of these differences as additional information becomes available is needed to reduce uncertainty. These differences should be considered in deriving conclusions from the data.

Station identification, various measures of distance and peak amplitude data, and geologic classifications of the sites are tabulated (Table 2-II). The measurements exceeding full scale at two stations are indicated. Measures of distance shown in Table 2-II are 1) distance to epicenter (E-Dist), 2) distance to hypocenter (H-Dist), 3) distance to projected rupture surface (Surf-Dis), and 4) distance to seismogenic rupture (SR-Dis; depth below surface, 4 km). Distances to the surface projection of the fault rupture surface were approximated as the closest distance to the straight line implied by the seismicity and determined by endpoints defined by coordinates [34° 29.4`N, 134 53.2E] and [34 45.7N, 135 16.3E].

Table 2 - II Preliminary list of strong motion stations for the Hanshin-Awaji earthquake

Station Name	Sta Code	Geol.	Site Clas	N. Lat. (deg)	E. Long. (deg)	Azm (deg)	Epi. (km)	Hyp. (km)	Surf. (km)	SR (km)	PGA (gal)	Sta Azm	H1 (gal)	H2 (gal)	UD (gal)
Fukiai	OG-FUI	Qp-Q3	III	*34.710*	*135.202*	52	18.5	23.4	0.4	4.0	833				
Shin-Kobe	JR-SNK	Qp-Q3	III	**34.704**	**135.200**	53	18.0	22.9	0.8	4.1	561	NS	-530	-267	-344
Kobe Marine	JM-KBM	Qh	IV	**34.688**	**135.180**	54	15.4	21.0	0.9	4.1	817	NS	817	617	332
Kobe University	KC-KBU	Qp-Q3	III	*34.725*	*135.240*	54	22.3	26.4	1.3	4.2	305	NS	270	305	447
Takatori	JR-TKT	Qh	IV	**34.649**	**135.139**	62	9.9	17.4	1.7	4.3	616	NS	635	553	175
PHRI Kobe	PH-KOB	Qh	IV	*34.697*	*135.225*	59	19.4	24.1	2.7	4.8	394	NS	394	169	275
Port Island	MC-PRI	Qh	IV	*34.691*	*135.226*	61	19.1	23.9	3.3	5.2	341	NS	341	284	557
Kobe Motoyama	KC-KOB	Qh	IV	*34.718*	*135.273*	60	24.4	28.2	3.8	5.5	775?	NS	421?	775?	379?
Port Island Array	MC-PIA	Qh	IV	*34.669*	*135.206*	65	16.4	21.8	4.0	5.6	340	NS	340	282	567
Nishinomiya	OG-NSM	Qh	IV	*34.732*	*135.346*	63	31.0	34.1	7.5	8.5	792				
Takaraduka	JR-TKD	Qh	IV	**34.809**	**135.344**	51	35.5	38.2	8.5	9.3	601	NS	595	530	377
Nishi-Akashi	JR-NSA	Qh	IV	**34.664**	**134.964**	311	9.7	17.2	10.1	10.8	481	NS	481	-389	338
Amagasaki 1	KC-AMG	Qh	IV	*34.718*	*135.408*	70	35.6	38.3	13.4	14.0	>321	NS	271	322	328
PHRI Amagasaki	PH-AMG	Qh	IV	*34.689*	*135.388*	74	32.9	35.8	13.4	14.0	475	NS	475	320	312
Amagasaki 2	MC-AMG	Qh	IV	*34.715*	*135.410*	70	35.7	38.4	13.7	14.3	310	TR	310	274	336
Amagasaki 3	JH-AMO	Qh	IV	*34.724*	*135.432*	70	37.9	40.4	15.3	15.8	580	NS			
Inagawa River	TD-OKI	Qh	IV	*34.826*	*135.426*	55	42.6	44.9	15.8	16.3	421				
Hokko	OG-HOK	Qh	IV	*34.666*	*135.432*	80	36.2	38.9	18.1	18.5	266				
Fukushima	KC-FKS	Qh	IV	*34.681*	*135.446*	78	37.8	40.3	18.3	18.8	212	NS	180	212	195
Yodo R (Ooyodo)	MC-YRO	Qh	IV	*34.688*	*135.458*	77	39.0	41.5	18.9	19.3	336	TR	150	200	300
Hitokura Dam	TD-HTD	sed	I	*34.900*	*135.408*	46	46.7	48.7	19.8	20.2	478				
Toyonaka	KC-TYN	Qp-Q1	III	*34.800*	*135.492*	62	46.3	48.4	20.6	21.0		NS			
Senri	OG-SEN	Tp-N3	I	*34.801*	*135.501*	63	47.1	49.2	21.4	21.8	312				
Minoogawa Dam	TD-MND	sed	I	*34.860*	*135.475*	55	48.5	50.5	21.6	21.9	127				
Shin-Osaka(SS)	JR-SNO	Qh	IV	**34.737**	**135.516**	72	45.6	47.7	22.5	22.8	245	NS	-218	-217	56
Kakogawa Ozeki	MC-KGO	Qh	IV	*34.791*	*134.913*	330	23.8	27.7	23.9	24.2	139	TR	136	139	114
Osaka	JM-OSK	Qp-Q3	III	**34.678**	**135.522**	80	44.5	46.7	24.7	25.0	80	NS	80	66	-65
Kansai Int'l. Airport	KA-KIA	Qh	IV	*34.421*	*135.212*	143	25.8	29.5	25.2	25.6	160				247
Kakogawa	JR-KKG	Qh	IV	**34.764**	**134.843**	314	25.3	29.0	25.7	26.0	229	NS	165	262	98
Abeno	KC--ABN	Qp-Q3	III	*34.636*	*135.519*	86	43.7	45.9	26.6	26.9	226	NS	217	226	136
Morikawachi	OG-MK	Qh	IV	*34.678*	*135.545*	80	46.5	48.6	26.6	26.9	210	NS	210	123	159
Kawachi	OG-KAW	Qh	IV	*34.732*	*135.574*	74	50.5	52.4	27.8	28.1	177				
Sakai S	KC-SAS	Qh	IV	*34.564*	*135.469*	97	39.3	41.7	28.4	28.7	150	NS	150	125	100
Sakai N	OG-SKN	Qh	IV	*34.573*	*135.487*	95	40.8	43.2	28.8	29.0	173				
Fujiidera	OG-FU2	Qh	IV	*34.501*	*135.387*	111	33.6	36.5	28.9	29.2	168				
Shin-osaka	KC-AHN	Qh	IV	*34.679*	*135.572*	81	49.0	51.0	28.9	29.2	243	NS			
Minami-Osaka	JH-MNO	Qh	IV	*34.755*	*135.600*	72	53.5	55.3	30.0	30.3	202				
Izumi	OG-IZ1	Qh	IV	*34.498*	*135.409*	110	35.6	38.4	30.5	30.7	178				
Iwasaki	OG-IWS	Qh	IV	*34.632*	*135.567*	87	48.1	50.1	30.6	30.9	185				
Yodo River (Hirakata)	MC-YRH	Qh	IV	*34.803*	*135.614*	67	56.6	58.3	31.6	31.9	253	TR	144	253	57
Tadaoka	KC-TAD	Qp-Q3	III	*34.480*	*135.408*	113	36.3	39.0	31.9	32.2	290	NS	290	190	137
Yae	KC-YAE	Qh	IV	*34.680*	*135.612*	81	52.7	54.5	32.4	32.6	155	NS	155	145	127
Izumi 2	OG-IZ2	Qp-Q3	III	*34.406*	*135.324*	131	34.0	36.9	33.2	33.4	240				
Sasayamaguchi	JR-SMG	sed	I	**35.053**	**135.180**	14	51.2	53.0	33.5	33.7	195	NS	139	-177	39
Higashi-Kishiwade	JR-HGK	Qp-Q3	III	**34.445**	**135.388**	120	36.3	39.0	33.7	33.9	149	NS	-110	-144	49
Shirahama	OG-SHR	Qh	IV	*34.779*	*134.729*	304	34.5	37.3	33.7	34.0	189				189
Shijonawate	OG-SHJ	Qh	IV	*34.734*	*135.639*	76	56.3	58.0	33.8	34.0	224				
Yodo River, Hirakata City	TD-HKC	Qh	IV	*34.810*	*135.645*	68	59.5	61.1	34.5	34.8	313				
Hashiramoto	OG-HSM	Qh	IV	*34.860*	*135.634*	63	60.9	62.5	34.8	35.1	251				
Onji	OG-ONJ	Qh	IV	*34.625*	*135.624*	88	53.2	55.0	35.6	35.9	169				
Fujiidera	OG-FJ3	Qp-Q3	III	*34.567*	*135.594*	95	50.6	52.5	36.5	36.7	149				
Shin-Takatsuki(SS)	JR-SNT	Qh	IV	**34.859**	**135.654**	63	62.5	64.0	36.6	36.8	323	NS			
Matsuo	OG-MTS	Qh	IV	*34.241*	*135.150*	167	41.8	44.2	36.7	36.9	180				
Shikama	KC-SHM	Qh	IV	*34.799*	*134.691*	304	38.7	41.2	37.7	37.9	253				
Fujiidera	OG-FU1	Qp-Q3	III	*34.558*	*135.611*	96	52.3	54.1	38.4	38.6	149				
Kino-Kawa Ohashi	TD-KKO	Qh	IV	*34.231*	*135.167*	165	43.3	45.6	38.6	38.8	150				
Himeji	KC-HIM	volc	I	*34.835*	*134.723*	311	38.8	41.3	38.9	39.1	189				
Nakanoshima	OG-NKS	Qh	IV	*34.240*	*135.191*	162	43.0	45.3	39.3	39.5	126				
Wakayama Br	JH-WKY	Qh	IV	*34.254*	*135.211*	159	42.2	44.5	39.3	39.5	109				
Oimosaka-Kameoka	JH-OMK	Qp-Q2	III	*34.983*	*135.609*	51	66.5	67.9	39.4	39.6	273				

Table 2 - II (continued) Preliminary list of strong motion stations for the Hanshin-Awaji earthquake

Sonobo	JR-SNB	Qh	IV	**35.100**	**135.487**	37	68.2	69.6	42.4	42.6	163	NS	-102	163	-47
Keiji Bypass	JH-KJB	Qh	IV	*34.898*	*135.741*	63	71.5	72.8	45.4	45.6	249				
Tatsuno	JH-TSN	volc	I	*34.871*	*134.626*	308	48.2	50.2	47.7	47.9	136				
Fushimi	OG-FUS	Qh	IV	*34.941*	*135.772*	61	76.2	77.4	49.8	49.9	206				
Chihaya	KC--CHY	ig/meta	I	*34.439*	*135.659*	108	59.4	61.1	50.4	50.6	109	NS	91	109	74
Nijo	JR-NJO	Qh	IV	**35.007**	**135.744**	55	77.9	79.1	51.0	51.1	84	NS			
Nara	JR-NRA	Qh	IV	**34.677**	**135.821**	84	71.6	72.9	51.1	51.2	113	NS	112	104	-36
Amagase Dam	TD-AMD	Qp-Q1	III	*34.875*	*135.815*	67	76.6	77.8	51.2	51.3	172				
Kyoto	OG-KYO	Qh	IV	*35.012*	*135.755*	55	79.1	80.2	52.1	52.3	67				
Higashiyama	JR-HGY	sed	I	**34.978**	**135.797**	59	80.3	81.4	53.6	53.8	113	NS			
Shirakawa Dam	TD-SKD	TmN1/	II	*34.615*	*135.858*	90	74.6	75.9	56.1	56.2	169				
Fukuchiyama	JR-FHY	Qh	IV	**35.293**	**135.121**	5	76.7	77.8	60.7	60.8	110	NS	72	107	21
Ikuno	JR-IKN	volc	I	**35.160**	**134.792**	339	65.7	67.1	62.1	62.2	59	NS	-36	53	20
In	JR-IN	volc	I	**34.750**	**134.227**	282	76.3	77.6	66.9	67.0	101	NS	-36	53	20
Kusatsu	OG-KUS	Qh	IV	*35.008*	*135.956*	62	94.5	95.5	68.2	68.3	6				
Gobo	JR-GBO	sed	I	**33.904**	**135.162**	172	78.9	80.1	69.9	70.0	170	NS	-111	132	26
Ritto	JR-RTO	Qh	IV	**35.028**	**135.996**	62	98.8	99.7	72.4	72.5	67	NS			
Nishi-Maiduro	JR-NSM	sed	I	**35.438**	**135.333**	16	96.1	97.0	75.4	75.5	87	NS	-60	79	-20
Maizura	JM-MAZ	ig/meta	I	**35.448**	**135.320**	15	96.9	97.8	76.4	76.5	67	NS	-67	-52	-40
Himeji	JR-HMJ	volc	I	**34.821**	**134.075**	285	91.7	92.7	82.9	83.0	125	NS	82	125	48
Tsuge	JR-TSG	Tp-N3	III	**34.843**	**136.259**	77	114.2	114.9	90.6	90.7	97	NS	77	-67	33
Obama	JR-OBM	Qh	IV	**35.488**	**135.749**	33	117.2	117.9	91.7	91.8	74	NS	70	-57	-24
Gokasou	JR-GOK	volc	I	**35.139**	**136.184**	61	119.7	120.4	93.1	93.2	128	NS	-125	119	-44
Toyooka	JR-TYK	TmN1/	II	**35.541**	**134.800**	348	106.2	107.0	96.7	96.8	124	NS	103	-90	-27
Shin-Malbara(SS)	JR-SNM	Qh	IV	**35.316**	**136.293**	56	138.5	139.1	111.6	111.6	227	NS	217	135	-25
Kji-Nagashima	JR-KNG	sed	I	**34.205**	**136.342**	111	127.2	127.9	116.0	116.1	46	NS			
Matsuzaka	JR-MTZ	Qh	IV	**34.573**	**136.538**	92	136.9	137.5	117.7	117.8	49	NS			
Kumancshi	JR-KUM	volc	I	**33.889**	**136.105**	130	126.1	126.8	123.5	123.6	52	NS			
Yokkaichi	JR-YKC	Qh	IV	**34.960**	**136.633**	75	150.4	150.9	126.2	126.2	65	NS			
Sekigahara	JR-SKH	Qh	IV	**35.360**	**136.472**	58	154.8	155.2	127.9	128.0	95	NS			
Shin-Sekigahara(SS)	JR-SNS	Qh	IV	**35.354**	**136.483**	58	155.3	155.7	128.4	128.5	106	NS	106	72	-29
Hashima	JR-HSM	Qh	IV	**35.326**	**136.675**	62	168.8	169.2	142.3	142.4	57	NS	57	-31	10
Kisogawa	JR-KIS	Qh	IV	**35.343**	**136.783**	63	178.4	178.8	152.0	152.1	67	NS			
Biwajima(SS)	JR-BWJ	Qh	IV	**35.195**	**136.867**	69	178.7	179.1	153.1	153.2	21	NS	-21	18	-7
Odaka(SS)	JR-ODK	Tp-N3	III	**35.066**	**136.953**	74	181.6	182.0	157.0	157.1	18	NS	-17	-14	-7
Anjo(SS)	JR-ANJ	Qp-Q3	III	**34.929**	**137.099**	80	191.2	191.5	167.8	167.8	26	NS	-22	-19	-7
Okazaki	JR-OKZ	Qp-Q3	III	**34.920**	**137.160**	80	196.5	196.8	173.2	173.3	9	NS			
Mino-Ota	JR-MNO	Qh	IV	**35.443**	**137.022**	63	202.8	203.0	176.3	176.4	50	NS			
Tajimi	JR-TJM	TmN1/	II	**35.330**	**137.122**	68	205.8	206.0	179.9	180.0	15	NS			
Toyohashi	JR-TYH			**34.760**	**137.385**	86	214.8	215.0	193.1	193.1	12	NS			
Gero	JR-GRO			**35.802**	**137.242**	57	239.9	240.1	213.0	213.0	10	NS			
Nakatsugawa	JR-NKT			**35.495**	**137.505**	67	244.9	245.0	218.9	218.9	14	NS			
Nagiso	JR-NGS			**35.596**	**137.612**	66	258.3	258.3	232.1	232.1	19	NS			
Takayama	JR-TKY			**36.138**	**137.254**	50	263.0	263.0	235.9	236.0	7	NS			
Shin-Iwata(SS)	JR-SHI			**34.723**	**137.901**	88	261.7	261.8	240.3	240.3	14	NS	10	13	-4
Hiraoka	JR-HRK			**35.271**	**137.857**	75	266.9	267.0	242.2	242.2	8	NS			
Ida	JR-IDA			**35.517**	**137.825**	69	272.7	272.7	246.9	246.9	18	NS			

KC - Kansai Committee for Earthquake Observation and Research
OG - Osaka Gas
JR - Japan Railway
JH - Japan Highway
MC - Ministry of Construction
PH - Port and Harbor Research Institute
JM - Japan Meterological Agency
KA - Kansai International Airport
TD - To be Determined
Bold faced coordinates provided by agencies.
Italicized coordinates inferred from maps

Acceleration contours, derived from the peak acceleration values tabulated in Table 2-II, are shown in Figure 2-4. The contours were derived from a grid of values interpolated at a spacing of 0.5 km (Wentworth, et al., 1995). The contours are shown with a contour interval of 50 gals. Inadequate station spacing in some areas contributes to generalized grid values and hence generalized contours. The contours suggest a linear zone of intense ground shaking underlain by Holocene soil deposits parallel to the surface projection of the crustal rupture zone. The suggested zone of intense ground shaking includes the zone mapped as JMA intensity 7.

Record sections showing the north-south, east-west, and vertical components of motion as recorded at stations located at increasing distance from the fault are shown in Figure 2-5. These recordings, shown with the same amplitude scale, indicate a well-defined velocity pulse near 1 second period. They suggest that the peak amplitude of ground velocity decreases rapidly within the first few kilometers of the projected surface rupture, with the duration of shaking extending from about 11-15 seconds for a site on Pleistocene deposits (KC-KBU) near the source to more than 60 seconds at several sites on Holocene soil deposits (see e.g. sites KC-FKS, KC-YAE, KC-SAS).

Acceleration, velocity and displacement time histories as derived by Nakamura (1995) for four locations are reproduced in Figures 2-6a through 2-6d. These analyzed versions illustrate effects of source rupture, wave propagation and local geology on the resultant motions. Corresponding response spectra are provided by Nakamura (1995).

Ground motions recorded at the Kobe Ocean Meteorological Station (JM-KBM) within 1 km of the surface projection of the rupture surface are of special note. The peak acceleration amplitude of 818 gal on the north-south component is one of three recording sites near the source region for which motions exceeded 0.8g. The measurements at the JM-KBM site were obtained using accelerometers and 16 bit digital recorders (K. Ohtani, pers. commun., 1995). These recordings were obtained on a concrete pier inside a single story concrete building. The building is located atop a hill with a steeply dipping slope near the building. The station is located near the boundary of Holocene and Pleistocene deposits. Inspection of the site by the author revealed a collapsed brick wall outside the instrument structure, but relatively minor amounts of damage to structures located at the base of the hill. Detailed studies to infer the role of topographic amplification at this site are needed.

Response spectra were provided by the Building Research Institute for several significant earthquake recordings (Figure 2-7a, 2-7b, and 2-7c) . They show that the JM-KBM spectra are greater than the other spectra in the period band 0.8 to 2.0 seconds. Comparison of the spectra with those used for tall building design in Japan (Figure 2-7c) shows that the JM-KBM spectra exceed the design spectra in the period band 0.25 to 2.0 seconds by about a factor of 2 at periods near 1 second.

Measurements obtained from a three-component vertical borehole array of sensors located on Port Island at a distance of about 4 km from the projected surface rupture are of special importance. They provide measurements of shaking at the ground surface and at depths of 12, 27, and 79 meters. With liquefaction occurring at this site, these measurements provide an

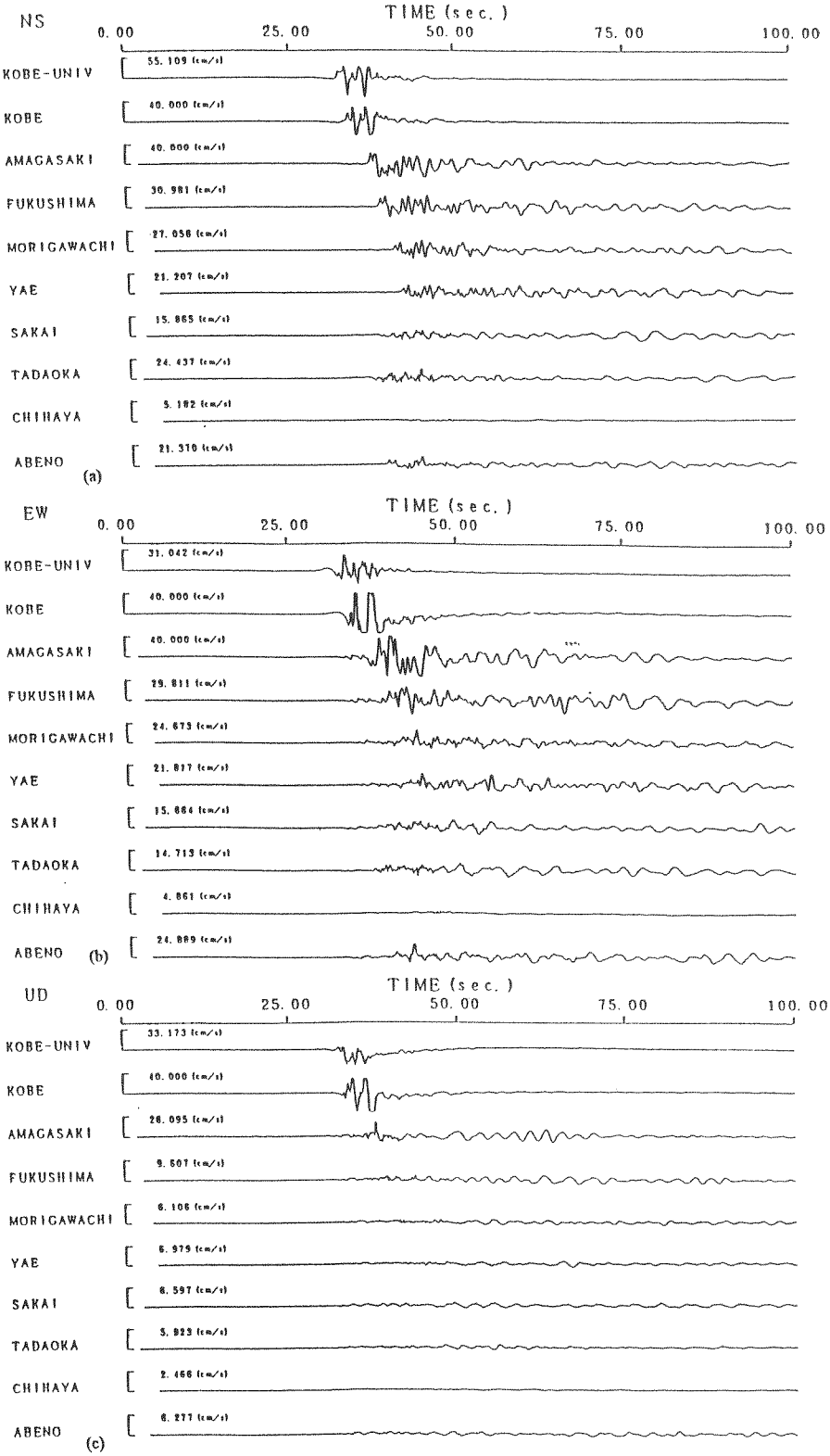
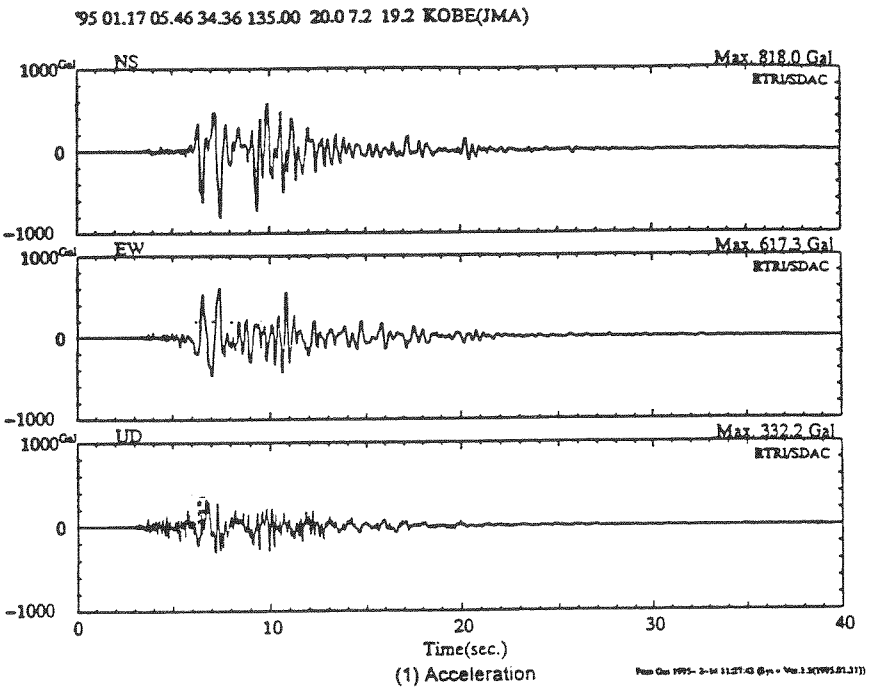


Figure 2-5 Record Section Showing Ground Velocity in the (a) NS, (b) EW, and (c) UD Directions
(from The Committee on Earthquake Observation and Research in the Kansai Area, CEORKA)



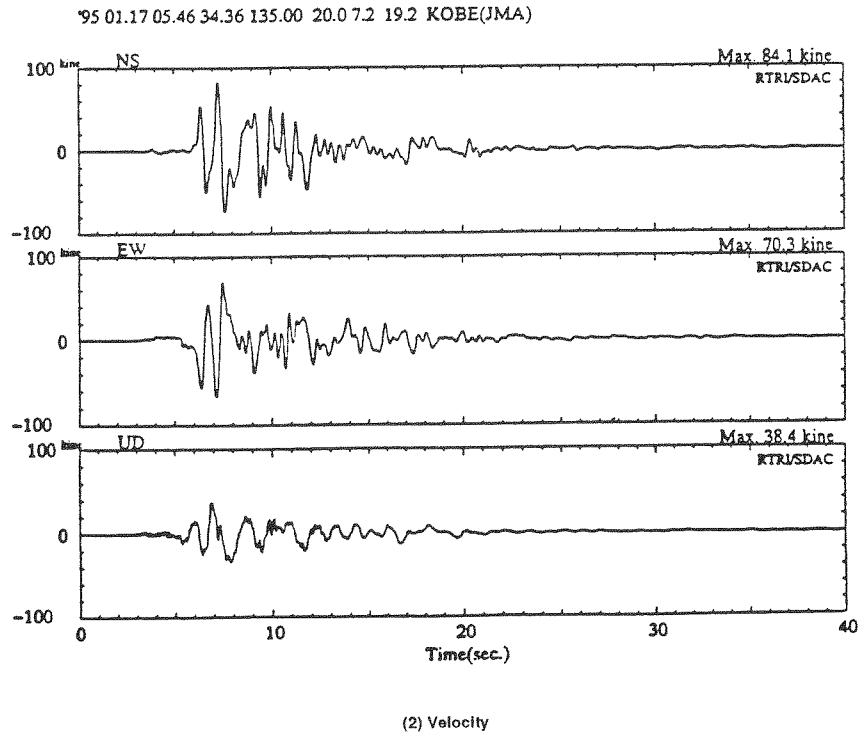


Figure 2-6 Three-Component (1) Acceleration, (2) Velocity, (3) Displacement, and (4) Displacement Loci Inferred by Nakamura (1995) from Strong-Motion Recordings at Site (a) Kobe Marine (JM-KBM), (b) Takatori (JR-TKT), (c) Takarazuka (JR-TKD), and (d) Nishi-Akashi (JR-NSA)

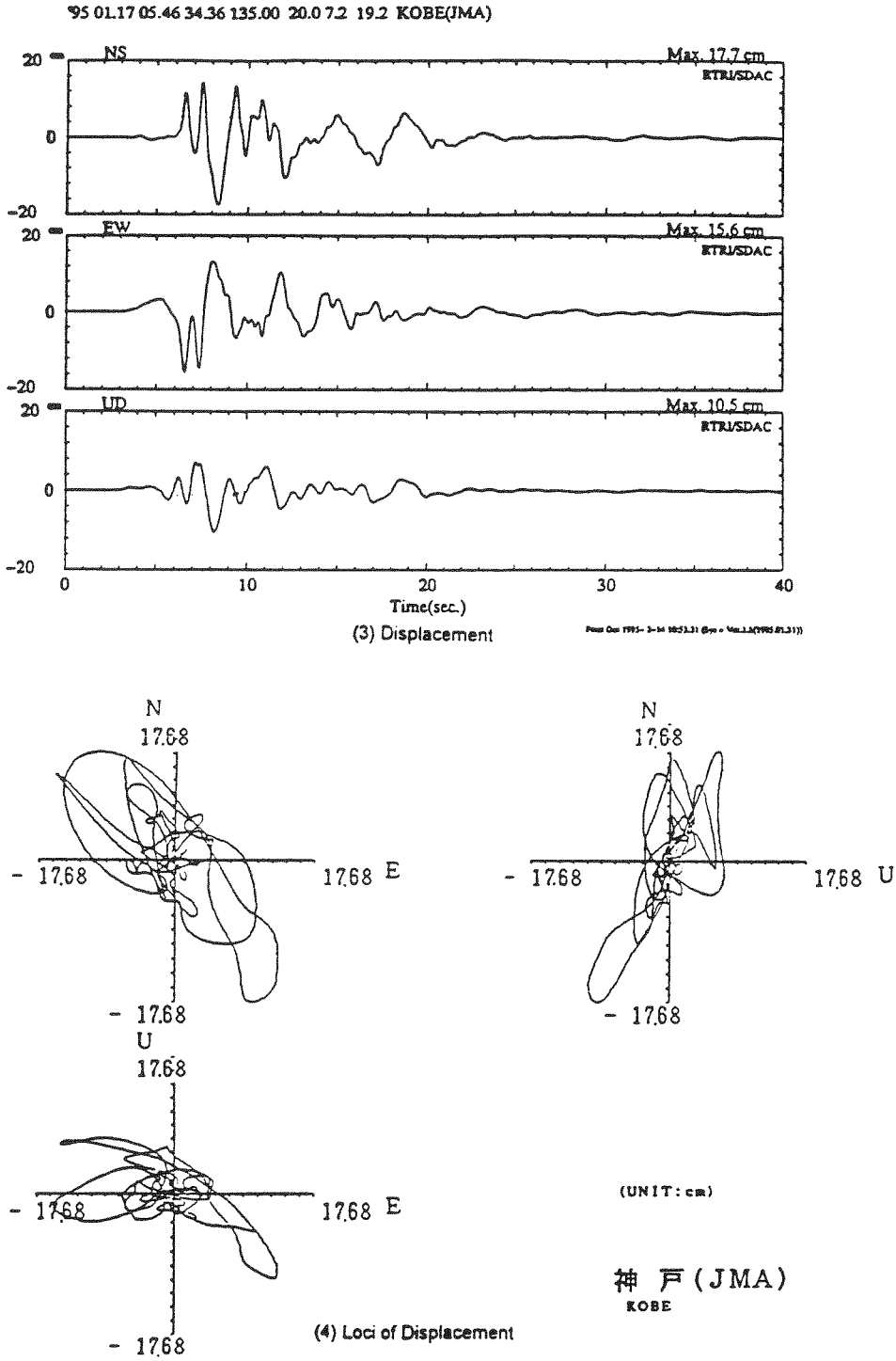
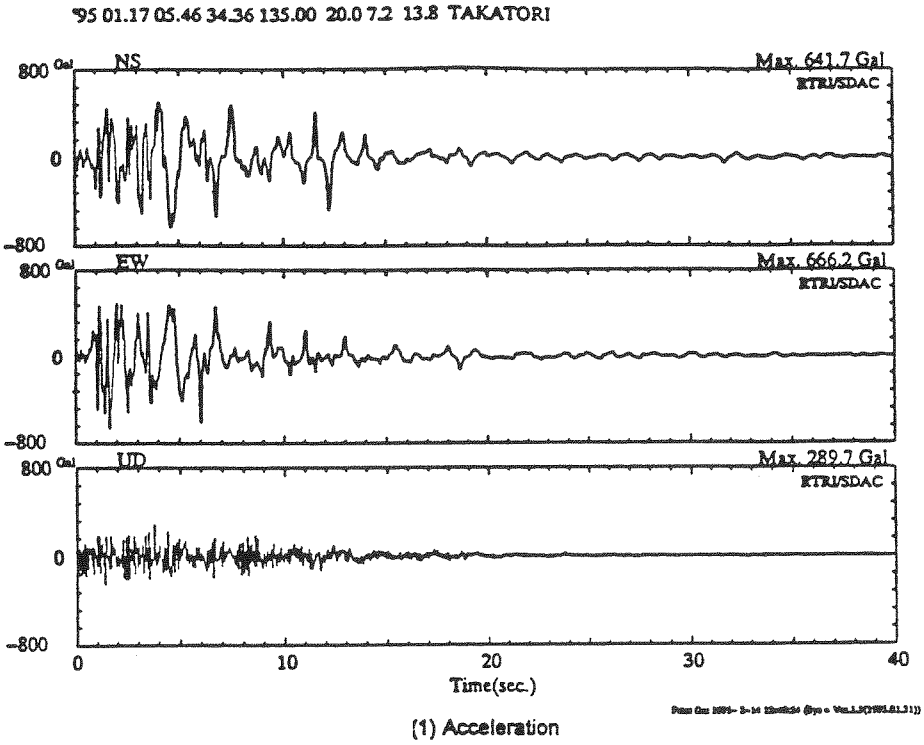
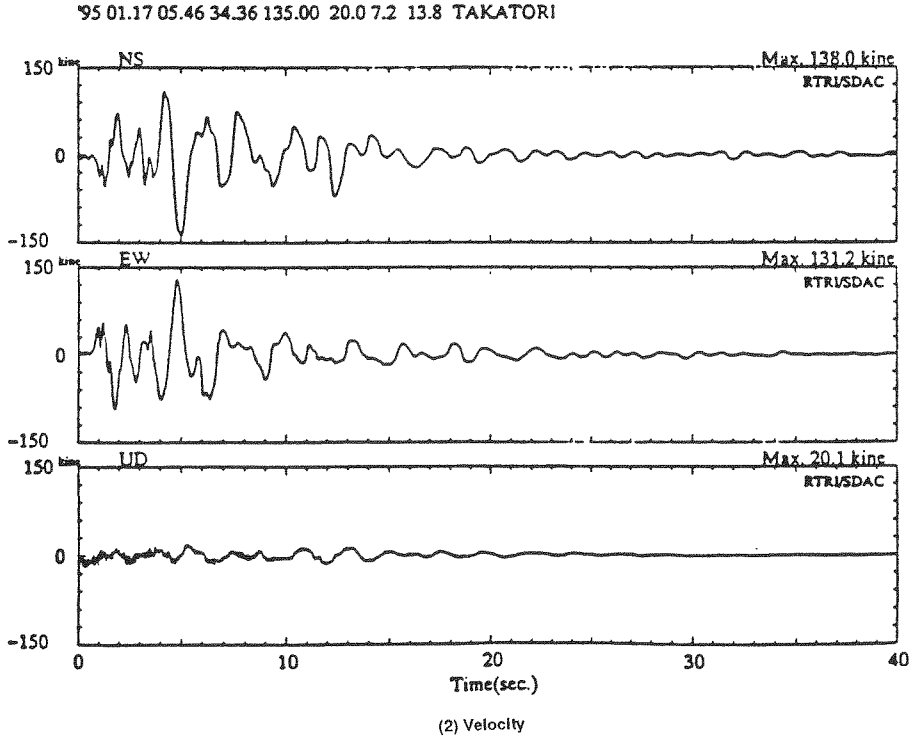


Figure 2-6 Three-Component (1) Acceleration, (2) Velocity, (3) Displacement, and (4) Displacement Loci Inferred by Nakamura (1995) from Strong-Motion Recordings at Site (a) Kobe Marine (JM-KBM), (b) Takatori (JR-TKT), (c) Takarazuka (JR-TKD), and (d) Nishi-Akashi (JR-NSA) (Cont'd)



(1) Acceleration



(2) Velocity

Figure 2-6 Three-Component (1) Acceleration, (2) Velocity, (3) Displacement, and (4) Displacement Loci Inferred by Nakamura (1995) from Strong-Motion Recordings at Site (a) Kobe Marine (JM-KBM), (b) Takatori (JR-TKT), (c) Takarazuka (JR-TKD), and (d) Nishi-Akashi (JR-NSA) (Cont'd)

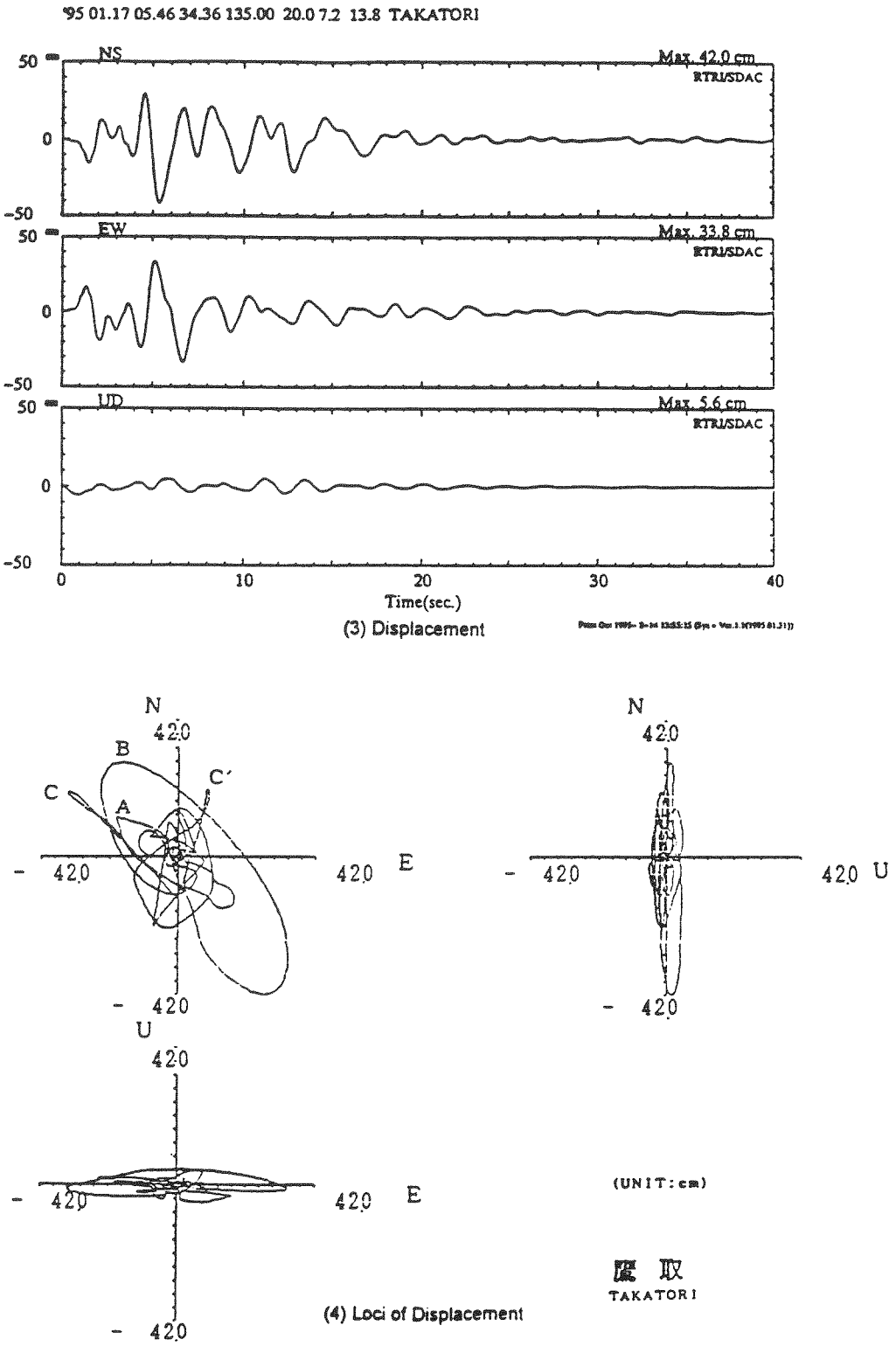
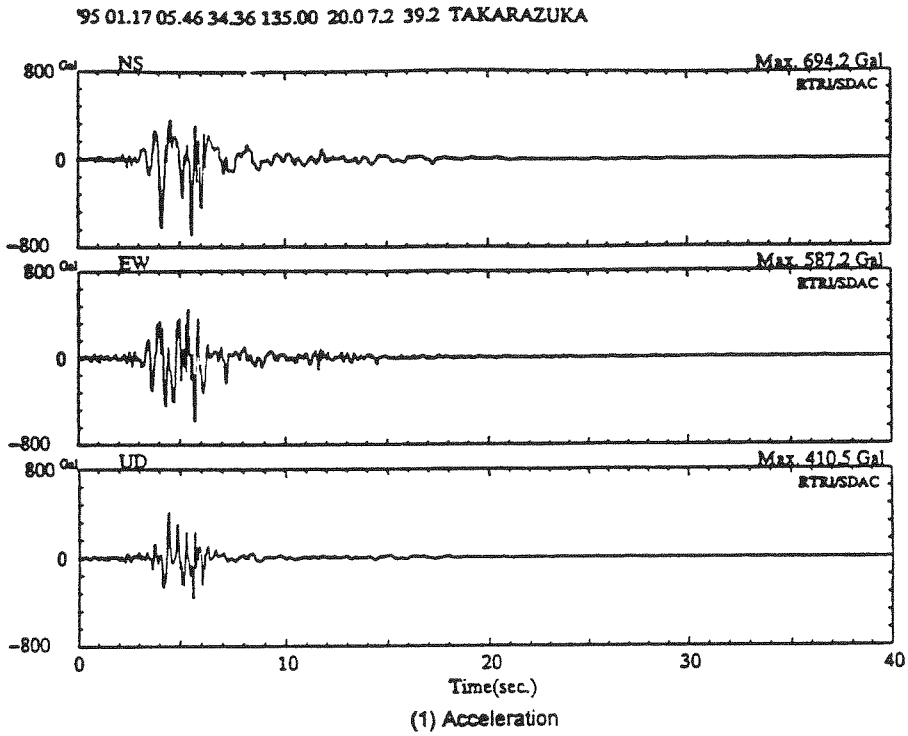


Figure 2-6 Three-Component (1) Acceleration, (2) Velocity, (3) Displacement, and (4) Displacement Loci Inferred by Nakamura (1995) from Strong-Motion Recordings at Site (a) Kobe Marine (JM-KBM), (b) Takatori (JR-TKT), (c) Takarazuka (JR-TKD), and (d) Nishi-Akashi (JR-NSA) (Cont'd)



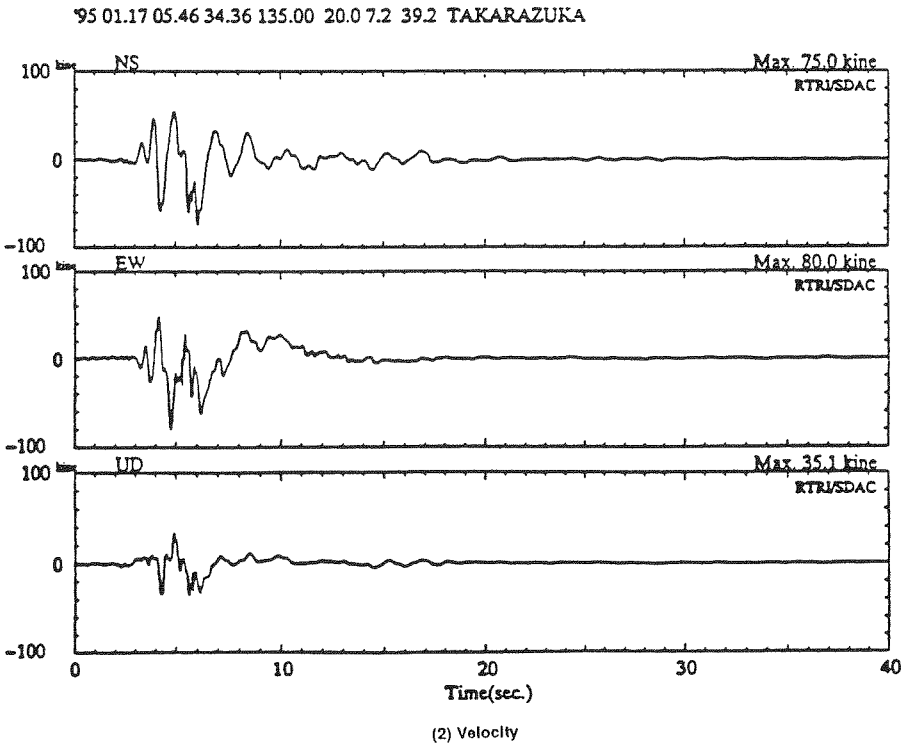


Figure 2-6 Three-Component (1) Acceleration, (2) Velocity, (3) Displacement, and (4) Displacement Loci Inferred by Nakamura (1995) from Strong-Motion Recordings at Site (a) Kobe Marine (JM-KBM), (b) Takatori (JR-TKT), (c) Takarazuka (JR-TKD), and (d) Nishi-Akashi (JR-NSA) (Cont'd)

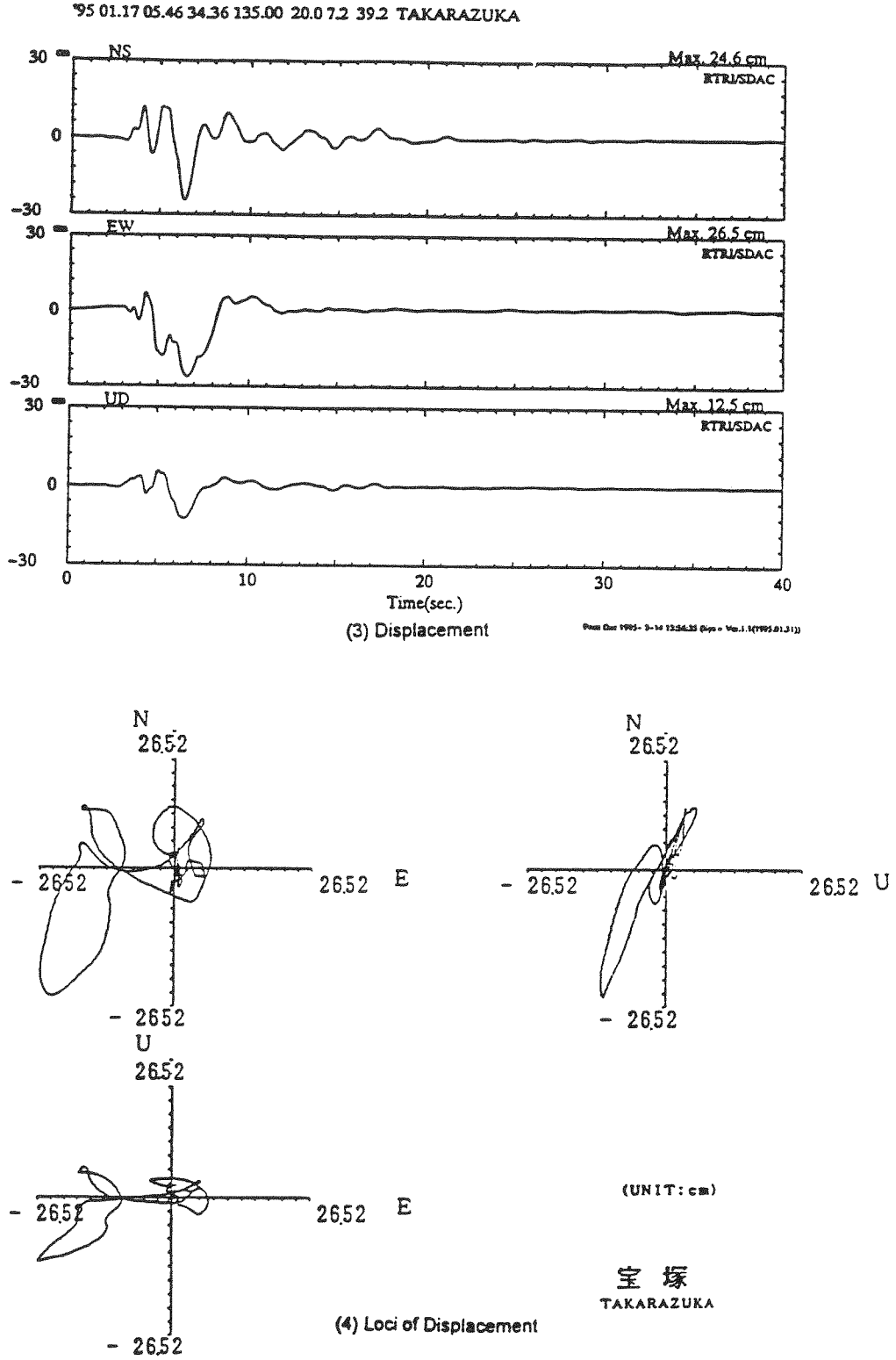
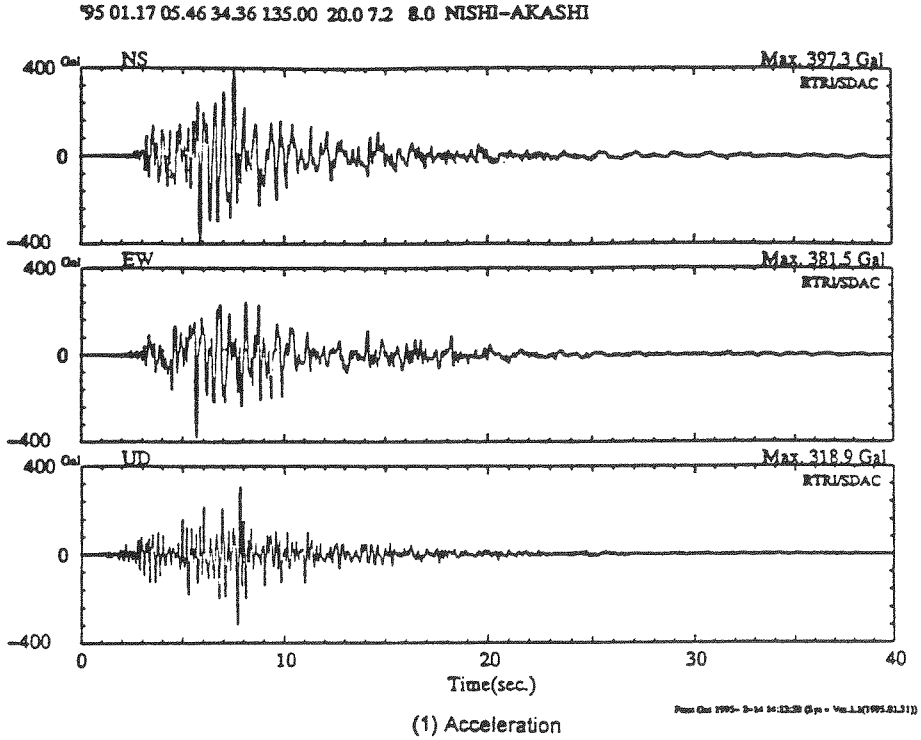
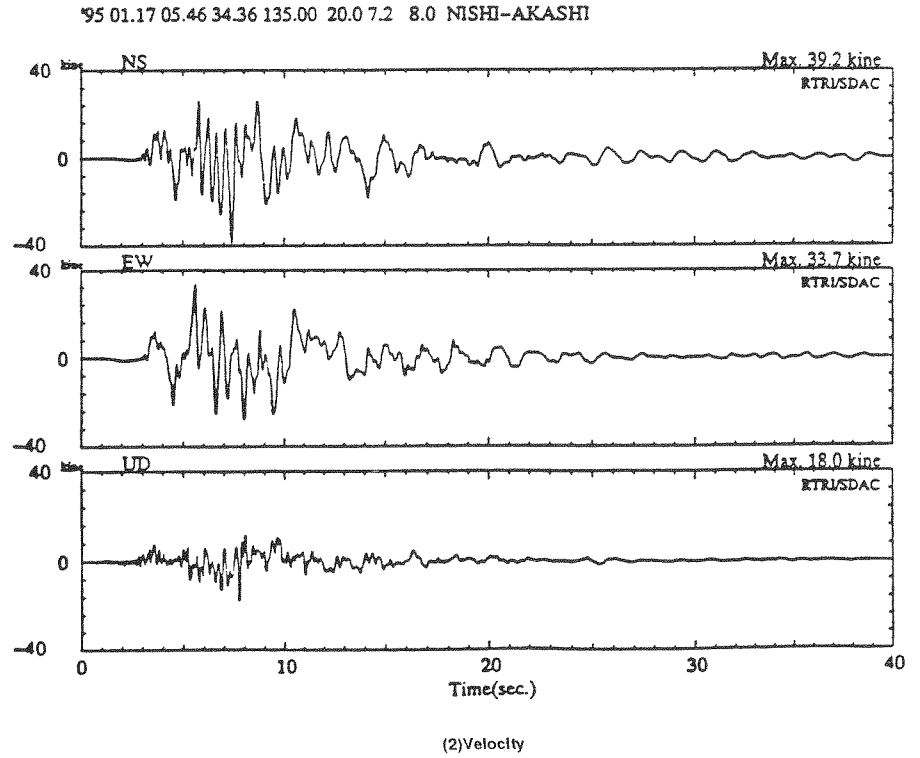


Figure 2-6 Three-Component (1) Acceleration, (2) Velocity, (3) Displacement, and (4) Displacement Loci Inferred by Nakamura (1995) from Strong-Motion Recordings at Site (a) Kobe Marine (JM-KBM), (b) Takatori (JR-TKT), (c) Takarazuka (JR-TKD), and (d) Nishi-Akashi (JR-NSA) (Cont'd)



(1) Acceleration



(2)Velocity

Figure 2-6 Three-Component (1) Acceleration, (2) Velocity, (3) Displacement, and (4) Displacement Loci Inferred by Nakamura (1995) from Strong-Motion Recordings at Site (a) Kobe Marine (JM-KBM), (b) Takatori (JR-TKT), (c) Takarazuka (JR-TKD), and (d) Nishi-Akashi (JR-NSA) (Cont'd)

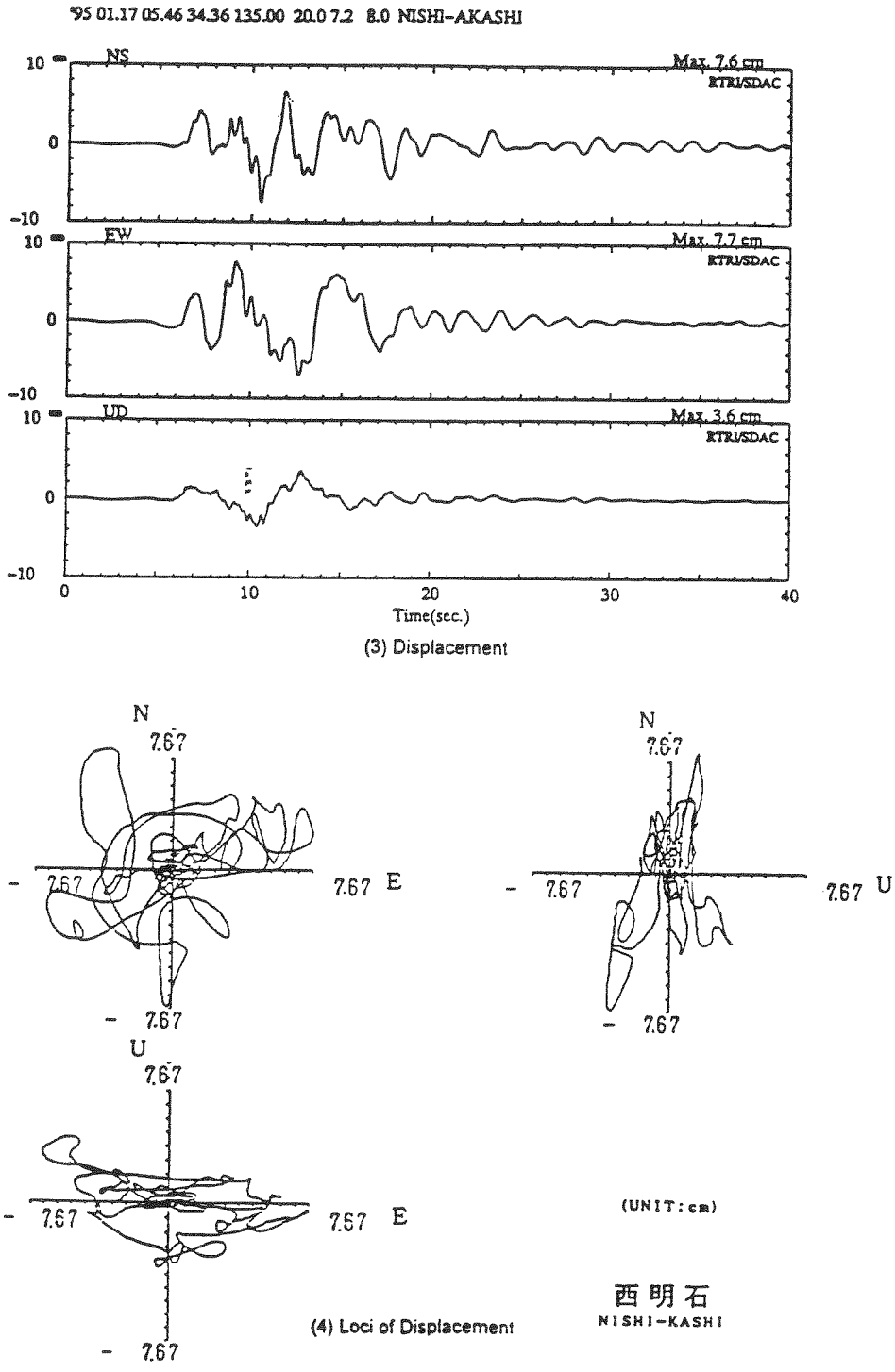


Figure 2-6 Three-Component (1) Acceleration, (2) Velocity, (3) Displacement, and (4) Displacement Loci Inferred by Nakamura (1995) from Strong-Motion Recordings at Site (a) Kobe Marine (JM-KBM), (b) Takatori (JR-TKT), (c) Takarazuka (JR-TKD), and (d) Nishi-Akashi (JR-NSA) (Cont'd)

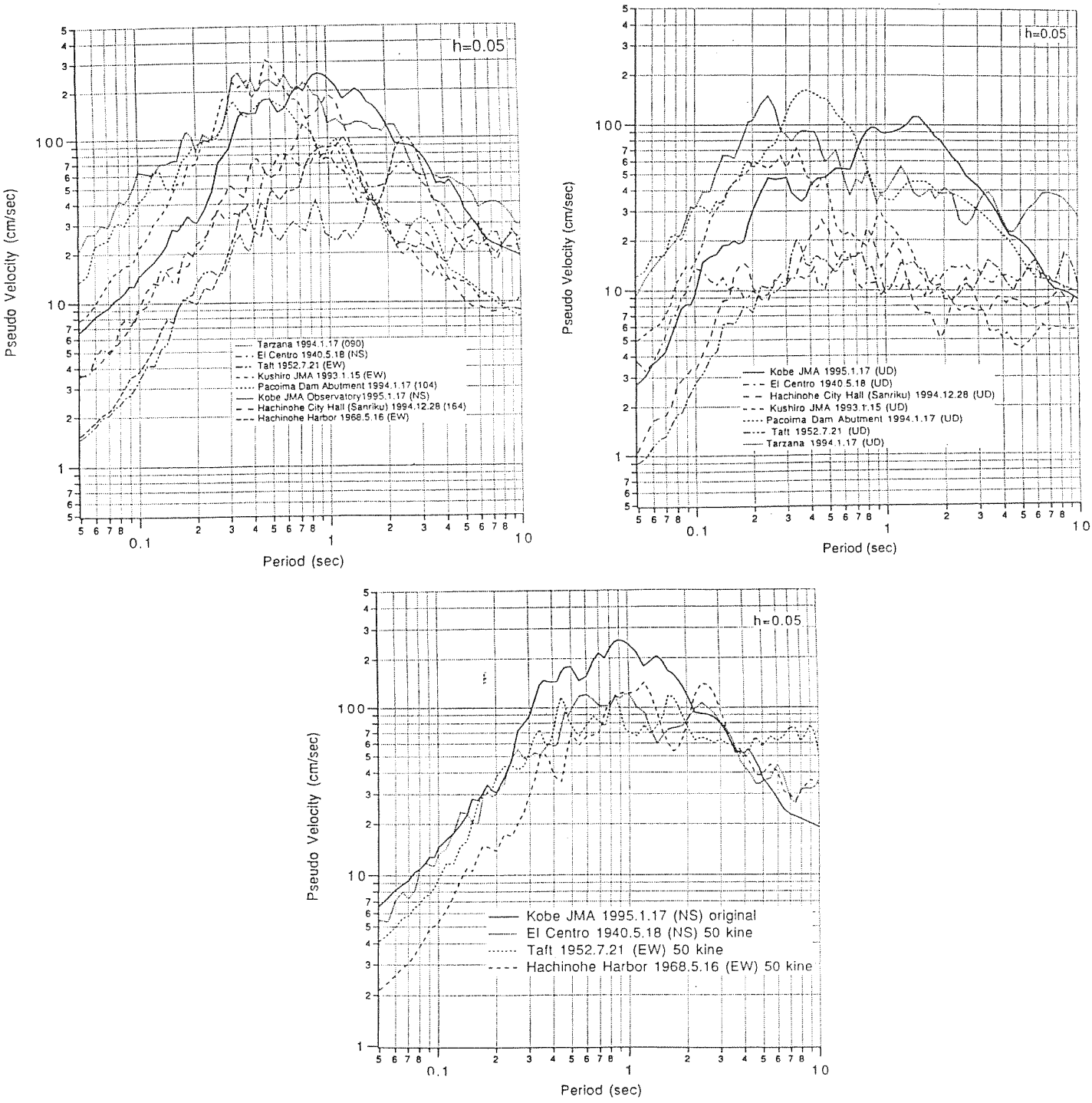


Figure 2-7 Pseudo Velocity Response Spectra for Recent Devastating Earthquakes for (a) the Horizontal Components, (b) the UD Component and (c) for Design Spectra for Tall Buildings
(from Building Research Institute, Courtesy M. Watabe)

exceptionally important data set for inferring the *in-situ* response characteristics of soils at ground-motion levels sufficient to induce failure. Some preliminary observations follow.

The simplified geologic log and velocity profiles for the Port Island site are shown in Figure 2-8. The corresponding ground-motion recordings obtained on the vertical array are shown in Figure 2-9. The site is underlain by about 13 m of fill, which in turn is underlain by at least two thick layers of clay and several layers of interbedded sands and clays. Depth of bedrock at the site is thought to exceed 100 m.

Peak acceleration, velocity and displacement values inferred at the various depths (Figures 2-9a, 2-9b, and 2-9c) reveal several effects of the soil deposits on resultant ground motions. Horizontal motions at the surface above the liquefied layer show a marked reduction in high-frequencies, but a significant amplification of low frequency motion. The peak horizontal accelerations increase slightly as they propagate upward toward the bottom of the liquefied layer, but are reduced by factors of 1.7 and 1.9 in the north-south and east-west directions respectively, upon reaching the surface. Peak horizontal velocities atop the liquefied layer are comparable to those at the bottom of the layer, which are larger than those at depth by factors of 1.7 and 1.3. Peak displacement values inferred at the surface are about 1.5 and 1.9 times larger than corresponding values measured at a depth of 79 m.

Each measure of vertical motion (acceleration, velocity and displacement) is larger at the surface than at depth. The vertical motions probably are predominantly dilatational energy. The various measures of vertical motion are amplified by the liquefied layer by factors of 1.0 for acceleration, 1.9 for velocity, and 1.6 for displacement.

The shear-wave velocity profile shows that the velocity of the near-surface fill, clay, and interbedded sands and clays within the first 30 m of the surface range between 170, 210 and 245 m/s, resulting in an average shear velocity to a 30 m depth of 196 m/s. These velocities clearly illustrate that the upper shear-wave velocity limit of 183 m/s as it has currently evolved for consideration in the proposed NEHRP and UBC site definitions should be reinstated at a minimum of 200 m/s as initially proposed (Borcherdt, 1994a). Otherwise, soft-soil sites with interlayered sands and clays with a high failure potential, such as this site, will be inappropriately classified.

2.2.2 Attenuation

Peak horizontal accelerations as reported for the Hanshin-Awaji earthquake (Table 2-II) are plotted versus the closest distance to seismogenic rupture approximated to be at a depth of about 4 km beneath Kobe City (Figure 2-10). Peak horizontal accelerations from the Northridge earthquake with a minimum depth to seismogenic rupture of 6 km are superimposed. Also superimposed are attenuation curves developed by Boore et al. (1994) and Campbell and Borzognia (1994).

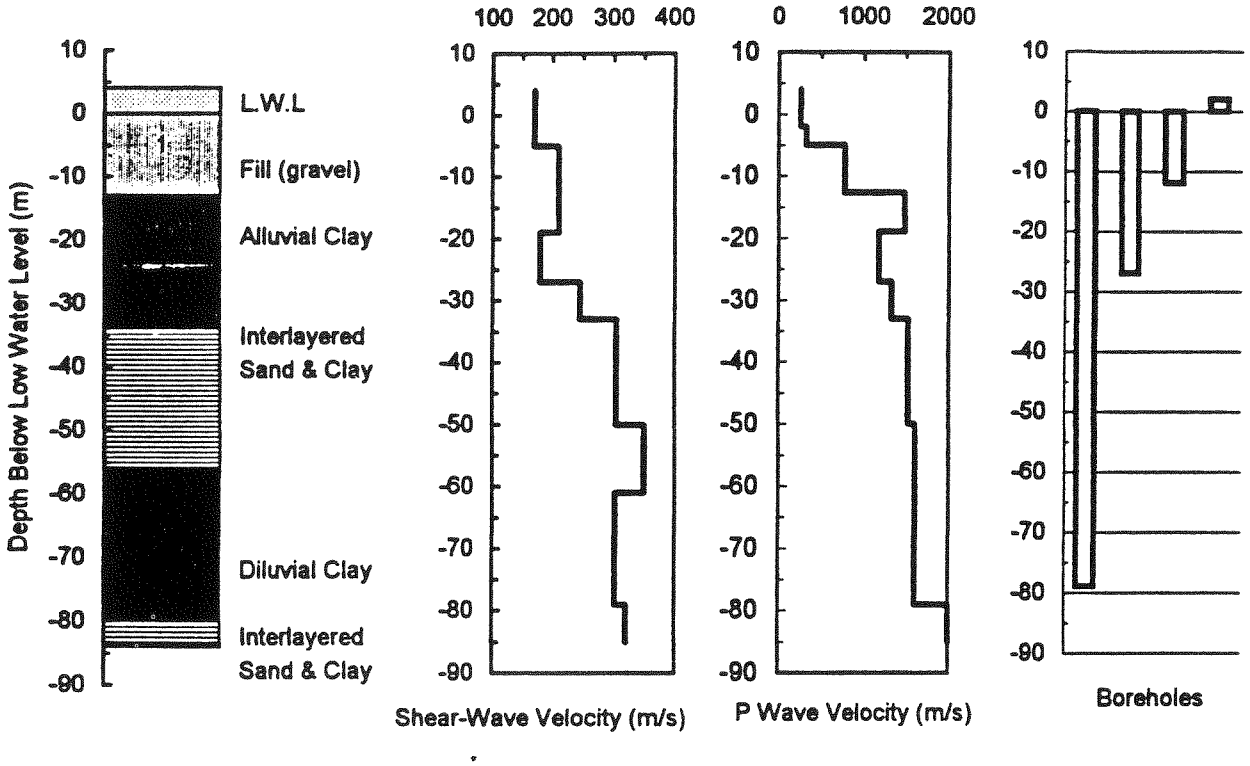


Figure 2-8 Geologic and Seismic Logs for the Port Island Vertical Array Site
(Modified from Logs Provided by The Committee on Earthquake Observation and Research in the Kansai Area, CEORKA, Courtesy Y. Iwasaki)

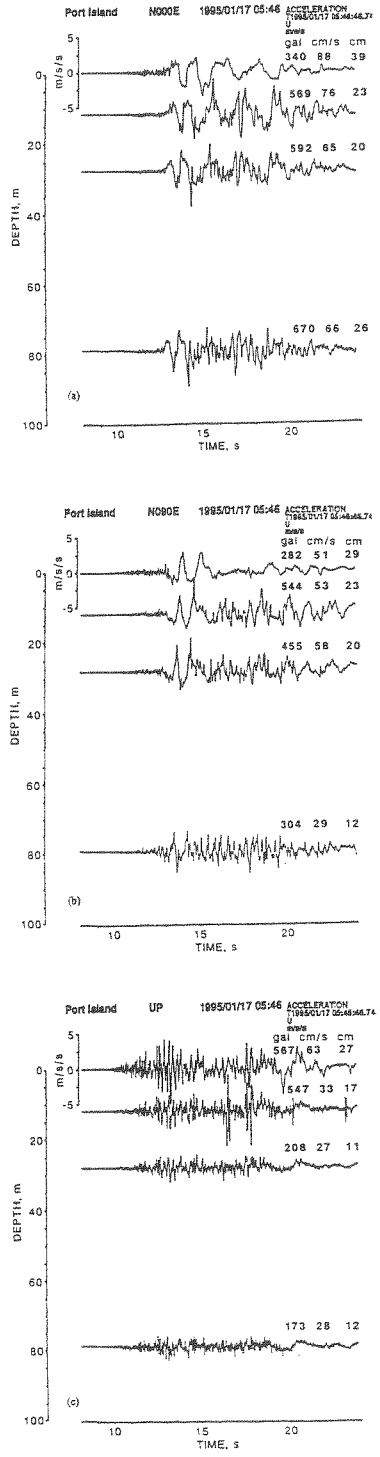


Figure 2-9 Strong Motion Recordings Obtained on the Port Island Vertical Array at the Surface and at Approximate Depths of 12, 27, and 79 m for the (a) NS, (b) EW and (c) UD Components
(from The Committee on Earthquake Observation and Research in the Kansai Area, CEORKA, Courtesy Y. Iwasaki)

The peak values for the Hanshin-Awaji earthquake tend to be less than those for the Northridge earthquake for sites within 4 to 20 km of the seismogenic source, but greater at distances exceeding about 30 km. These differences in amplitude are roughly consistent with differences in source mechanism and types of geologic site conditions. The source mechanism for the Northridge earthquake is predominantly vertical movement on a thrust fault. Such source mechanisms typically generate higher peak accelerations near the source than comparable sized strike-slip mechanisms. The geologic conditions beneath a majority of the recording sites for the Hanshin-Awaji earthquake are soft-soil (Holocene) deposits with higher amplification capabilities for ground motions near one second period than the stiff Pleistocene deposits beneath many of the recording sites for the Northridge earthquake. Consequently, the high frequency motions near the source might be expected to be larger for the Northridge earthquake, but the longer period motions at some distance from the source might be expected to be larger for the Hanshin Awaji earthquake.

The peak acceleration values plotted as linear function of distance (Figure 2-11) emphasize the rapid decrease in peak acceleration values with distance. The recent attenuation curves derived by Boore, et al, 1994 when extrapolated to soft soils using an average shear-wave velocity of 200m/s fit the data quite well. Peak values observed at sites in a $\pm$ 22.5 degree window centered along strike with apex at the epicenter are superimposed on those observed in a $\pm$ 67.5 degree window centered at the epicenter perpendicular to strike. Similar trends in each data set suggests that a significant directivity effect is not apparent in these two samples of peak acceleration values. However, a similar comparison of peak velocity values reflecting the mid-period characteristics of the ground motion might be expected to yield a different result.

Site-specific amplification factors were computed for each site by normalizing the peak values by corresponding peak values observed at the nearest station on rock or firm alluvium at seismogenic-rupture distances (*SR-Dis*, Table 2-II) of about 4, 25, 50 and 75 km in 45 degree azimuthal windows centered along strike of the fault with apex at the epicenter. The amplification factors also are normalized by the reciprocal ratio of the seismogenic-rupture distances for each site. Sites for normalization were chosen from those for which coordinates had been provided by owner agencies. If chosen normalization sites were not on rock (*SC-Ib*, Borcherdt, 1994b), then corresponding average amplification factors were used to adjust resultant amplifications to rock.

The mean and standard deviation for amplification factors inferred for Holocene sites in the azimuthal window of 45 degrees centered along strike are 1.8 and 1.5, respectively. Corresponding values inferred for the azimuthal window of $\pm$67.5 degrees perpendicular to strike are 1.7 and 1.5. The Holocene sites are thought to be categorized as soft-soil sites as defined by Borcherdt, 1994, that is the sites are classified as *SC-IV* or as D sites as initially proposed for the NEHRP code revisions. The preliminary 1.8 value is slightly smaller than the 2.0 value for *SC-IV* sites as initially inferred from the Loma Prieta strong-motion for input ground motion levels near 0.1g (Borcherdt and Glassmoyer, 1992).

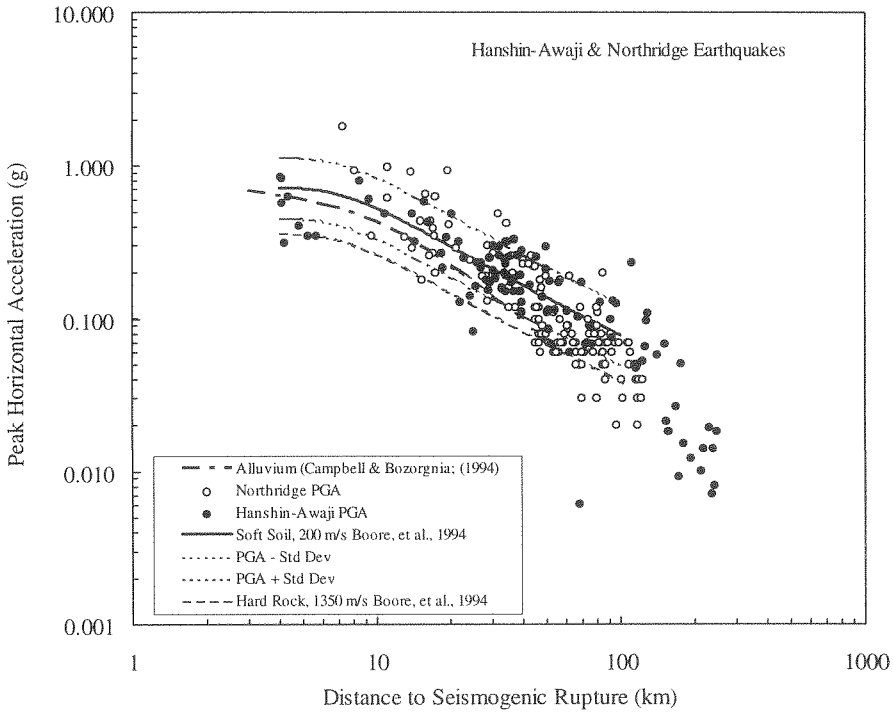


Figure 2-10 Preliminary Compilation of Peak Horizontal Acceleration as a Function of Closest Distance to Seismogenic Rupture for the Northridge and Hanshin-Awaji Earthquakes
(Attenuation Curves Courtesy of K. Campbell and D. Boore)

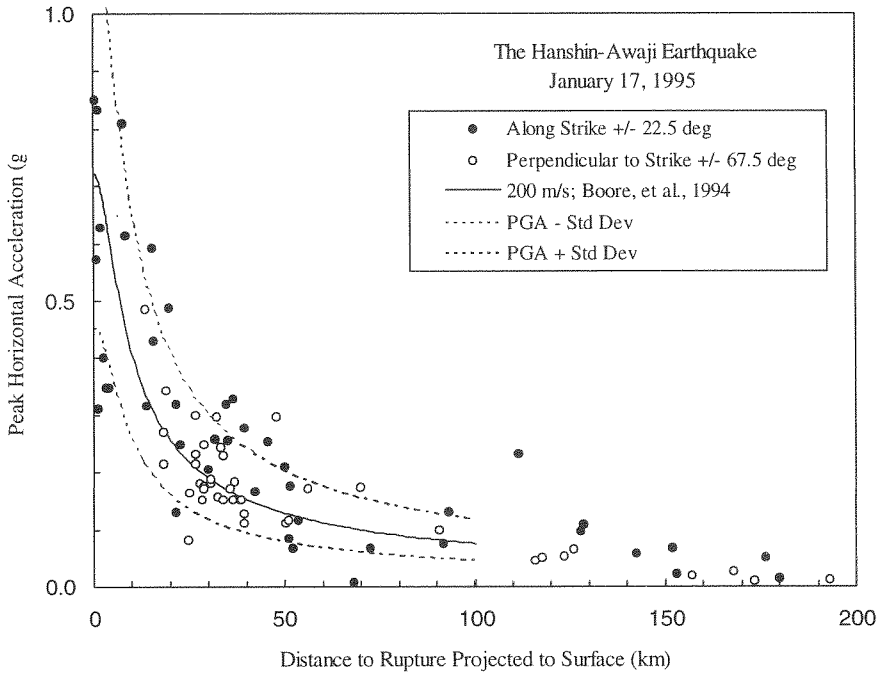


Figure 2-11 Preliminary Compilation of Peak Horizontal Acceleration Compiled Along Strike (± 22.5 Degree) and Perpendicular to Strike (± 67.5 Degrees)

Comparison of the peak vertical acceleration recorded at each of the sites with the peak horizontal (Figure 2-12) shows that on the average the peak vertical accelerations are about 62% or 2/3 of the corresponding horizontal values. Peak vertical accelerations that exceed the peak horizontal values are most evident for sites near or on Port Island (MC-PRI, MC-PIA). These larger vertical accelerations are consistent with larger amplification factors observed for vertical motion above the liquefied layer on the Port Island array.

2.2.3 Amplification Effects of Soft-Soil Deposits

The geologic classification of the sites shown in Table 2-II provides a basis for a preliminary evaluation of the effect of local site conditions on recorded peak accelerations. The geologic classification was inferred from superposition of the strong-motion station coordinates on the 1:1,000,000 scale geologic map of Japan. The resultant classification is dependent on both the accuracy of the station coordinates and the published map scale. Consequently, the geologic classification for sites inferred from map projections and associated results must be regarded as preliminary.

As a preliminary attempt to quantify the response characteristics of the Holocene deposits at high input ground motion levels near the source, amplification ratios were computed with respect to the Shin-Kobe site (JR-SNK) for which a peak acceleration of 0.57 g was recorded at a distance of about 0.8 km from the surface projection of the crustal rupture zone. The geologic map and site coordinates imply that the site is underlain by geologic unit QP3 (gravels, sands, and clays of Late Pleistocene age). The amplification ratios, normalized by the reciprocal ratio of the seismogenic-rupture distance, are plotted for sites along strike at distances less than 22 km (Figure 2-13). The mean and standard deviation for the amplification factors are 2.0 and 1.1, respectively. The linear trend fit to the data do not show a tendency to decrease with increasing peak acceleration level. Liquefaction induced ground failure is known to the author to have reduced the amplification at only the Port Island vertical array station. These preliminary observations suggest that the amplification factors for these Holocene sites do not decrease with increasing peak amplitude. Confirmation of this important result with futher analyses would suggest that amplification factors currently being suggested for the NEHRP and UBC code revisions should be modified so as to reduce the influence of nonlinearity on site factors at sites for which the potential for ground failure is low.

2.3 Summary

The strong ground motion measurements of the Hanshin-Awaji earthquake provide an important new near-source strong-motion data set. The data set provides an unprecedented set of measurements on soft soils at high input ground motion levels near the causative crustal rupture. Horizontal ground acceleration exceeded 500 gal at ten sites and 800 gal at two sites near the surface projection crustal rupture zone. Measurements at ten other sites within distances of 20 km were between 200 and 500 gal. About sixty percent of the measurements are located on "soft-soil" deposits of Holocene age. These deposits are comprised of interbedded sand, clay, and gravel layers, with a majority of the interval shear-wave velocities for the deposits between about 100 and 350 m/s (Iwasaki, et al., 1991).

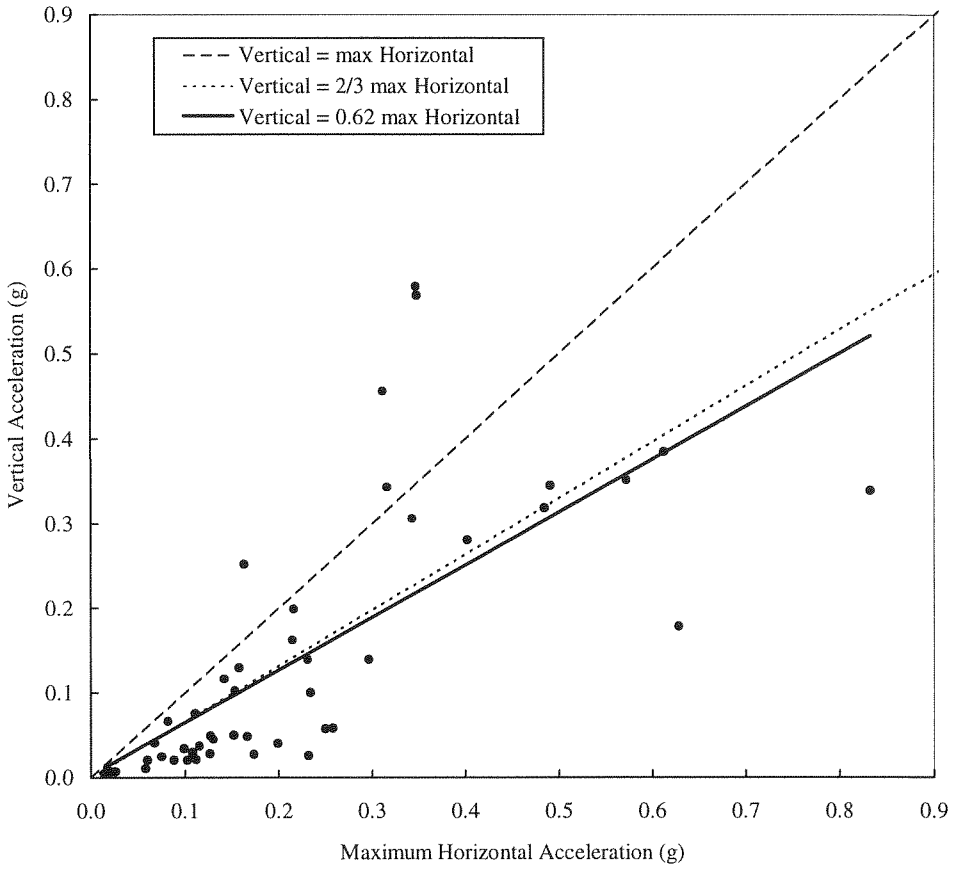


Figure 2-12 Preliminary Compilation of Peak Vertical and Peak Horizontal Acceleration

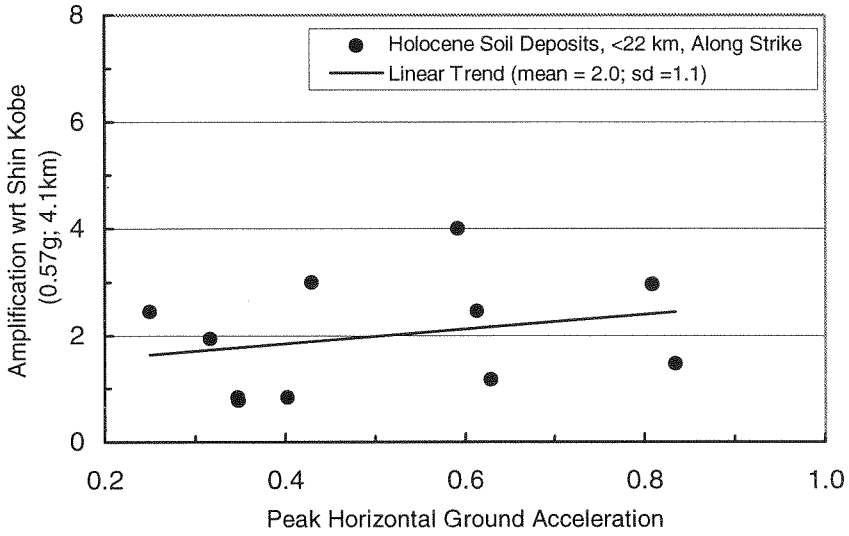


Figure 2-13 Amplification of Peak Horizontal Acceleration With Respect to Corresponding Value at Shin-Kobe Station (0.57g) as Normalized by the Reciprocal Ratio of Respective Distances to Seismogenic Rupture for Sites Within a +/- 22.5 degree Azimuthal Window of Fault Strike (51^0)

Acceleration contours for the higher levels of motion (>400 gal) show a linear southwest-northeast trend roughly parallel to and inclusive of the surface projection of the crustal rupture zone. Preliminary compilations of the peak acceleration data suggest that the peak levels decrease rapidly with increasing distance from the surface projection of the implied fault rupture. This rapid attenuation is apparent on plots of peak acceleration with distance compiled with linear scales and the generalized acceleration contours. This attenuation rate is anticipated well by recently derived empirical attenuation curves for peak acceleration extrapolated to sites with mean shear velocity of 200 m/s (Boore, et al., 1994). Input ground motion levels of 0.3 to 0.4g implied by the recording at KC-KBU are less than 0.5 to 0.6 g inferred for the Northridge, California earthquake of January 17, 1994 (Borcherdt, 1994). This difference is consistent with ground motion variations that might be expected for differences in source mechanisms for the two earthquakes, namely, strike-slip vs thrust.

Preliminary amplification factors derived for the Hanshin-Awaji earthquake are in general agreement with those derived from the Loma Prieta earthquake. This agreement suggests that site amplification and proximity to the crustal rupture zone contributed to the high levels of ground acceleration measured at sites near the source. The area of most intense motion as indicated by generalized acceleration contours for levels greater than 400 gal includes the zones of most intense damage mapped with JMA intensity level 7. This correspondence emphasizes the severity of the ground motion observed on soft soil near the surface projection of the fault rupture. These high levels of shaking confirm the significance of "near-source" factors currently being considered for U.S. building codes and the need to evaluate *in-situ* amplification factors at high input ground-motion levels.

2.4 Acknowledgments

Dr. Borcherdt is especially appreciative of the information and data provided by numerous agencies and colleagues on which this report is based. In particular, data and information provided by colleagues at The Public Works Research Institute, The National Research Institute for Earth Science and Disaster Prevention, Science and Technology Agency, The Disaster Prevention Research Institute, Kyoto University, the Earthquake Research Institute, University of Tokyo, Department of Civil Engineering, Gifu University, the Port and Harbor Research Institute, the Architectural Institute of Japan, The Committee on Earthquake Observation and Research in the Kansai area, Osaka Gas, Japan Railway, Japan Highways, Japan Meteorological Agency, Ministry of Construction, Building Research Institute, Geological Survey of Japan and others are appreciated. A special note of thanks is expressed to Y. Iwasaki, H. Kameda, K. Ohtani, M. Sugito, M. Watabe, and numerous other colleagues for information and personal contributions. The efforts of C. Wentworth in compiling the geologic map were essential for the preparation of Figure 2-4 and subsequent geologic classifications of the strong-motion stations. Manuscript reviews by W. Joyner and D. Boore are appreciated. Translations of Japanese text to English by Yoko Takauchi and Yoshiko Suzu were helpful.

2.5 References

Boore, D.M., Joyner, W.B., and Fumal, T., (1994), "Estimates of Response Spectra and Peak Accelerations from Western North American Earthquakes; An Interim Report, Part 2 (with insert)," U. S. Geological Survey Open File Report 94-127, 39 pp.

Borcherdt, R.D., (1994a), "Simplified Site Classes and Empirical Amplification Factors for Site-dependent Code Provisions," Proceedings NCEER, SEAOC, BSSC Workshop on Site Response During Earthquakes and Seismic Code Provisions, University of Southern California, Los Angeles, California, November 18-20, 1992.

Borcherdt, R.D., (1994b), "Estimates of Site-dependent Response Spectra for Design (Methodology and Justification)," Earthquake Spectra, Vol. 10, p. 617-653.

Borcherdt, R.D., (1995), "Seismology, Geology, and Geotechnical Issues," National Institute of Science and Technology, U. S. Geological Survey, Report in preparation.

Borcherdt, R. D. and Wentworth, C.W., (1995), "Preliminary Map of Peak Horizontal Ground Acceleration for the Hanshin-Awaji Earthquake of January 17, 1995, Japan, Part II of 2 - Description of Mapped Data Sets," U. S. Geological Survey Open File Report No. 259 B.

Borcherdt, R.D., and Glassmoyer, G., (1992), "On the Characteristics of Local Geology and Their Influence on Ground Motions Generated by the Loma Prieta Earthquake in the San Francisco Bay Region, California," Bulletin of the Seismological Society of America, Vol. 82, p. 603-641.

Campbell, K. W. and Borzognia, Y., (1994), "Near-source Attenuation of Peak Acceleration from Worldwide Accelerograms Recorded from 1957 to 1993," Proceedings of the Fifth U.S. National Conference on Earthquake Engineering, Chicago, Illinois.

Geological Survey of Japan, (1992), "Geological Map of Japan," CD-ROM Version, Third Edition, CD-ROM series of Earth Science Databases, CDGSJ92010, Map Scale 1:1,000,000.

Iwasaki, Y., Suwa, S., Yamamoto, K. and Hamada, T., (1991), "Regional Geo-data System for Seismic Zoning," Fourth International Conference on Seismic Zonation, Stanford, California, pp. 723-730.

Kikuchi, M., (1995), "The Mechanism of the Hyogo-ken Nanbu Earthquake of January 17, 1995," in YCU (Yokohama City University) Seismology Report No. 38.

Masaharu, T., (1995), personal communication.

"Maximum Accelerations Observed by JR," JR Earthquake Information No. 23a, Internet.

Nakamura,Y., (1995), "Waveform and its Analysis of the 1995 Hyogo-ken-Nanbu Earthquake," JR Earthquake Information No. 23c, 46 pp.

Nakamura,Y., Kazutoshi, H., Saita, J., and Sato, S., (1995), "Strong Accelerations and Damage of the 1995 Hyogo-ken Nanbu Earthquake," JR Earthquake Information No. 23b, 25 pp.

Ohtani, K., (1995), personal communication.

"Prompt Report on Strong-motion Accelerograms No. 46," (1995), The National Research Institute for Earth Science and Disaster Prevention, Science and Technology Agency, 42 pp.

Wentworth, C.W., Borcherdt, R. D., and Mark, R., (1995), "Preliminary Map of Peak Horizontal Ground Acceleration for the Hanshin-Awaji Earthquake of January 17,1995, Japan, Part I of 2," U. S. Geological Survey Open File Report No. 259 A.

SECTION 3
ELECTRIC POWER FACILITIES

3.1 Overview of the Kansai Electric Company

The Kansai Electric Power Company is one of nine major investor-owned electric utilities in Japan. It was established in 1951 as a result of a nationwide reorganization of the electric power industry. The service area of the company is located in the central part of the main island in the Japanese archipelago, and covers about 28,500 square kilometers, or about 8 percent of Japan's total land area. The area has a population of about 20 million people and the company supplies about 12 million customers (meter connections). The Kansai area ranks second after the Tokyo metropolitan area in economic importance to Japan. The company serves four major cities: Osaka with 2.5 million, Kyoto with 1.39 million, Kobe with 1.47 million and Nara with 0.35 million people (Kansai Electric Company, 1994). A summary of vital statistics is given in Table 3-I.

Table 3-I Summary of Vital Statistics of the Kansai Electric Company
(Kansai Electric Company, 1994)

Installed Generation	MW	35,035
Nuclear	MW	9,768
Fossil Fuel	MW	18,581
Hydro	MW	6,686
Energy Sales	Millions of KWH	123,300
Number of customers	Thousands	11,730
System Peak Demand	MW	28,411
Electric Operating Revenues	Millions of Yen	2,371,828
Assets	Millions of Yen	6,204,016
Number of Employees		26,205

While the Kansai District accounts for only eight percent of the land, it consumes 18 percent of the nation's power. The break down of power sales is given in Table 3-II.

3.1.1 System Description

In the earthquake impacted area, the transmission and sub-transmission voltages are 500 kV, 275 kV, 154 kV, and 77 kV. The 500 kV system lies primarily to the north, northeast, and east of the earthquake impacted area. These lines carry power from major nuclear generating stations on the Japan Sea, and large pumped storage facilities. There are eight fossil-fuel generating facilities on Osaka Bay east of the epicenter with a total capacity of 5912 MW. The 500 kV substations use gas-insulated circuit breakers and in some cases gas-insulated bus. Breaker-and-a-half bus configuration is used at most 500 kV substations. Most 500 kV substations in other parts of Japan use double bus-single breaker bus configurations. The lower voltage substations are configured as double bus-single breaker with a tie breaker between the busses. Figure 3-1 shows a simplified schematic diagram of the service area with major facilities and transmission lines. The

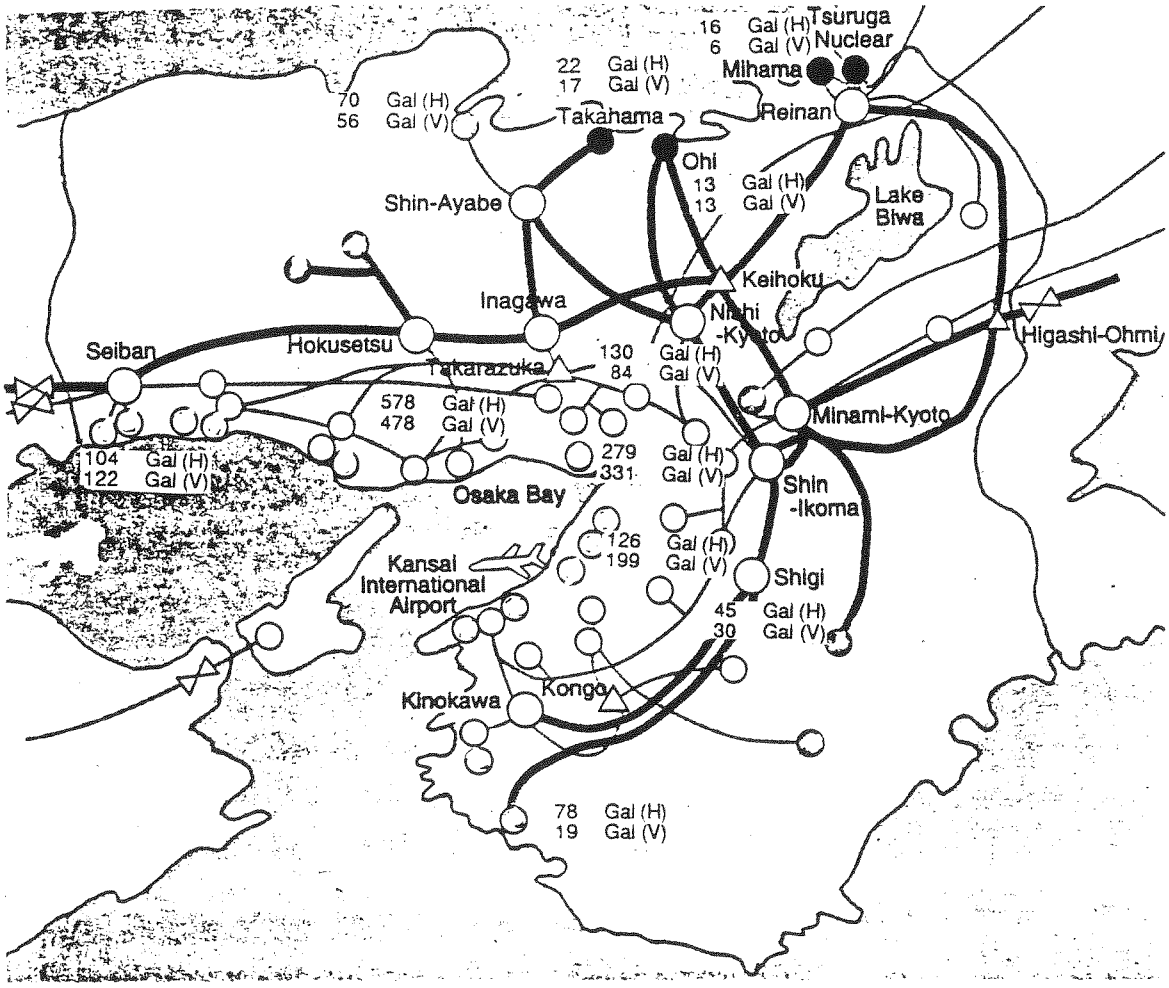


Figure 3-1 Schematic Diagram of Kansai Service Area and Peak Acceleration at Utility Instruments

primary distribution voltage is 6.6 kV, although there are some 22 kV and 33 kV distribution lines.

Table 3-II Breakdown of Kansai Power Electricity Sales (Kansai Electric Company, 1994)

Lighting (mostly residential)	28.4%
Light and Power (office buildings and hospitals)	19.7
Small Power (small- and medium-sized factories, shops)	13.6
Steel Industry	7.8
Chemical Industry	3.9
Machinery Manufacturing	5.9
Cement, Glass, and Ceramics	2.4
Textile Industry	1.0
Other Manufacturers	8.5
Transportation, Communications Electrical, Gas, Water, Construction, businesses, etc.	7.1
Others (water heaters, etc.)	1.7

Aerial lines and towers are used for most high voltage lines, although there are more than 275 kV cables in urban areas than is typical for 230 kV in California. Distribution is primarily aerial on concrete poles, with cables in steel conduit in central business areas like Kobe.

3.1.2 Differences in Equipment, Facilities, and Practices Between Kobe and the U.S.

There are notable differences between the facilities observed in the Kobe area and those found in California. It should be noted that these observations are based on visits to only three substations, two operating at 275 kV and one at 77 kV. No 500 kV facilities were visited.

The transmission towers tend to have heavier construction than in the U.S., probably due to large wind loading associated with typhoons, and the fact that they typically carry more circuits than in the U.S. (see Figure 3-2). The distribution system uses spun-concrete poles that were typically more heavily loaded than in U.S. (see Figure 3-3).

The three substations that were visited, all in urban areas in which residential and light industrial areas were adjacent to the substation, had acoustical enclosures around all transformers. High voltage transformers often had a separate, smaller line reactor nearby, but outside the acoustical enclosure. The units resemble power transformers with a 10 MVA rating. Under light load, these units are used to control system voltage. Transformers tended to be larger than in the U.S., with weights of about 800,000 pounds, not including radiators. All transformers were bolted to cast-in-place plates in foundation pads as compared to welding to embedments, which is common in the U.S. Different reports were given on transformer bushings. One description was that porcelain is grouted into pockets in flanges, and the other indicated that they are the same as those used in the U.S., that is, post-tension is used to hold the upper porcelain to the flange. Circuit breakers use post-tension connections of the porcelain to their flanges, as is common for transformers in the U.S. The radiators on some 77 kV transformers have substantial structural

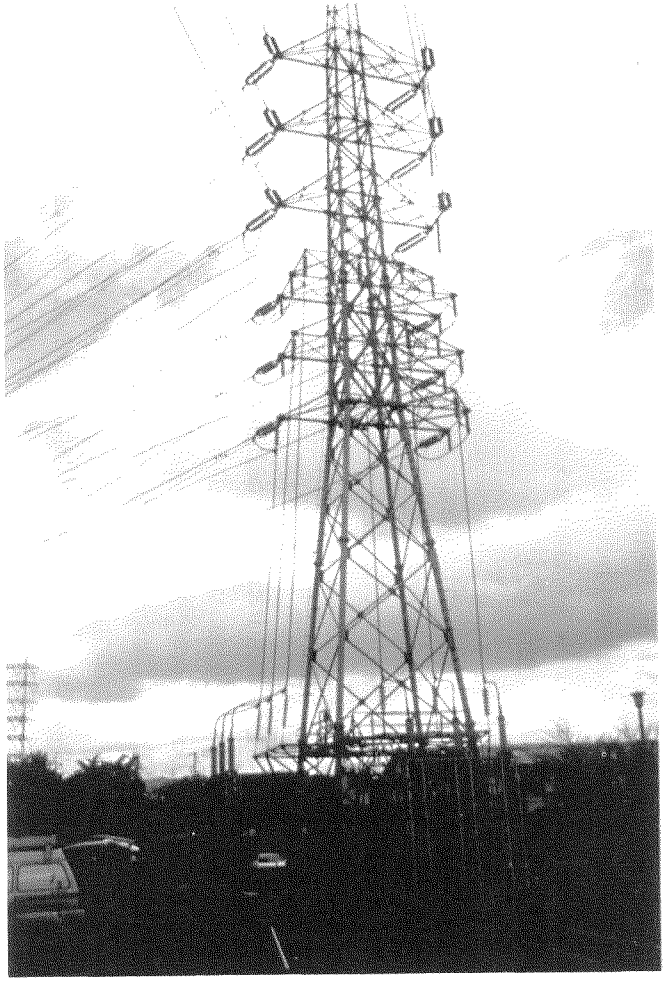


Figure 3-2 Transmission Tower Carrying Two 275 kV and Two 154 kV Circuits

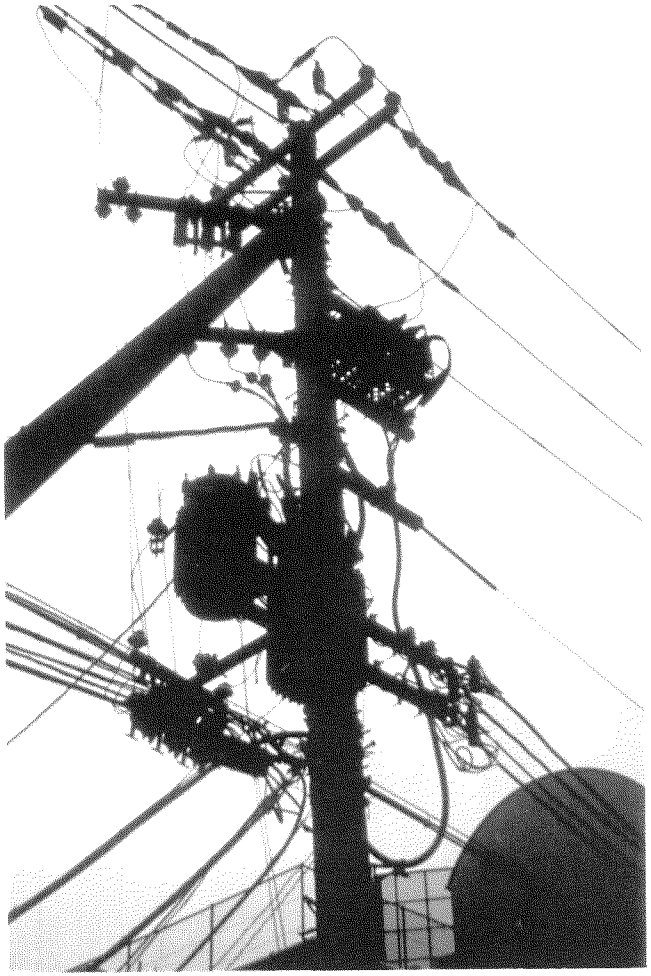


Figure 3-3 Spun-concrete Distribution Pole Used in Kobe

supports and piping connections to the transformer body included a flexible coupling (see Figure 3-4). The transformers at a distribution substation operating between 77 kV and 6.6 kV were designed differently than those observed in the U.S. in that they had a large metal box supported on a large porcelain insulator on top of the transformer (see Figure 3-5). Japan also uses a frail plate (busting plate) on top of transformers that can quickly release over pressures. In the U.S., pressure release valves are used. The valves are self-closing but have a more limited flow capacity and release pressure slower. On an earthquake investigation after the Off-Miyagi earthquake in 1978, thin (about 1-1/2 cm) rubber pads under the transformers were thought to contribute to extensive bushing damage. None of these pads were observed in this earthquake.

Much of the equipment, such as potential transformers (see Figure 3-6) and bulk-oil circuit breakers (see Figure 3-7), appeared to be much larger than one would expect based on 230 kV equipment found in the U.S. (see Figure 3-8). All capacitors are enclosed in large tanks and have transformers installed on the isolated rack (see Figure 3-9). A typical U.S. installation is shown in Figure 3-10. Flexible conductors were used to interconnect all equipment and in busses, however, liberal slack was not always provided. It was reported that Kansai Power uses flexible conductors, including their 500 kV switchyards, with the exception of some operating at 77 kV. Some equipment installations were designed to conform to seismic design practices that were instituted in 1980, although most substation equipment observed was installed prior to this date. The support structures for some of these newer installations were very massive and stiff (see Figure 3-11). Ground resistors were used, but they do not appear in this form in the U.S. Lightning arresters were frequently supported on short concrete pads just above the ground and surrounded by a railing to keep electrical clearances (see Figure 3-12). Wave traps which were suspended from overhead bus supports (see Figure 3-13) used a current-voltage transformer as a lower restraint rather than a separate insulator string that was attached to a structure or the ground as is done in the U.S. (see Figure 3-14). The two high voltage sites had large water tanks to store water for cleaning salt deposits off of porcelain after typhoons. There were also water spray nozzles distributed in the high voltage switchyard that are activated under certain wind conditions to add water to the atmosphere to reduce the salt concentration as there is a concern with flash-over. Many bushings are covered with a thin, green colored silicone rubber to improve surface properties of the porcelain. The transformers that provided station power were much larger than those found in the U.S., even at much larger substations. Their system uses a grounded neutral, as it is thought to reduce the chance of fire.

In general, Kansai Electric does not store any spare parts at substations. In the U.S., some spares, such as bushings, post insulators, and lightning arresters are distributed throughout the system at major transmission substations. As in Japan, small parts, hardware, and electronic parts used in control rooms, such as protective relays, are stored at service centers.

3.1.3 Seismic Design Criteria

During the visit to Kansai Power, a copy of the "Guide for Seismic Design of Substation Equipment," developed by the Japan Electric Association (1980) was provided (English translation) and represented as the current practice for the seismic design of high voltage



Figure 3-4 Distribution Transformers (77 kV to 6.6 kV) have Radiators with Structural Supports Independent of the Piping System and Flexible Couplings in Connections

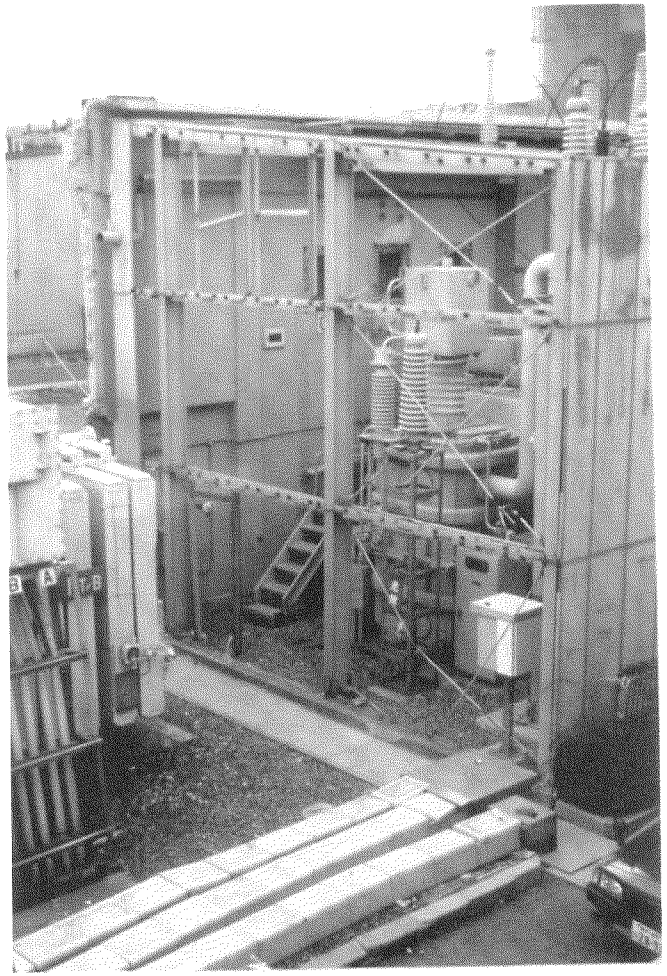


Figure 3-5 Box with Porcelain Support is a Design Feature on a Distribution Transformer Not Seen in the U.S.

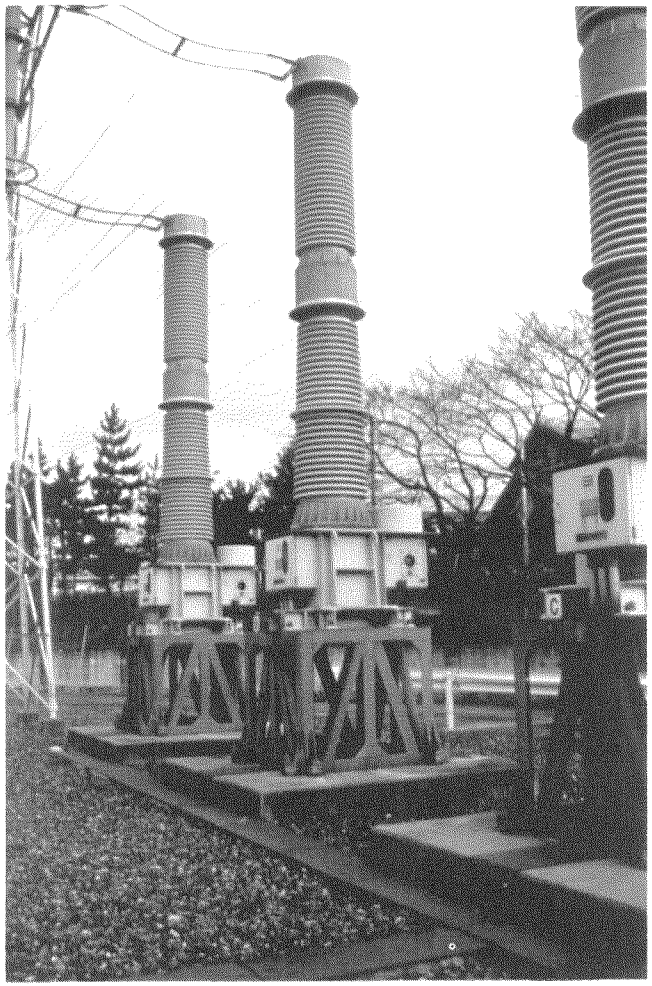


Figure 3-6 The 275 kV Potential Transformers are Much Larger than Their Counterpart in the U.S.

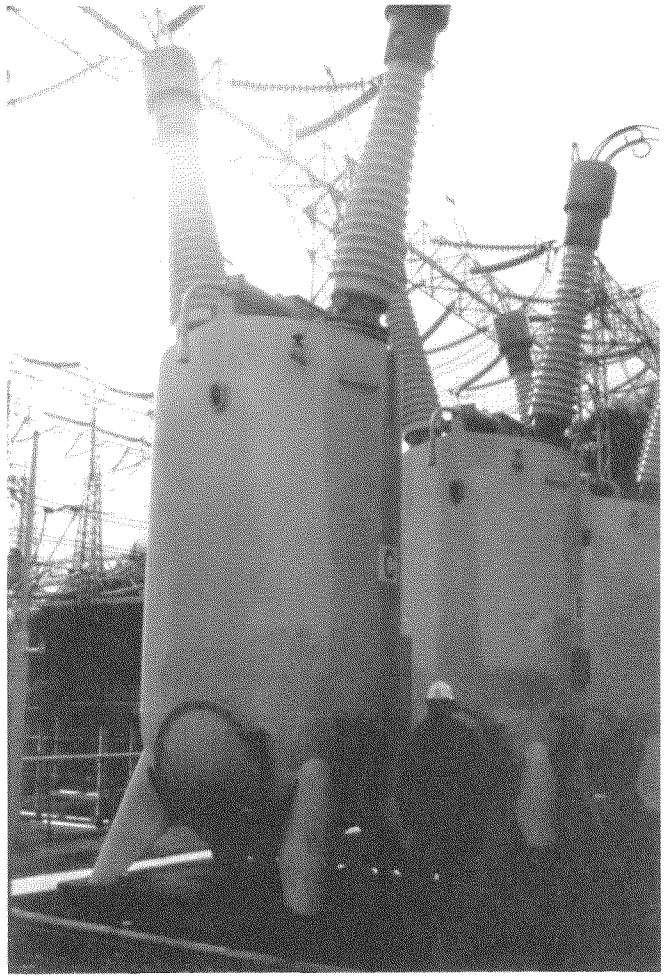


Figure 3-7 A 275 kV Bulk-oil Circuit Breaker which is Very Large Compared to 230 kV Units in the U.S.

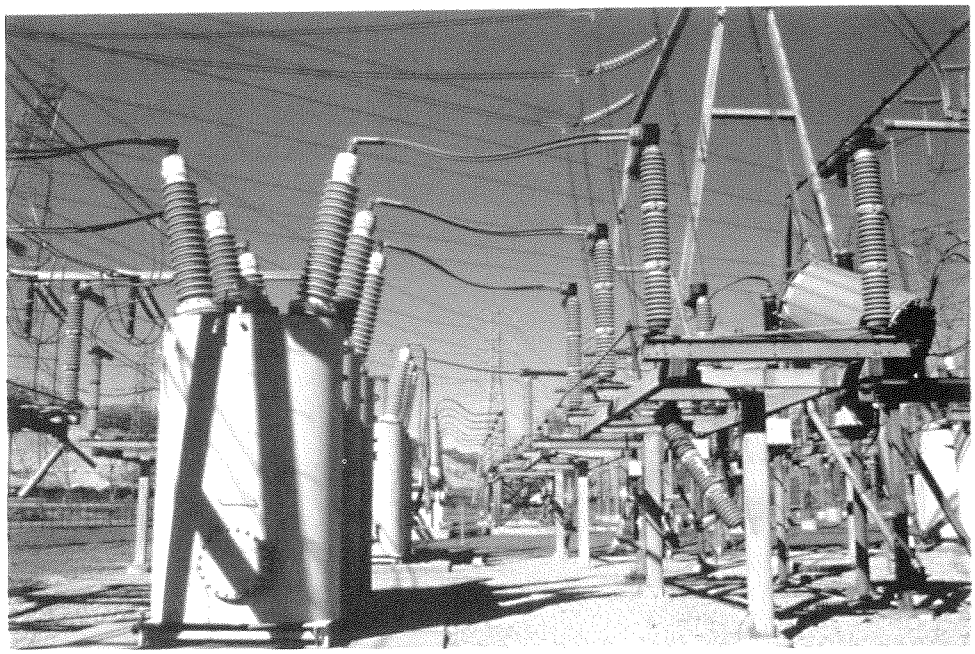


Figure 3-8 Typical 230 kV Bulk-oil Circuit Breaker in the U.S.

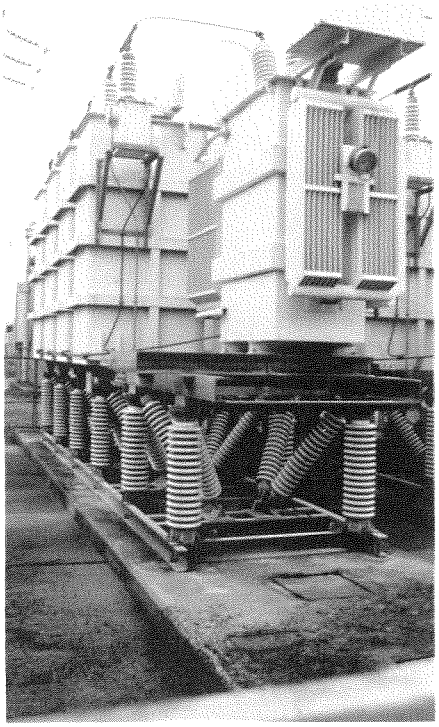


Figure 3-9 Capacitors Observed in Japan are in Large Tanks and have Small Transformers on Isolated Rack, a Different Configuration than in the U.S.

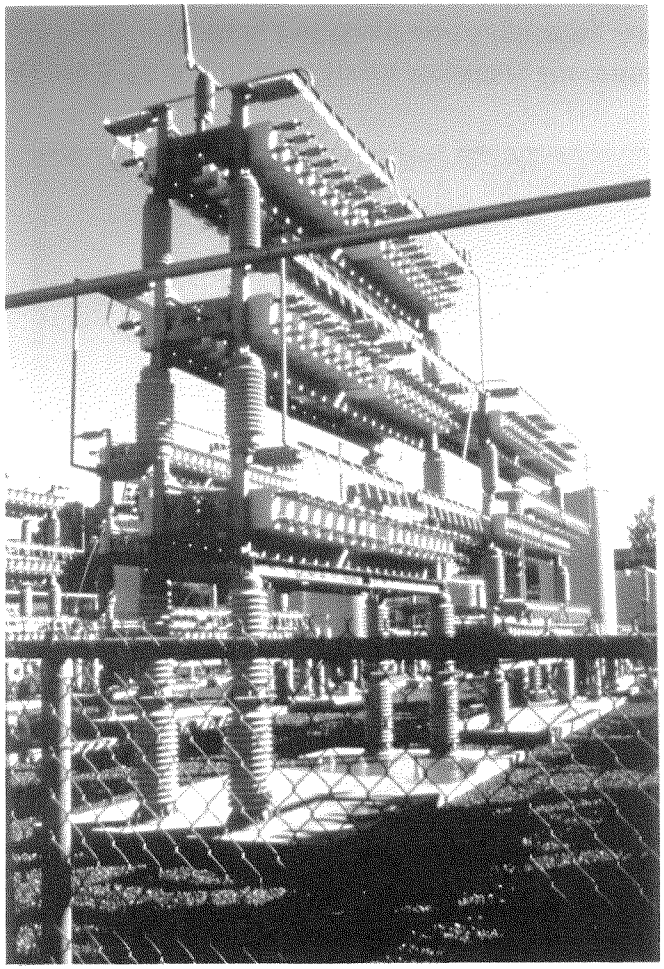


Figure 3-10 Typical Capacitor Rack in the U.S.

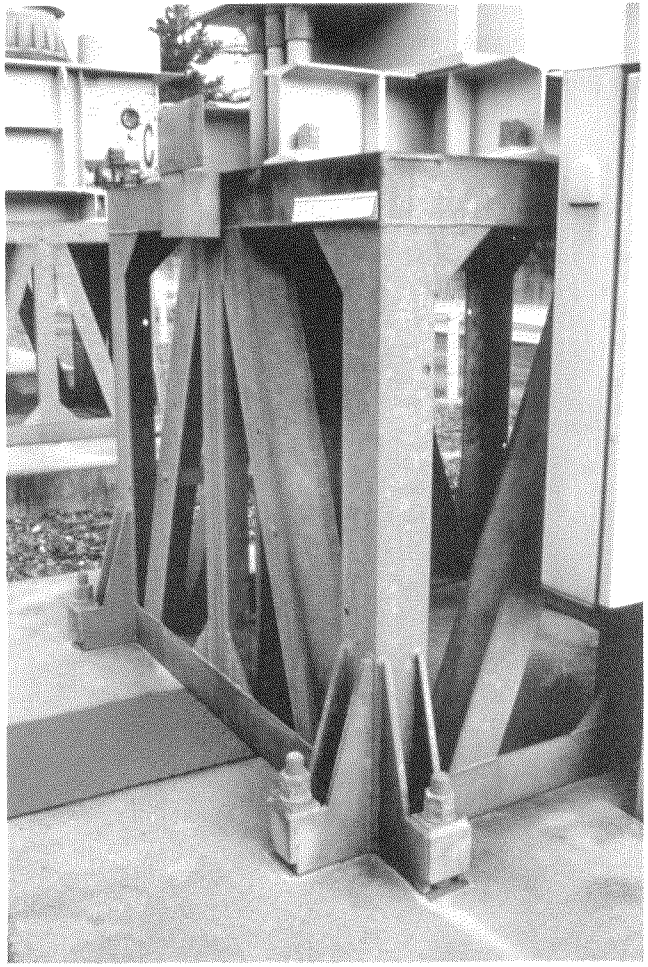


Figure 3-11 Very Stiff Support Structure for a Potential Transformer Installed After the More Stringent Seismic Design Practices were Adopted in 1980

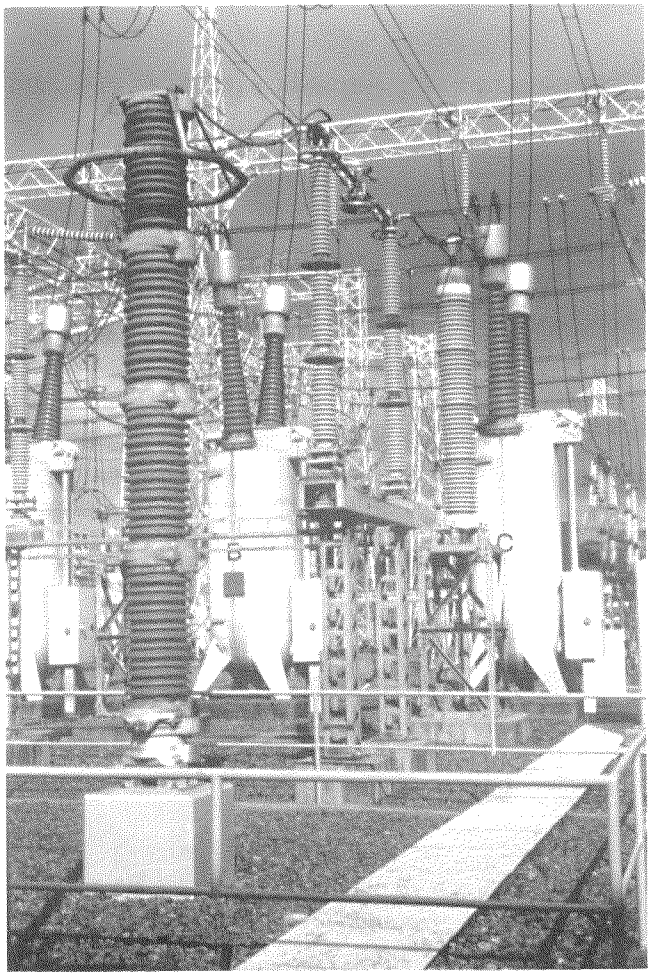


Figure 3-12 A 275 kV Circuit Breaker, Disconnect Switch, Pot Head and Lightning Arrester. Lightning Arrester Installed on Short Pedestal Reduces Cost and Amplification of a Taller Support Structure.

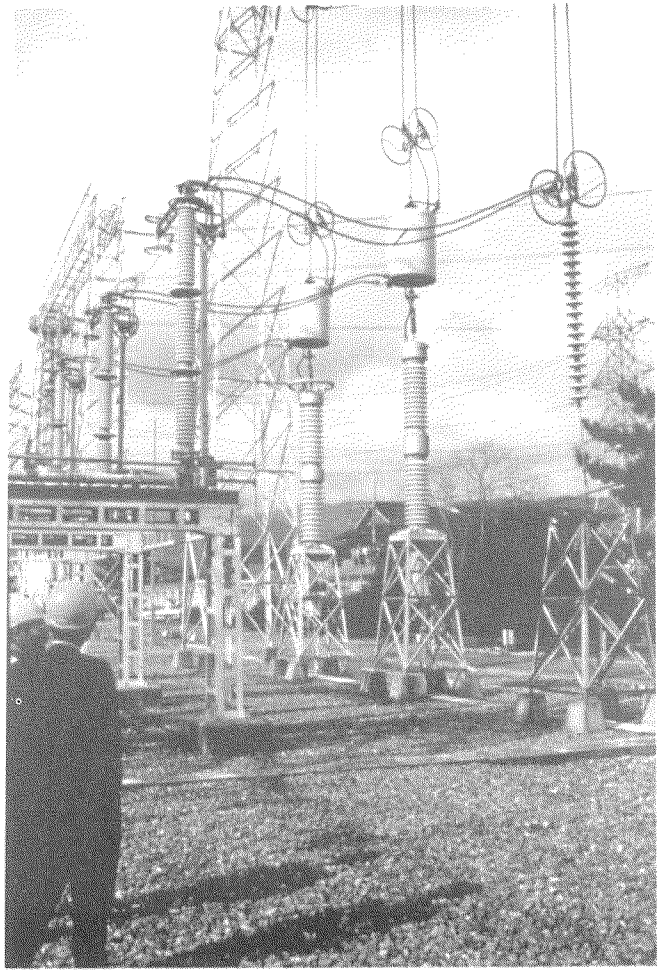


Figure 3-13 Current-Voltage Transformer is Used as the Lower Restraint for a Suspended Wave Trap

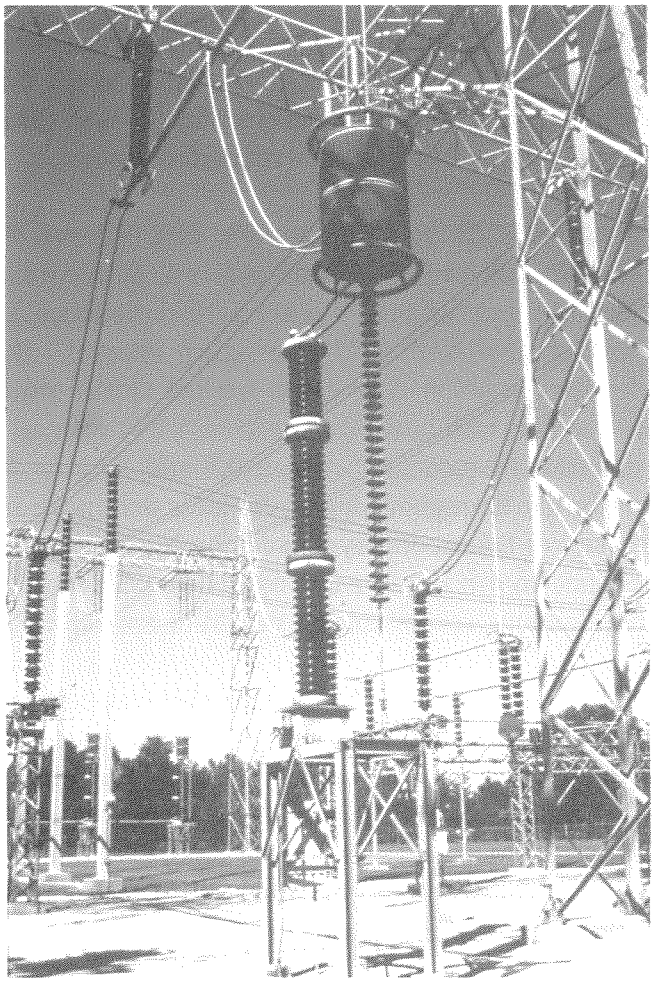


Figure 3-14 In the U.S., Suspended Wave Traps Usually have Independent Lower Restraints

substations. It was developed after the Off-Miyagi (Sendai) earthquake of 1978 and represents a consensus document of a committee representing the Ministry of International Trade and Industry (MITI), the Society of Electrical Cooperative Research, the Central Research Institute of Electric Power Industry (CRIEPI) (the Japanese counterpart to the Electric Power Research Institute in the U.S.), electric power companies and the equipment manufacturers. It was to serve as a "tentative substitute of Japanese standard..." Only the key points of this 42 page document are discussed here. The guide was to provide a design procedure to avoid serious problems in the supply of power resulting from earthquakes. It was limited to main circuit apparatuses and auxiliary equipment rated above 170 kV. Its criteria were to be used for new construction and when equipment had major renovation. There was no retrofit requirement.

The document, through a review of existing strong motion data in Japan (549 records including those from the Off-Miyagi earthquake of 1978) and a few U.S. records and past earthquake performance, sets forth a basic seismic design. Figure 3-15 reproduces a map of the expected distribution of horizontal accelerations with a 75 year return interval. Based on this plot, the maximum horizontal acceleration is set at 0.3g to be applied at the ground surface. Vertical accelerations, typically only used for wall bushings, are to be 1/2 horizontal values. Analysis and testing are to be done at resonant frequencies between 0.5 and 10 Hz. The provisions of the guide were to be applied uniformly throughout Japan, for sites that met a minimum requirement for soil properties. (The velocity of the secondary wave is higher than 150 m/s or the N value of the soil is higher than 5. It is not known if this test is consistent with those used in the U.S.) For sites that do not meet this requirement, special design should be applied to the equipment.

Additional requirements are to be applied to outdoor porcelain type apparatus and outdoor type transformers. For porcelain type apparatus, equipment shall be designed to withstand a quasi-resonant three cycle sinusoidal wave at its lowest support. For outdoor transformers, the tentative provisions call for bushings to be designed to withstand a quasi-resonant horizontal acceleration of a 0.5g three cycle sinusoidal wave to be applied to the bottom of the bushing turret. The main body of the transformer is to be designed for a 0.5 g static acceleration. A provision is made that a user of the equipment can stipulate a 2 cycle sinusoidal, 0.3 g test or actual earthquake waves may be used. Provisions for indoor equipment are covered in the document, but will not be discussed here.

The design practice used prior to the issuing of the document was to be applied to most other equipment, based on its good earthquake performance. It is noted that the use of aluminum pipe busbars are under investigation and are to be covered in a supplemental report.

3.2 Description of Damage to Kansai Electric Company

3.2.1 Seismic Environment at Power Facilities

Figure 3-1 shows a rendering of a map provided by Kansai Electric showing the peak horizontal and vertical accelerations at 11 strong motion instruments located at power facilities. Instruments on the Japan Sea coast are located at a gas turbine and three nuclear generating

stations and had peak horizontal accelerations between 13 Gal and 70 Gal and peak vertical accelerations ranging between 6 Gal and 56 Gal. The accelerations of 547 Gal horizontal and 478 Gal vertical were recorded at the Shin-Kobe substation located about 24 km east-northeast of the epicenter. The Amagasaki-Higashi and the Nanko generating stations had 279 Gal, 126 Gal horizontal and 331 Gal, 199 Gal vertical, respectively. The three sites with the largest accelerations had high vertical acceleration relative to their horizontal accelerations. It is noted that the record obtained at the Shin-Kobe substation and many other records recorded in this earthquake significantly exceed the 1980 design guide criteria. Table 3-III provides information about the characteristics of strong-motion instruments at Kansai Power facilities. It is interesting to note that these are digital instruments with 16 bit resolution, sample rates between 100 to 1,000 samples per second, a bandwidth from 1 Hz to between 30 Hz and 60 Hz, and full scale ranging from 300 Gal to 2,000 Gal. It is interesting to note that these bandwidths are comparable to instruments used in the U.S. It has been reported that most Japanese instruments have an upper cutoff frequency of about 10 Hz.

Table 3-III Specifications of Kansai Power Strong-Motion Instruments

Location	Year	Sensitivity Gal	Frequency Range, HZ	Number of Bits	Sample Rate	Components
Mihama PS	1976	0.1-600	0.1-30	16	100	3
Takasago PS	1983	0.2-2000	0.1-40	16	400	3
Ohi PS	1991	0.03-1000	0.1-30	16	100	3
Miyazu PS	1989	0.1-500	0.1-50	16	500	Vertical
Yamazaki	1986	0.1-1000	0.1-50	16	200	3
Nishikyoto SS	1987	0.1-1000	0.1-50	12	400	Vertical
Kobe SS	1988	0.1-1000	0.1-30	-	1000	3
Takasago PS	1987	0.3-300	0.1-30	12	400	3
Akaho PS	1987	0.1-1000	0.1-60	12	200	Vertical
Research Center	1988	0.3-300	0.1-30	12	400	3
Ahagasaki No 3	1987	0.1-1000	0.1-70	12	200	Vertical
Nanko PS	?	0.1-1000	0.1-20	16	100	Vertical
Yao SS	?	.0021-69kine				
Shigi SS	1987	1-320	0.3-30	12	400	3
Minami-Osaka SS	?	.0021-69kine	0.25-70	16	100	3
Kainanko SS	1981	0.03-300	0.1-30	12	400	3
Gobo PS	1984	0.1-1000	0.1-60	12	200	Vertical
Tuzaki SS	?	.0012-40kine	0.025-70	16	100	3

3.2.2 Restoration of Service

The overall performance of the power system, as measured by the restoration of power to substations and to areas that were not severely damaged, was very good. It should be noted that power could not be restored to some areas as this presented life-safety hazards until some

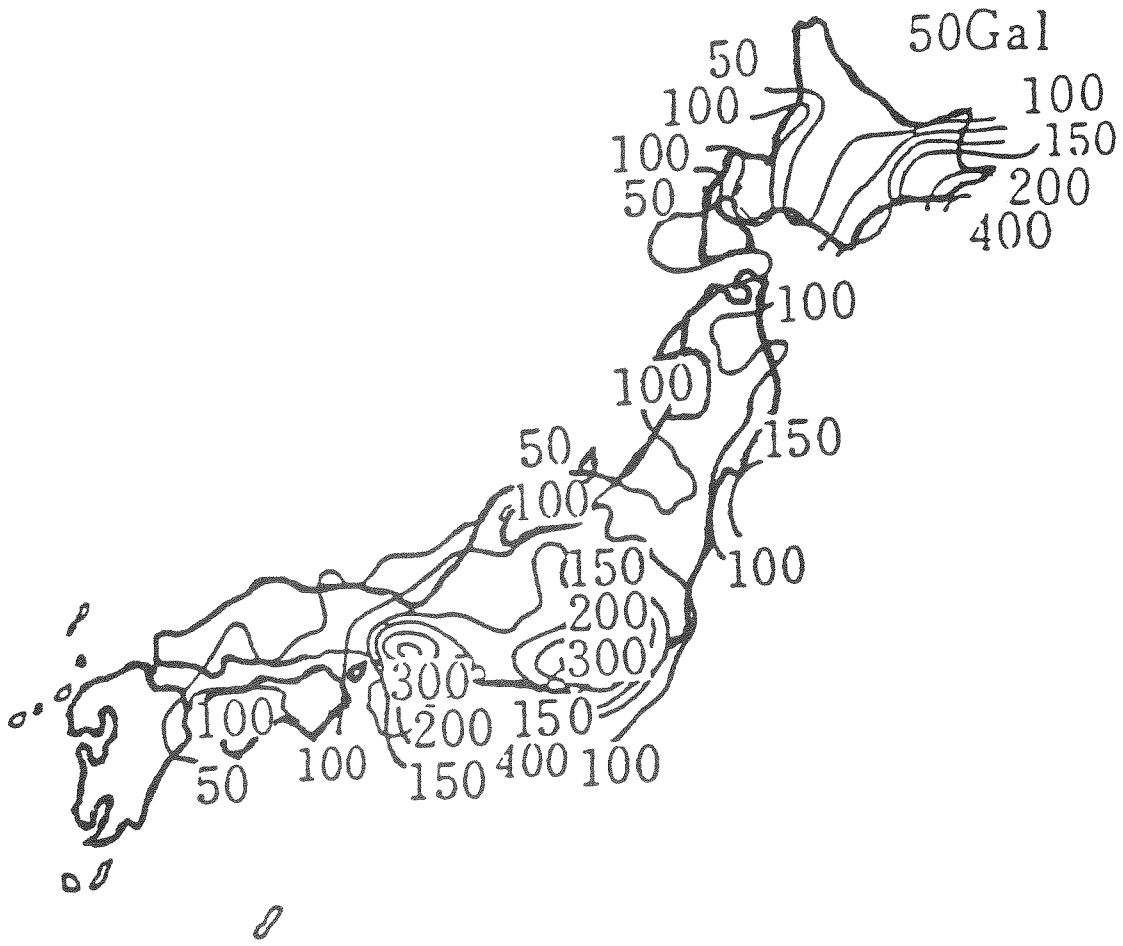


Figure 3-15 **Kawasumi Map Shows the Distribution of Horizontal Accelerations on the Ground Surface Expected at the Interval of 75 Years (Japan Electric Association Guide, 1980)**

damage could be cleared. Figure 3-16 shows the number of customers (meters - not individuals) without service as a function of time. The initial estimate of one million customers is very rough. It is interesting to note that the slight increase in the number of customers without power during the 17th was due to loss of service associated with the spread of fire. The disruption after the 18th is primarily due to the slow process of restoring the massive damage to the distribution system. It should be noted that some of the restoration was of a temporary nature to get power to customers, and substantial rework will be required. Figure 3-16 also shows the recovery of load following the earthquake.

Extensive mutual aid was provided, primarily to restore the distribution system. Work crews totaling 295 individuals, 46 high voltage generating vehicles (6.6 kV) with a total capacity of 16 MW, 74 vehicles with materials to support the crews, water trucks, substation and transmission line hardware, and two earth station vehicles for communication were provided. Figure 3-17 shows the sources and types of mutual air provided by utilities within Japan. The mobile generating units were distributed to critical facilities, such as hospitals. Table 3-IV shows the number and work assignment distribution of restoration personnel. The average length of stay of mutual aid personnel was about 10 days.

Table 3-IV Distribution of Workers During Restoration

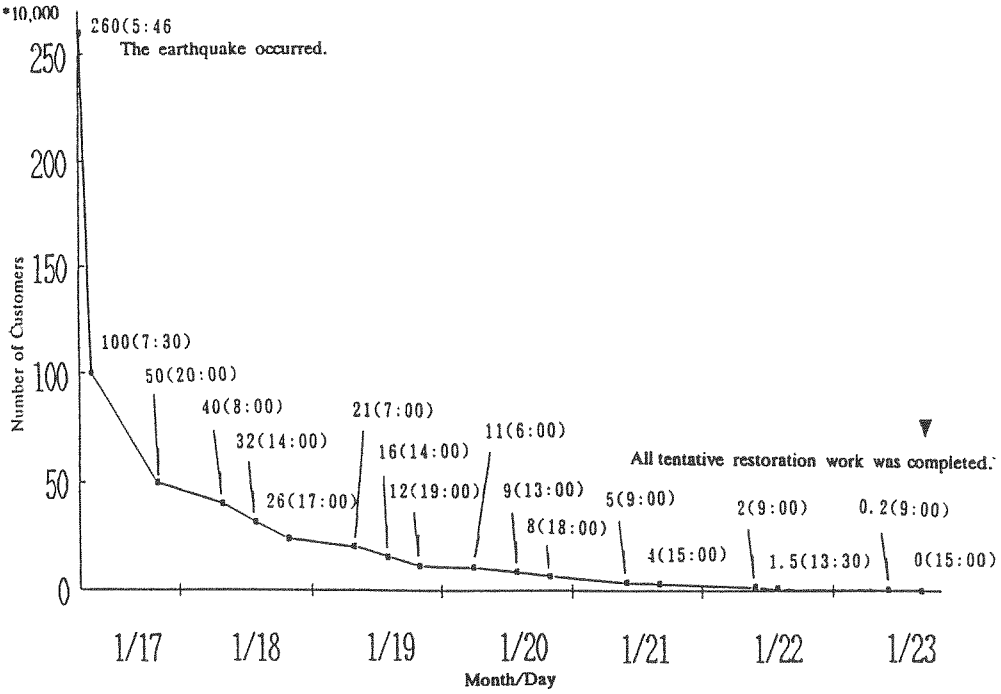
	Day	17	18	19	20	22	23	24
Distribution System	KEPCO	371	657	788	765	794	794	709
	Other Utilities	0	260	284	287	291	283	219
	Contractors	639	2,070	2,895	2,963	3,616	3,616	3,032
	Total	1,101	2,987	3,967	4,015	4,701	4,693	3,960
Power Transmission Communications	KEPCO	1,169	947	722	657	334	290	464
	Contractors	1,168	1,582	1,448	1,467	1,113	743	1,316
	Total	2,336	2,529	2,170	2,124	1,477	1,033	1,780
	Grand Total	3,346	5,516	6,137	6,139	6,148	5,726	5,740

It is interesting to note that some pictures contained in books published by newspapers show massive destruction to the power distribution system with a working traffic light (see Figure 3-18. To help control traffic, special power lines were set up for traffic signals. U.S. delegates who were attending a meeting in Osaka at the time of the earthquake observed special power distribution lines being strung to establish power outlets at residences. It is not known how wide-spread this practice was.

3.2.3 Overview of Damage to Kansai Electric Company

A summary of damage to power system facilities is given in Table 3-V. There were four 500 kV substations just outside of the damage area. Figure 3-19 is a composite of several figures provided by Kansai Electric Co. This figure shows transmission lines and substations that were damaged, substations that were blacked out as a result of damage, the times that power was restored to major substations, and the approximate time that power was restored to various service areas. There are five 275 kV substations that were de-energized as a result of damage at

Number of Customers Without Power



Load Losses Following the Earthquake

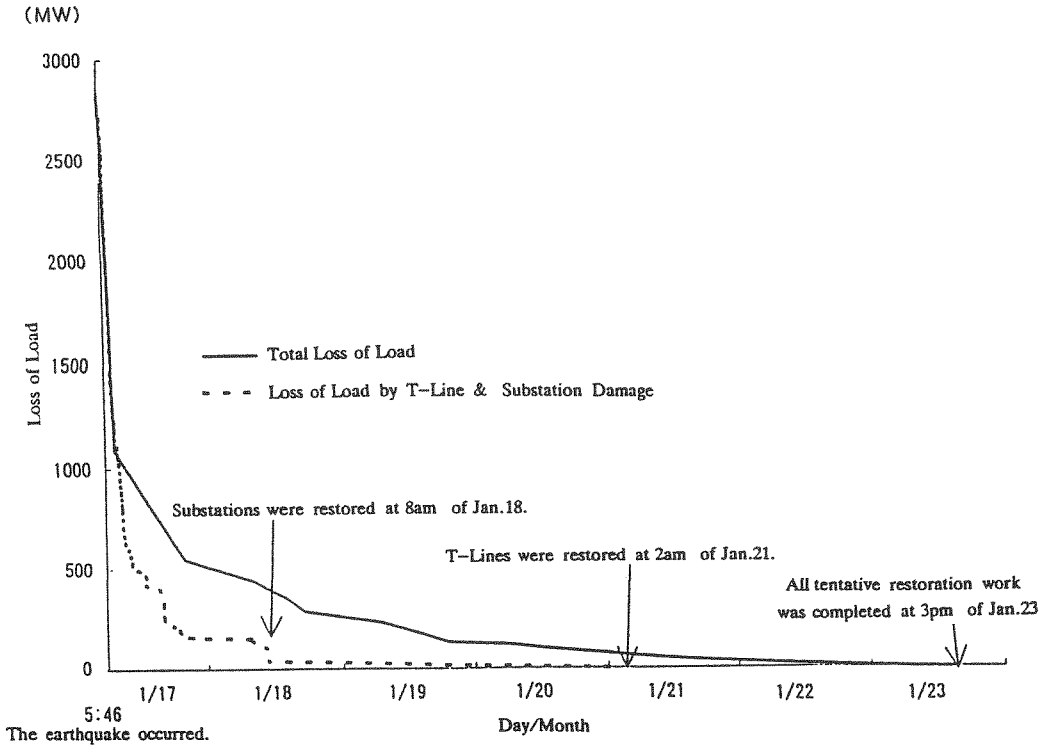


Figure 3-16 Number of Customers and Loss of Power vs. Time

Aid of Other Electric Utilities

TOTAL
Distribution
319 Workers, 52 High Voltage Power Generating Vehicles (17,890kVA)
77 Vehicles, Commodities of living, Water Wagons, etc.
Substation and T-Line
Disconnecting Switches, Hardware for Insulator Assembly, etc.
Communication
2 Earth Stations on Vehicles

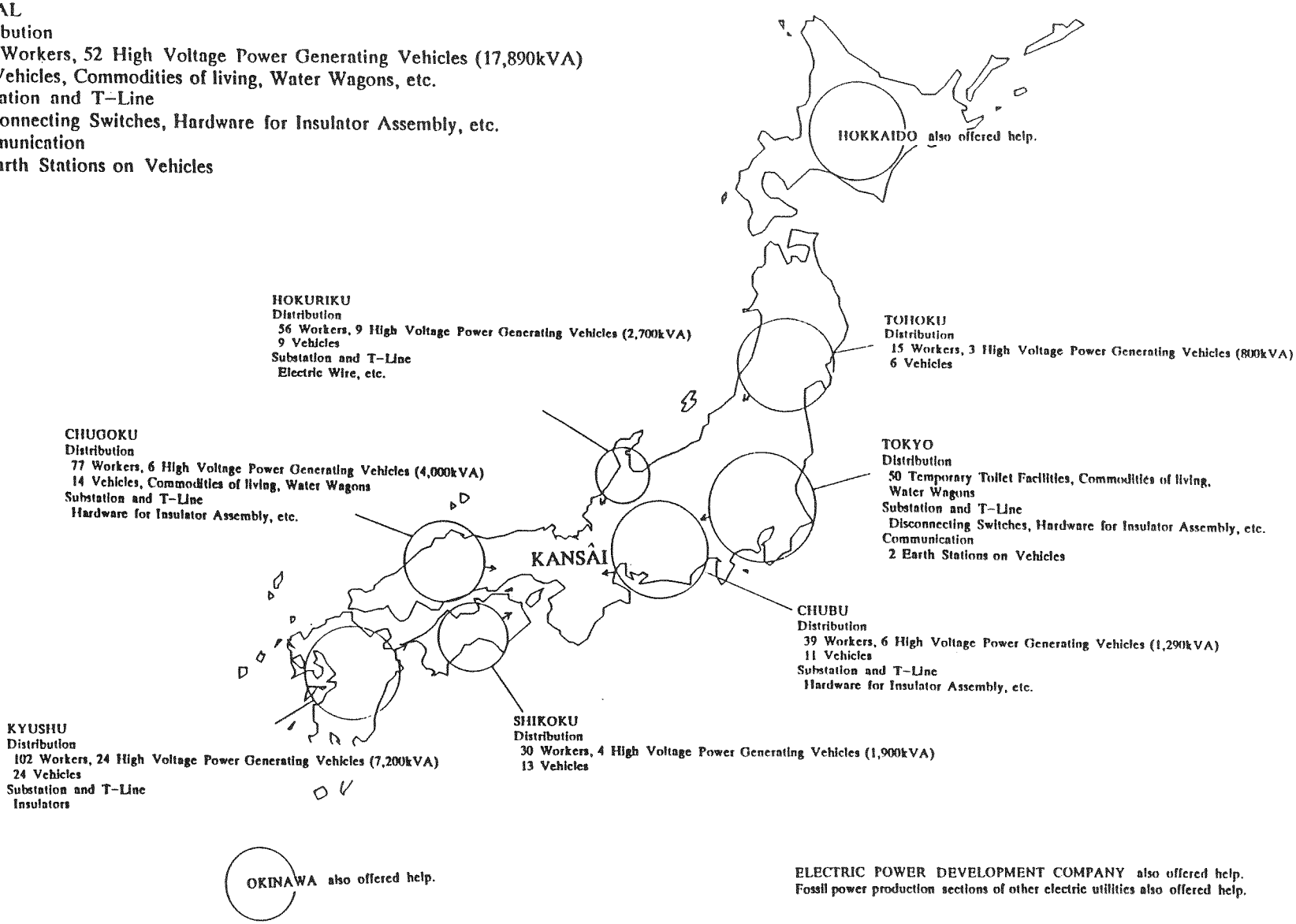


Figure 3-17 Sources and Types of Mutual Aid from Other Utilities



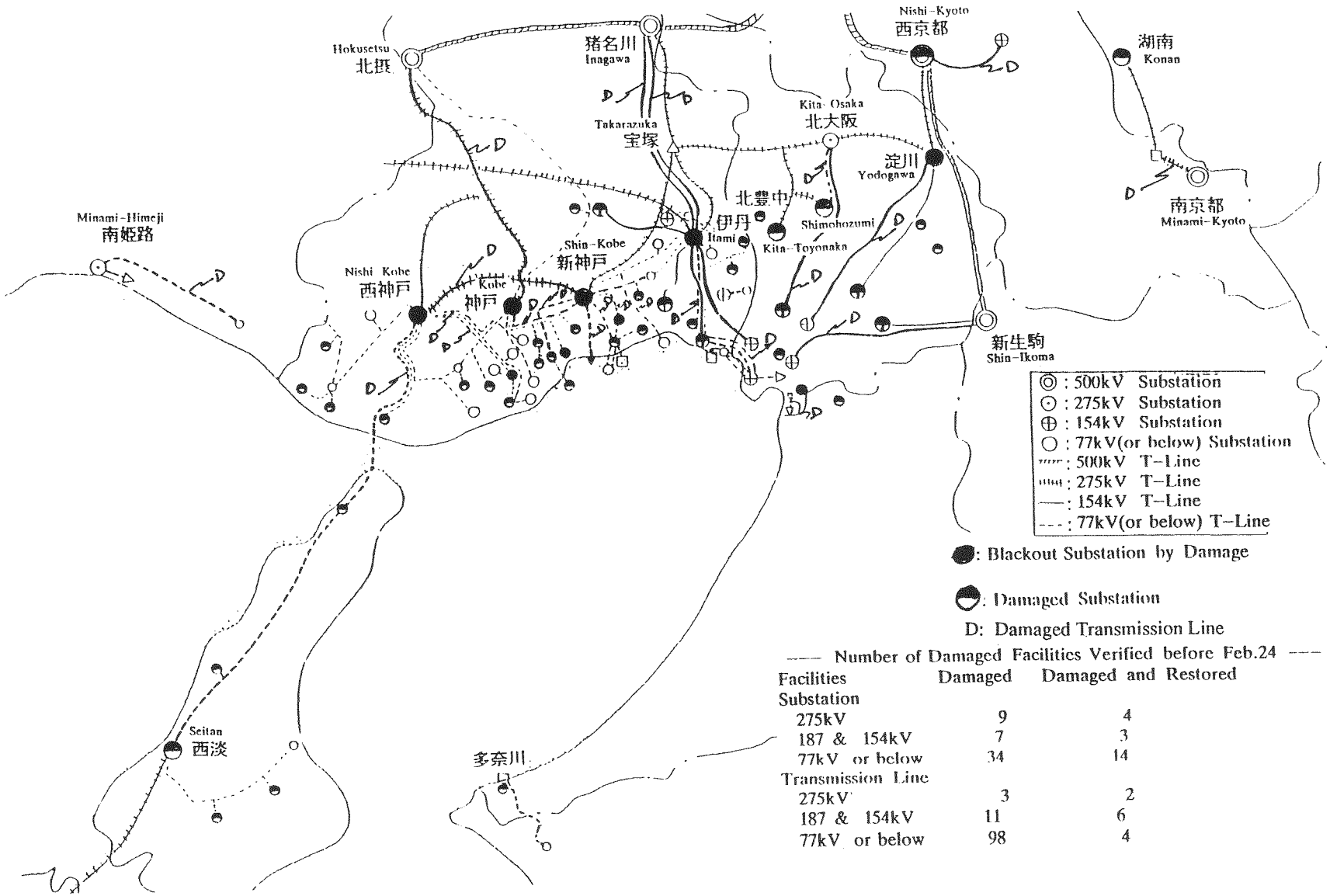
Figure 3-18 Damage to the Distribution System was Massive, but a Traffic Light in the Background is the Result of Special Restoration of the Traffic Control System

Table 3-V Summary of Damage to Power Facilities
(Kansai Electric Power Co., 1995)

	Damaged Main Facilities	Slightly Damaged Main Facilities and Damaged Other Facilities	Total
Fossil Power Stations	5	4	9
Boiler, Gas Turbine	8	12	20
Substations	17	30	47
Transformers	23	29	52
Circuit Breakers	9	1	10
Power Capacitors	4		4
Shunt Reactors	5		5
Disconnect Switches		41	41
Lightning Arresters		15	15
Busses		7 points	7
Buildings		12 points	12
Neutral Grounding Devices, etc.		32	32
Overhead Transmission Lines	11	12	**23
Wire	3 spans		3
Supporting Structures	11	9	20
Insulator Assemblies	3	36	39
Grounds, etc.		1	1
Underground Transmission Lines	3	92	**95
Cables	20	*384	404
Ducts		*183	183
Manholes		*257	257
Bridge Section of Line		*14	14
Support for Cable Termination		*4	4
Oil Feeding Equipment		*2	2
Distribution Lines (22 kV, 33 kV)	11		11
Overhead - Wire	1 span		1
Overhead - Insulator	1		1
Underground - Cable	11		11
Underground - Duct		8 spans	8
Underground Manholes		125	125
Distribution Lines (6.6 kV)	649		649
Overhead - Wire	*6,188 spans		6,188
Supporting Structures	*7,869		7,869
Transformers		*4,512	4,512
Underground - Cables	185	*1,317	1,322
Underground - Ducts		*247 spans	247
Underground - Manholes		*125	125
Communication Circuits		76	76
Cable		171 spans	171

* Verified before February 24, 1995

** 112 lines were damaged - 6 lines consist of overhead lines and underground lines.



—— Number of Damaged Facilities Verified before Feb.24 ——

Facilities	Damaged	Damaged and Restored
Substation		
275kV	9	4
187 & 154kV	7	3
77kV or below	34	14
Transmission Line		
275kV	3	2
187 & 154kV	11	6
77kV or below	98	4

Figure 3-19 Schematic Diagram Showing the Damage to Substations and Transmission Lines

the substation, four that were damaged but did not lose power because of the damage, and two substations and one switching station were undamaged. Six 154 kV substations were damaged but did not lose power because of the damage and six were undamaged. Of the forty 77 kV (and below) substations near the epicenter, four were de-energized as a result of damage, twenty-eight were damaged, but did not lose power as a result of the damage, and eight were undamaged. It is interesting that the island in Figure 3-19 did not lose power. The disruption in a large part of the west end of the disrupted area was due to damage to one of the 275 kV substations. It was reported (Electric Utility Week, 1995) that nearly all problems that caused disruption could be attributed to transformer bushings at five 275 kV substations, one at a 187 kV substation, and four at 77 kV substations.

As a result of the damage from this earthquake and the large amplitude of the recorded ground motions, the power industry is reviewing seismic design criteria. It is anticipated that this study will be competed in about two years.

The total cost of damage and some upgrading to the electrical system was reported by Kansai Electric as about $2.3 billion. About one billion was attributed to the distribution system and the remainder to transmission, generation and possibly the loss of the Kobe office building. In the review of damage to the distribution system, it was impossible to get a feeling of the losses, but as will be seen below, extensive damage was done in the Kobe business district to buried conduit and surface facilities that were damaged over a much broader area. Damaged generating facilities were not visited, but most were generally put back into service quickly. Three generating stations experienced soil subsidence and the Higashinada generating station (120 MW) was going to require substantial restoration time. A large office building in Kobe was taken as a total loss, although it did not collapse.

3.2.4 Itami Control Center and Substation

The Itami substation was reported to be the most severely damaged substation. The substation is located approximately 39 km east-northeast of the epicenter on what was wetlands adjacent to the Mukogawa river. The substation was originally built in 1941 and the 275 kV switchyard was added in 1960. The age of specific banks or bus positions is not known, but much of the equipment in the switchyard is over 20 years old. The control house is three years old and it was built on a specially prepared foundation, but piles were not used. The 275 kV switchyard has a double-bus single-breaker configuration with eleven positions. There are four 275 kV lines supplying the bus, six transformer banks (three 275 kV to 154 kV and three 275 kV to 77 kV), and one tie breaker. The 275 kV and 154 kV busses have bulk-oil circuit breakers. Figure 3-20 shows a modified schematic one-line diagram for the 275 kV and 154 kV switchyards that is approximately configured with the same physical layout at the site. Note that for a few items of equipment, individual phases are shown. The control house, two water tanks, transmission and microwave towers, and two large fissures in the ground are also shown.

The review of seismic response of the equipment at the facility will start where the high voltage lines enter the switchyard and work through to the lower voltage switchyards, the control house and its equipment, and then the transmission-line towers.

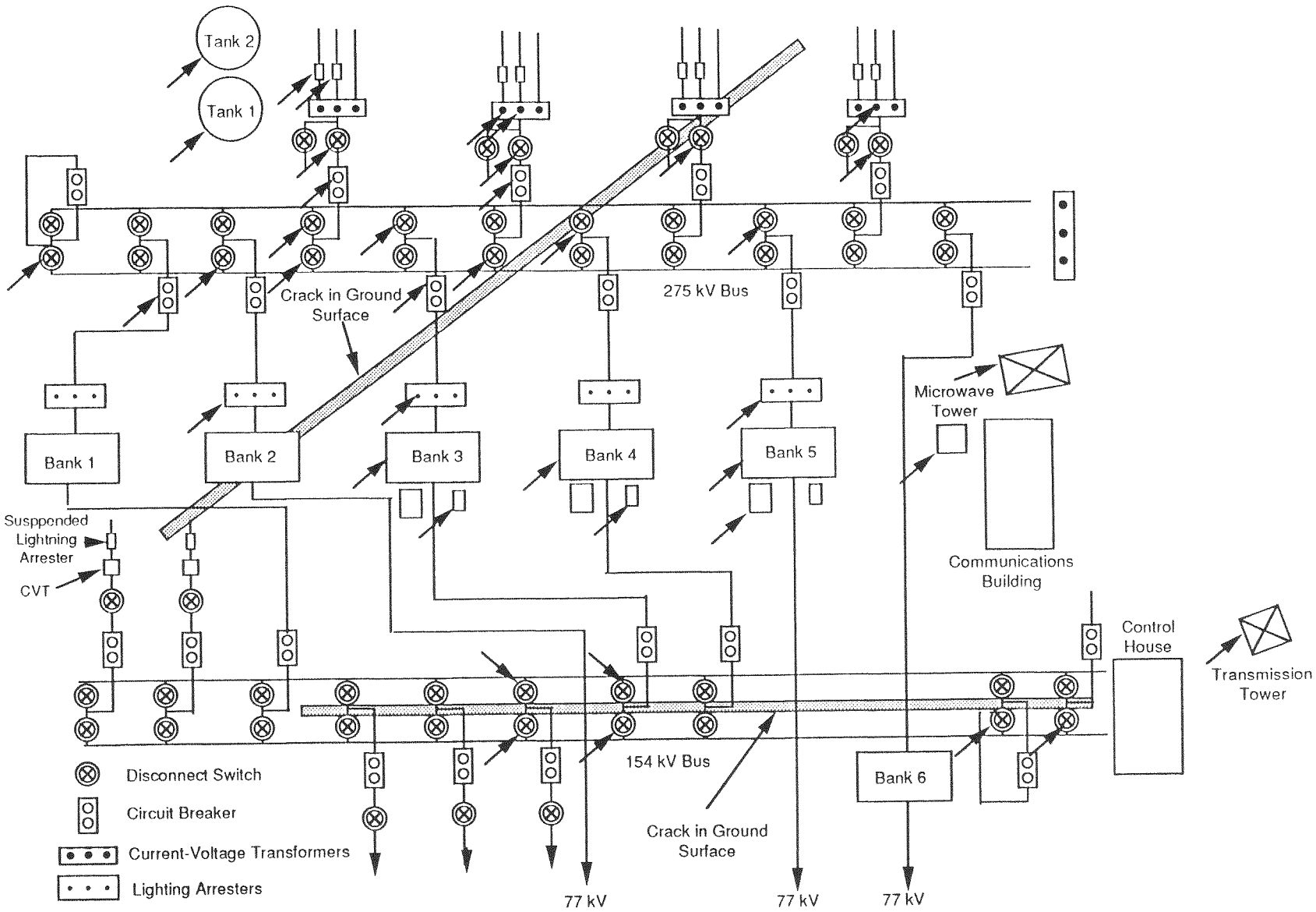


Figure 3-20 A Modified One-line Diagram for the 275 kV and 154 kV Switchyard

The four 275 kV circuits enter the substation from drops from dead-end structures. Two phases of each circuit have wave traps (see Figure 3-13). Note that there is relatively little slack between the wave trap and the adjacent disconnect switch. Several failures were observed. In two cases, one of the four cast iron legs on the lower flange of the current-voltage transformer failed. One unit was observed in the graveyard (see Figure 3-21), and one unit was still in service with a cracked base support (see Figure 3-22). One current-voltage transformer had a porcelain failure at the base just above its lower flange (see Figure 3-23). Several other current-voltage transformers developed leaks at "O" rings used to seal the units, but these were repaired and put back into service. Two damaged wave traps were also observed in the graveyard. Notation on an operating diagram indicated that disconnect switches on each circuit were damaged, but the number of phases or type of damage is not known. These were the units adjacent to the wave traps and vibration of the wave trap could generate interaction loads.

In the U.S., the lower wave trap restraint of suspended wave traps is typically configured like the phase without a current-voltage transformer (CVT) or wave trap. That is, the wave trap restraint is connected to a structure or to the ground with an insulator string. The CVT would have its own support adjacent to the wave trap restraint. In the configuration shown, the lower support is provided by the CVT, so that it must withstand its own inertial loads and the wave trap restraint loads. In the U.S., CVTs and similar devices, such as potential transformers, have been very seismically vulnerable, even without interaction loads. As noted earlier, the CVTs appear to be large for their operating voltage as compared to the U.S. In Japan, all of the CVTs were supported on lattice-type structures that were probably relatively still. In the U.S., most CVTs are supported on a tubular steel column that is probably relatively flexible. CVTs in the U.S. with stiffer supports appear to perform better.

One bulk-oil circuit breaker was used in each of the 275 kV circuits that fed into the bus (see Figure 3-24). Two of these units were marked as damaged and one had a slipped bushing (see Figure 3-25). The damage patterns in the U.S. and Japan appear to be reversed. That is, in the U.S., transformer bushings tend to slip, with over 50 examples in the Northridge earthquake, and circuit breaker bushings do not. The opposite is true in Japan. There were two spare bushings at the site, an unusual occurrence since most spares are stored at service centers in Japan. The bushings from two circuit breakers, twelve bushings, were removed to replace damaged units at other sites (see Figure 3-26).

A double-bus single break configuration is used on the 275 kV bus. The potential transformers on the bus were much larger than those typically found in the U.S. (see Figure 3-6). These units were installed after 1980, when more stringent design standards were used and the support structure and anchorage details reflects this (see Figure 3-27). These units were not damaged. Twelve of the thirty disconnect switches in or adjacent to the double bus were indicated as being damaged. A picture of one unit, Figure 3-28, shows that the post insulator failed at its base. Note that this is an isolated failure and that there is relatively little slack between the drop and the disconnect switch. In the Northridge earthquake, several switches were damaged due to the dynamics of the switch and probably interaction loads associated with the insulator string used in the drop. However, in Northridge, the metal supports below the post insulators of the switch were

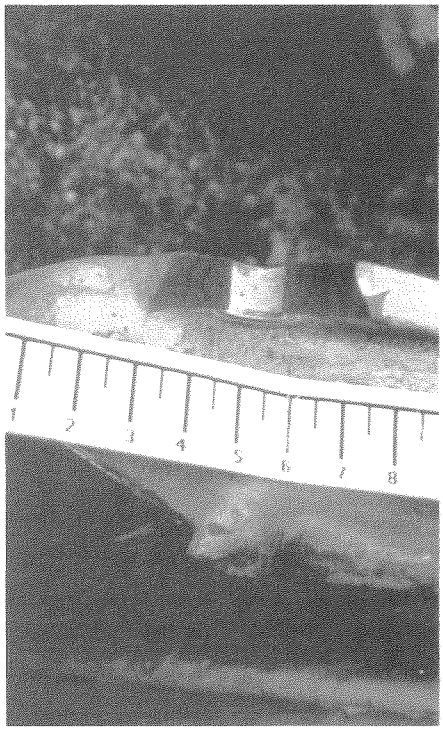


Figure 3-21 Failure of a Current-Voltage Transformer Base Flange

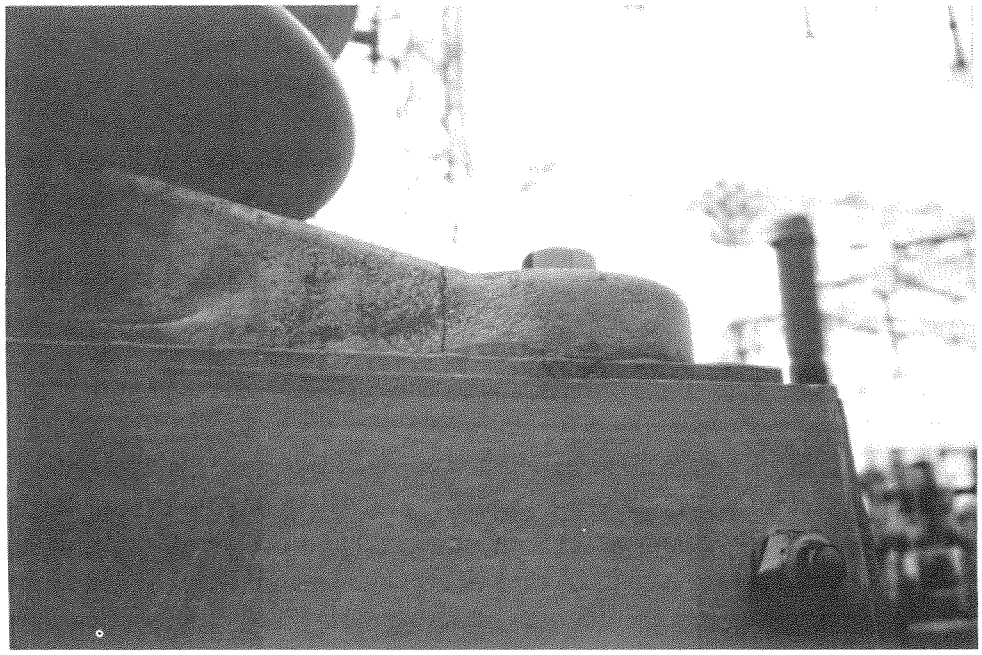


Figure 3-22 A Cracked Cast Iron Anchor Tab on a Current-Voltage Transformer Remained in Service

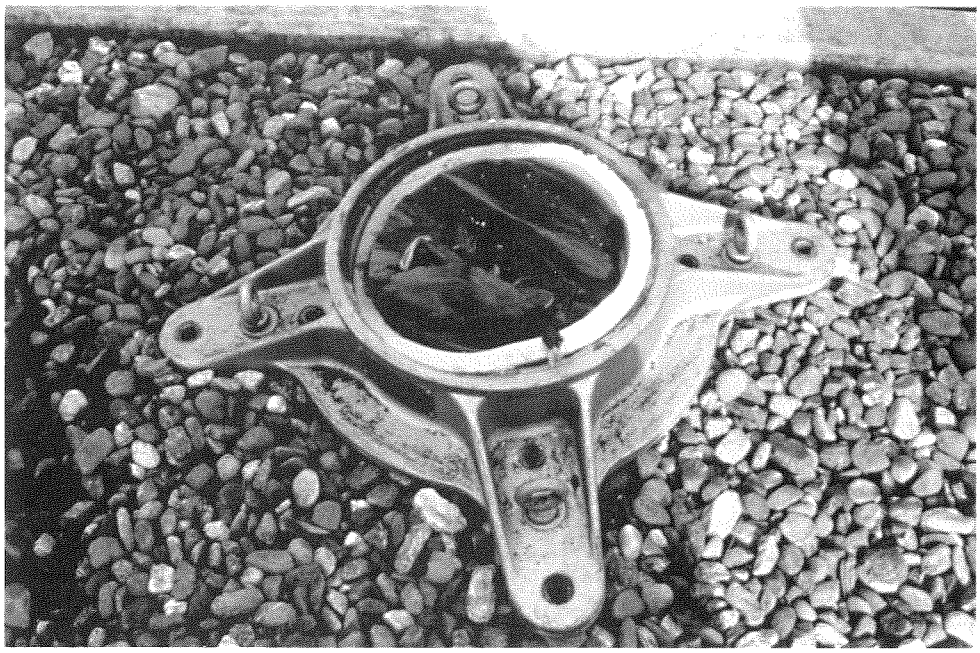


Figure 3-23 Porcelain Failed at the Base Plate of this Current-Voltage Transformer

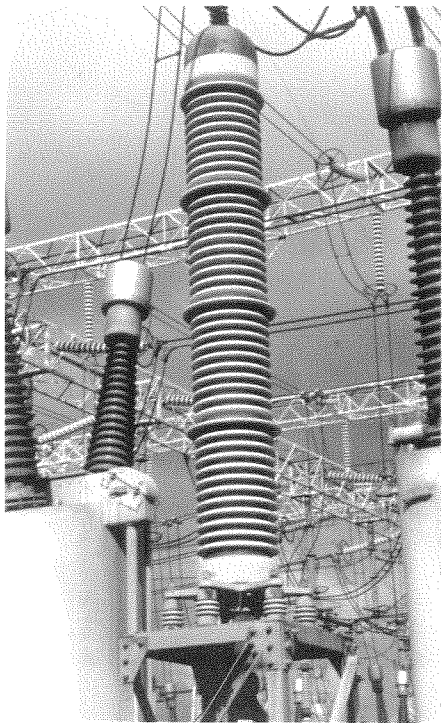


Figure 3-24 Bulk-oil Circuit Breaker and Pot Head on a 275 kV Circuit

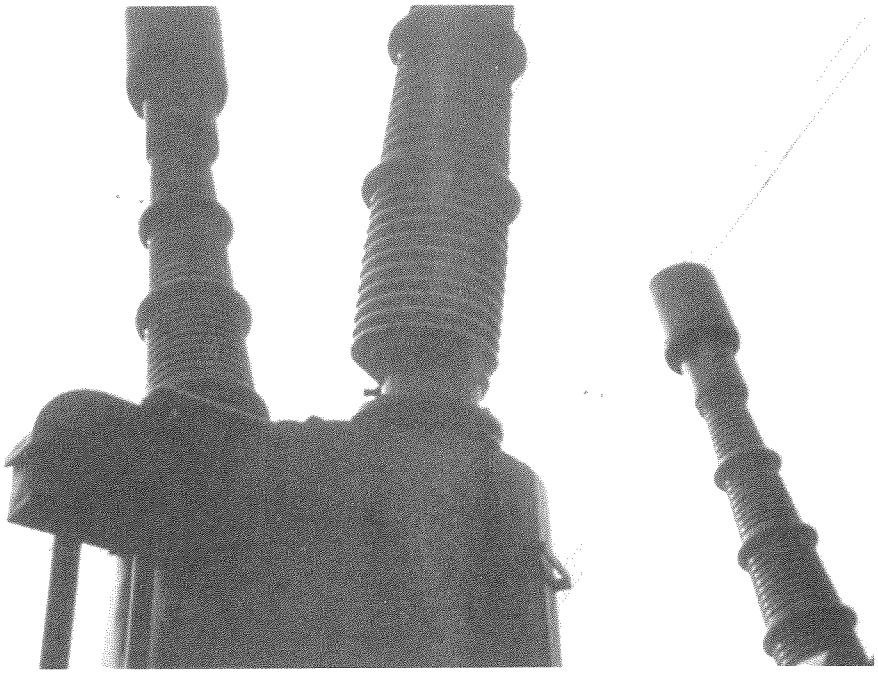


Figure 3-25 Porcelain Slipped on its Lower Flange on a 275 kV Bulk-oil Circuit Breaker

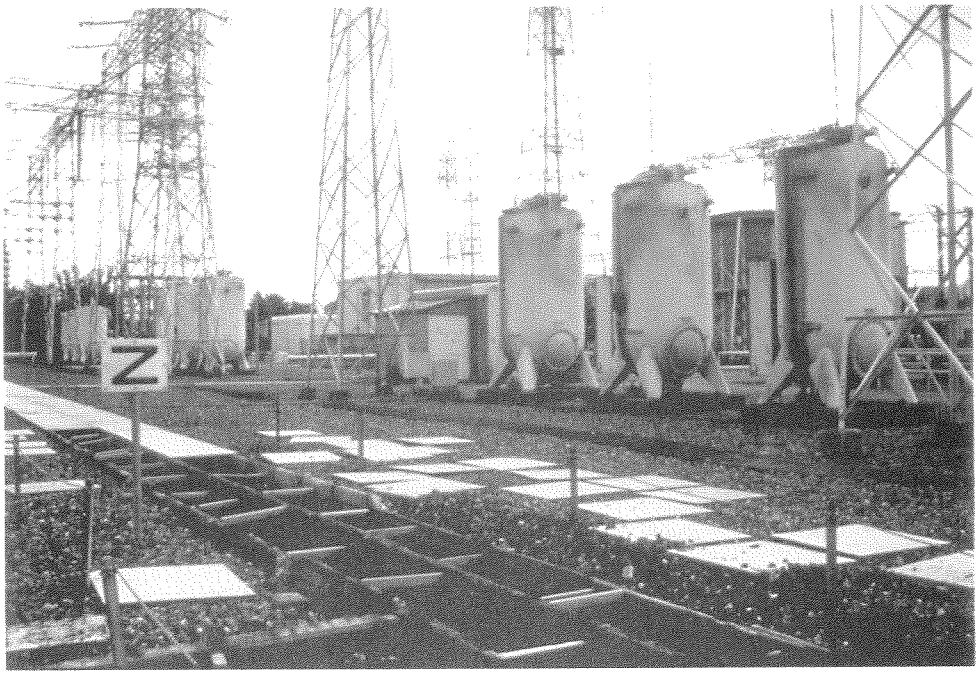


Figure 3-26 Bulk-oil Circuit Breakers with the Bushings Removed to Replace Damaged Units at Other Sites

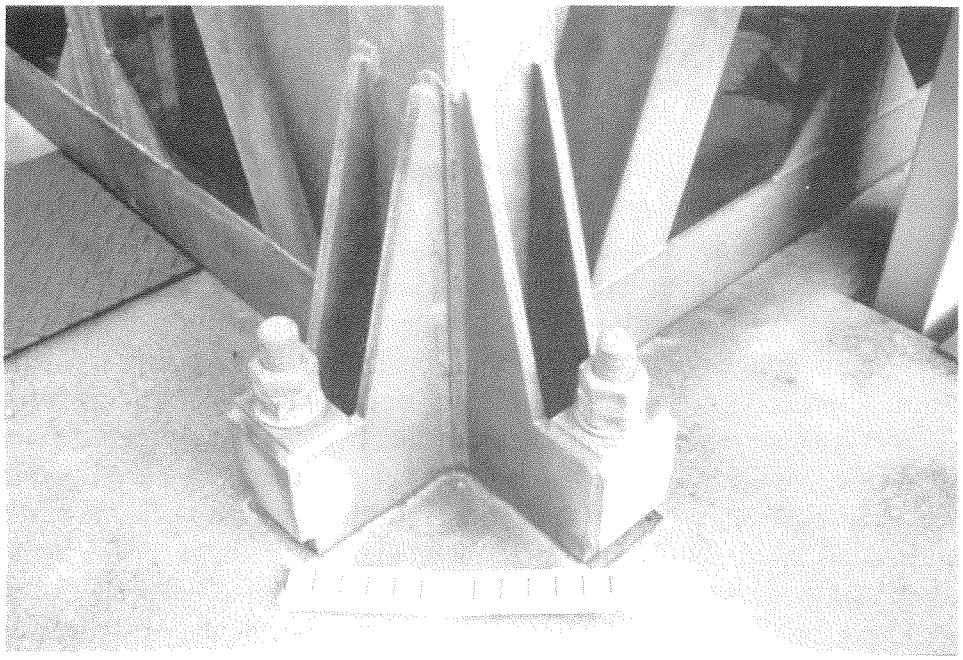


Figure 3-27 Very Strong and Stiff Anchorage Detailed Used on a Large Potential Transformer to Meet More Stringent 1980 Seismic Design Criteria

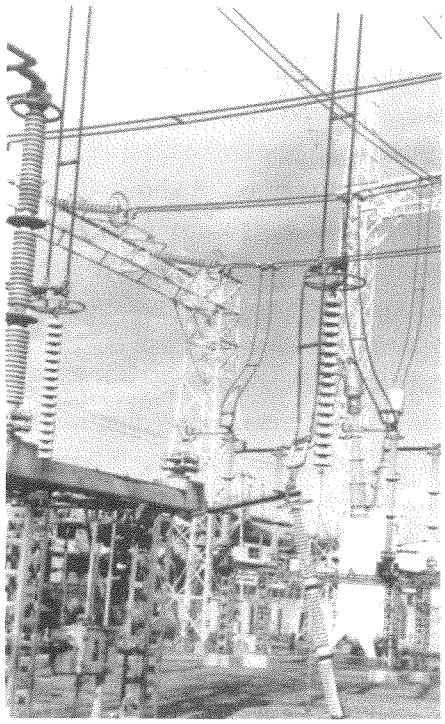


Figure 3-28 Isolated Failure of Disconnect Switch May be Due to Interaction with the Bus Drop and Insulator String

deformed, while in Japan the post insulators failed. Since the insulator string is relatively light weight, nonlinear effects due to the interaction of the string, slack in the connections, and vertical motions of the conductor support tower may cause larger than expected loads. The post insulators in the graveyard, which had solid cores, had an unusual failure mode, as they appeared to split in half longitudinally (see Figure 3-29).

In the position shown in Figure 3-12, adjacent to the circuit breaker is a pot head of a cable to Bank 6, a disconnect switch and a lightning arrester. The pot head design is different from that used in the U.S. in that there are standoffs between the bottom flange of the pot head porcelain and its support structure, similar to lightning arresters. The disconnect switch is similar to the center break disconnect switches used in the U.S., except arms are fabricated from copper rather than aluminum. The three lightning arresters in this position failed (see Figure 3-30), and probably damaged the B-phase disconnect switch in the background. The lightning arrester is supported from a short concrete pedestal. This configuration avoids the expense of a support structure and the dynamic amplification that it contributes to the response of the lightning arrester. Note that there is a small fence around the lightning arrester to maintain adequate clearance. Under U.S. rules, a tall fence would probably be required to prevent access. The lightning arrester has a standoff that is the same diameter as the lighting arrester. This design is occasionally used in the U.S., but small insulators are much more common. Seven of the fifteen lightning arresters failed in this elements, as indicated by items in the graveyard (see Figure 3-31). The lightning arresters were also positioned much further from transformer bushings than in the U.S. It is also interesting to note that many of the porcelain members were a bright green color, which was from a thin silicon rubber coating applied to the porcelain, as can be seen in Figure 3-32.

The site has six transformer banks, each bank consisting of a three-phase transformer. Some units weigh about 800,000 pounds and were anchored by eight 3-3/4 cm to 4-1/2 cm diameter bolts. All units were bolted to nuts or plates embedded in the transformer pad. Three of the banks had anchorage failures, with one unit moving about 45 cm (see Figure 3-33). As a result of the displacement, flexible covers on a tertiary bus were severely stressed (see Figure 3-34), control cables that entered the transformer junction box through a hole in the concrete pad were almost sheared off (see Figure 3-35), a low voltage bushing failed at its top due to interaction load with the adjacent item of equipment, and the case of the transformer hit and shorted out connections in a cabinet that contained tertiary circuits (see Figure 3-36). A decision was made to replace some of these transformers and a soil investigation was underway to determine the requirements for the foundation of the new transformer. Because of the proximity of residential and light industry to the substation, transformers have acoustical enclosures. In one case, the enclosure supports were damaged and the enclosure had shifted (see Figure 3-37). A small line reactor, which looks like a transformer and controls line voltage under light loads, was connected to the main banks and also had damaged or failed anchorage. One unit sheared its anchor bolts and slid about 25 cm in the opposite direction from that of the main transformer (see Figure 3-38), aggravating the interaction problems with the transformer bushings.

Capacitor banks observed at several sites have a different form than those typically found in the U.S. The capacitors are enclosed in relatively large tanks and have small transformers located

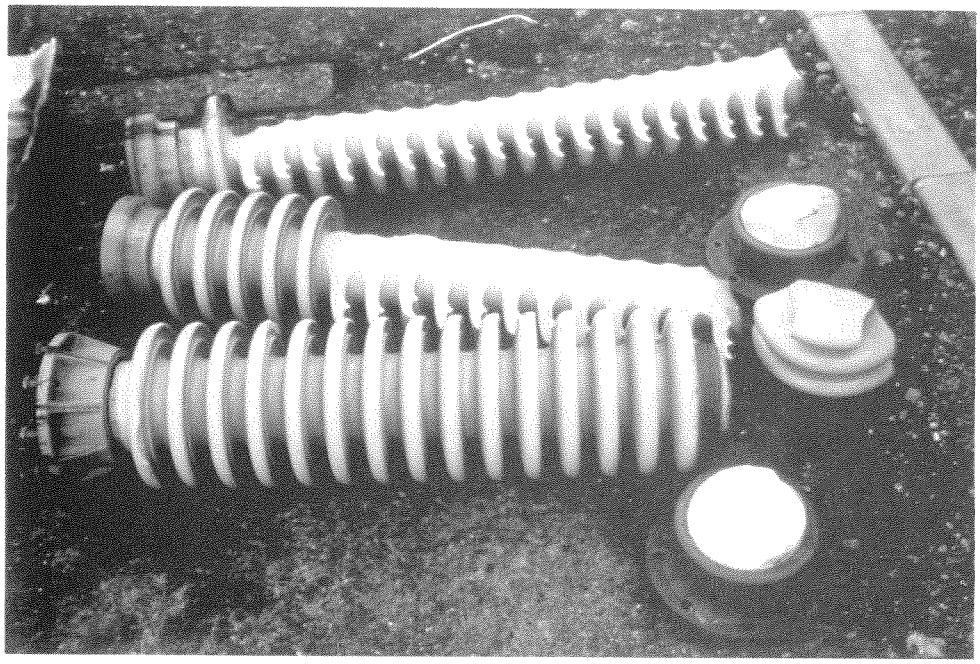


Figure 3-29 Damaged Post Insulators in the Graveyard Exhibit Unusual Longitudinal Cracks

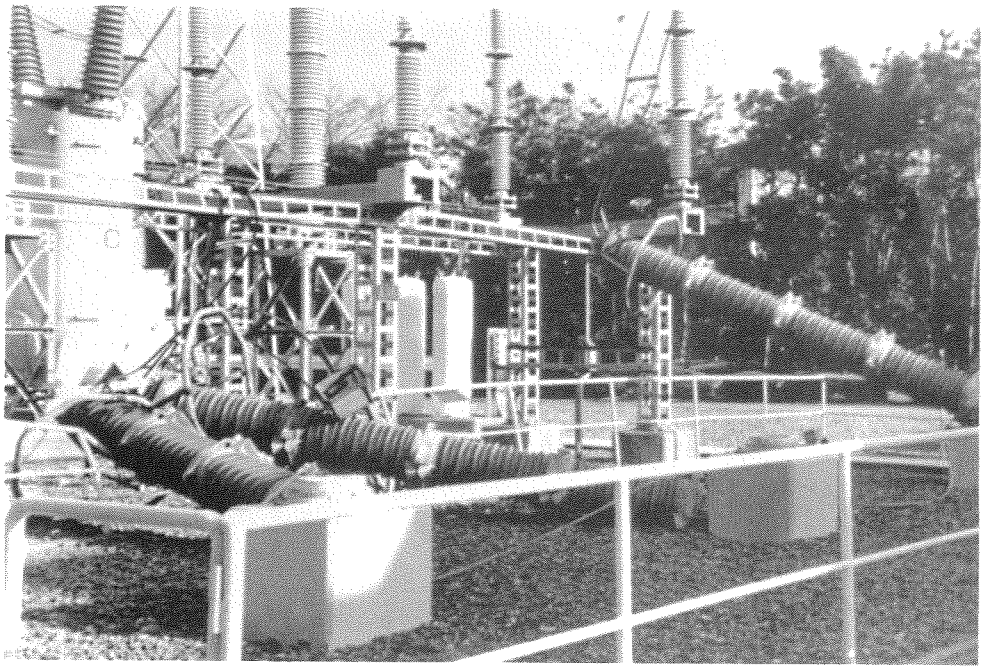


Figure 3-30 Standoff Incorporated into the Design of the Base of the Lightning Arrester Failed

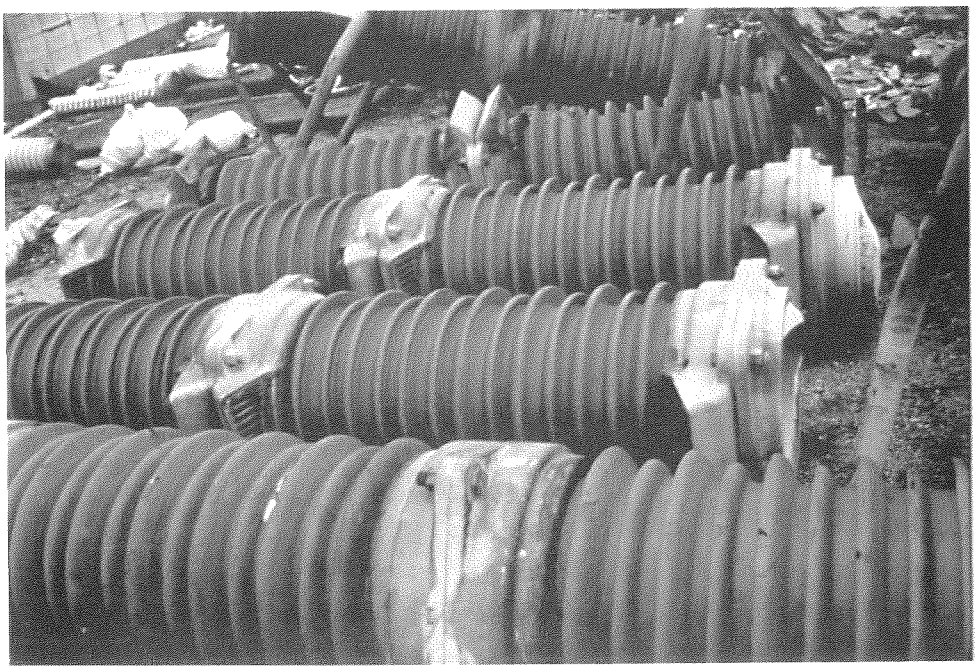


Figure 3-31 Damaged 275 kV Lightning Arrester in the Graveyard

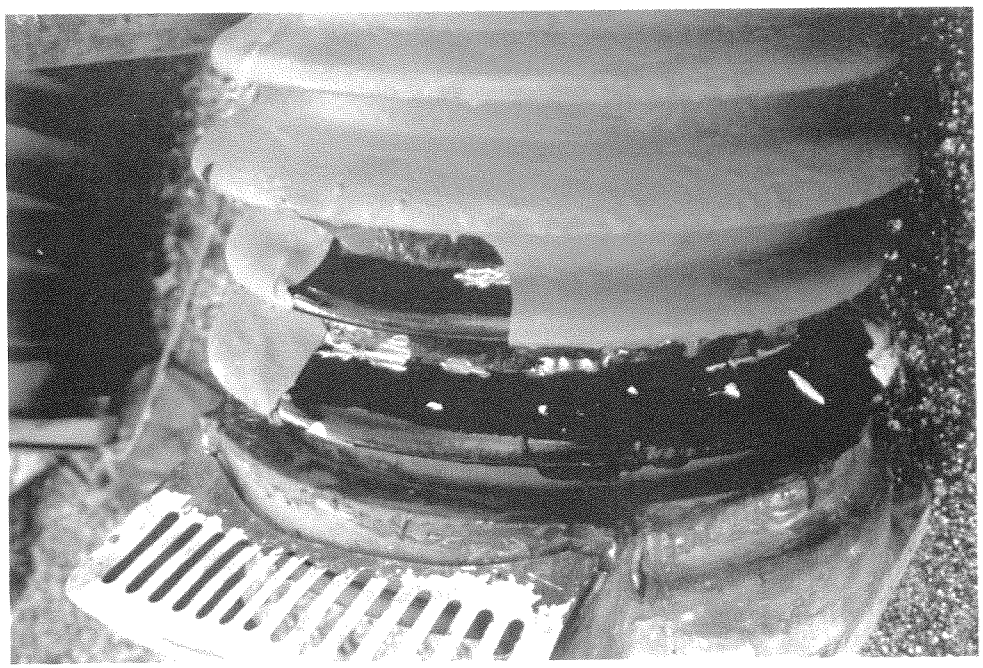


Figure 3-32 Silicon Rubber Used to Improve Contamination Problems has Peels from this Damaged Equipment in the Graveyard

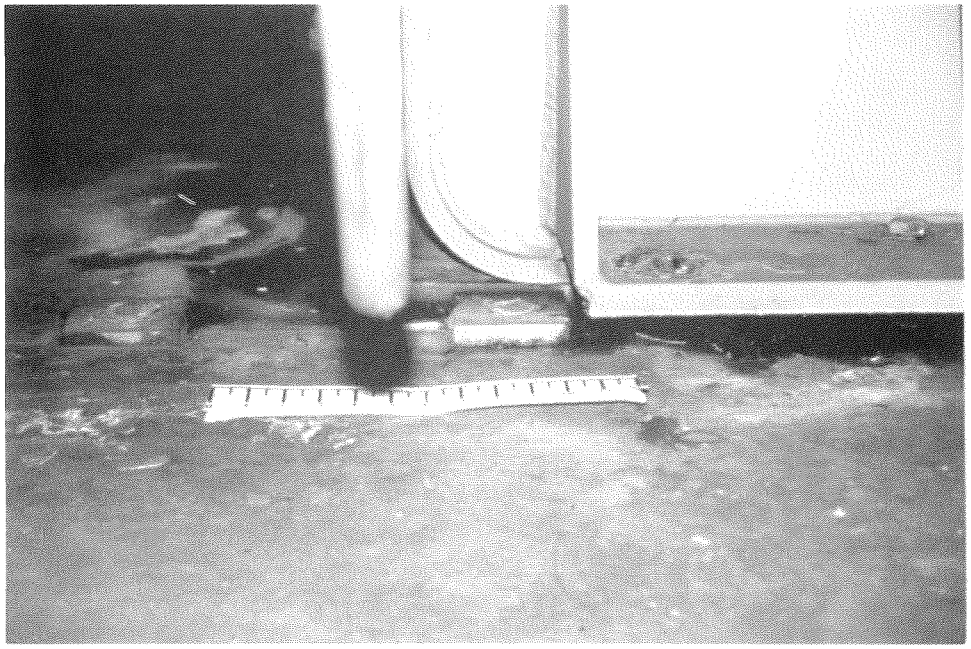


Figure 3-33 Bolts Anchoring a Transformer Failed Allowing the Unit to Slide 45 cm and Causing Damage to Bushings

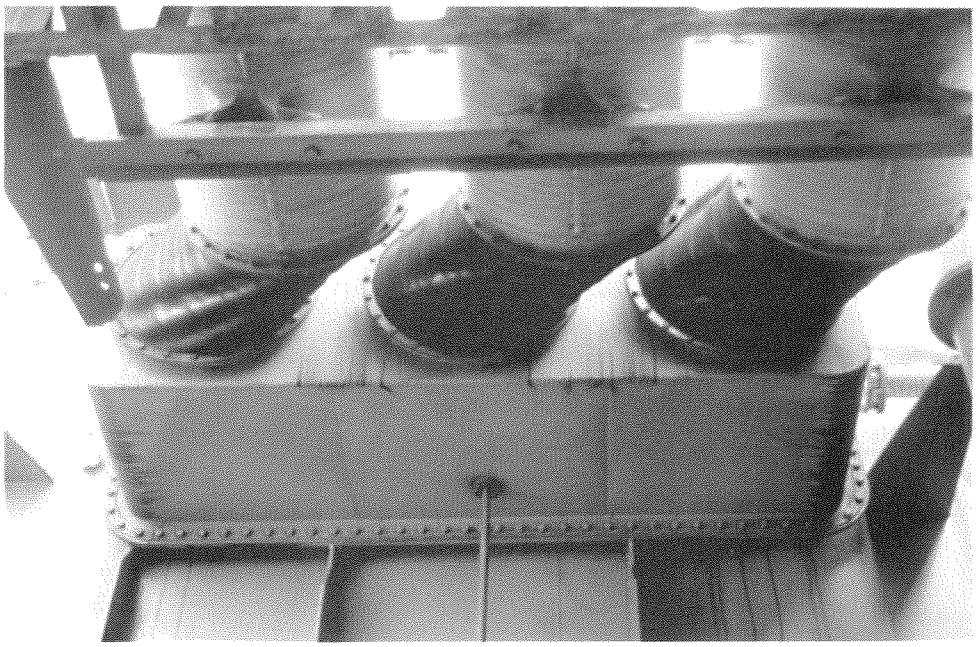


Figure 3-34 Offset in Bus Covers Caused by the Failure of Transformer Anchorage and its Movement

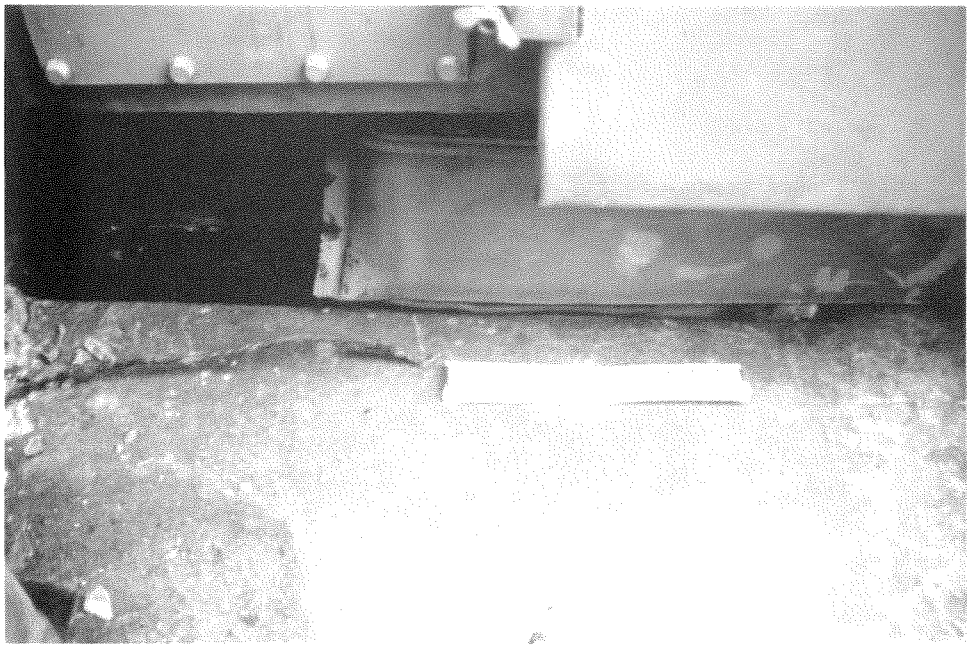


Figure 3-35 Transformer Control Cables were Almost Sheared Off Due to Movement of the Transformer

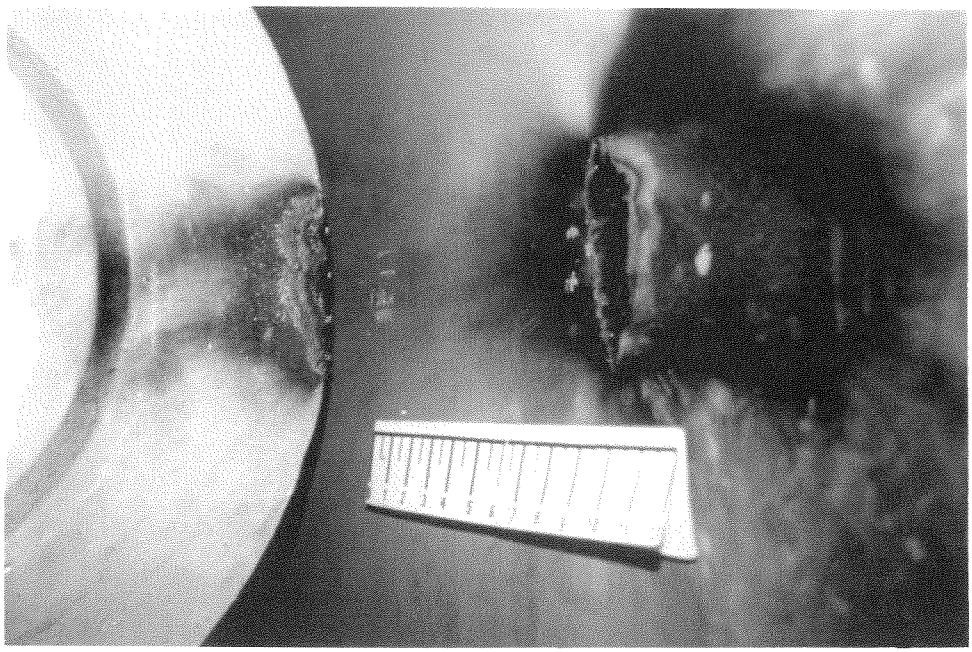


Figure 3-36 Movement of Transformer Shorted Transformer Case to Cabinet Containing Tertiary Output

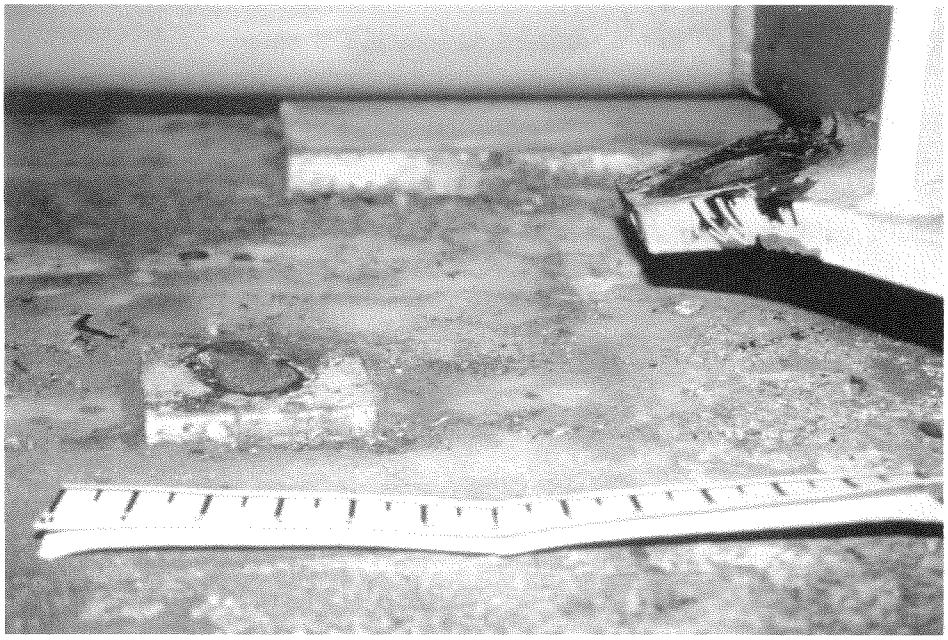


Figure 3-37 Transformer Acoustical Enclosure Support was Damaged and the Enclosure Shifted

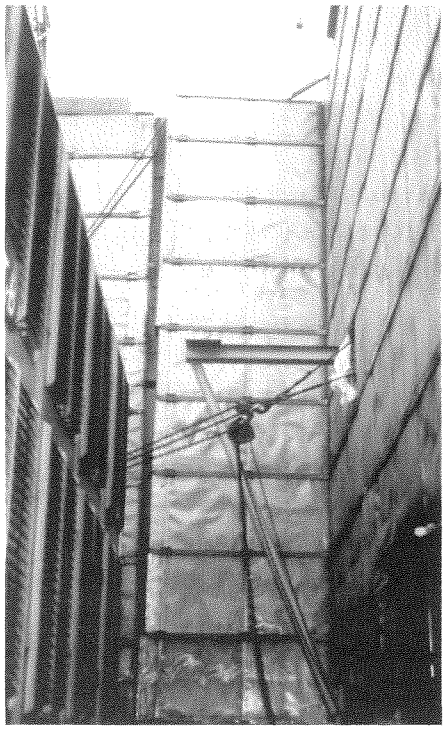


Figure 3-38 Small Transformer Sheared its Anchor Bolts and Moved 25 cm Increasing the Load on Bushings

on the electrically isolated rack (see Figure 3-9). Note that the post insulators that form diagonal braces are mounted so that they can take tensile and compressive loads.

Station batteries were secured to well-braced and anchored battery racks (see Figure 3-39). A rack of a different design, positioned close to the floor, reduced the need for bracing (see Figure 3-40). A common detail found at several Japanese facilities was the use of stiff rubber spacers between the cells and between the cells and their restraints (see Figure 3-41). Cabinets associated with the batteries were well-anchored. Just outside of the battery room there was a relay cabinet that was unanchored at the time of the earthquake and it fell over and relays had to be replaced. The cabinet is now anchored at its base and braced at the top. The cable trays were similar to those used by the power industry in the U.S., except that they have rungs rather than solid bottoms (see Figure 3-42).

Several soil effects were observed at the site. As noted above, the site was constructed on wetlands adjacent to a river. Figure 3-20 shows two large cracks in the surface of the site. Figure 3-43 shows one of the large cracks that opened about 25 cm in the switchyard. Where these cracks crossed concrete cable trenches, the trenches were fractured or deformed (see Figure 3-44). The crack which crossed the site diagonally opened between 20 cm and 30 cm. Because of the potential of control cable damage (see Figure 3-45), all transformers were operated manually rather than by using the controls until the cables could be checked. None of the cables were damaged, but a pipe for a system of compressed air in one of the trenches failed. Bus support structure and equipment foundation pads were also disturbed. The footings on a bus support structure rotated and there was a crack in the soil about a foot deep (see Figure 3-46). A lightning arrester support structure tipped over about 2-1/2 degrees (see Figure 3-47), which probably contributed to the failure of the lightning arrester. The diagonal crack also passed though the six separate footings of a 275 kV disconnect switch. This switch has been removed and a monolithic pad of reinforced concrete about 1-1/4 m thick was being installed (see Figure 3-48). At the time of the visit, work was in progress to repair water pipes near the control house. This did not have any effect on equipment or technical operations, but it did make it difficult for operating personnel as sanitary facilities were not available.

Water stored in two 100,000 liter tanks was used to clean porcelain after typhoons. These were old installations and their response was somewhat puzzling. Each tank was surrounded by a 10 cm thick concrete ring about 45 cm outside of the outer diameter of the tank. The annular ring between the tank and the concrete was covered with asphalt. It has been suggested that these rings were to retain the soil that was compacted below the tanks. Each tank was secured by about eight bolts on chairs. The details of the anchorage of the bolts is not known, but it was reported that they were not secured to the concrete ring. The bolts on the southern tank were stretched or pulled out, the asphalt strip between the tank and the concrete ring was broken and deformed, and some of the chairs were deformed indicating that there was a large force between the anchor bolt and the chair (see Figure 3-49). On the north tank, the bolts appeared similar to those on the south tank, and some chairs were deformed, but there was no disturbance to the asphalt at the bottom of the tank or by the concrete ring. There was no indication that the tank had rocked, other than the bolt position. The good detailing in the flexible pipe connection



Figure 3-39 Batteries are Secured to a Well Braced and Anchored Battery Rack

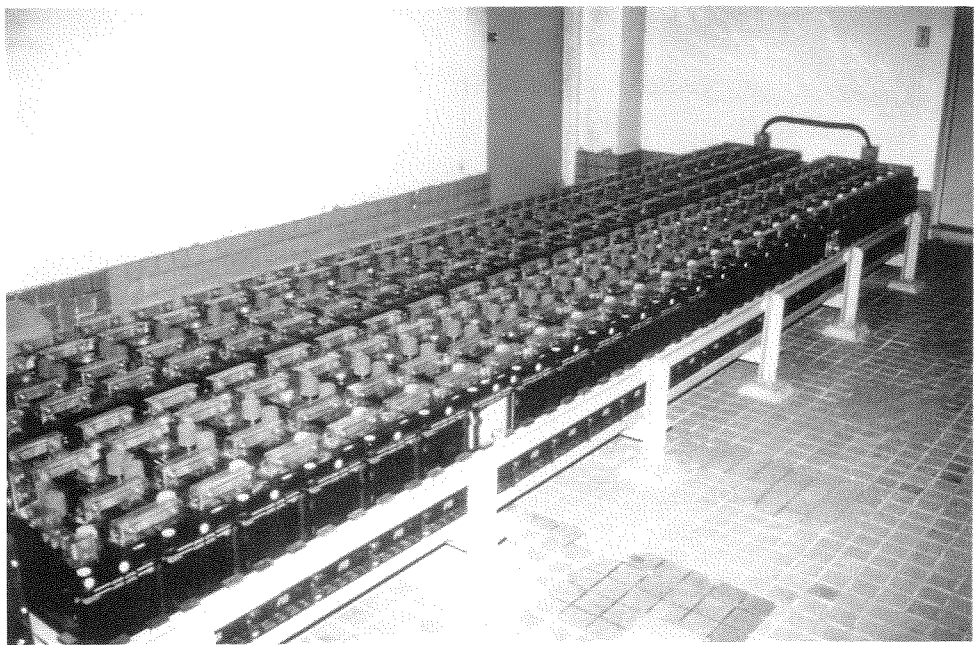


Figure 3-40 Low Slung Battery Rack Configuration Not Found in the U.S. Reduces Bracing Requirements of the Rack

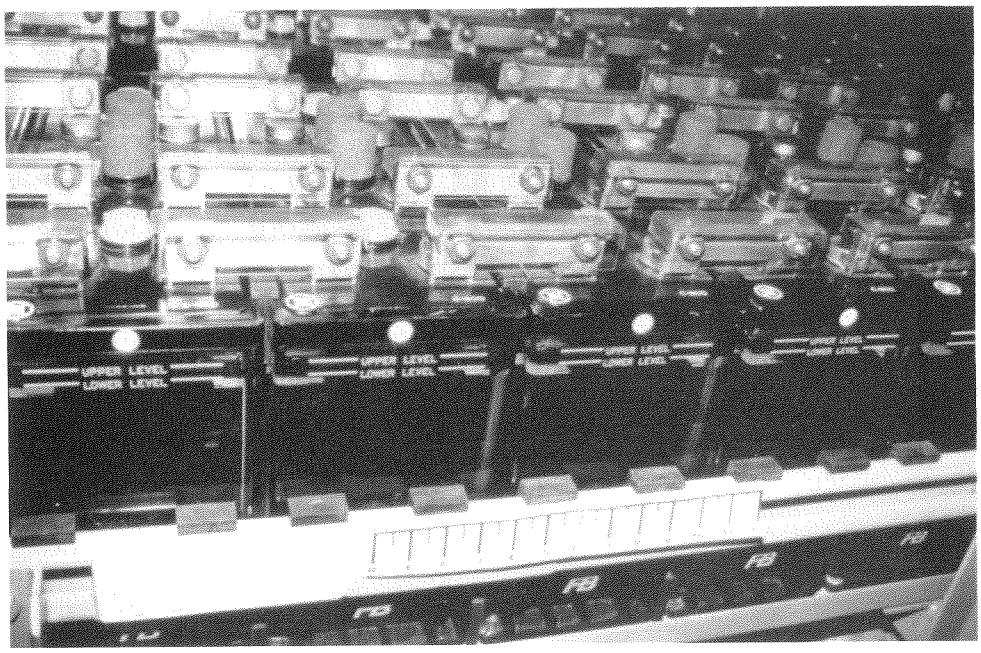


Figure 3-41 Different Approach Using Rubber Spacers in Japan to Restraining Cells to Battery Racks

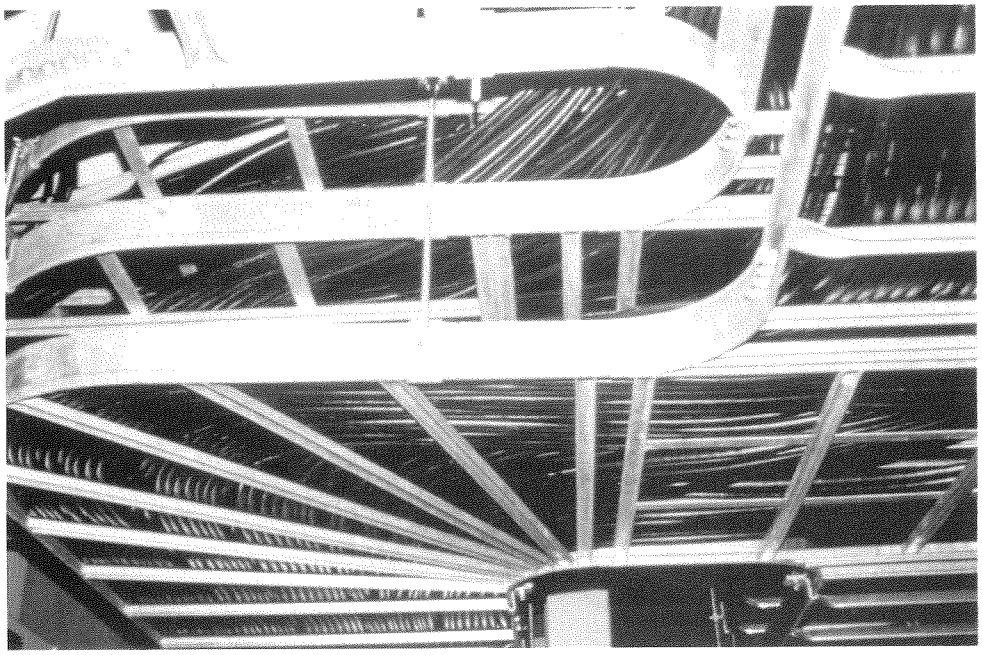


Figure 3-42 Cable Tray Sections are Bolted Together and Cables Restrained with Ties to the Tray



Figure 3-43 Long Crack in the Ground Surface Opened About 25 cm and Damaged Cable Trenches

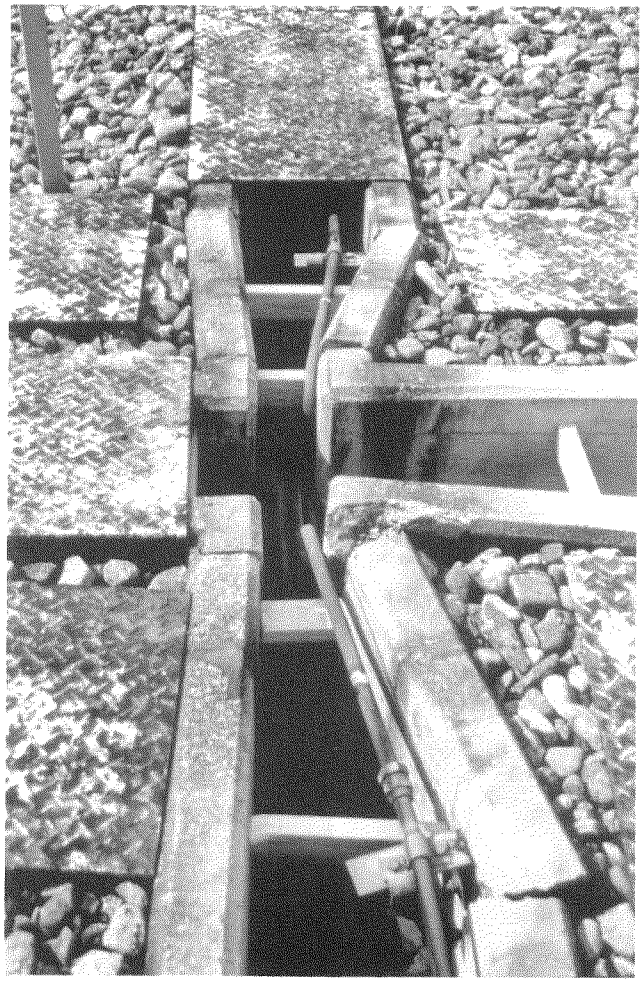


Figure 3-44 Cable Trenches were Deformed with the Ground Fracturing an Air Line but Leaving Control Cables Undamaged

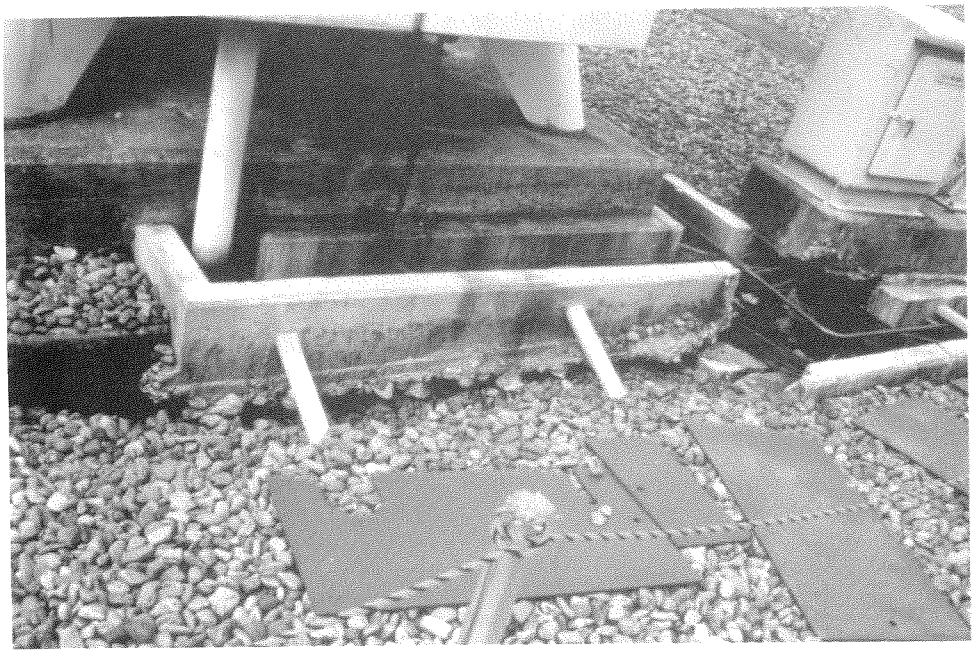


Figure 3-45 Large Soil Deformations at Equipment and Pedestal Foundations Did Not Damage Control Cables

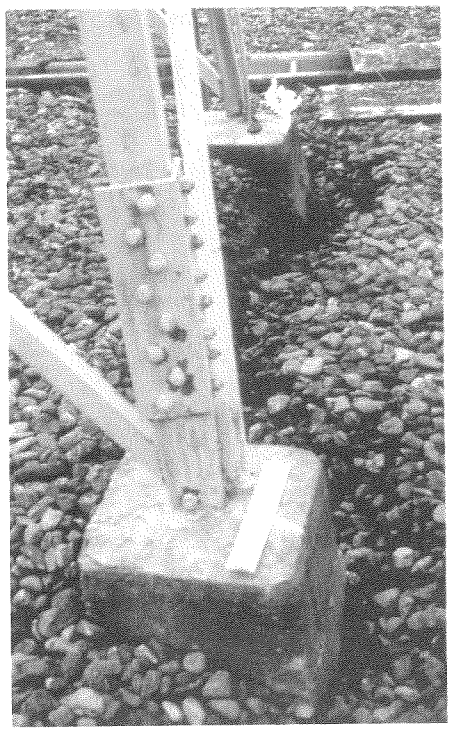


Figure 3-46 Foundations of Conductor Support Structures were Disturbed and Individual Footings Rotated as Much as 25 Degrees

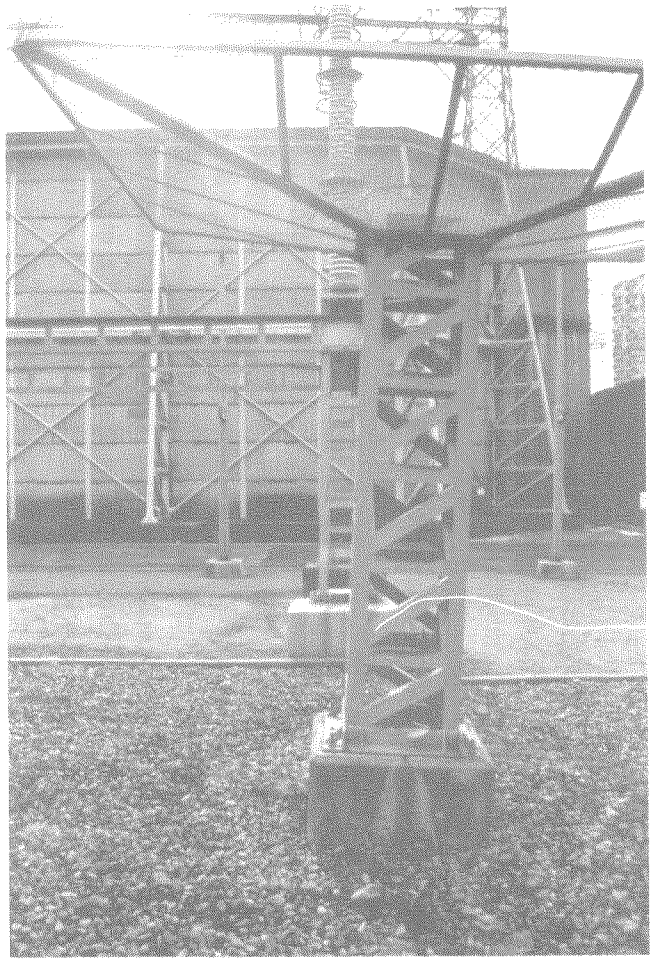


Figure 3-47 Lightning Arrester Support Structure Tipped About 2-1/2 Degrees and Probably Contributed to the Failure of the Lighting Arrester

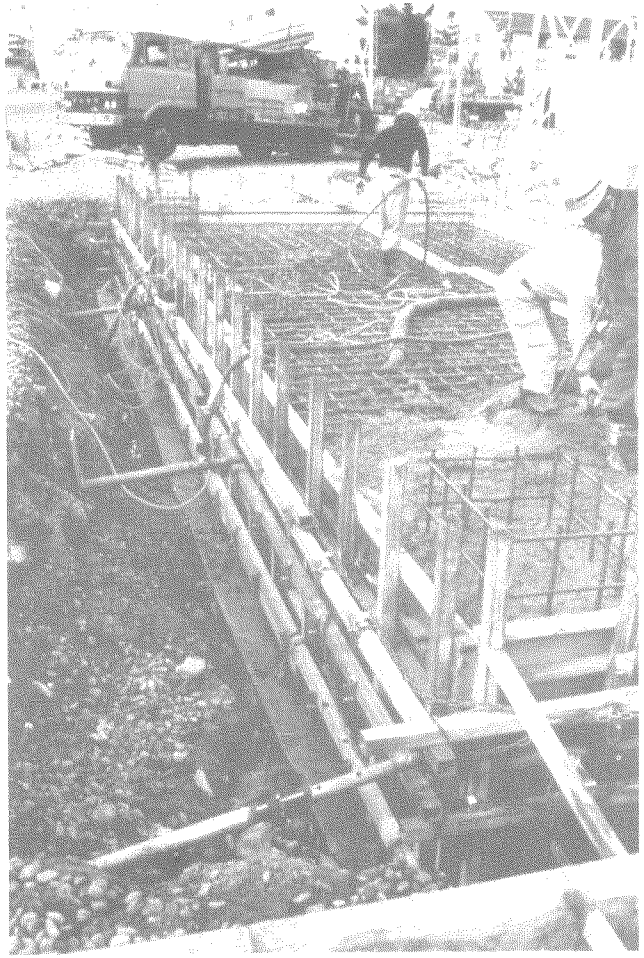


Figure 3-48 New Monolithic Disconnect Switch Pad Replaced Individual Footings that were Disturbed by a Surface Crack in the Soil

provided to this old installation (see Figure 3-50), is rarely seen in the U.S. Other soil effects are discussed below relative to a transmission-line tower.

A transmission tower adjacent to the control house had the ground around the tower footings settle about 15 cm (see Figure 3-51). Conduit attached to the tower by a "U" bolt was pulled down with the soil about 8 cm (see Figure 3-52), and there was damage to concrete cable trenches near the base of the tower. Relative movement of the soil and the tower could damage signal lines coming off of the tower, such as optical fibers, if adequate slack was not provided.

The transmission tower adjacent to the one described above also carried two 275 kV circuits and two 154 kV circuits. These were dead-end types structures (see Figure 3-53). That is, the insulator string was in the load path of the line to the tower, rather than the line being supported by a string hanging from the arm. Note that the lines on the left side of the tower were supported by post insulators below the tower arm. On those and several other transmission lines, the post insulators failed at the sand ring and were hanging from the line. This did not put the line out of service, but did require repair. Some towers carry optical fiber communication cables in their transmission tower ground wire that are used for protective relay signaling. This provides a redundant path with the microwave system, but there are no plans to eliminate carrier signals and wave traps, as has been done by some utilities in the U.S.

A microwave tower at the site had two members that were bent or had minor buckling (Figure 3-54), which did not effect operations. While this damage was minor, it is very unusual for earthquakes to damage communication towers. The foundation did not appear to be disturbed. Communication equipment and an engine-generator at the site were not visited.

3.2.5 Shin-Kobe Substation

The Shin-Kobe substation is located about 30 km northeast of the epicenter on a hillside on at least three man-made terraces. The back of each cut was faced with a concrete wall. While grading diagrams were not seen, it appears that the back part of the terraces were on cut and the front part were on fill. This appears to be born out by cracks and separation in a wall at one side of the site and subsidence and cracks at other locations. Circuit breakers were frequently located on the fill part of the terrace.

Damage to equipment at the site was similar to that at Itami. Lightning arresters failed and damaged disconnect switches when they fell (see Figure 3-55). Bulk-oil circuit breaker bushings slipped on their lower flange (see Figure 3-56), probably due to inertial rather than interaction loads because of the configuration of the conductors. Post insulators on disconnect switches failed (see Figure 3-57). The failures could have been from the combined effect of interaction and inertial loads. Insulators in general did not fail at the base of the insulator stack, but in the body of the porcelain, and in some cases fractured the porcelain longitudinally. The three insulators in the stack were graded, that is, successive segments from the bottom were thinner. The vast majority of post insulator failures in the U.S. are at the sand ring rather than in the body of the insulator.

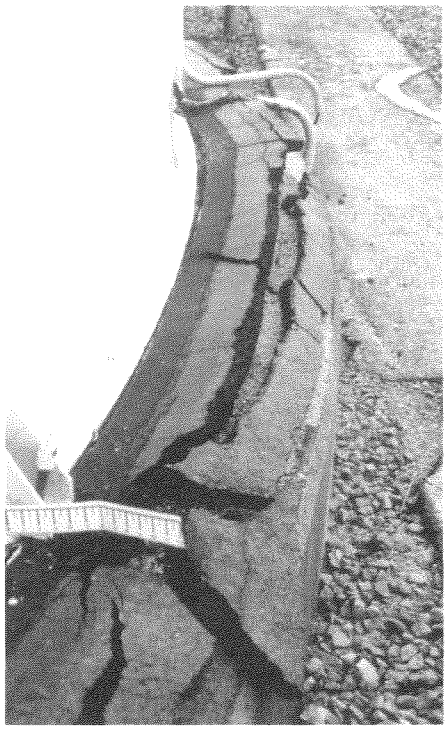


Figure 3-49 Asphalt Surface Between the Tank and the Concrete Ring was Broken and the Bolts Stretched or were Pulled Out Due to Rocking of the Tank

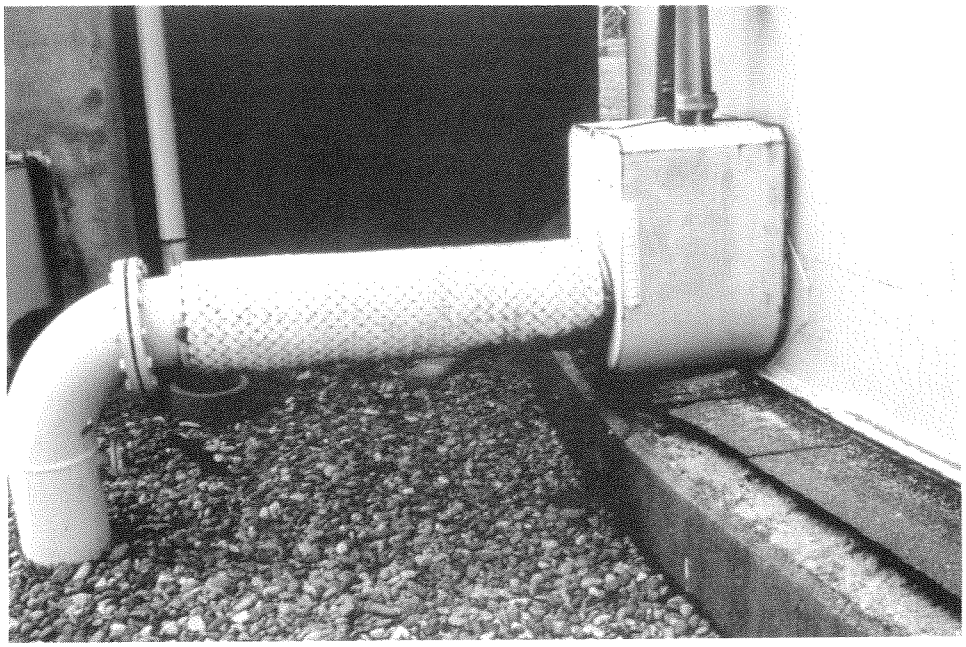


Figure 3-50 While These Were Old Installations, the Tanks were Provided with Flexible Coupling at Pipe Connections



Figure 3-51 Soil Around Footing Subsided About 15 cm

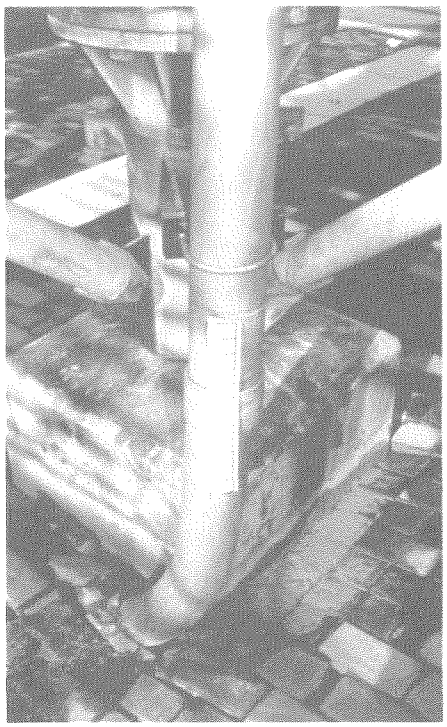


Figure 3-52 Conduit Attached to the Tower and Buried in the Ground was Displaced About 8 cm and has the Potential of Damaging Internal Signal Cables as they are not Provided with Adequate Slack

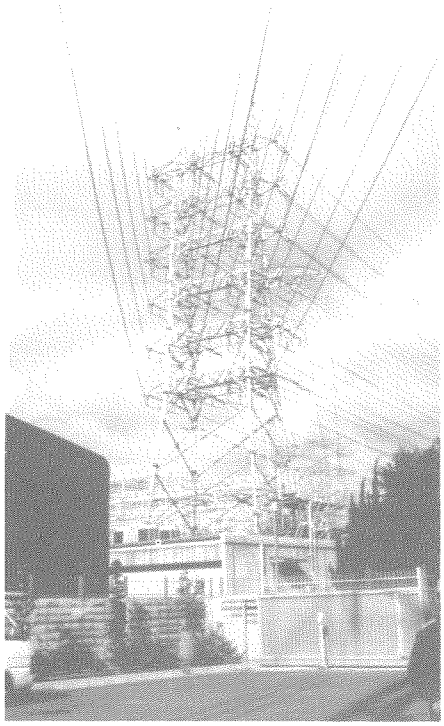


Figure 3-53 Post Insulators that Restrain the Lines as They Pass Under the Support Arm Failed On Several Towers, but Did Not Cause Disruption

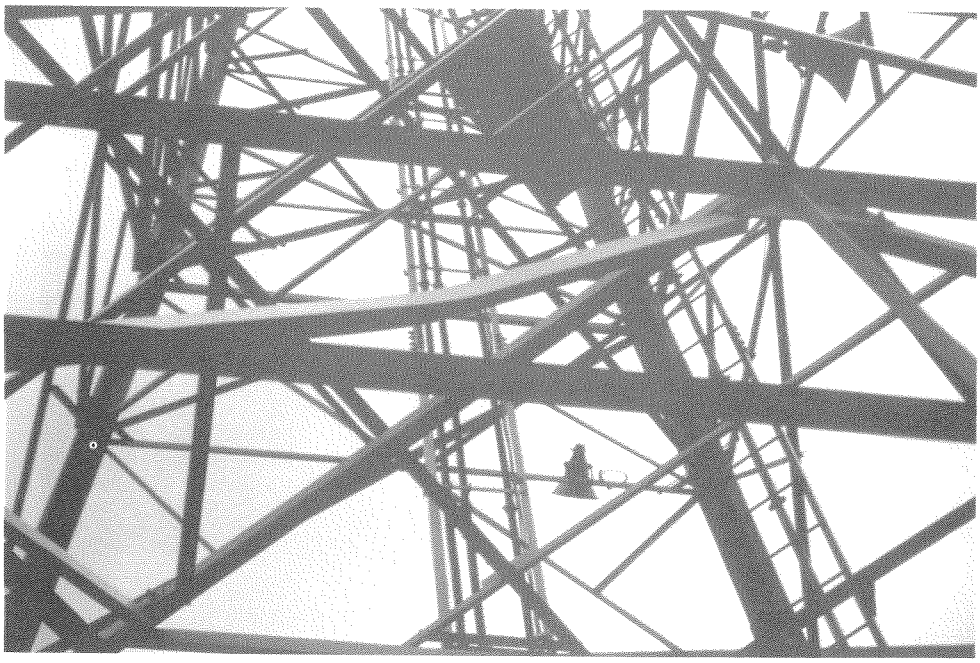


Figure 3-54 Bent Member in a Microwave Tower is Very Unusual, but it Did Not Effect Operations

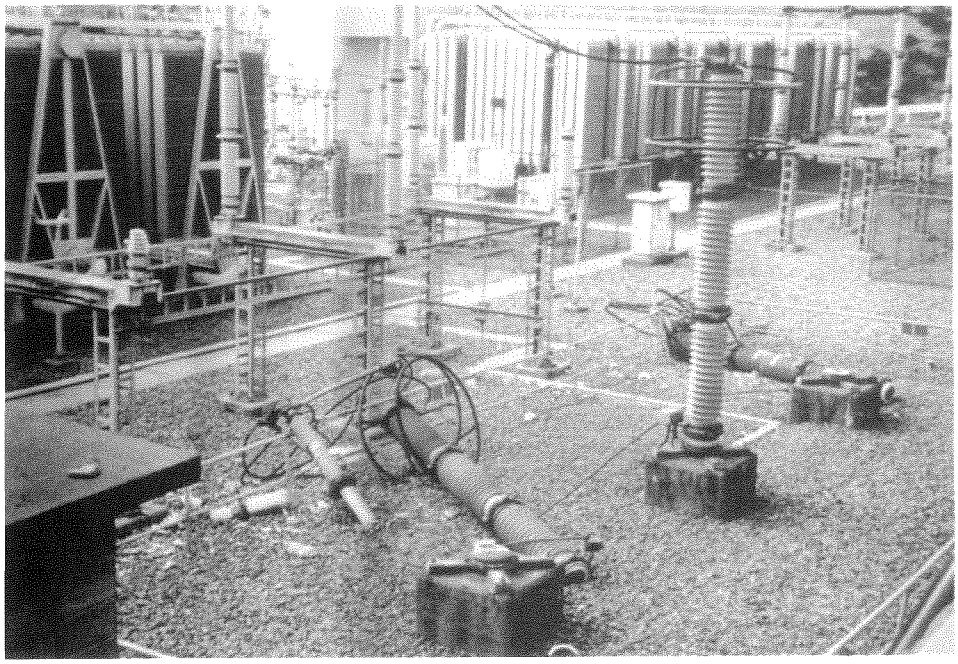


Figure 3-55 Lightning Arresters Failed and Probably Pulled Down Adjacent Disconnect Switches

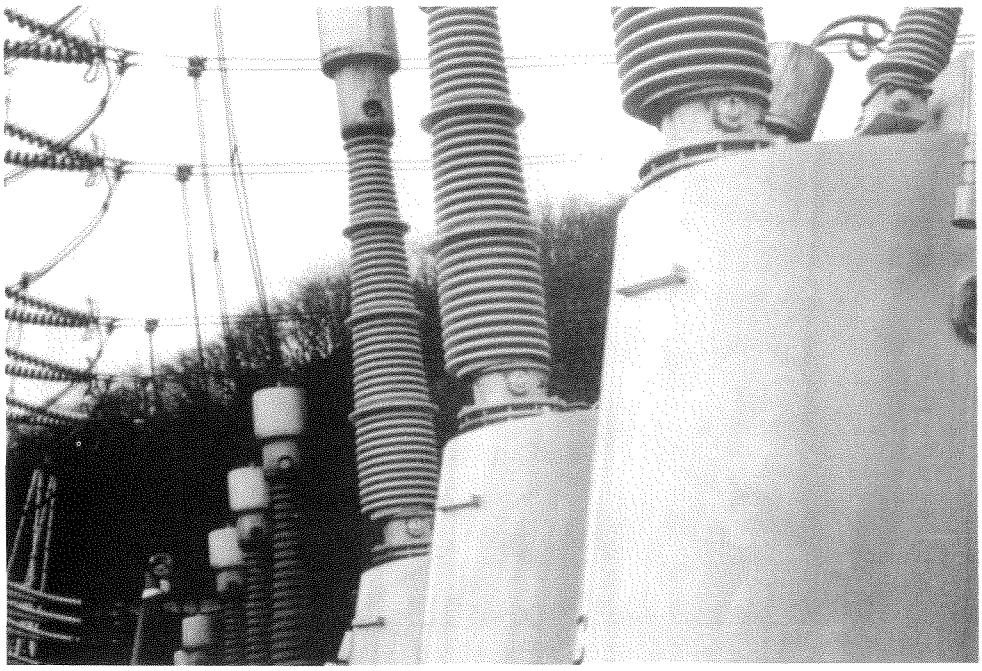


Figure 3-56 All Three Bushings Shifted on this 275 kV Bulk-oil Circuit Breaker

There were several differences in the damage between this and the Itami substation. Transformer anchorage did not fail. Post insulators supporting neutral resistors failed (see Figure 3-58). Of particular interest, a 77 kV, three-phase, gas-insulated circuit breaker lost three bushings (see Figure 3-59). In the U.S., the failure of any equipment at this voltage is unusual, and a dead-tank circuit breaker has never failed. One possible cause of the failure was that the ground settled and the bus support structure did not because of its better foundation. If the vertical drop to the circuit breaker did not have slack, as is often the case, the relative displacement could have pulled the internal conductor from the bushing.

Another feature not observed in the U.S. was fresh water spray heads that were used during certain wind and atmospheric conditions to lower the concentration of salt in the air to reduce the potential for flash-over in the 275 kV switchyard (see Figure 3-60).

3.2.6 Fukiai Control Center and Substation

The Fukiai substation is a distribution substation operating between 77 kV and 6.6 kV, the primary distribution voltage of Kansai Power Co. The substation has three, three-phase transformer banks and the 77 kV switchyard is gas insulated. A control center is located in a building adjacent to the substation.

Transformer Bank 1 failed its anchorage, slid into an acoustical or fire wall, and caused it to lean (see Figure 3-61). A pot head connected to one phase of the transformer primary failed (see Figure 3-62), probably when the bushing hit the pot head. The radiators were supported by structural members at the top and bottom, and the piping connections at the top and bottom incorporate flexible couplings (see Figure 3-63). This design feature would eliminate a common seismic problem in the U.S. of leaking radiator connections on transmission transformers. Relative motion between the control cable support structure and the radiators was sufficient to overcome the current 60 cm gap and cause the radiators to be crushed and leak (see Figure 3-64).

The anchorage on transformer Bank 2 apparently failed, but some bolts were still in their holes, suggesting that the transformer may have rocked back and forth. Diagonal rods bracing the fire walls all failed, indicating that there had been significant motion of the wall. Conductors, supported from post insulators connected to the fire wall structure, appear to have loaded the bushings and caused leaks. The design and damage to Bank 3 was similar to that on Bank 2. Three mobile transformers temporarily replaced the damage units. Due to severe traffic congestion, the first transformer arrived from Osaka about 3 p.m. The second unit arrived in the afternoon of the next day, delayed again due to very heavy traffic. Each unit has a 10 MVA rating.

The site had 77 kV and 6.6 kV gas insulated switchyards (see Figure 3-65), which were undamaged.

There was a small control center in a building adjacent to the switchyard. The earthquake caused computer monitors to fall to the floor, but caused little significant damage. Station batteries

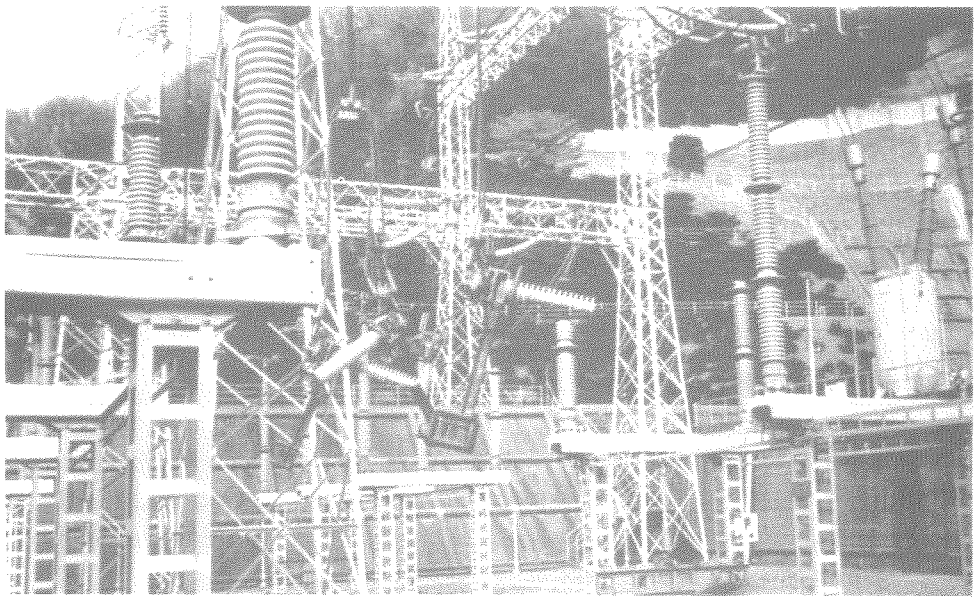


Figure 3-57 Failure Pattern of Splits in the Post Insulators of These Disconnect Switches is Unusual



Figure 3-58 Neutral Resistors Failed, a Device Not Used in This Configuration in the U.S.

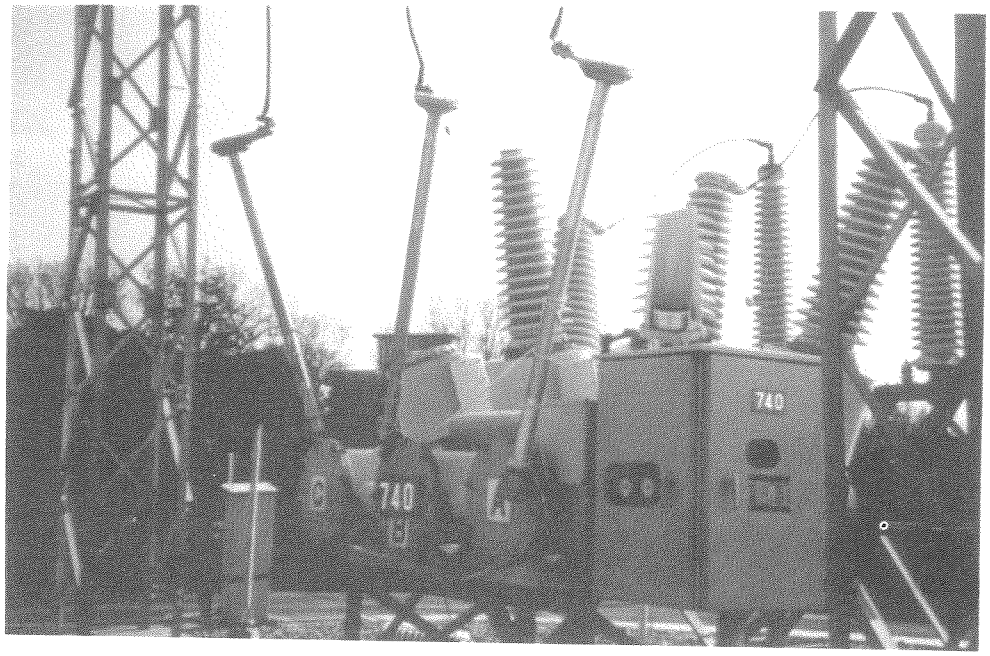


Figure 3-59 A 77 kV Three-phase, Dead-tank Gas Insulated Circuit Breaker Failed at its Bushings, Probably Due to Inadequate Slack to Accommodate Soil Settlement at the Site

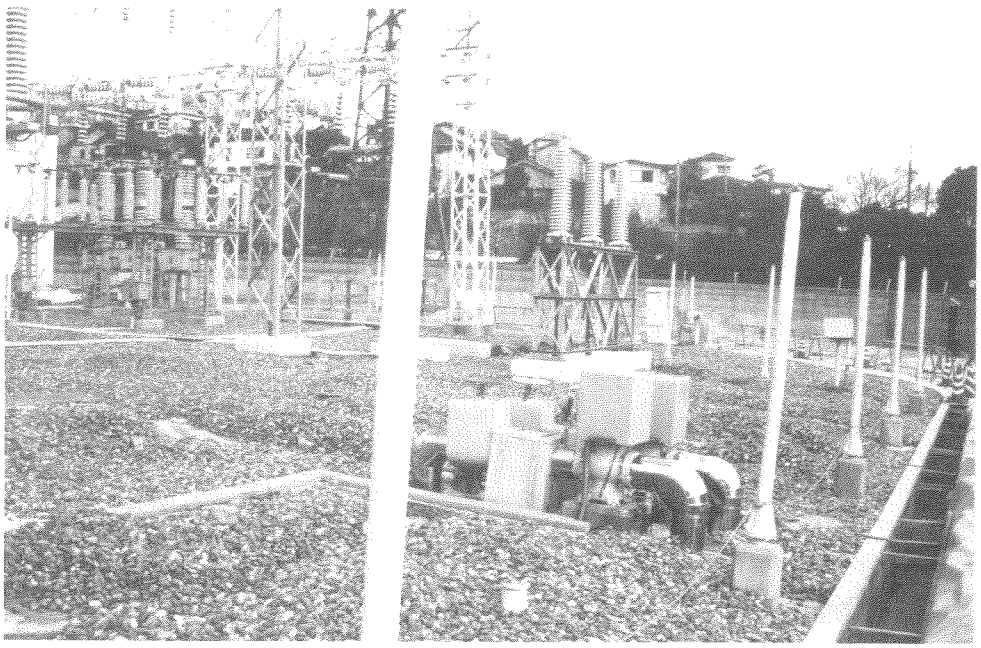


Figure 3-60 Water Spray Heads Near the Fence are Used to Reduce Salt Concentration and the Potential of Flash-over Under Certain Atmospheric Conditions

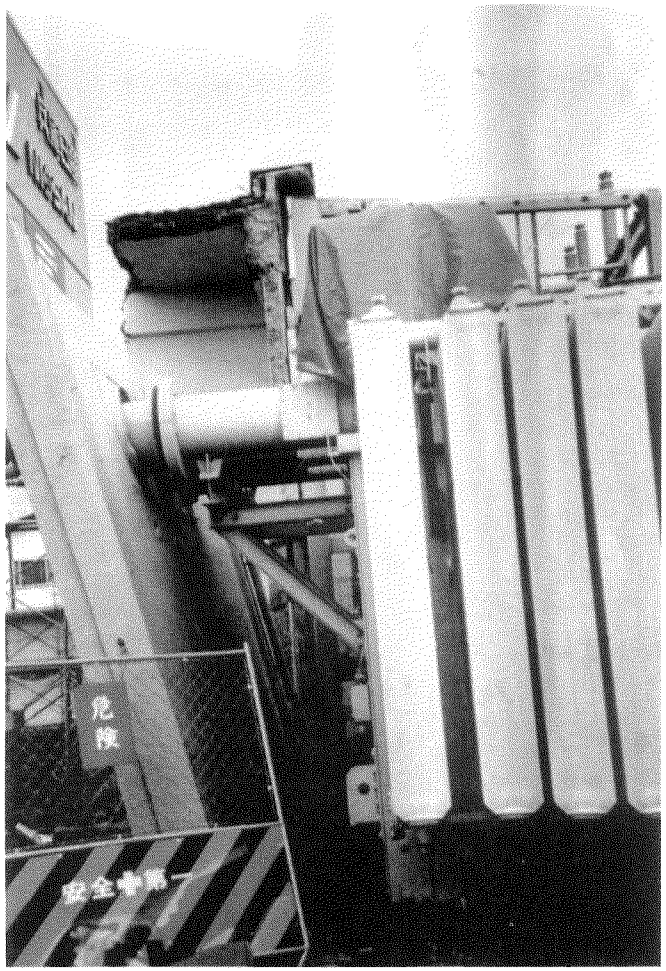


Figure 3-61 Transformer Pushed Over the Fire Wall After it Failed its Anchorage

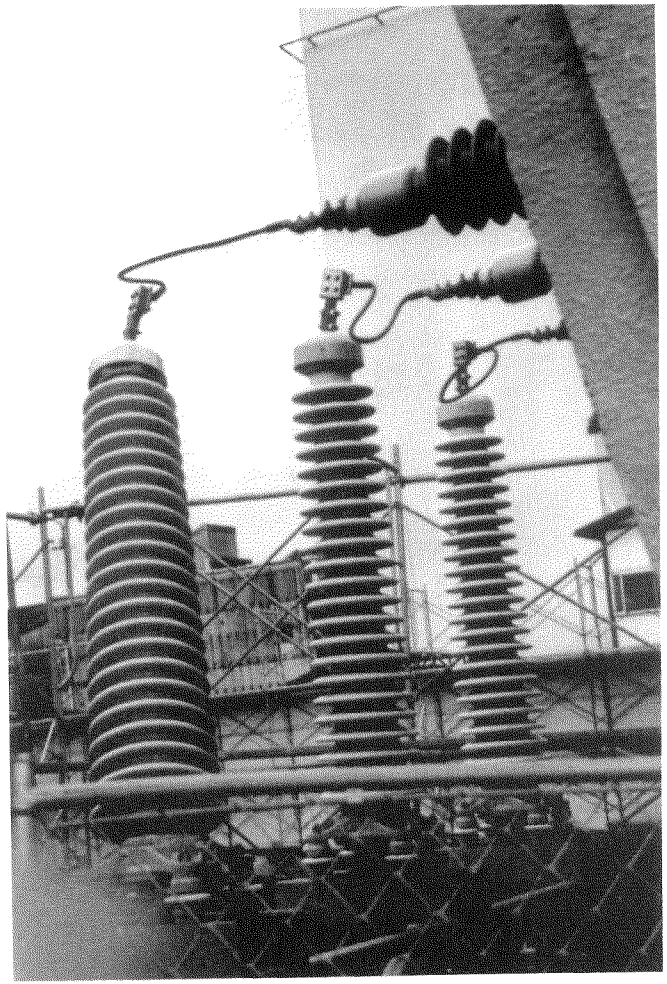


Figure 3-62 Pot Head Connected to the Bushing Failed, Probably When it was Hit by the Bushing

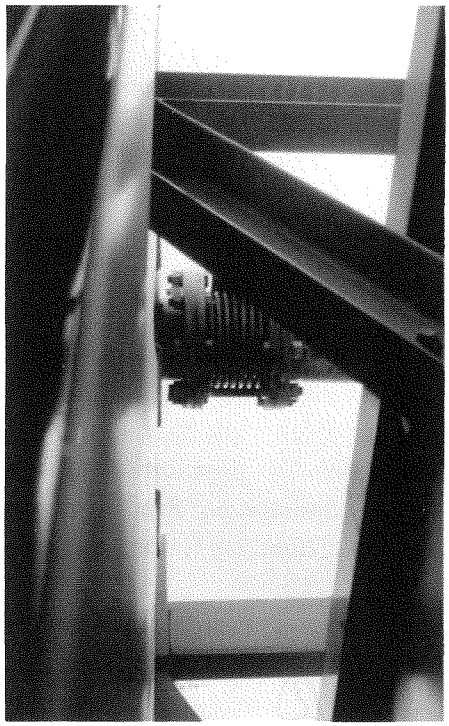


Figure 3-63 Radiator on This Distribution Transformer has a Structural Support and the Piping Connections have Flexible Couplings



Figure 3-64 Movement of the Transformer After its Anchorage Failed Allowing the Radiators to Hit a Nearby Structural Support Causing a Leak

associated with the control center and substation were well-restrained in battery racks that were well-braced and anchored and similar to those shown in Figure 3-39.

3.2.7 Performance of Generating Facilities

Just prior to the earthquake, 35 generating units were operating or in a startup process. However, of these 35 units, 12 units (eight units that were operating and four units that were in startup process) stopped due to excessive turbine shaft vibrations and other causes triggered by the earthquake. Among those units which automatically stopped, no damage was found to the facilities of four units, and these units were started up the same day. The remaining eight units, however, had leakage at boiler tubes and other problems and temporary repairs were completed by January 27, 1995. Figure 3-66 shows the location of generating stations in the earthquake impacted area. Table 3-VI summarizes damage reported to thermal power generating units that shut down as a result of the earthquake. Table 3-VII summarizes damage to generating units that

Table 3-VI Power Stations Sustaining Damage to Main Facilities and Experiencing Trouble in Power Generation

Power Station	Unit No.	Restoration Date	Equipment Damage
Higashi Nada gas turbine	1, 2	June 1996	o Land subsidence spread across the entire yard (fissures and liquefaction occurred) o Uneven settling of buildings and equipment foundations (gas turbine foundations and the like) o Exposed fuel tan foundation piles (fuel tank does not appear to be leaning) o Cracked, leaning time embankments
Amagasaki Higashi	**1, 2**	Jan. 19,18	o Land subsidence and fissures (areas surrounding the main building, on-site roads, and the like) Distilled water tank leaning, purified water tank has settled, drainage gutter damage, and partial cracking of oil retention embankment o Steel frame damage to turbine building (braced portions and the like) ● Pipe support damage (main steam pipes, high temperature reheating steam pipes, and the like)
Osaka PS	**1, 2, 4**	Jan. 22, 27, 23	● Boiler tube damage (cooling spacer tubes bent and fractured; wall tubes partially deformed from impacts)
Sakaiko PS	**2**	Jan. 20	o Boiler tubes bent (bending of cooling spacer tubes) ● Economizer header drain tube nozzle fractured
Sanpo PS	**1**	Jan. 23	● Economizer element damage (cracks developed on welded portions of attached metal fixture)
Himeji No. 2 Takasago Himeji LNG Terminal, etc.	**2**	Jan. 18	● Thermal insulation dropped off (high temperature reheating steam pipes and the like) o Building structure damage (cracks developed on the main building and service building) o Partial cave-in of soil bank

Legend: ● Repaired o To be repaired

Unit numbers in bold face type automatically stopped. The following units stopped, but were not damaged and were re-started - Himeji No. 2 (1, 3, 5), Takasago (2).

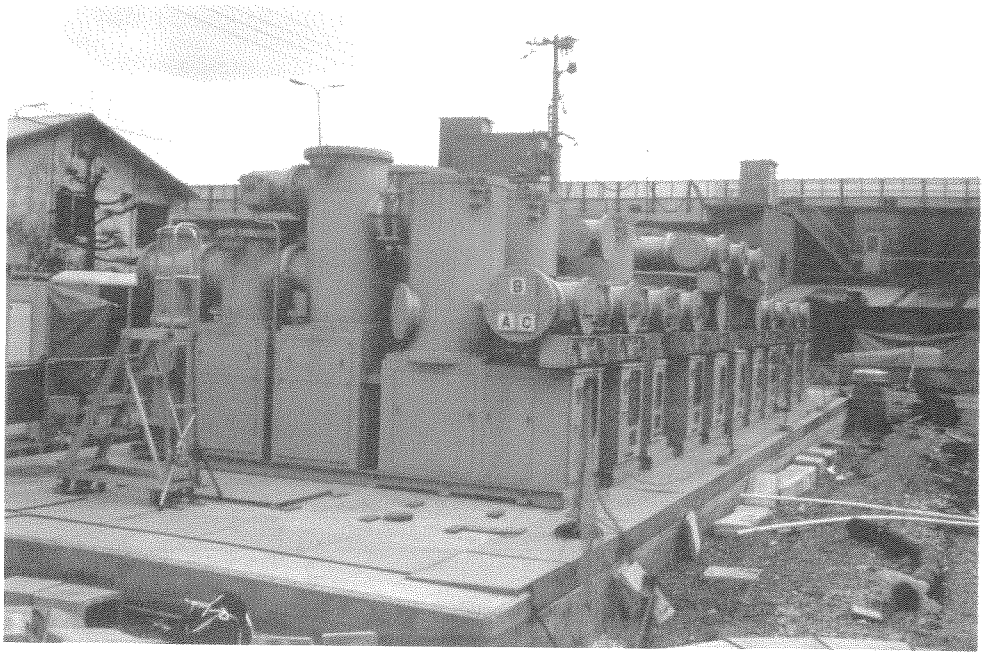


Figure 3-65 A 77 kV and 6.6 kV Gas Insulated Distribution Substation

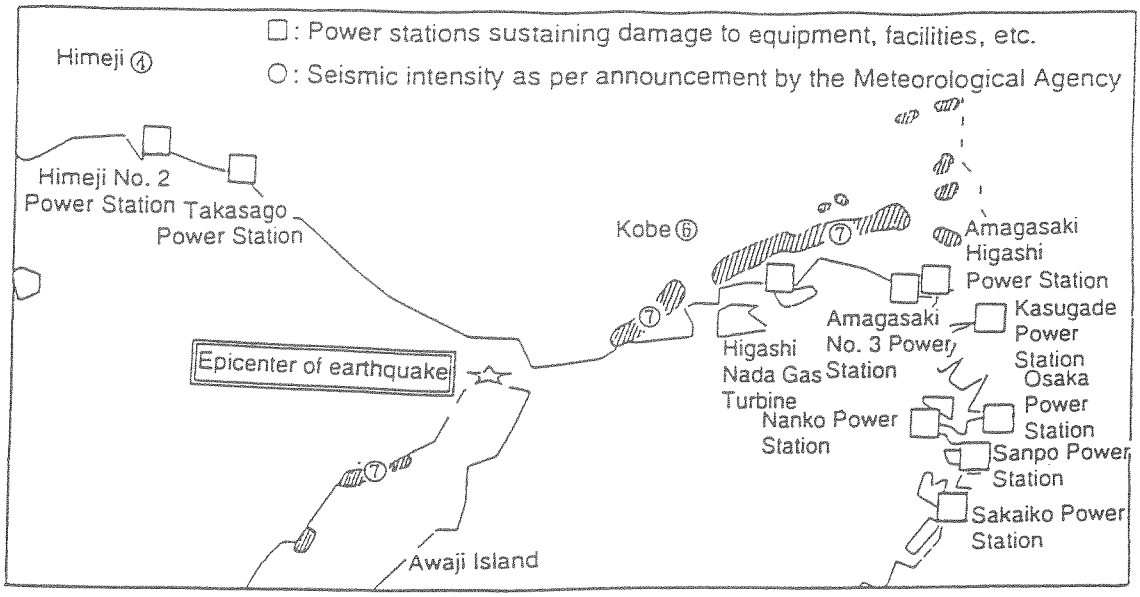


Figure 3-66 Location of Generating Stations in the Earthquake Impacted Area

continued to operate during and after the earthquake. No damaged generating station sites were visited. There were no leaks in fuel oil tanks at generating sites, but one tank was emptied as there was concern that it would leak due to a nearby soil failure. Soil deformation and liquefaction at generating stations, which were located adjacent to Osaka Bay, had the largest impact on generation facilities.

Table 3-VII Power Stations Sustaining Damage to Facilities

Power Station	Unit No.	Restoration Date	Equipment Damage
Amagasaki No 3	1 -3	Summer '95	Damage to boiler seismic-tie Deformed boiler frame
Kasugade	1, 2	Summer '95	Superheater and reheater spacers became detached from boiler
Nanko	1	February 2	Boiler tubes bent (cooling spacer tubes bent)
Osaka	2	February 3	Bent boiler tube
Sakaiko	1 4 7	April 26 May 11 June 10	Bent boiler tube
Takaigo	-	End Sept.	Cracked road on premises

3.2.8 Performance of High Voltage Transmission Lines

Problems with transmission towers was discussed in the section on the Itami substation (section 3.2.4). The damage did not disrupt the operation of the lines and was of a character described above. It was reported (Electric Utility Week, 1995) that ten transmission lines suffered damage, three 154 kV and seven 77 kV. In addition, two 275 kV towers, one 154 kV tower, sixteen 77 kV towers, and one 22 kV tower suffered slight damage, but did not effect service. Conductors opened on one 77 kV line and two 22 kV lines. There were broken insulators on thirteen 275 kV towers, twenty six 154 kV towers, and three 77 kV towers. One tower had problems with its footings. All lines were temporarily restored within two days.

3.2.9 Performance of the Distribution System

Because of the pervasiveness of the distribution system, only an extremely limited assessment of the damage was possible. Statistics for the distribution system are summarized in Table 3-V and were taken from a Kansai Electric report (March 7, 1995). Based on pictures that appeared in publications (Figures 3-67 and 3-18), much of the damage to the aerial system had been cleared and many repairs had been made at the time of the site visit, almost one month after the earthquake. Several types of damage were observed from the visit and a review of pictures in publications. In the Kobe business district, where the distribution system is underground in steel conduits, relatively little had been done to the system, and major demolition activities were underway to remove damaged buildings, many in excess of eight stories. It was reported (Electric Utility Week, 1995) that there were 446 circuits damaged along the Kobe districts 57,614,000 miles of distribution lines. Restoration required that 900 poles and 300 transformers be replaced, although the data in the Kansai Electric Power Co. report (1995) has much higher numbers.



Figure 3-67 Damage to the Aerial Distribution System was Severe in Many Regions

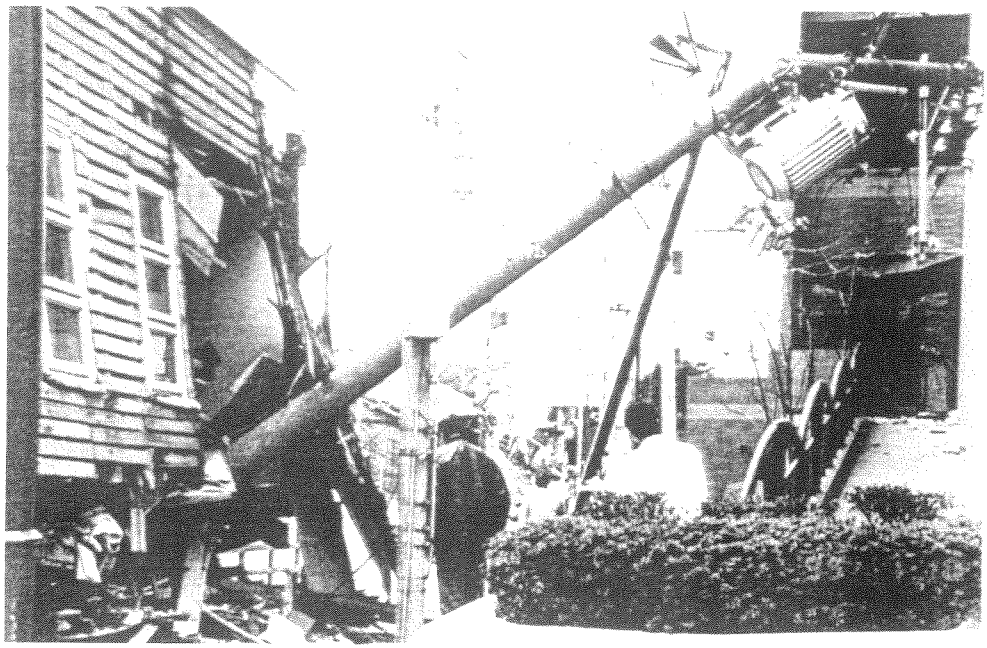


Figure 3-68 Fallen Houses Pushed Over Some Distribution Poles

The limited observations of the aerial system used outside of the central business district shows extensive damage to spun concrete utility poles. Clearly, many poles were pushed over when nearby houses fell into the street (see Figure 3-68). Other poles appeared to fail as a result of severe shaking, although some may have been pulled over by power lines connected to nearby poles that were knocked down by falling houses (see Figure 3-69). Downed poles were also a serious impediment to foot traffic (see Figure 3-70), and to a much lesser extent, to passage of vehicles. There were many cases where poles settled when the ground liquefied (see Figure 3-71). In this case, one of the most extreme examples, the stirrup protruding from the pole at a level just below the knee of the individual in the picture, was originally about 2 m above the ground, thus, this pole has settled about 1-1/2 m. To the casual observer, this damage is not obvious. It is not clear how extensive this type of damage is. There were many areas with liquefaction, particularly on Rokko and Port Islands.

The damage to underground facilities in the central Kobe business district was indicated by the distortion of some of the above ground transformers and disconnect switches (see Figure 3-72), and the distortion in pavements. In the business district, steel conduit, rather than plastic, was used. To the extent that the system has been inspected, there appears to be very little damage to the electrical cables, not withstanding the deformations experienced by the conduit. In a few locations, rather unconventional temporary repairs have been made to restore service (see Figure 3-73). Here, a 6.6 kV primary distribution line has been connected to a conduit below grade and strung on existing poles to a third floor window in a building across the street. The line was then brought to the units substation in the basement of the building so that power could be temporarily restored.

3.3 Lessons from Damage to Electric Power Facilities

The use of post tensioning to fabricate high voltage bushings appears to contribute to the poor seismic performance of transformers and circuit breakers in the U.S. and Japan.

The use of flexible coupling in piping connections of transformer radiator to the transformer body may reduce problems with leaks observed in the U.S.

The performance of instrumentation transformers in Japan appears to be better than in the U.S. Some units acted as lower restraints to suspended wave traps, and still performed better than in the U.S.

At potentially liquefiable sites, the need for adequate slack was demonstrated.

The use of concrete poles appear to increase the vulnerability of the aerial distribution system. In the 1992 Cape Mendocino earthquake, over 600 wooden poles were about to be replaced because they were weakened due to dry rot, and none of these failed.



Figure 3-69 Some Poles Failed Due to Inertial Loads or were Pulled Down by Other Fallen Poles

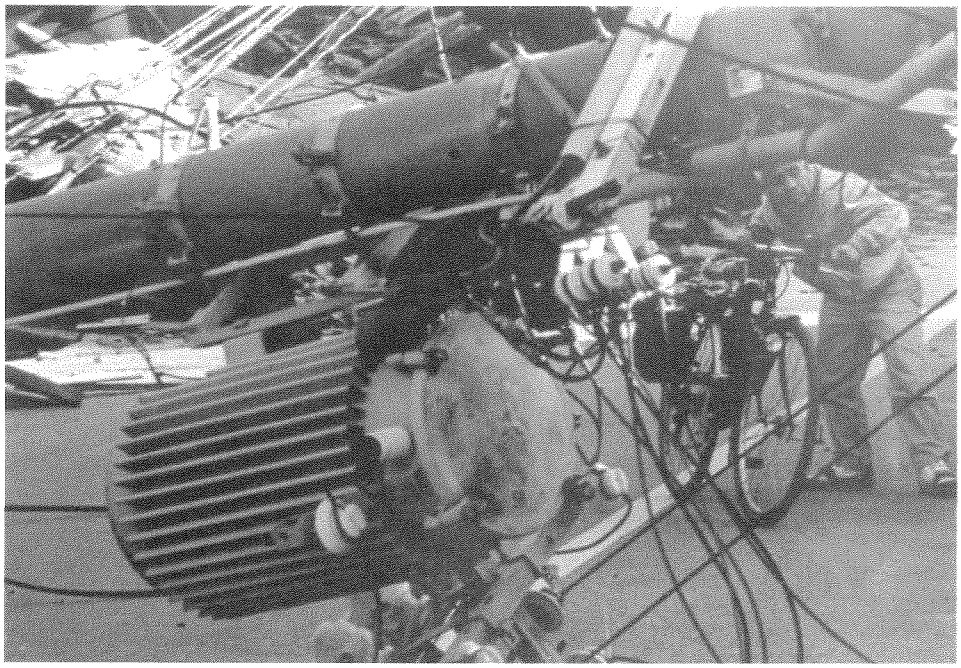


Figure 3-70 Fallen Poles Contributed to the Disruption of Traffic



Figure 3-71 This Pole Settled About 1-1/2 m Due to Liquefaction at the Site



Figure 3-72 Conduit and the Foundation Pad Under this Transformer Pad was Disrupted in Downtown Kobe Due to Soil Liquefaction



Figure 3-73 A Primary Distribution Line of 6.6 kV was Temporarily Installed to Restore Power to a Building

3.4 Summary

The overall performance of power systems, as measured by the extent and duration of disruption, was very good. The seismic performance of high voltage equipment was different than that observed in the U.S. In Japan, dead-tank circuit breakers were damaged and transformers failed their anchorage which contributed to bushing damage. In the U.S., more damage appeared to be associated with transformer bushing, the failure of current-voltage transformers, potential transformers, and disconnect switches. This earthquake indicated that if sites are subject to liquefaction, it is important that a flexible bus be used with liberal, but manageable slack. Transformer anchorage frequently failed. There was relatively little damage to high voltage substations as compared to what was observed in the Loma Prieta and Northridge earthquakes. The subsidence of substation sites appears to have contributed to the failure of bushings connected to vertical conductor drops, as little slack was typically provided. There was uniformly high quality use of good design and installation details in station batteries. The bushing performance of transformer and circuit breaker bushings in the U.S. and Japan were very different and unexplained. Discounting the direct damage to poles from falling houses, there appeared to be very high damage to the aerial system resulting from the failure of concrete poles.

3.5 Acknowledgments

Dr. Schiff gratefully acknowledges the help of Mr. O. Usuda and Mr. K. Matsuno in visiting the Itami substation, and many others at the Kansai Electric Power Co. who took time from their busy schedules to provide information on the earthquake response of their facilities. In addition, their openness to share information on the earthquake performance of their facilities is acknowledged. The help provided by Jim Stoner, Duke Power, in interpreting one-line drawings is also acknowledged.

3.6 References

Current Information on Kansai Electric Company, March 1994.

"Guide for Seismic Design of Substation Equipment," Japan Electric Association Guide: JEAG 5003-1980.

Electric Utility Week, January 30, 1995.

"Impact of The Earthquake of Southern Hyogo Prefecture on Electric Facilities," Kansai Electric Power Co., Inc., March 7, 1995.

SECTION 4
GAS DELIVERY SYSTEM

4.1 Overview of the Gas Delivery System

Natural gas for the areas most severely affected by the earthquake, including Kobe City, Ashiya, Amagasaki, and Nishinomiya, is supplied by the Osaka Gas Company, Ltd. The company provides gas to more than 5.6 million metered customers, accounting for 30% of the total gas sales volume in Japan. Major trunklines, pipelines, and distribution mains total 49,430 km. The Osaka Gas system is comparable in size to the gas delivery network operated by the Southern California Gas Company, which is the largest U.S. gas supplier with approximately 4.6 million metered customers and nearly 74,000 km of transmission, distribution supply, and distribution pipelines. Liquefied natural gas (LNG) accounts for about 94% of the Osaka Gas system feedstock. Most of the supply is imported by means of tankers from Brunei, Australia, and Indonesia.

Residential gas operations accounted for nearly 40% of total volume sales in 1994 and about 95% of the customer base. Industrial gas sales accounted for nearly 42% of total volume in 1994, compared to only 30% in 1989. The rapid increase in industrial supply shows the increasing dependency of industrial heat energy demand on gas. At the time of the Hanshin-Awaji earthquake, about 41% of the industrial heat energy demand in the Osaka Bay region was being met with natural gas to fuel heating units, such as furnaces and boilers.

Figure 4-1 is a map of the main facilities and pipelines of the Osaka Gas system. Three LNG terminals provide the primary sources for distribution. The two Senboku terminals have a combined capacity of 25.6 million m^3, and the Himeji terminal has a capacity of 8.1 million m^3. Gas is conveyed regionally through a system of major trunklines, which operate at internal pressures of 4 MPa. Transportation of gas also is accomplished through what is termed a "medium pressure" system of A lines, at internal pressures of 0.3 to 1.0 MPa, and B lines at internal pressures of 0.1 to 0.3 MPa. There are 19 gas distribution stations where 37 gas holders are located for a nominal overall capacity of 4.15 million m^3. Only the major trunklines, medium pressure A lines, and distribution stations in Kobe and Nishinomiya are shown on the map.

The Osaka Gas system is divided into what company personnel call "super blocks". The eight super blocks of the network are large areas which can be isolated through telemeter control by closing valves activated by compressed carbon dioxide. Closing valves with carbon dioxide allows for control independent of electric power supply. The system can be subdivided further into about 55 "middle blocks," each of which may provide service to hundreds of thousands of customers. The middle blocks must be isolated by means of manually operated valves. The low pressure pipeline system within the middle blocks can be subdivided again into sectors, each of which provides service to between 3,000 and 4,000 customers.

From 1976 to 1991, Osaka Gas was involved in a conversion program in which artificial gas plants, producing methane from coal and petroleum sources, were decommissioned and replaced with supply from LNG terminals. As a consequence of these changes and other operational

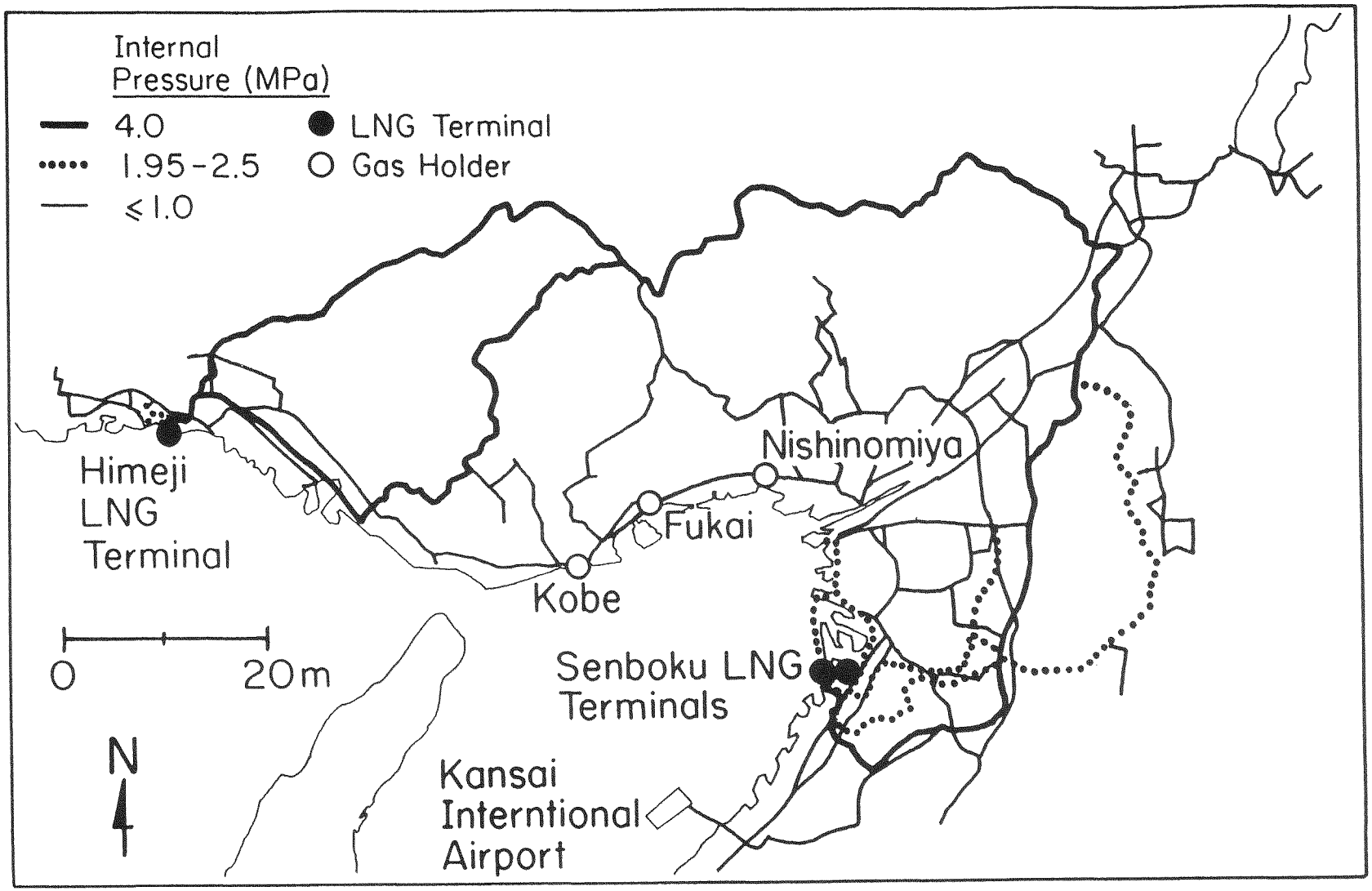


Figure 4-1 Map of Principal Facilities, Trunklines, and Major Pipelines Operated by the Osaka Gas Company

considerations, the distribution network was divided into the aforementioned sectors, each of which could be isolated and converted to natural gas. This partitioning of the system is typical of the way in which gas delivery systems are organized and can be used for system restoration in the event of major supply disruption.

4.2 Description of the Gas Delivery System

There was no significant damage reported at the Senboku and Himeji LNG terminals, and at the gas distribution stations. As shown in Figure 4-1, there were three distribution stations with gas holders at Kobe, Fukiai, and Nishinomiya. No significant damage was reported at these structures even though they were subjected to high levels of acceleration. Peak accelerations at the Fukiai and Nishinomiya stations of 0.85 and 0.81 g, respectively, were recorded.

At the time of the earthquake, there were 490 km of transmission, or trunk lines, in the system. The trunk lines were composed of X-42 or X-52 steel pipe with full penetration, electric arc, girth welds. Typical wall thickness for a 600-mm-diameter pipe is 12 mm. There was no damage reported in the trunk lines.

The medium pressure A lines were composed principally of steel pipe with full penetration, electric arc, girth welds. The oldest pipelines in this system were constructed in 1952. The medium pressure B lines were composed either of electric arc welded steel pipe or ductile iron pipe with restrained mechanical joints on 5 m spacings. The mechanical joints are similar to the S-type joints deployed in the water supply system. The joints are equipped with a locking mechanism, and were installed to allow 6 cm of extension and 2 cm of compression. There were 1,245 km and 3,800 km of A and B lines, respectively, at the time of the earthquake.

The greatest earthquake damage was sustained in the low pressure distribution system which operates at internal pressures equivalent to 150-210 mm of water column, or about 1.8 kPa. There were 43,895 km of low pressure lines at the time of the earthquake. In Kobe and adjacent communities, the low pressure system is composed predominantly of steel pipe with threaded steel couplings, or screw joints. A small portion of the low pressure system, approximately 5%, is composed of polyethylene mains and services. Some steel piping with restrained mechanical joints and polyethylene linings was deployed in areas of artificial fill as a seismic countermeasure.

4.3 Gas Pipeline Damage

Oka (1995) has summarized the number of repairs and principal types of damage sustained by both the medium pressure and low pressure distribution pipelines. Tables 4-I and 4-II provide tabulated data pertaining to the medium and low pressure pipelines, respectively.

Table 4-I indicates that there were a total of 35 and 71 repairs to medium pressure A and B lines, respectively. The damage was concentrated primarily at Dresser couplings and bolted flange joints. The Dresser couplings were typically 600-mm-long sleeve joints with compression gaskets and restraining devices against pullout. Damage was predominantly in the form of

Table 4-I Summary of Repairs of Medium-Pressure Gas Pipelines (after Oka, 1995)

	Steel Pipe					Ductile Iron Pipe				Total for Joints	Total for Pipe Bodies	Grand Total
	Welded Joint	Flange Joint	Mechanical Joint (Dresser)	Subtotal	Pipe Body	Mechanical Joint		Subtotal	Pipe Body			
						GM II	Bell-and-Spigot					
Medium-A pressure	8	5	22	35	0	NA	NA	NA	NA	35	0	35
Medium-B pressure	6	17	38	61	0	3	7	10	0	71	0	71
Total	14	22	60	96	0	3	7	10	0	106	0	106

NA - Not Applicable
GM II - Gas Mechanical Joint with a Compression Gasket

leakage where compression gaskets had loosened. A total of 14 low grade girth welds were damaged on steel pipelines. The low grade welds were installed before 1962 and were characterized by poor root penetration of the welds. Steel pipelines installed after 1962 were constructed in accordance with modern welding practices and did not sustain weld damage.

At several locations, medium pressure steel pipelines were subjected to large permanent ground deformation. Even though the steel pipelines were deformed at these locations, no leakage was observed. For example, the collapse of the Daikai Station (see Section 7.3 on Underground Rapid Transit Systems) imposed 2.5 m of settlement over a length of about 25-50 m on a 400-mm-diameter A-line. No leakage was reported at this location. Oka (1995) cites other examples of substantial steel pipeline distortion with no gas leakage at a landslide site and a location of liquefaction-induced bridge abutment deformation. These pipelines, which were composed of X-grade steel with full penetration electric-arc, girth welds, provides field evidence for the high degree of ductility and resistance to rupture of this type of modern steel pipeline.

Table 4-II summarizes damage in the low pressure distribution system. There was no observed failure in the bodies of steel pipe segments, and only 36 locations of ruptured cast iron pipe walls. The predominant type of damage was failure at the threaded, or screw, joints of steel piping and leakage and cracking at the joints of cast and ductile iron pipelines. There was a total of 5,190 repairs to distribution mains and branches within city streets, compared with 10,161 damaged service lines and 11,108 locations of damage at piping attached to buildings. Over 80% of the low pressure system damage was sustained by services. There were no repairs to polyethylene piping, although this type of piping accounted for less than approximately 5% of the overall system.

Table 4-II Summary of Repairs of Low-Pressure Gas Distribution Pipelines (after Oka, 1995)

	Steel Pipe						Ductile and Cast Iron Pipe					PE	Steel Pipe		Total for Joints	Total for Pipe Bodies	Grand Total
	Welded	Flanged	SGM	Screw	Sub-total	Pipe Body	GM II	Bell-and Spigot Type	Socket Type	Sub-total	Pipe Body		Joint	Pipe Body			
Main	0	NA	NA	NA	0	0	76	439	34	549	34	0	NA	NA	549	34	583
Branch	NA	NA	156	4451	4607	0	NA	NA	NA	NA	NA	0	NA	NA	4607	0	4607
Service Pipe	NA	NA	106	6045	6151	0	5	28	NA	33	0	0	NA	NA	6184	0	6184
Service Pipe on Customer's Property	0	0	59	3906	3965	0	3	7	0	10	2	0	NA	NA	3975	2	3977
House Pipe Between Meter and Cock	0	0	13	11085	11098	0	1	1	0	2	0	0	8	0	11108	0	11108
Total	0	0	334	25487	25821	0	85	475	34	594	36	0	8	0	26423	36	26459

NA - Not Applicable
SGM - Steel Gas Mechanical joint: special polyethylene-coated steel joint for mechanical joint connections
GM II - Gas Mechanical Joint with a compression gasket
Bell-and-Spigot Type - Joint with lead caulking and jute packing and a compression gasket
Socket Type - Conventional lead caulked joint with jute packing in cast iron pipelines
PE - Polyethylene

4.4 Emergency Response and System Restoration

The Osaka Gas Company operates a system of seismic sensors throughout its service area to provide rapid feedback about the likelihood of earthquake damage to pipelines and associated facilities. The theoretical aspects of seismic monitoring and control and the application of such measures to the gas system in the Osaka area have been described by Takada, et al. (1992). The monitoring system works by telemetering data from an array of seismic sensors, which were deployed throughout the service area, to the company control center in Osaka. Data from the sensors, which includes acceleration and velocity, provide information about the severity of ground motion. In combination with the appropriate algorithms, these data can be used to estimate levels of damage. With these preliminary damage assessments, field crews are directed to confirm or modify the estimates and proceed with emergency operations.

At the time of the earthquake, 34 sensors had been installed throughout the service area, and company plans had been implemented to install an additional 30 sensors. Strong motion data were acquired from the seismic sensor array, and additional information was obtained through emergency calls from customers and reports from field personnel during the morning of 17 January.

Figure 4-2 is a map showing the eight super blocks and middle blocks of the Osaka Gas system. The gas supply was shut down in the five middle blocks shaded in the figure. Osaka gas personnel report that by 11:30 a.m. on 17 January, gas supply was suspended to 386,000 customers in Blocks 2 and 3. Blocks 7 (102,000 customers), 1 (221,000 customers), and 4 (124,000 customers) were shut down by 4:15 p.m., 5:10 p.m., and 9:00 p.m., respectively, suspending gas supply to a total of 836,000 customers. By 23 January, gas supply had been discontinued to 857,400 customers, or 15% of the total in Osaka Gas' service area. Venting from gas pipelines was accomplished by radio-controlled venting regulators on major trunk lines and manually operated valves on medium pressure lines. In areas of the system outside the five shaded blocks in Figure 4-2, there were 24,844 reports of gas leakage.

Approximately 6,000 employees of Osaka Gas and 2,300 personnel from 86 other utility companies were engaged in the repair and restoration shortly after the earthquake. The outside work force from other utilities was increased to approximately 3,700 by early March.

Restoration was performed on a sector-by-sector basis. After a sector was isolated, each customer meter box was closed and air pressure tests were performed on mains and services. Leaks were repaired and additional air pressure tests were performed. After repairs to mains and services, leakage tests and repairs, if needed, were performed in each customer building. Restoration progress was hampered by the need to clean water and debris which had washed into broken gas lines from adjacent soil and ruptured water mains. Restoration also was restricted by blocked and damaged roads and traffic congestion. Full restoration of a single sector often required four to five days.

By 13 February, all medium pressure A lines had been put back into service, and the B lines were almost completely restored. By 13 and 22 February, gas service had been restored to 32% and

46% of the customers, respectively. It was not until mid-April, however, that gas service had been restored throughout the system, excepting severely damaged structures. As of 24 April, gas was restored to 700,000 customers. Because of structural collapse, fire, and associated damage, service could not be restored to roughly 160,000 customers.

The total expense of restoration is estimated at 190 billion yen, or approximately $2.3 billion. This cost covers network repair, replacement, administration, and related activities.

4.5 Seismic Gas Shut-Off Valves

Approximately 74% of customers were equipped with intelligent meters according to Osaka Gas personnel. A three-dimensional view of an intelligent meter is provided in Figure 4-3. The meter is equipped with a seismic sensor triggered by acceleration exceeding 0.2 g, a pressure sensor, and a flow rate transducer. The pressure and flow rate sensors detect abnormal drops in pressure and increases in flow, respectively, which are indicative of broken and disengaged piping and gas appliances. A microcomputer monitors the incoming signals and shuts off flow, if required. A lithium battery is used as a power supply for the microcomputer and gas shut-off valve.

Gas company personnel report that the intelligent meters appear to have functioned as intended. Data were not available, however, at the time of writing this report from which to assemble statistics about meter performance or to assess the extent to which the meters reduced fire initiation.

4.6 Lessons from Damage to the Gas Delivery System

One of the most important lessons associated with gas system performance during the Hanshin-Awaji earthquake is the need to coordinate the restoration of electric power with an assessment of the state of gas system repair. In the first day after the earthquake, electric power was restored to 60% of customers at the same time that shutting down and venting of middle blocks were being performed and appraisals were being made of gas system damage. It appears that there was no pre-arranged coordination between gas and electric company personnel to restore electric service in concert with shutting off and venting gas in areas severely damaged by the earthquake. Although the consequences of restoring electricity in areas of gas leakage have not been fully evaluated, it appears that early restoration of electric power in areas with leaking gas contributed to additional fires.

Emergency plans should be drawn up and hard, formal communication procedures should be established between gas, electric power, water supply, and fire department personnel. Specific checking mechanisms should be embodied in emergency response and restoration procedures so that gas and electric power personnel cannot proceed beyond a certain recovery level until there has been formal confirmation by their counterparts that gas systems are secure.

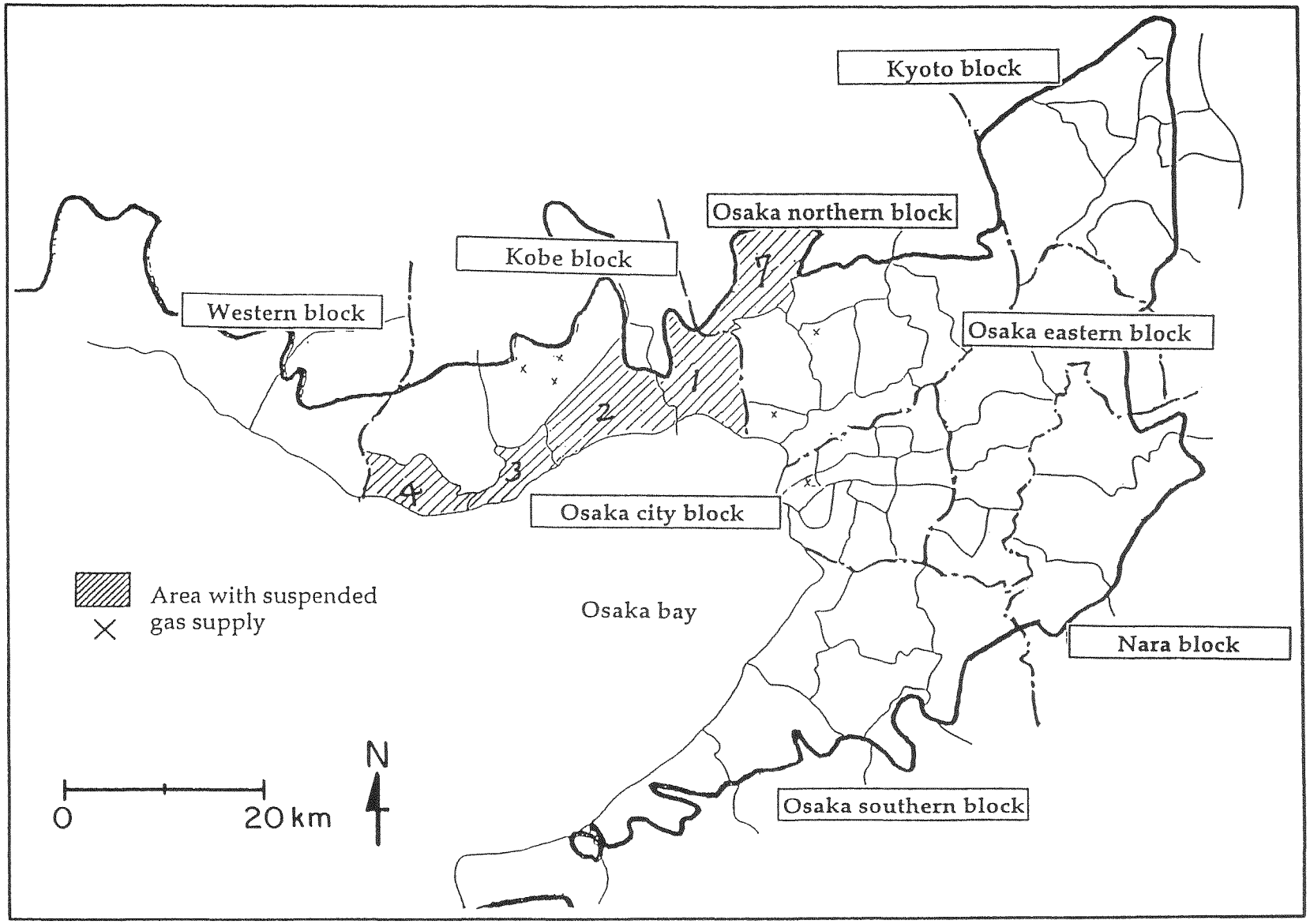


Figure 4-2 Map of Super Blocks and Middle Blocks in the Osaka Gas System Showing Areas Where Gas Flow Was Shut Off After the Earthquake

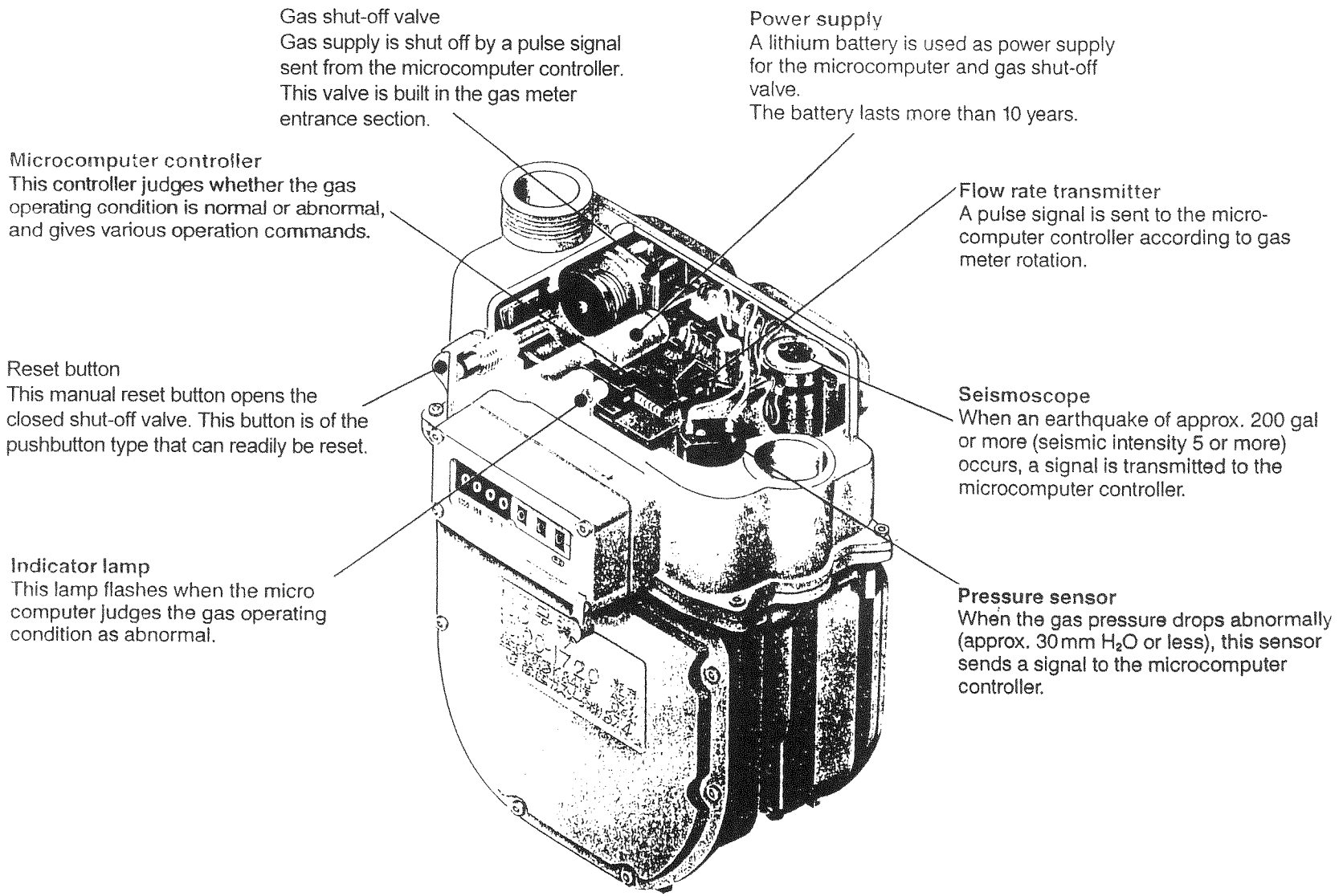


Figure 4-3 Three-Dimensional View of the Osaka Gas Intelligent Meter

The difficulty and substantial time required for restoration of gas service in Kobe is an important reminder of the complexities and resources required for the resumption of gas supply after large areal shutdowns. Restoration of gas can be especially critical in winter, as it was in Kobe. It may be advantageous, therefore, to provide for remote control and other rapid means of isolation of smaller, more manageable areas of the gas system. Strategies of this type require microzonation techniques which are capable of identifying areas with the potential for locally severe site response and soil liquefaction. Hazard mapping and scenario earthquake planning can be especially valuable to identify and isolate troublesome areas.

Although the widespread damage to steel pipe with threaded steel couplings occurred at an unprecedented scale, the vulnerability of this type of piping has been recognized and reported in the technical literature (Katayama and Isoyama, 1983; O'Rourke, et al., 1985). Threaded steel sections are not only vulnerable to earthquake effects because of reduced cross-sectional area, but because threaded sections tend to be locations of corrosion concentration. A threaded coupling provides for a rigid connection, and thus lacks the longitudinal flexibility inherent in a pipeline with mechanical couplings that maintain a seal with compression gaskets.

The extensive damage to vulnerable piping is a very important lesson and a sobering reminder of potential earthquake effects in older systems. Although threaded steel piping is used rarely in U.S. gas systems, many U.S. systems do use cast iron mains for low pressure distribution. Several of these systems are located in midwestern, eastern, and west coast portions of the U.S. which are susceptible to serious earthquakes, albeit with various return intervals. Although cast iron pipelines have provided generally long and reliable service, they nonetheless are composed of brittle material that does not possess sufficient ductility to accommodate large ground deformation caused by liquefaction or locally high transient motion. Given the vulnerable nature of cast iron pipelines to large differential movement, it is especially important to identify portions of cast iron systems in liquefiable soils as the basis for network isolation, replacement, and special emergency response planning.

4.7 References

Katayama, T. and R. Isoyama, (1983), "Damage to Buried Distribution Pipelines during the 1971 San Fernando Earthquake," Earthquake Behavior and Safety of Oil and Gas Storage Facilities, Buried Pipelines and Equipment, PVP-Vol. 77, American Society of Mechanical Engineers, pp. 124-132.

Oka, S., (1995), "Damages of Gas Facilities by Great Hanshin Earthquake and Restoration Process," Proceedings, 6th U.S.-Japan Workshop on Earthquake Disaster Prevention for Lifeline Systems, Osaka, Japan, Public Works Research Institute, Tsukuba, Japan.

O'Rourke, T.D., M.D. Grigoriu, and M.M. Khater, (1985), "Seismic Response of Buried Pipes", Pressure Vessel and Piping Technology - A Decade of Progress, C. Sundararajan, Ed., ASME, New York, NY, pp. 281-323.

Takada, S., T. Fuke, and J. Ueno, (1992), "Seismic Monitoring and System Control for Lifelines," Technical Memorandum No. 3198, Proceedings of the Fifth U.S.-Japan Workshop on Earthquake Disaster Prevention for Lifeline Systems, Tsukuba Science City, Japan, pp. 481-502.

SECTION 5
HOSPITALS

7.1 Overview of Hospitals

The investigation of hospitals focused on the impact of lifeline disruption on hospital operations. Some additional information was gathered, but issues related to the medical response and patient treatment were not investigated. The Kobe Medical College of the University of Kobe was visited (Medical College of Kobe University, 1995). A limited amount of information about the Hyogo Medical Center was also obtained through a brief interview (Hyogo Medical Center, 1995).

The Kobe Medical College is located about 10 km east-northeast of the epicenter. It is about 1 km north of the Japan Railroad Kobe station and up a slight hill from the shore. Thus, the buildings on the campus are not on reclaimed land adjacent to the Osaka Bay. There are several buildings associated with the college including a new hospital building, built about 1985, an old hospital building, built about 1967 and at least one large classroom and laboratory building. The two hospital buildings are about 10 stories high. They were joined by a narrow section that contained corridors connecting the two buildings. The old hospital building did have cracks in a first floor wall between windows that was being repaired with injected epoxy (see Figure 5-1). This damage indicates that there was significant ground motion at the site.

The hospital appears to be similar in some respects to teaching hospitals in the U.S. It is a critical care facility and obtains its patients primarily by reference from physicians of patients that have special needs. The earthquake did not have a significant impact on admissions to the pediatric section of the hospital.

5.2 Description of Damage to Hospitals

Kobe Medical College of the University of Kobe

There appeared to be relatively little structural damage to the hospital, except as noted above. In the new wing of the hospital, a section of a wall that joins the new and old wings had severe local damage due to interaction of the two buildings where the corridor connects the two buildings (see Figure 5-2). There was some spalling of concrete adjacent to at least one seismic joint observed during the short visit to the hospital.

There were reports that equipment in a ward on the 10th floor moved and some items fell from work tables to the floor.

There apparently was some damage to the oxygen distribution system causing a drop in pressure in the system. The hospital has a centralized oxygen source that is then distributed throughout

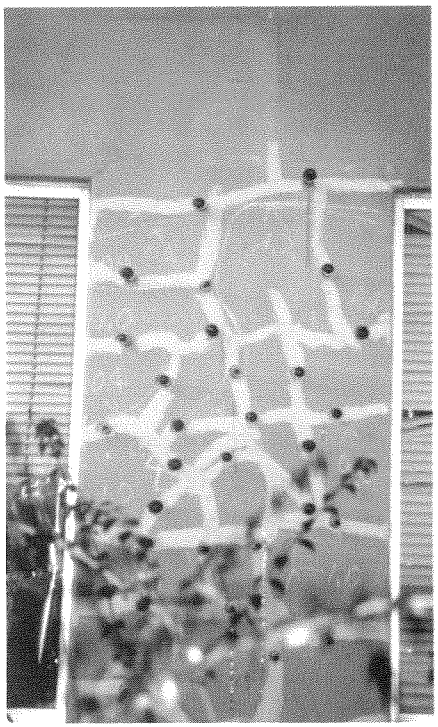


Figure 5-1 Column on First Floor of Old Hospital Being Repaired with Epoxy Injection



Figure 5-2 Beam Shattered Due to Interaction Between the Two Wings of the Hospital at Crosswalks Connecting the Buildings

the hospital. One patient in the pediatric ward, who was dependent on oxygen, was transferred to another hospital. The cause of the problem could not be explored because of a lack of time.

The hospital has two emergency generators, one each in the old and new wings of the hospital. The unit in the new wing, which was assumed to be 10 years old - the same age as the wing - is a large diesel-generator. It was designed to start automatically when there is a loss of commercial power and provides emergency power to the hospital complex. It was installed on elastimer vibration mounts (see Figure 5-3). This type of mount was observed on all emergency generators in Japan, including some units that were about 30 years old (see Figure 5-4). This type of engine mount has not been observed in the U.S., although it would appear to have some advantages over mounts used in the U.S. The elastimer probably has good damping characteristics and the mount does not need a snubber to limit motion. This was an advantage because when vibration-isolated equipment hits snubbers, large accelerations can result. All utility connections to the engine-generator were provided with flexible couplings. The engine-generator, like many large units, uses compressed air to start the generator. The air tanks and compressor were well anchored (see Figure 5-5). The day tank was supported on a well-braced and anchored structure (see Figure 5-6). There was a 3,000 liter water storage tank used for engine cooling water that was well anchored and provided with flexible couplings. The cooling system for the diesel engine uses a single pass system. That is, water from the water tank passes through and cools the engine, and then is dumped into the sewer system. Water to refill the tank was provided from the municipal water supply.

The engine-generator in the old wing of the hospital was a smaller unit and was a quality installation similar to the unit in the new wing (see Figure 5-7). This unit was started manually and serves as a back up to the new unit. This engine had a closed loop cooling system that included a cooling tower on the roof of the hospital. This type of system makes much better use of the available water, but still requires that evaporative losses, which take place in the cooling tower, be made up. The make up water for the engine cooling system comes from the building water supply, which will be discussed below.

The engine in the new wing started when commercial power was lost. However, due to the loss of the municipal water supply, when the small tank near the engine was empty, there was a loss of cooling water and the unit shut down due to overheating. The old generator, with the closed loop water cooling system, was switched manually to pick up the load in the new wing, and this appeared to meet the emergency needs of the hospital.

There were no provisions to simply connect an external generator to the facility should both generators have failed to operate.

Commercial power was restored to the hospital at 8:40 a.m. on the 17th, and the generator was shut off two hours later after commercial power continued without interruption.

Three large buildings in the hospital complex have an integrated water system depicted in Figure 5-8. The system consists of a tank on top of each building and a common large water storage

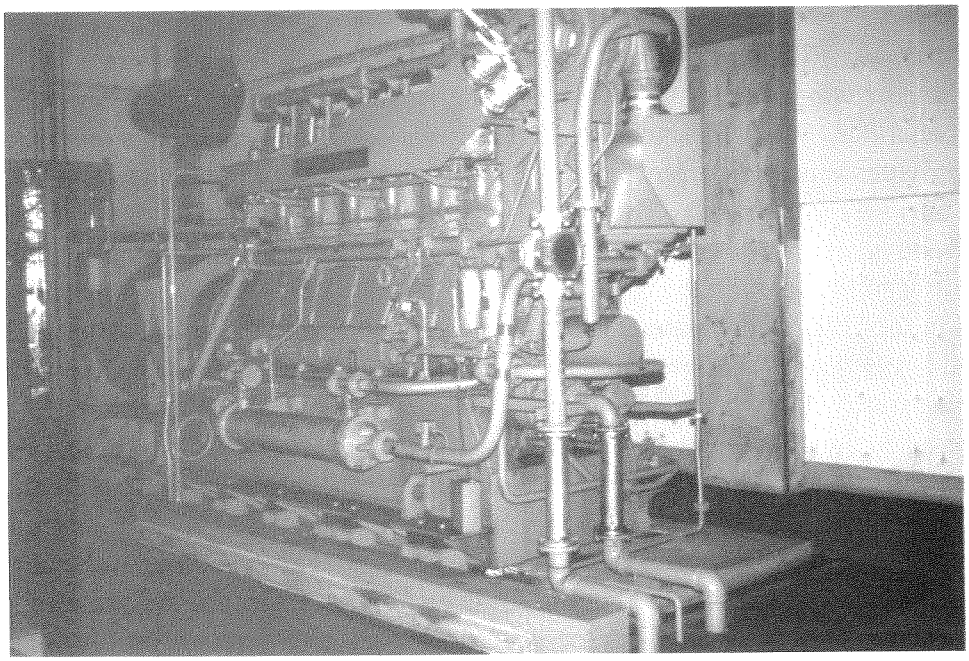


Figure 5-3 Engine-Generator in the New Hospital Wing, which has Vibration Isolators and Flexible Connections on Utilities

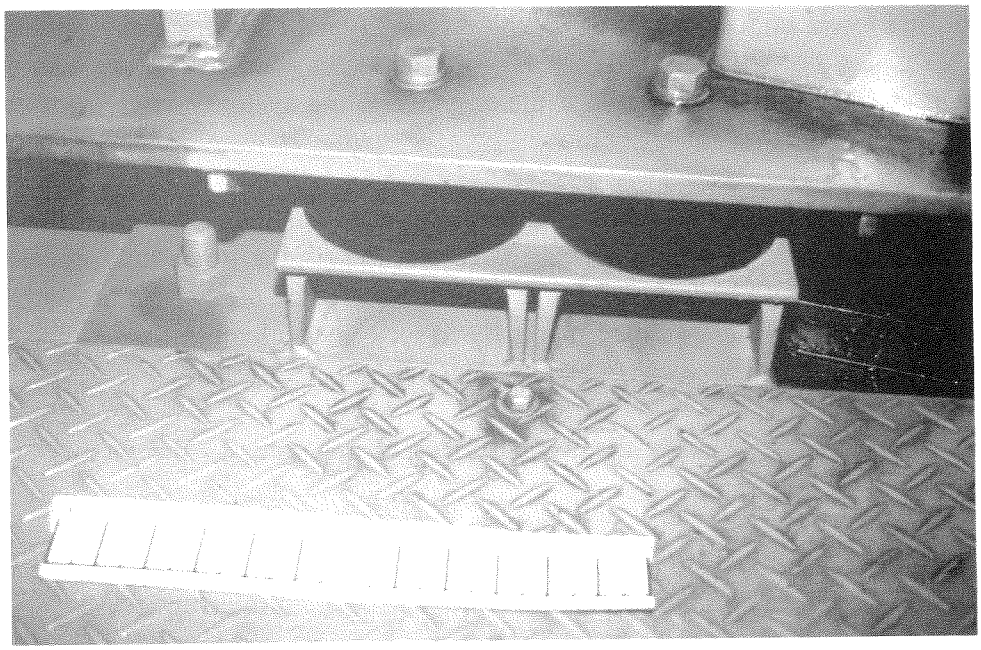


Figure 5-4 Detailed View of Vibration Isolators Used on Emergency Power Engines

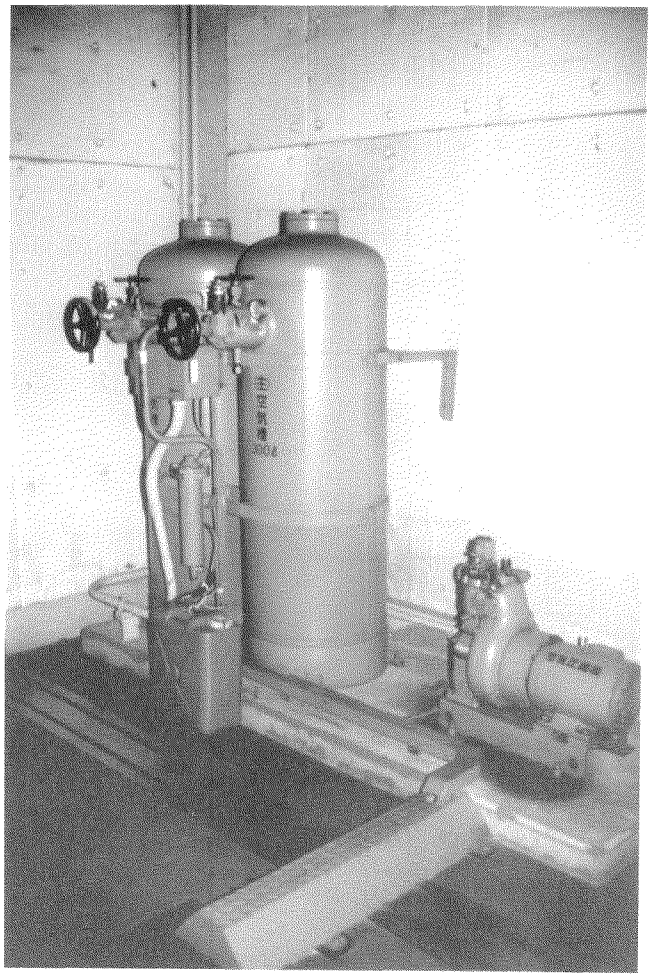


Figure 5-5 Compressor and Air Storage Tanks Used to Start the Diesel Engine

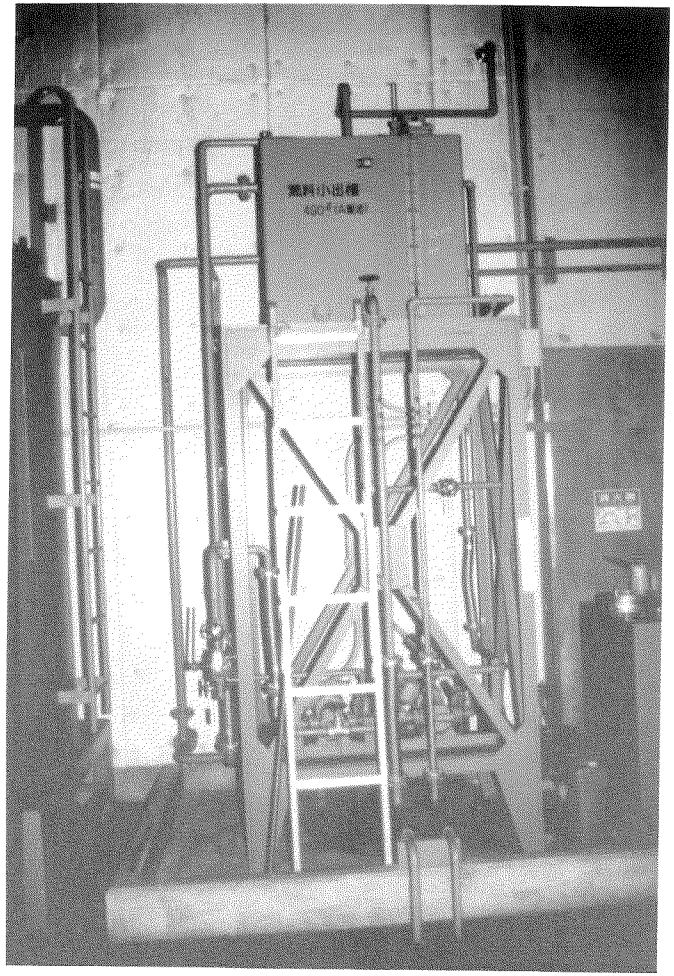


Figure 5-6 Day Tank and Pump for the Fuel Supply to the Diesel Engine

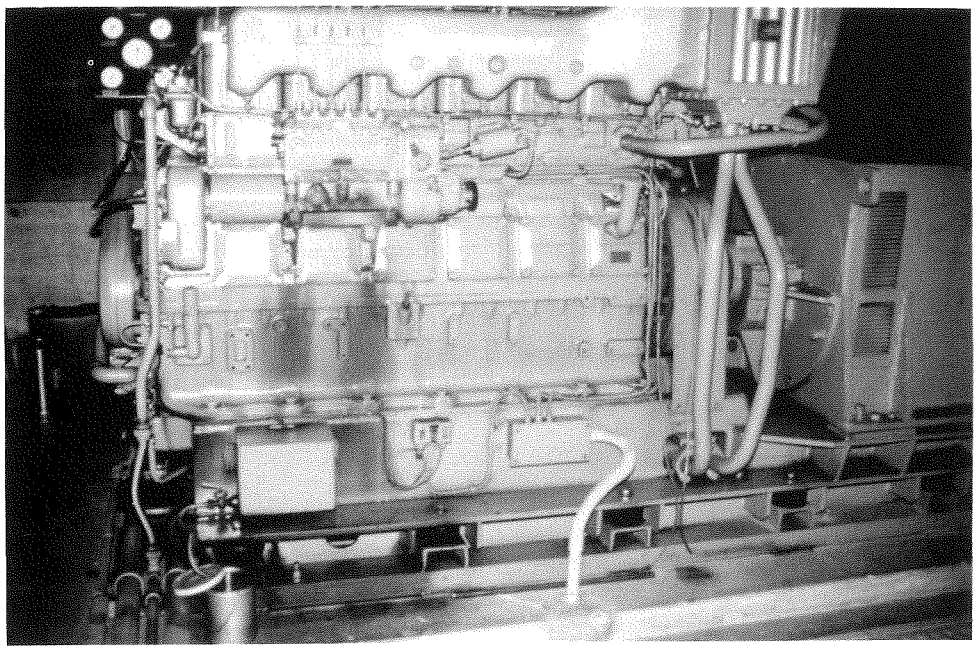


Figure 5-7 Diesel Engine Used for Emergency Power in the Old Wing of the Hospital

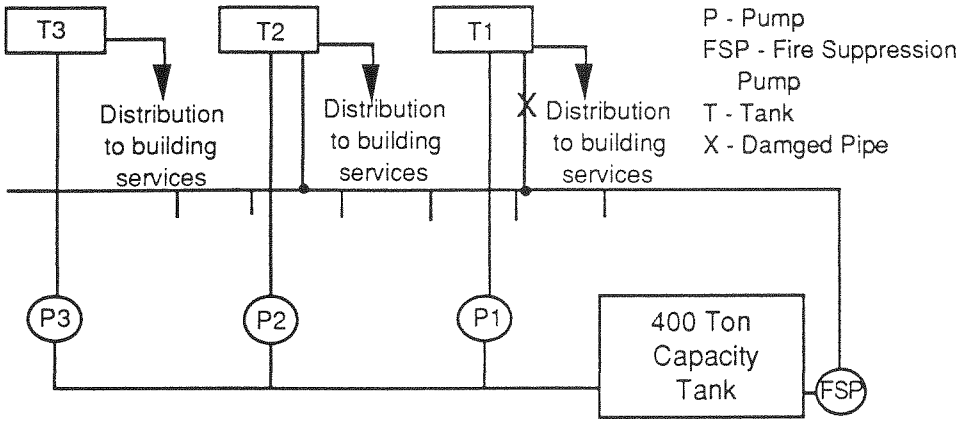


Figure 5-8 Schematic Diagram for the Kobe Medical College Water System

tank with a capacity of 400 tons (400,000 liters). It should be noted that very few hospitals in the U.S. have the water storage capacity of the Kobe facility. This tank, which is supplied with water by the municipal water supply, has four pumps associated with it. Three supply tanks are located on the roof of each of the buildings. Each of these tanks supplies the water needs for their respective buildings. A fourth pump supplies water to the fire suppression system in the three buildings. This pump also supplies water to two of the building tanks. There was a pipe failure in the line connecting the fire suppression system to the tank in the old hospital, Building No. 1. This system also supplied make up water to the emergency engine in the old hospital wing.

There was a break in the pipe connecting the fire suppression system to the tank in Building 1. The pump that feeds this tank and the fire suppression system were shut off after the danger of fire had passed. It was not known if Building 1 lost all of its water supply or the extent of flooding that may have occurred due to the pipe failure. The water contained in the roof tanks and the main storage tank lasted for six hours. Provision was made for a tanker truck to deliver water to the hospital - 20 tons every two hours. However, there was no simple way of getting the water from the tanker truck into the hospital system. Initially, this water was carried to the top of the building manually, as none of the elevators were operating. By the second day, one of the elevators was operating so that the water did not have to be carried to the roof manually, but other than the elevator ride to the roof, it was a manual operation. This operation continued until the municipal supply was restored after four or five days.

The telephone system within the hospital consisted of a main distribution frame (see Figure 5-9) Private Branch Exchange (PBX), an uninterruptable power supply (UPS), cable trays, and a remote switch. The Private Branch Exchange was connected to Nippon Telephone and Telegraph (NTT) trunks through the main distribution frame. The uninterruptable power supply (batteries) were charged by commercial power or the emergency generator in the complex, if commercial power was lost. In addition, there were a few telephones connected to NTT through the main distribution frame without going through the Private Branch Exchange (see Figure 5-10). These were to provide communications in the event that there was a failure in the Private Branch Exchange. The communication equipment was well anchored to a regular building floor (raised floors were not used in the communications room). The batteries for the uninterruptable power supply were mounted in a cabinet, and restrained by brackets attached to the shelves (see Figure 5-11). The restraints were not snug at the ends and they were made of relatively light weight metal. It was interesting to note that the cells and bus straps connecting the cells are constructed so that the top edges of the cells butt against each other, thus, there was no need for spacers between the cells. The battery cabinet was well anchored. The communication cable tray sections were bolted together (see Figure 5-12) so that they formed a structural system. The communication cable trays typically used in the U.S. were fabricated with friction clips, so that units cannot withstand tensile loads (see Figure 5-13). The trays were bolted to structural walls (see Figure 5-14). This was a more reliable method of anchoring the cable trays that the J bolts that are often used in the U.S. (see Figure 5-15). The main distribution frame was bolted to the cable tray to provide bracing at the top of the frame to limit its motion (see Figure 5-16). There were no problems with the main communication facilities. The remote system had unspecified

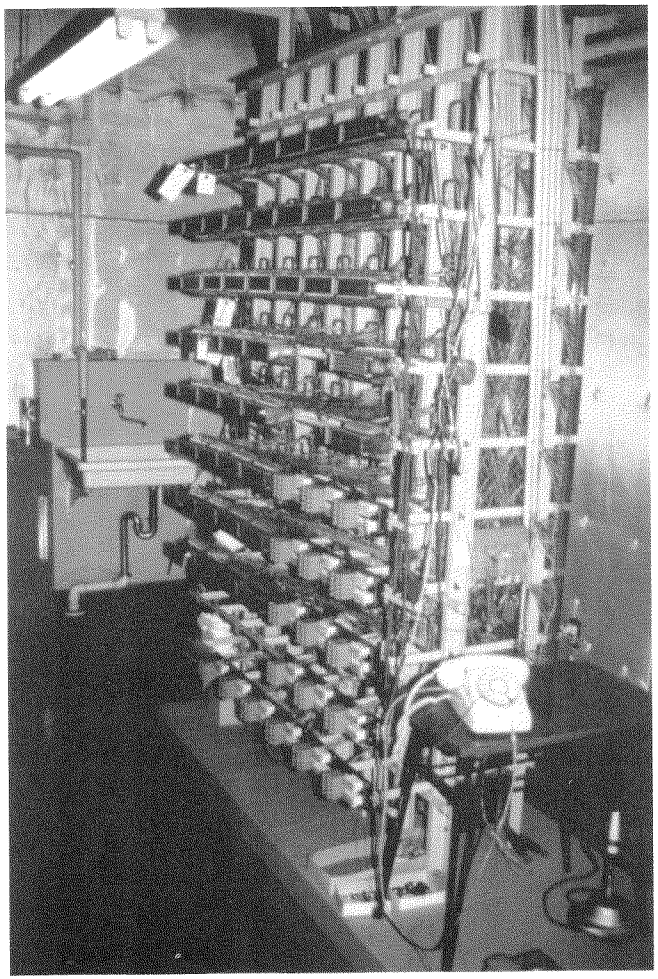


Figure 5-9 Main Distribution Frame for the Hospital Communication System

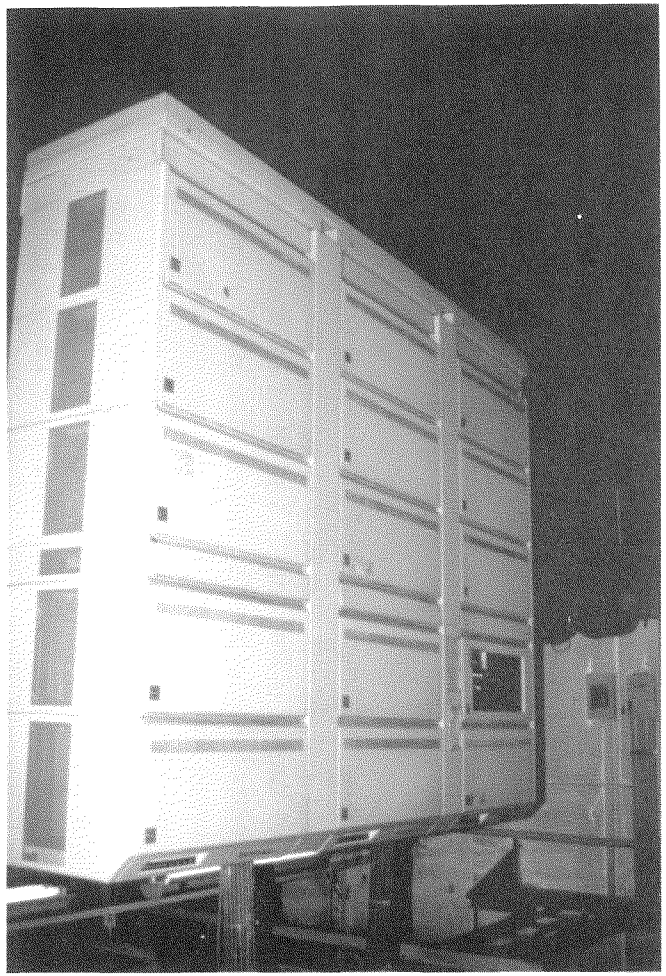


Figure 5-10 Part of the Private Branch Exchange (PBX) Switch Used by the Hospital

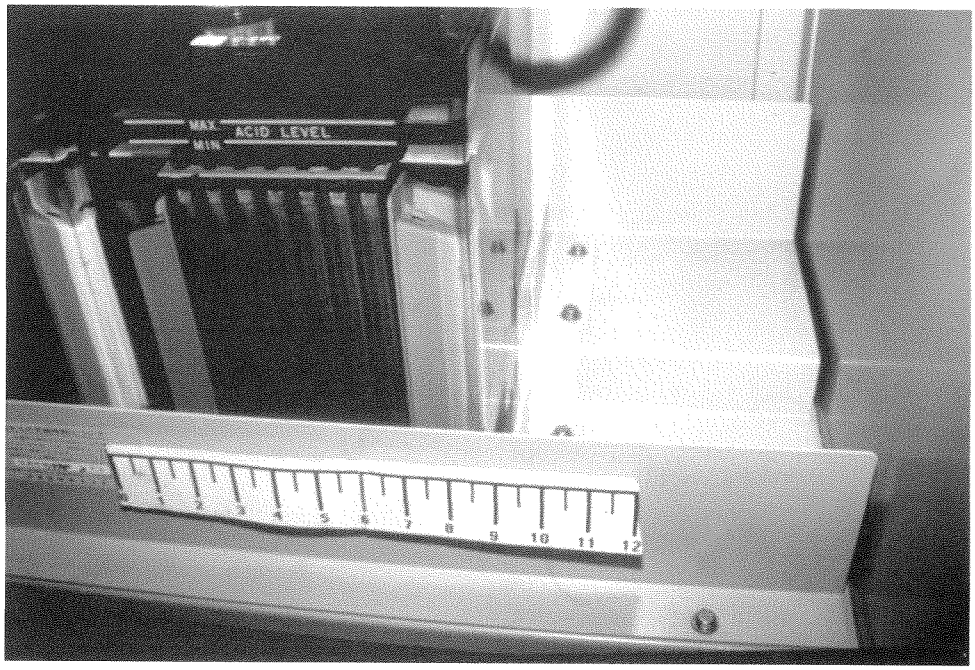


Figure 5-11 Battery Within UPS Used by the PBX (Note that cells fit snugly together, that there is a gap between the end restraint and the cell, and that the end restrain is light weight.)

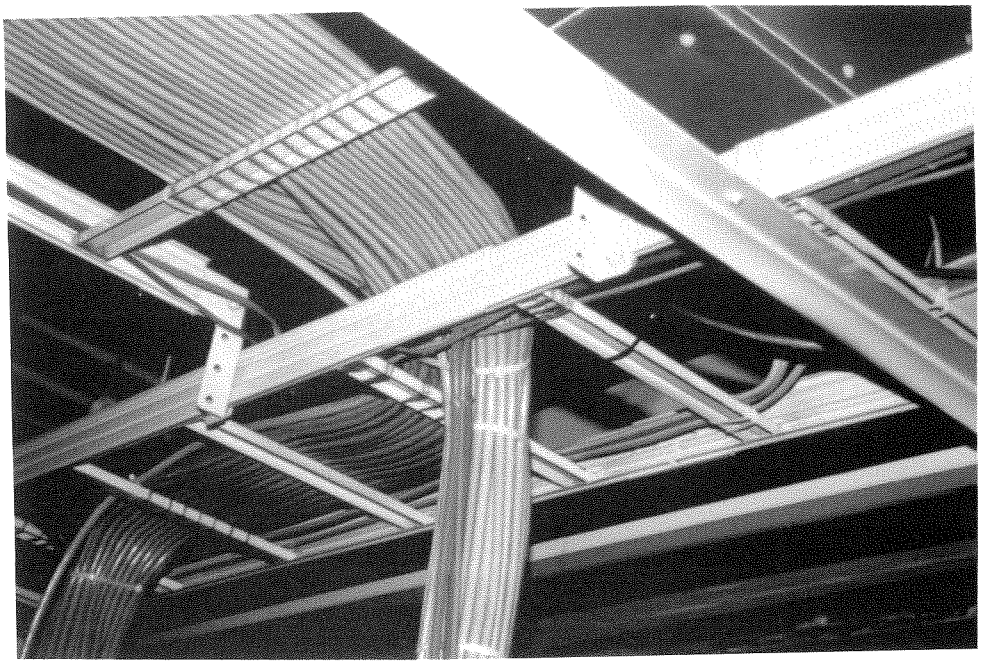


Figure 5-12 Cable Trays Used by the Telecommunication System Use Bolted Connections



Figure 5-13 Typical, Low Tensile Strength, Friction-Clip Type Communication Cable Tray Hardware Used to Join Tray Sections in the U.S.

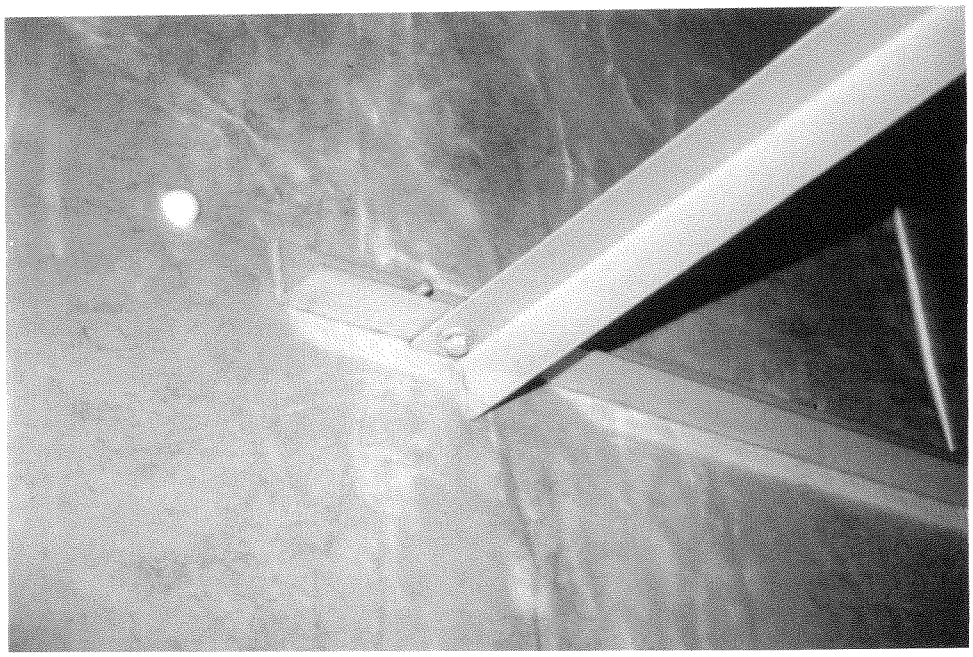


Figure 5-14 Bolted Connections are Used to Anchor Cable Trays to Structural Walls

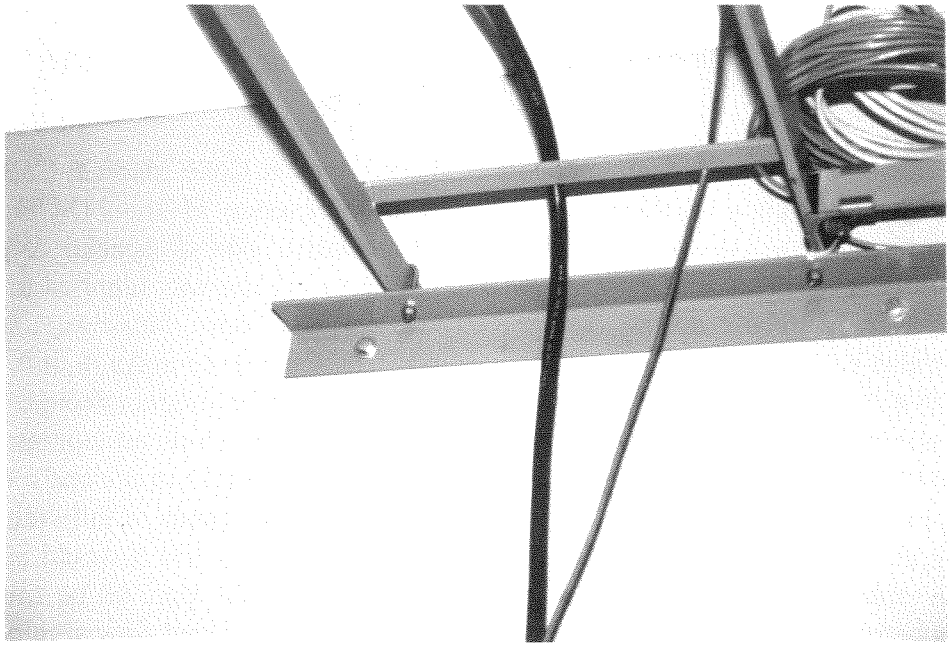


Figure 5-15 J bolts are Often Used to Secure Cable Trays to Walls; These Type of Connections have not been Reliable

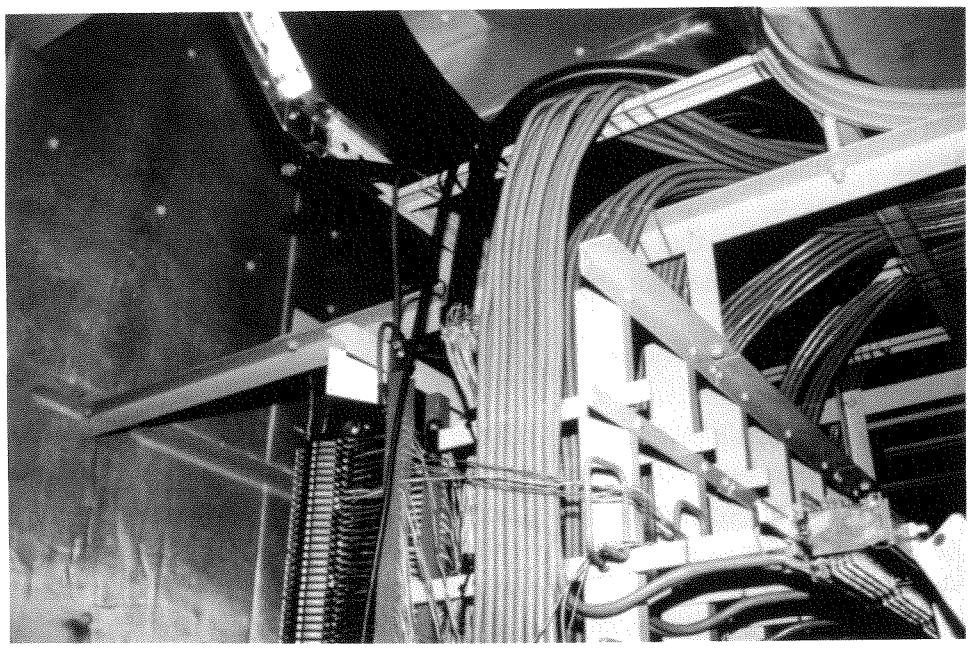


Figure 5-16 Main Distribution Frame is Bolted to Cable Tray to Provide Bracing at the Top of the Frame

problems, however, there was insufficient time to explore the difficulties. The impact of congestion on the NTT telephone system on hospital operations was not known.

The loss of the gas supply also had a large impact on hospital operations, as gas was used for preparing patient food.

It might be interesting to briefly compare some of the lifelines at Kobe Medical College with a university teaching hospital in California, namely Stanford University Hospital (SUH). It should be noted that no comparison was made between the relative size or special roles that the respective institutions may have in their unique environments. Water was supplied to SUH from the municipal system. There are no storage facilities for raw water, however, a well at the university can also be connected to supply the hospital. There are three tanks (6,000, 1,600, and 600 gallons) that store water treated by reverse osmosis that can be interconnected. The water used for dialysis was treated by a special processing unit and there was no storage capability. There was a 6,000 gallon liquid oxygen tank that supplies the hospital's needs and a distribution system. There are also many small portable units that can meet the needs of individual patients. The main oxygen distribution system has many sectionalizing valves, but it would be very time consuming to isolate sections to find a leak, as all patients would have to be transferred to portable tanks before a section could be isolated. The reduction in overall flow would have to be compared with use in the isolated section to determine if there was a leak. There are shut off valves for gas within the hospital. Research labs and the kitchens use gas. The kitchens also have electric stoves. Emergency power for the main hospital complex was provided by a large co-generating unit located on campus. It was interesting to note that if there was a loss of the municipal water supply, the co-generating plant will have to shut down.

Hyogo Medical Center

The location of this 200 bed facility was not known. As a result of the earthquake, a water tank on the roof of the hospital collapsed, flooding part of the hospital. As was true in many parts of Kobe, there was a loss of water and power. Because of the loss of water, the emergency generator would not operate so that the hospital lost all power and it had to be evacuated. The water to the hospital was disrupted for about two weeks.

5.3 Lessons from Damage to Hospitals

The loss of water supply at Kobe Medical College indicates that hospitals need to establish an emergency water use policy and procedures as normal water use was well beyond what one could expect in resupply after a major earthquake. There was also a need to facilitate getting delivered water in to the hospital water system. This requires that there be appropriate water hookups and pumps. The hookups do exist for fire service on some facilities. That was, there was an external access to a stand pipe that was fitted with a valve or check valve so that an external source can be attached to the system when the system was pressurized. As in the Loma Prieta and Northridge earthquakes, it appears that some critical facilities, such as hospitals, should have a method for quickly hooking up an external generator should the emergency power fail. The impact of the

loss of gas on food preparation was also significant, as many patients require special meals. As in the U.S., the loss of elevators in a hospital was a common problem.

5.4 Summary

The quality of lifeline facilities and their installation, from an earthquake engineering perspective, observed in the hospital visited was very high as compared to U.S. installations. Few U.S. hospital would have a large emergency water supply as existed at Kobe Medical College. The loss of water still had a large impact on hospital operations. It disabled one generator at the hospital and also caused the loss of all emergency power at another medical facility. The 400 ton capacity water storage tank only lasted six hours, which implies that almost 70 tons were used per hour immediately after the earthquake. The resupply by tanker truck was only at a rate of 10 ton an hour, so that water use had to be significantly reduced. The dependence on gas for food preparation was disruptive to hospital operations. The distribution of lifelines within a hospital needs review. Special services, such as the distribution of oxygen, can be disrupted, particularly when lines pass through seismic joints.

5.5 References

Through contact established by Dr. David Stevenson, Department of Pediatrics, Stanford University Hospital, and his colleague in Japan, Dr. Nakamura, Head Pediatrics, Medical College of University of Kobe, an interview was conducted with the help Dr. Tanaka, Department of Pediatrics, with the head of building services, 1995.

Information about the Hyogo Medical Center was gathered through a brief interview of a physician who was familiar with some of the impacts of lifelines at the hospital, 1995.

SECTION 6
TELECOMMUNICATIONS FACILITIES

6.1 Overview of Nippon Telegraph and Telephone (NTT) Corporation

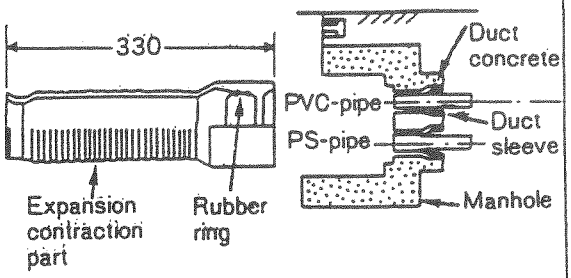
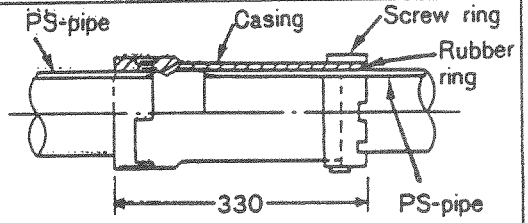
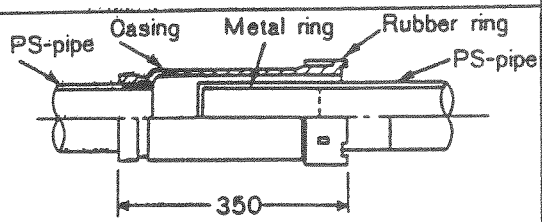
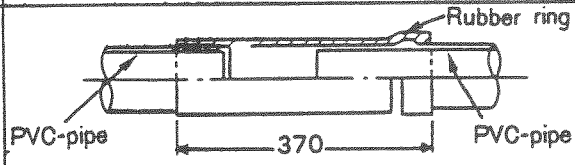
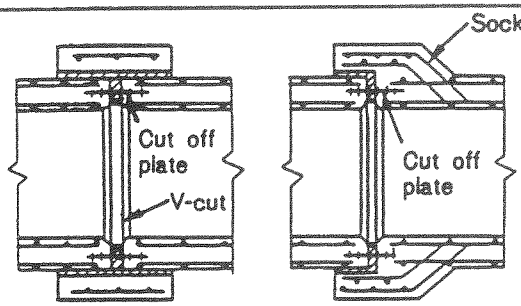
The telephone communication system is dominated by NTT, although independent companies are now providing long-distance services. The large metropolitan areas of Tokyo, Nagoya, and Osaka have diverse communication routing systems installed (IEEE, 1990). The Osaka regional center has connections to five district centers, and there is a loop connecting the district centers providing multiple redundant transmission routes. There are also priority service lines in Japan that are available to customers at additional charges that connect the customer to two central offices, although diverse routes from the customer may not be used. It appears that this option is available at lower cost in Japan than in the U.S. as it is used more frequently. In addition, special provisions have been made to new conduit installations to improve their earthquake resistance. Table 6-I shows current measures used to improve the earthquake resistance of conduit joints. It was reported that welded steel conduit was exclusively used. This is in contrast to the U.S., where plastic conduit is used. Central offices are connected by optical fiber, copper cable and microwave trunks. Tunnels are used to carry communication trunk lines. NTT has two types of tunnels; bored or shielded tunnels make up 60% of the tunnel system, and cut and cover tunnels make up the other 40%. The shielded tunnels are from 7 m to 20 m deep and are about 4.5 m in diameter. The cut and cover tunnels are from 2 m to 4 m deep, and their cross sections are 2 m to 3 m square. In addition, there are joint utility tunnels made by the government that have separate sections for communication, power, and gas lines that are paid for by a utility tax. These tunnels tend to be very costly, but are encouraged by the government because they reduce the impact of surface transportation caused by the installation of tunnels or repair of buried lines. Tunnels have sumps or pumps to remove water that leaks into the tunnel.

The annual capital expenditures of NTT are about $200 billion; annual revenues are about $400 billion.

6.2 Description of Damage to NTT

A briefing was held at an NTT facility at which system damage was described and pictures of damage were distributed. An NTT news release was also distributed (Damage and Restoration, etc., 1995). The earthquake reconnaissance team of the Technical Council on Lifeline Earthquake Engineering (TCLEE), ASCE, also provided information on system response. No damaged central offices were visited in Kobe. The total loss was estimated by NTT to be ¥300 billion, which at today's exchange rate (83¥/$) is over $3.6 billion. It is understood that NTT was not insured for earthquake damage to network facilities. It is unknown whether this cost will be recovered through rates.

Table 6-I Current Measures Used to Improve Earthquake Resistance of Conduit Joints

Name	Structure (Unit : mm)	Application
Duct sleeve		At manhole duct
Expansion Joint		At end of protection concrete
Stopper Joint		On the side of the bridge abutment
Expansion Joint for Pipe Installed in a Bridge		At movable pier
Expansion Joint for Tunnel	 (a) Collar type expansion joint (b) Socket type expansion joint	On the side of telephone office and in places where topographical changes are extreme

6.2.1 Central Offices

Three central office buildings sustained damage, but the damage had no effect on operations except for one office. The three damaged central offices at Kobe, Kobe Sai, and Nishi Ku were restored by January 29. Three building-mounted towers were damaged. One, which was removed later, is shown in Figure 6-1. A buckled member can be seen on the inner cord on the right leg. Because of the concern that the tower may collapse, the building was evacuated until the tower was removed. The tower on the Daikai building was back to normal on January 21 and the one on the Kobe Port building was back to normal by January 24. They have been reinforced.

There was a loss of commercial power in most of the earthquake impacted area (see Section 3). Of the 1,440,000 lines in the Kobe area, 285,000 had problems related to power failures. By noon on January 18, electrical problems were solved by the restoration of commercial power or the use of mobile emergency generators. As in the U.S., central offices have large battery power plants that can provide power for several hours and there was an engine-generator to recharge the batteries to provide long-term emergency power. There was no battery damage. It was reported that at one central office, the engine-generator would not operate because there was a loss of municipal water needed for cooling. The central offices do not appear to have provisions for a quick electrical hookup when a generator fails, as are now being added by some California utilities. It is not clear why only one central office was impacted by water disruption, as most of the area was without water. It was also not clear why the loss of air conditioning, which also requires water, would not have impacted operations, as switches usually require cooling, even in winter.

6.2.2 Outside Plant

There was extensive damage to conduit at manholes and at locations where it entered central offices. The information received at the briefing indicated that there were no failures to optical fiber trunks and only a few to copper trunks. Reliable, independent sources indicate that there was damage to optical fiber trunks. The news release (Damage and Restoration, etc., 1995) notes that the earthquake caused damage to 193,000 lines, and approximately 100,000 were restored by January 31. The remaining lines that were out of service were due to collapsed or fire destroyed buildings. There was also damage to 3,170 special service lines, and approximately 2,730 were restored by January 31. There were 440 of these lines that could not be restored and temporary lines were laid.

There were varying degrees of damage to tunnels. A superimposition of a seismic intensity map on the NTT tunnel network indicated that about 6 km were in JMA 7+ zone, 2 km in JMA 6 zone, and 4 km in JMA 5 zone. After the earthquake, 10 sump pumps that were used to remove water that collected in the tunnels due to leaks and seepage had to be operated using mobile generators due to the loss of commercial power. These generators were obtained through contract. It was noted that waterproofing specialists were in short supply after the earthquake to make tunnel repairs, and were thus critical in terms of making timely repairs.

The shield tunnels had no damage. There were problems with some of the cut and cover tunnels. A manager and three supervisors checked out the 12 km of buried tunnel in Kobe area, and the damage was repaired by March 26. At the Mindato Central Office, which is located about 200 m from Kobe Bay just north of Highway 43, the tunnel settled relative to the building about 7 cm and shifted about 7 cm laterally, however, there was no damage to trunk lines. Figure 6-2 shows a schematic diagram of the tunnel-building connection and a post-earthquake repair used to stop water leaks. This detail is used throughout Japan. There was minor damage to the Joint Utility Tunnels, primarily slight movement at construction joints resulting in leaks, as shown in Figure 6-3. Communication cables in the Joint Utility Tunnel had fire resistant covers near entrances and staircases, but were generally unprotected (see Figure 6-4).

At many manholes, the conduits were pushed into the manhole boxes by up to 30 cm. This can exceed the available cable slack and cause a cable failure (see Fig 6-5). The relative motion also can damage the manhole-conduit seal, and water seepage can also damage the cables. In older conduits, cable slack was 2 cm at the manholes, and some of these broke. At new conduits, cable slack was up to 15 cm, and these did not break. It appears that there can be large variations in slack provided to cables at manholes. In an earlier visit to Tsukuba City, an NTT Outside Plant research group proposed service loops of about 8 cm diameter before each splice joint. However, a tie-wrap to secure the loop to a tray or shelf was also recommended, so that the deployment of the slack may be impeded. Liquefaction and soil movement also moved junction boxes (see Figure 6-6). Figure 6-7 shows a schematic diagram of a 4 cm offset of plates used to form the manhole entry. Subsidence of soil around manholes also caused conduit failures (see Figure 6-8). Conduit carried on bridges were also damaged due to the motion of the bridge deck (see Figure 6-9). Subsidence in roadways also caused extensive damage as can be seen in Figures 6-10 and 6-11. Telephone booths were also severely damaged by soil failures (see Figure 6-12).

At a stream crossing, the telephone conduits were supported on their own bridge. The slope on one side slumped into the water, imposing large deformations on the bridge and conduits, and causing the failure of the conduits. Visually, the displaced conduits appeared to have moved up to 1 m. The walls of a canal moved towards each other causing conduit spanning the canal to buckle (see Figure 6-13).

The extensive damage to concrete poles used to carry aerial lines is discussed in Section 3.2. In addition to the failure of poles due to liquefaction, inertial loads, and interaction with fallen houses and other poles, some lines were damaged due to fire (see Figure 6-14).

6.2.3 Network Operations

There were significant problems with congestion, that is, attempts to place more calls than the system could accommodate, a situation common in the U.S. from even minor earthquakes. On January 17, call volume from other parts of Japan to Kobe increased by a factor of 50 over normal traffic. This dropped to 20 times normal traffic on January 18. There were reports that it would typically take 10 attempts to complete a call. At the same time, it may only take three



Figure 6-1 Microwave Tower on Top of a Central Office which was Damaged and Later Removed

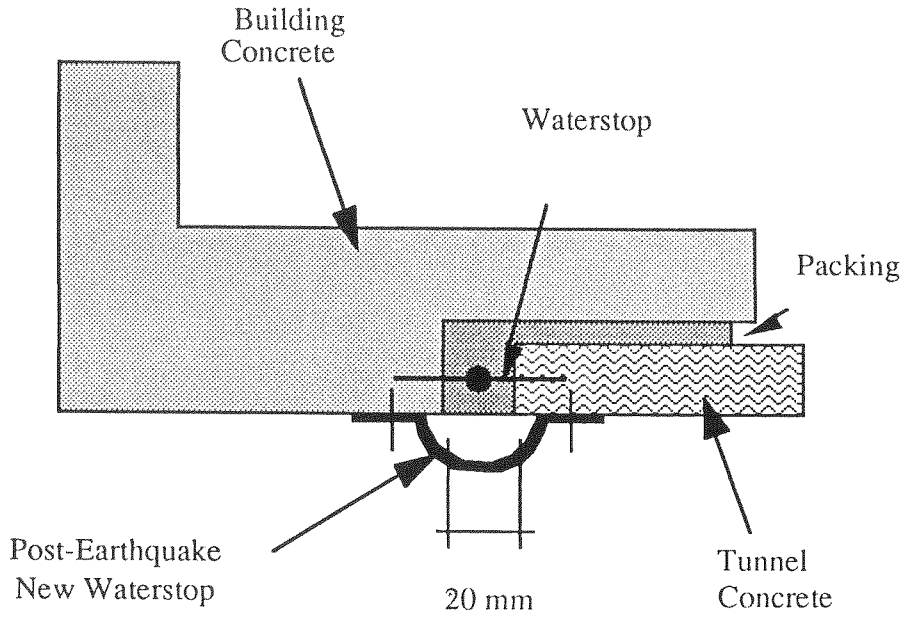


Figure 6-2 Schematic Diagram of Tunnel-Building Connection Detail and Post-Earthquake Repair

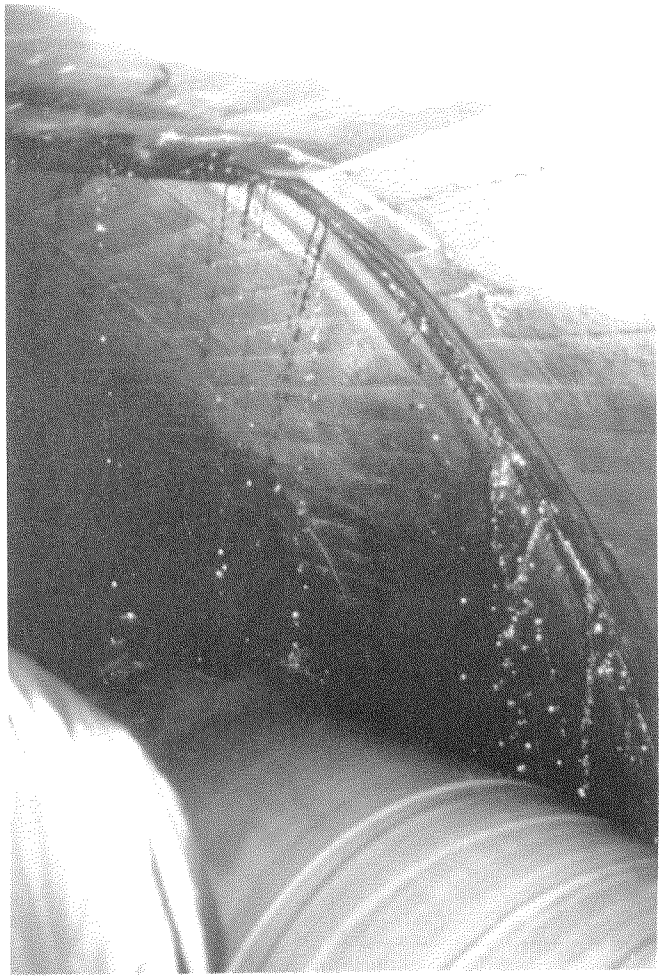


Figure 6-3 Slight Movement at a Construction Joint Caused a Small Water Leak in a Joint Utility Tunnel



Figure 6-4 Trunk Lines in the Joint Utility Tunnel had Fire Retardent Covers Near Entrances and Stairways

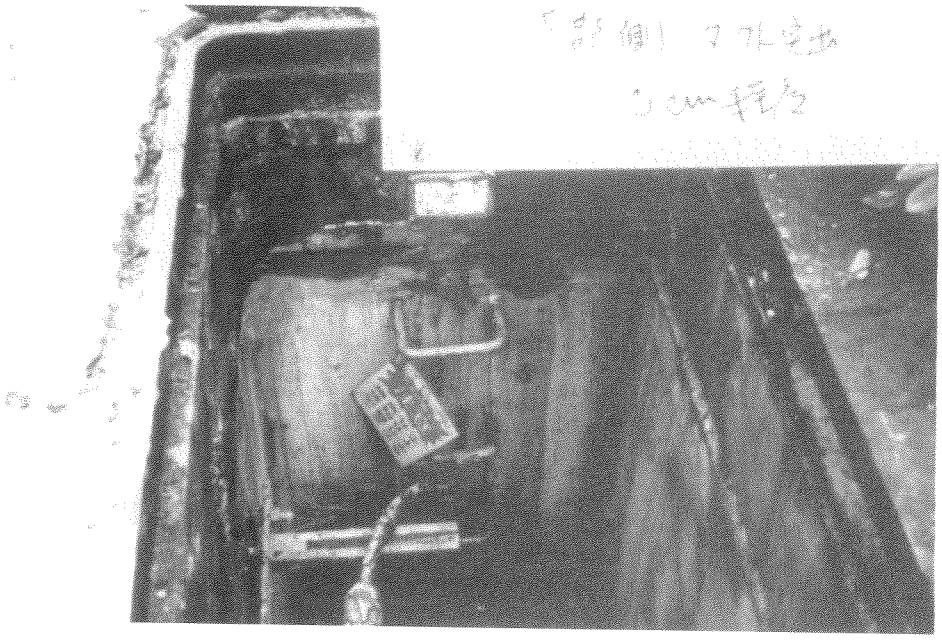


Figure 6-5 Cables were Pushed into Manhole Box Breaking Water Seals and in Some Cases Damaging Cables



Figure 6-6 Movement of Manhole Box can Damage Conduits and Trunk Lines

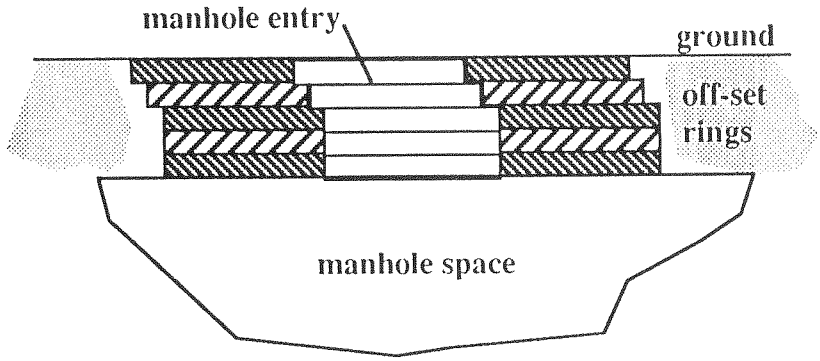


Figure 6-7 Entry of a Manhole Built by Stacking Rings Was Offset by 4 cm Due to Soil Failure



Figure 6-8 Subsidence Around Manhole can Damage Conduit and Trunk Lines

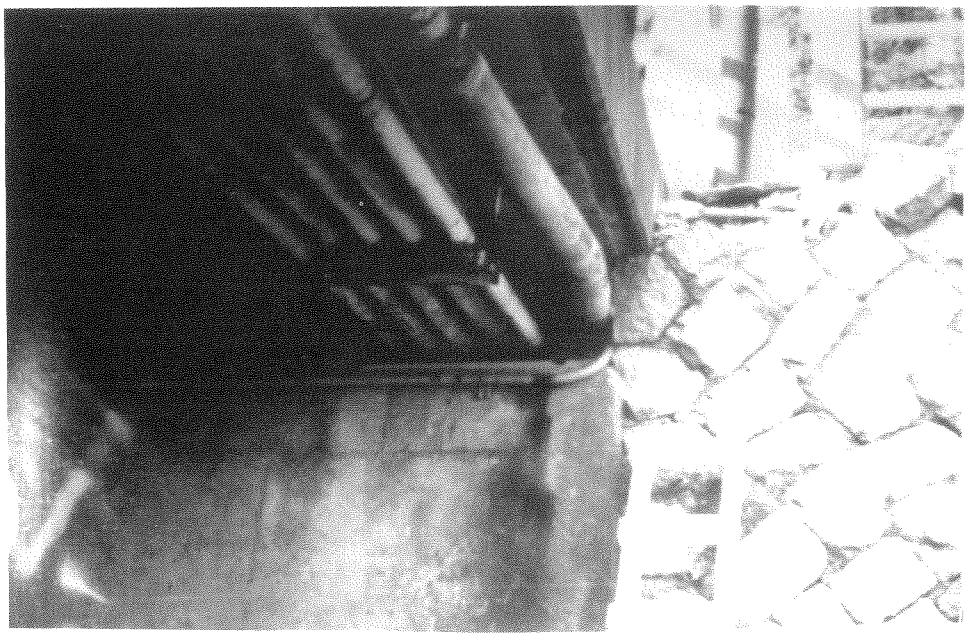


Figure 6-9 Conduits Carried on Bridges were Damaged when Bridge Deck Moved



Figure 6-10 Large Differential Settlements in Roadways can Damage Conduit and Trunk Lines



Figure 6-11 Settlement of a Walkway Adjacent to a Building Shears Conduit and Cables

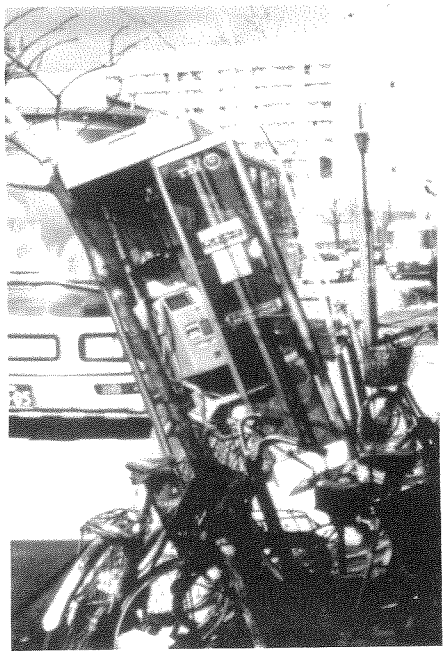


Figure 6-12 Soil Instability Damaged Telephone Booths



Figure 6-13 Walls of a Canal Moved Causing Conduit Bridge and Conduit to Buckle



Figure 6-14 Fire Damaged Aerial Lines and Cables Along the Pole

attempts to complete a call using the cellular system. During a visit of one of the reconnaissance teams at the end of March, some areas required as many as five attempts to complete a call using a pay telephone.

To prevent switch saturation, line control was implemented. Restrictions on calling were removed on January 22, when call volume was about twice normal levels. Due to load control efforts by NTT, some areas away from the earthquake, for example in area code 0742 south of Osaka, could not call other parts of 07 areas, even though those areas had no telephone system damage. About 50,000 extra lines have been installed to the Hyogo area by using mobile switching units and mobile satellite transmission units. Telephones were connected directly to mobile switching units.

6.2.4 Restoration

Initially 7,000 NTT personnel, many from other parts of Japan, were working on restoration. During the TCLEE visit at the end of March, there were still 3,000 personnel working on locating damage and restoration of outside plants.

Six mobile satellite units were used after the earthquake to provide transmission capacity due to damaged towers. In addition, 11 diesel-generators were used to provide power where commercial power was disrupted and emergency power was not provided or had failed.

On Port Island, television inspection of 7.5 cm steel conduit had just been started at the time of the visit. They found two of five steel conduits that had been inspected had failed due to differential settlement, but the cables were not damaged.

It was reported (Damage and Restoration, etc., 1995) that NTT will examine the current disaster management program based on Japanese intensity 6 by organizing a Large Scale Disaster Management Committee to review the impact of the earthquake and submit a report with recommendations by July, 1995.

6.2.5 Special Post-Earthquake Services

NTT provided free telephone service, including long distance, with 2,700 phone sets, including 350 fax machines at 760 locations in the disaster area.

Telegram service was provided for the people who evacuated Kobe. E-mail providers also established a data base of the displaced, injured and diseased persons so that relatives could obtain information quickly.

6.3 Lessons from Damage to Telecommunications Facilities

Three building-mounted microwave towers were damaged, one of which was removed. One of the striking features about communications towers in Japan, where there are large wind loads

associated with typhoons, is their massive construction as compared to those found in the U.S. The damage to Japanese towers suggests that those in the U.S. may also be vulnerable, particularly where central offices are built on poor soil.

The loss of water to communication facilities and its effect on emergency power further substantiates this vulnerability to U.S. facilities.

6.4 Summary

There was relatively little service disrupting damage to central offices. Emergency power was disrupted due to the loss of water at central offices, which caused the loss of service to 285,000 lines. There was extensive damage to the outside plant. A massive restoration effort was required to restore service and the restoration of conduit and other facilities continues, two months after the earthquake. Total cost of damage from the earthquake is estimated by NTT at $3 billion. NTT has established a committee to review the impacts of the earthquake and will make recommendations for changes.

6.5 Acknowledgments

Dr. Schiff acknowledges the translation of the news release (Damage and Restoraton, etc., 1995) by Alex Tang, Nortel, and Satoshi Tanaka, Princeton University.

6.6 References

"Disaster Prevention Measures of NTT for Telecommunications Network Systems," IEEE Communications Magazine, June 1990, pp. 18-24.

A news release in Japanese, dated February 1, 1995, "Damage and Restoration of Hyogo-Nanbu Earthquake," was distributed at the NTT briefing.

SECTION 7
TRANSPORTATION SYSTEMS

7.1 Airport Facilities

7.1.1. Overview of Airport Facilities

The Kansai area is served by three airports: Kansai International Airport (Kansai Airport), Osaka International Airport (Osaka Airport), and Yao Airport. The Terminal Radar Approach Control (TRACON), which is located at Kansai Airport, controls airplanes in the area before each is turned over to the respective control towers. Kansai Airport was opened for service on September 1, 1994, and it primarily serves international flights, although emergency services, such as police, rescue and news media have access. Prior to the opening of the Kansai Airport, Osaka Airport served as the area domestic and international airport. Osaka Airport now primarily serves domestic flights and a few international flights. Neither of these airports allows general aviation, which is served by Yao Airport. The control towers and some support facilities at Kansai and Osaka Airports were inspected.

7.1.1.1 Kansai Airport

The Kansai airport is built on a 511 hectare island of reclaimed land in Osaka Bay. The bay at the site was about 18 m deep and it took about five years to complete the island. It is 28 km southeast, and across the bay from downtown Kobe and 38 km southwest of downtown Osaka. It is located 27 km southeast of the epicenter. The island has subsided about 2 m since it was completed and currently has about 5 m freeboard. Recently, subsidence has slowed and it is anticipated that the island will subside another 1-1/2 m in the next 50 years. There is a single runway about 3,200 m. Several tanks store 100,000 kl (kilo liter) of jet fuel, and at a typical use of about 3,500 kl/day, there is about a month's supply of fuel. The airport is connected by a bridge to the mainland that carries auto and train traffic. It is also served by ferry companies from Kobe and four other cities. There is a pier for off-loading jet fuel. Expansion is planned in about 10 to 15 years when another 700 hectares of land will be reclaimed and two additional runways and a second terminal will be added. Figures 7-1 and 7-2 show an overview of the airport from the control tower looking east and west, respectively. Figure 7-3 shows a schematic diagram of the airport, access bridge and the location of strong-motion instruments discussed later.

It was noted that in the winter, there are normally strong winds. It was fortunate that at the time of the earthquake there was no wind.

Air Traffic Control Tower

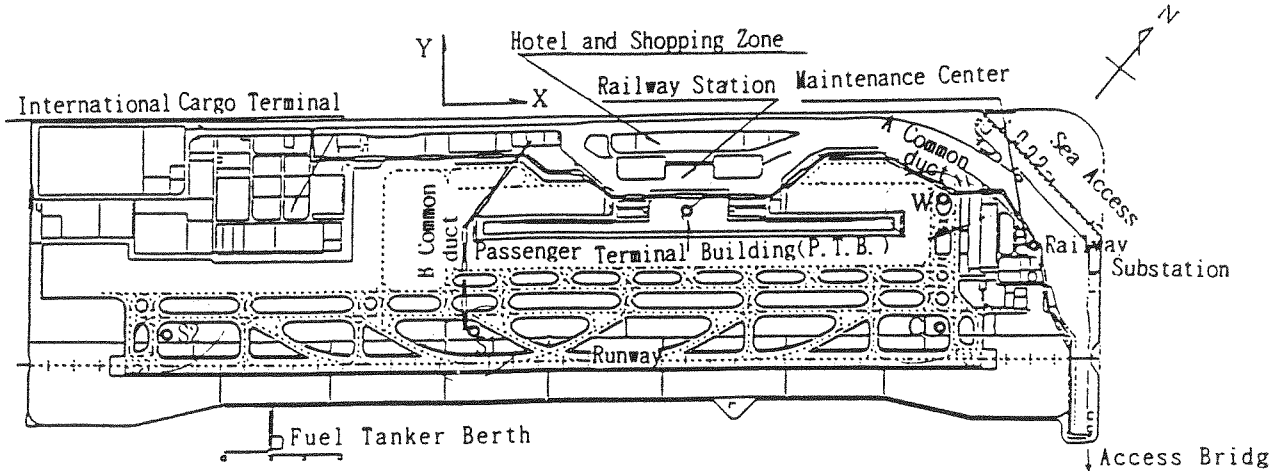
The Air Traffic Control Tower (ATCT) at Kansai is a 19 story steel-tubing braced frame. The frame is comprised of four exterior pipe-columns outside the building envelope and four pipe-columns inside the building envelope. The exterior and interior columns are tied to each other at



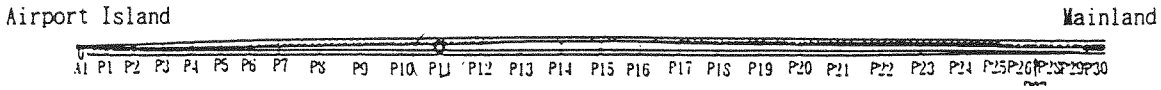
Figure 7-1 Overview of Airport Looking East from Control Tower



Figure 7-2 Overview of Airport Looking West from Control Tower



Schematic Diagram of Kansai Airport
(Instrument Locations: SW, C, S1, S2)



Profile of Kansai Access Bridge

Figure 7-3 Schematic Diagram of Airport, Access Bridge and Strong-Motion Instrument Locations

each floor level by a horizontal truss (see Figure 7-4). The lateral force resisting system is provided by vertical cross bracing between each of the interior columns. An interior column, which is about 75 cm in diameter, can be seen in Figure 7-5. Beam/column connections were made by shop welding short beam sections to the columns in the shop and bolting the connecting beam to the beam stub in the field. Figure 7-6 shows such a detail in the penthouse above the cab. Based on a brief review of control tower drawings, the tower and the adjacent administrative building appears to have a stiff foundation mat. The drawings did not show any piles. The tower is connected to an administration building by two catwalks, on the fifth and seventh floors (see Figure 7-4). The control tower contained an active control system to reduce wind induced vibration.

The vibration control system consists of two systems located on opposite sides of the control tower on an upper floor. Each system has a mass consisting of metal blocks filling a 1.2 m by 1.2 m by .3 m box. The mass is suspended on an arm that has a universal joint at its top, which is supported by a box shaped frame. The frame is connected to the floor. There are two actuators, which lie in a horizontal plane, connected to the arm. The angle between the actuators is ninety degrees (see Figure 7-7). Rubber snubbers are connected to the frame to limit the motion of the suspended mass. The strategy for the operation of the vibration control system is not known.

As noted above, Kansai Airport is built on reclaimed land which has experienced significant subsidence prior to airport construction, so that ground settlement is a serious concern. If settlement occurs, the building can be leveled by using two hydraulic rams at each of the eight columns located on the foundation slab (see Figure 7-8). The columns were held against the action of the hydraulic rams by about 12-ten cm studs. The shear capacity of the columns was not known, but there were two shear keys on each side of the tower (see Figure 7-9). These shear keys were detailed to carry lateral load parallel to the foundation wall, including torsion of the building, but no vertical axial load (see Figure 7-10). The lower end of each ram was supported by the foundation pad and the upper end was connected to a stiff diaphragm, consisting of the deep beams shown in Figure 7-11. The shear keys were configured so that they stay engaged when the rams were used to relevel the structure. It is not known if the leveling mechanism was used to compensate for differential settlement of the tower to prevent leaning, or if it was also used to maintain the level between the structure and the surrounding ground. This may have been needed to prevent damage to utility lines that enter the building. It was reported that the terminal building also has leveling devices.

The control tower cab was constructed differently than those found in the U.S., in that the cab roof was supported by four columns in the interior of the cab (see Figure 7-12). The column cross-section decreases in the cab, just above the floor and below the ceiling. In the U.S., the cab roof was supported only by the window mullions, in order to allow a 360 degree view from anywhere in the cab with the only obstruction being the narrow mullions. In the U.S., the failure of control tower windows, which is generally attributed to the flexibility of the cab roof relative to its floor, is relatively common. The columns at Kansai should provide the cab with much larger lateral stiffness.

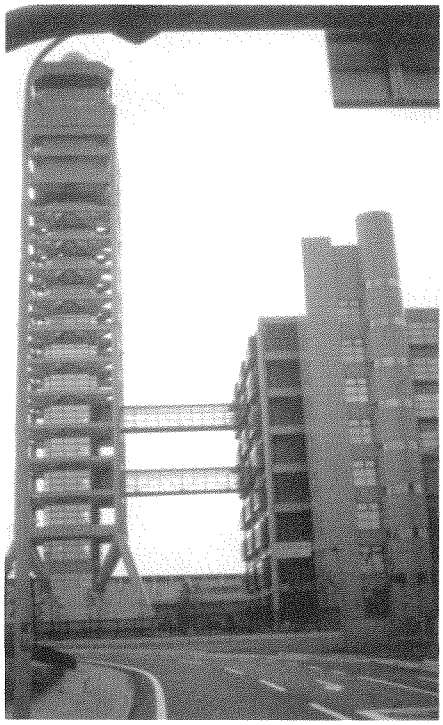


Figure 7-4 Kansai Airport Air Traffic Control Tower

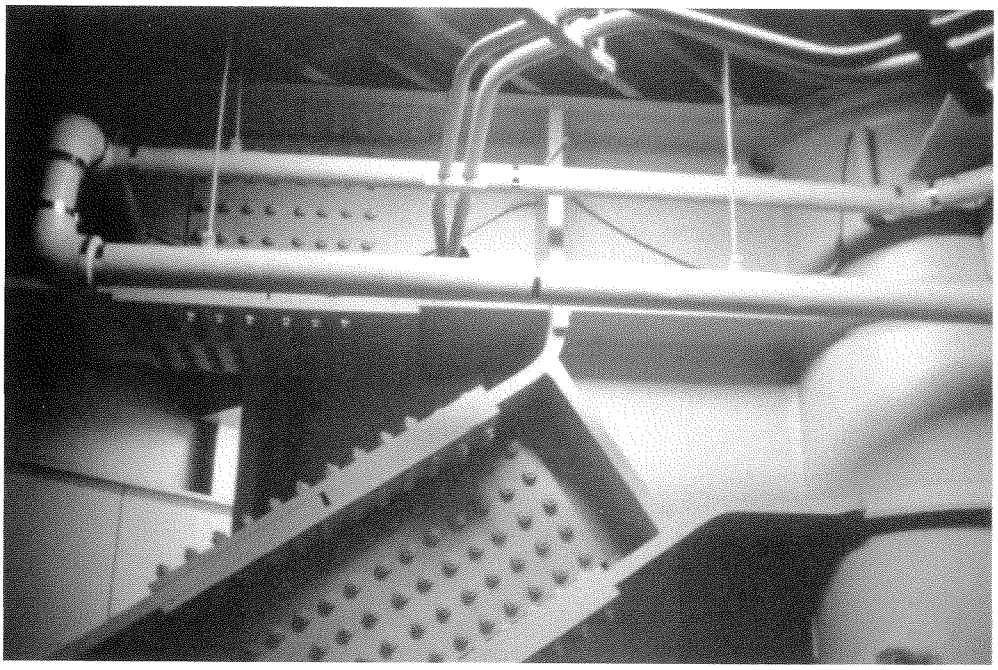


Figure 7-5 Connection Between an Interior Pipe Column and a Vertical Truss in the Shaft of the Tower

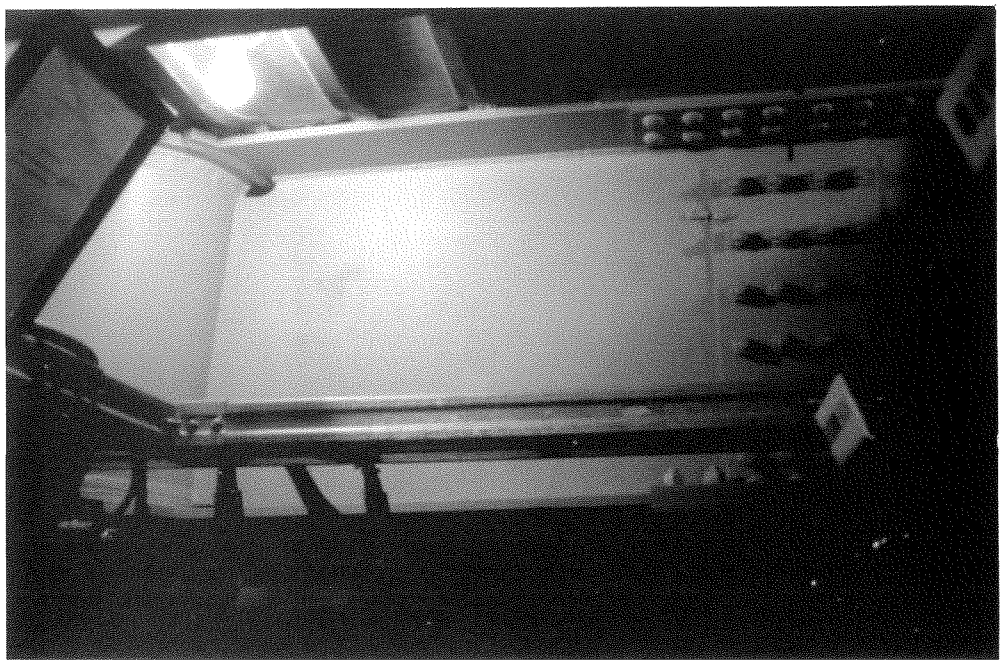


Figure 7-6 Beam/Column Connection in the Penthouse Above the Cab

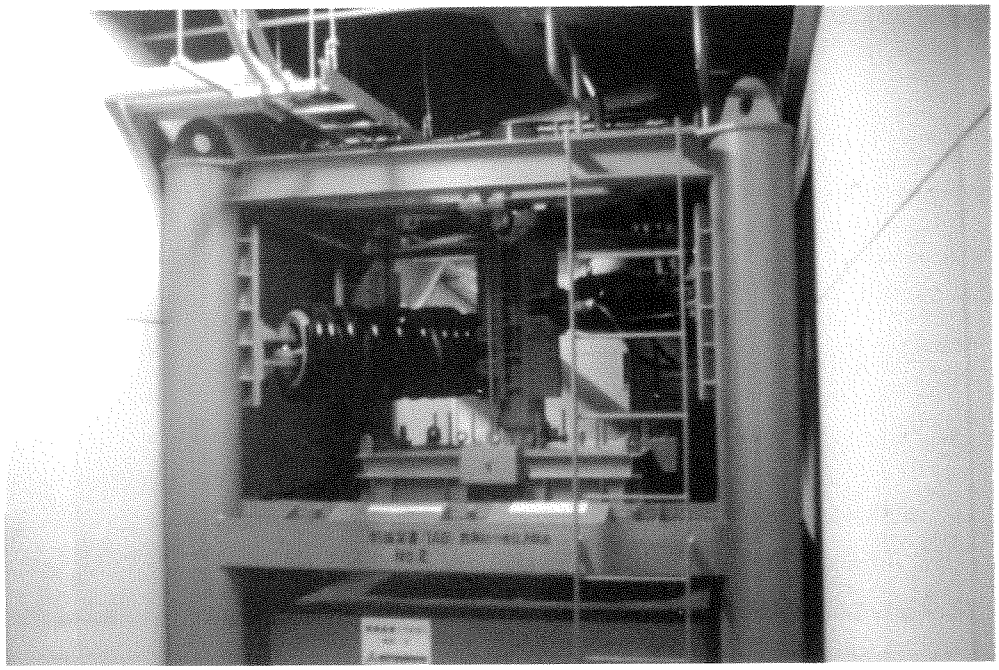


Figure 7-7 Active Control System to Reduce Wind Induced Vibration

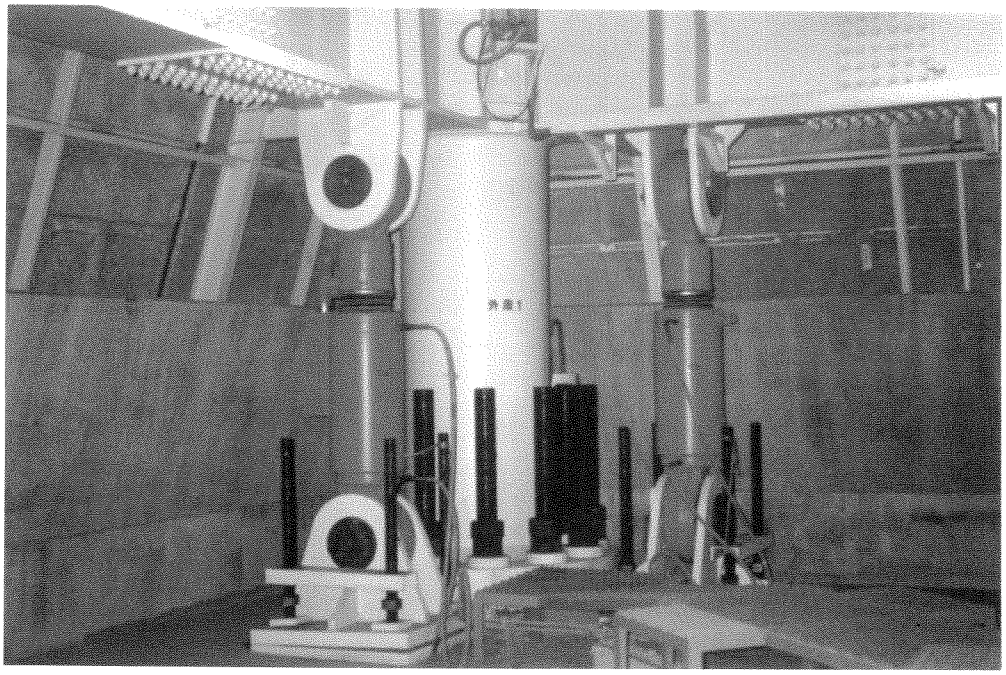


Figure 7-8 Hydraulic Rams on Either Side of a Column

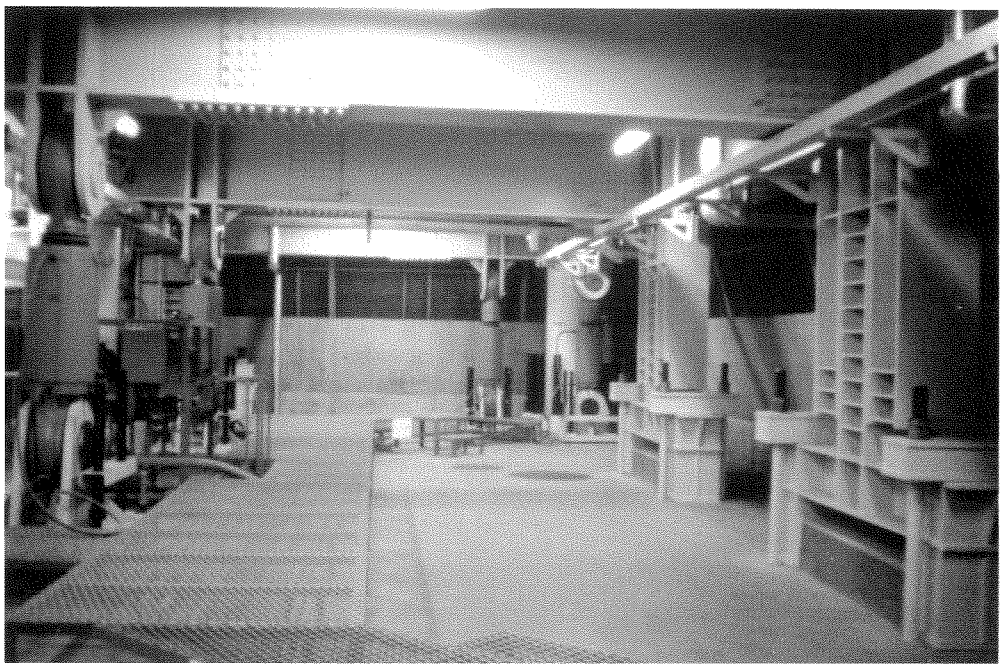


Figure 7-9 Basement of the Tower Showing System for Leveling the Building and Shear Keys

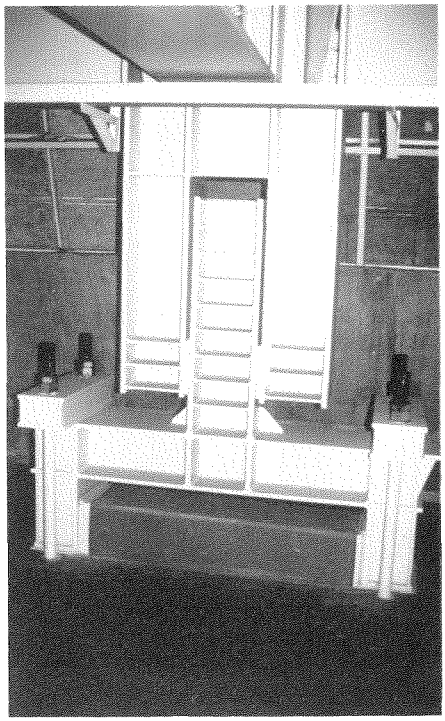


Figure 7-10 One of Two Shear Keys Parallel to Each Side of the Control Tower

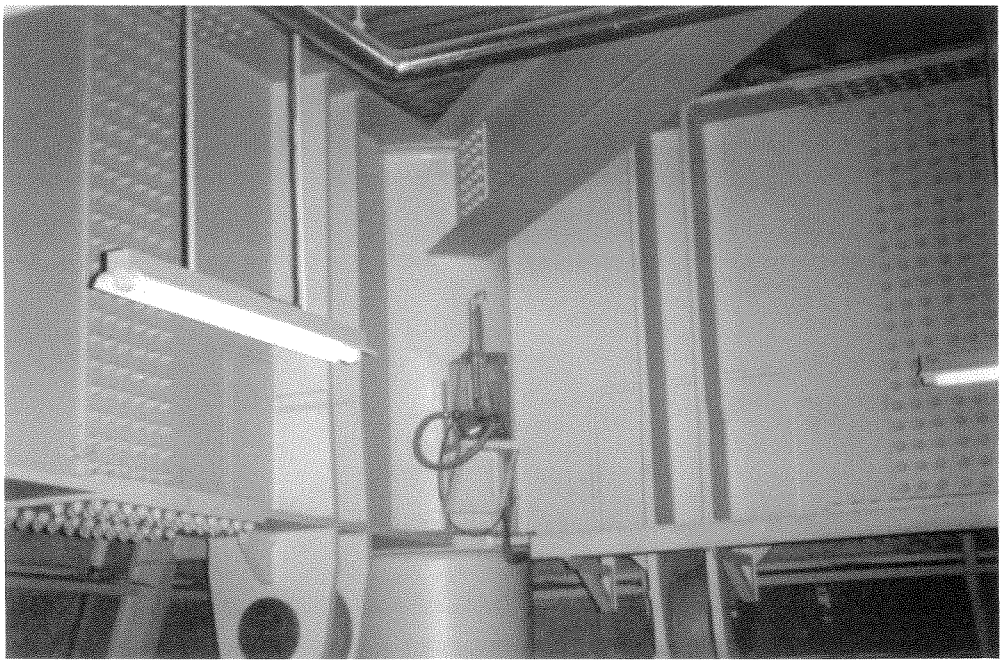


Figure 7-11 Deep Girders of the Rigid Diaphragm Above a Column

The cab is octagonal in plan, with four wide sides and four more narrow sides. The windows are supported with twenty structural tubing mullions, with three larger members (20 x 10 cm) along the interior of the wide window face and two smaller members (15 x 7.5 cm) at the corners of the narrow sides. The window panes are inserted in slots in the mullions with an engagement of about 2-1/2 cm on the sides and about 3-1/2 cm at top and bottom. An outside view of the cab is shown in Figure 7-13.

Operationally, the control towers are different from the U.S. Communication control councils and monitoring oscilloscopes form controller positions around the periphery of the cab, as is done in the U.S. However, near the center of the control tower is a master monitor for a supervisor (see Figures 7-14 and 7-15). These appear to be used when there is more traffic than was the case during the visit. It is interesting to note that the monitors in Japan were much smaller than those used in the U.S. and are incorporated into the control council. In the U.S., they are often suspended from the ceiling. The computers that control the displays were not visited, as they were located in another building. It was noted that at one time, Japan used the same system that is currently used in the U.S., but Japan is now in the second generation of equipment that replaced the old U.S. equipment.

Support Facilities

A small room above the control tower cab contained communication transmission equipment, heat exchanger and cable trays. The communication equipment was well anchored. The cable trays used for communication lines resemble those used by the power industry for control cables in the U.S., in that sections are bolted together (see Figure 7-16). Cable trays were typically supported by trapezes suspended by threaded rod. At some locations they were restrained by friction clips (see Figure 7-17).

A heat exchanger on the roof was well anchored, as was most equipment observed (see Figure 7-18).

A battery plant provided an uninterruptable power supply. Battery support structures observed in Japan tended to be short and close to the ground, well braced, and provided with rubber spacers between the batteries and their restraints and between cells (see Figure 7-19). Because of the high operating voltage, very long battery strings were used.

A large diesel-generator that supplied emergency power was supported on vibration mounts typical of those seen at other Japanese facilities (see Figure 7-20). Utilities connected to the diesel-generator were provided with flexible connections to accommodate the motion of the vibration isolation system. Large diameter pipes, such as those used for cooling water, had flexible couplings (see Figure 7-21). The diesel engine used compressed air for starting, typical of larger engines. The compressor and air storage tanks were well anchored.

The cooling system for the diesel used a small cooling tower adjacent to the building. The cooling tower was supported on a large concrete water storage tank that measured about 6 m by



Figure 7-12 Column Supporting the Cab Roof in Kansai Control Tower



Figure 7-13 Cab of the Osaka Airport Control Tower

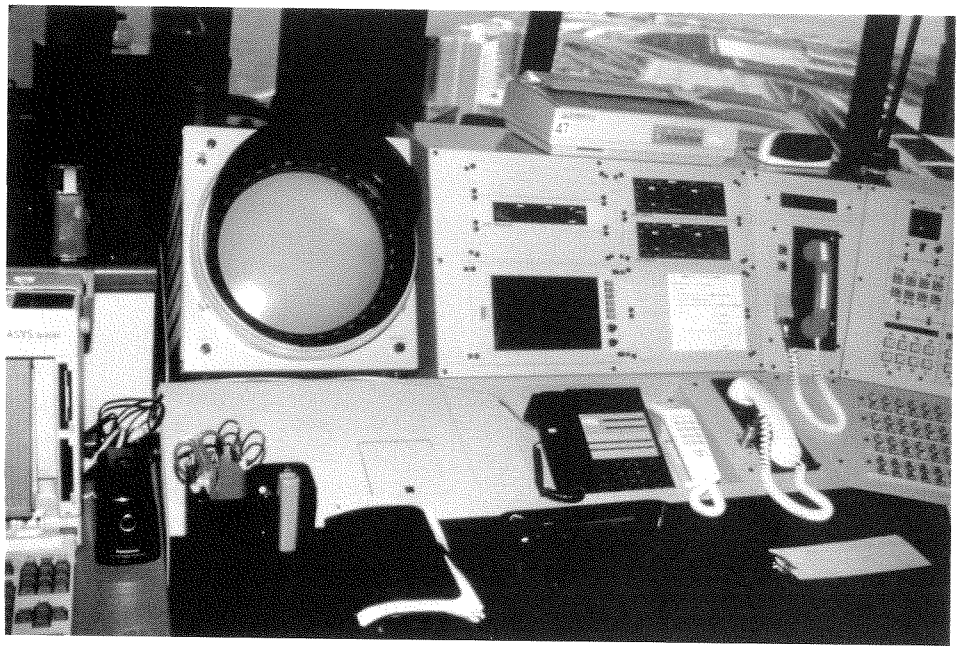


Figure 7-14 Supervisor Control Position Located in Center of Control Tower Cab

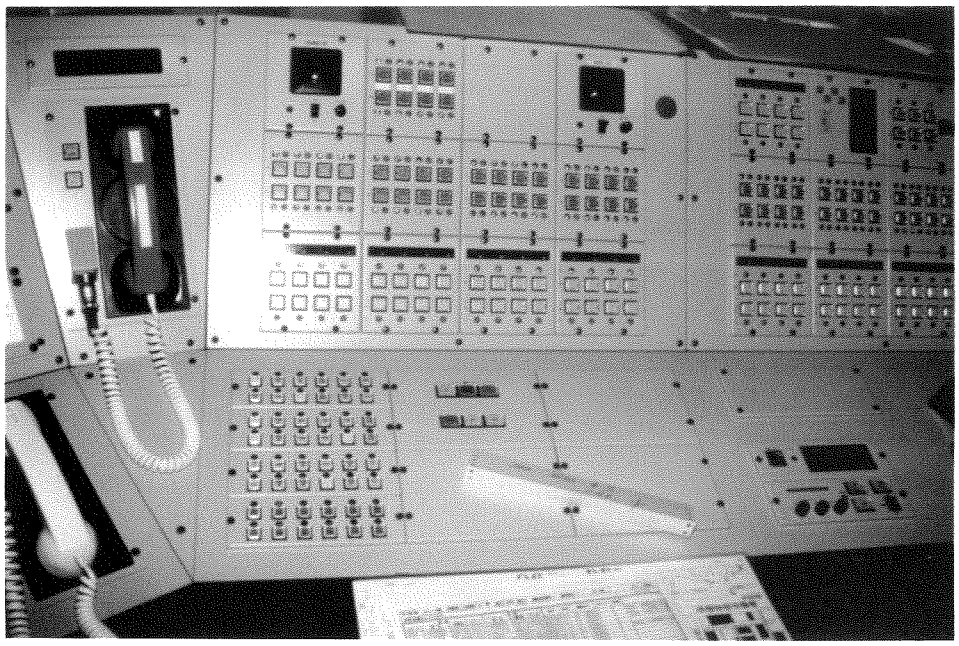


Figure 7-15 Supervisor Control Position Communication Council

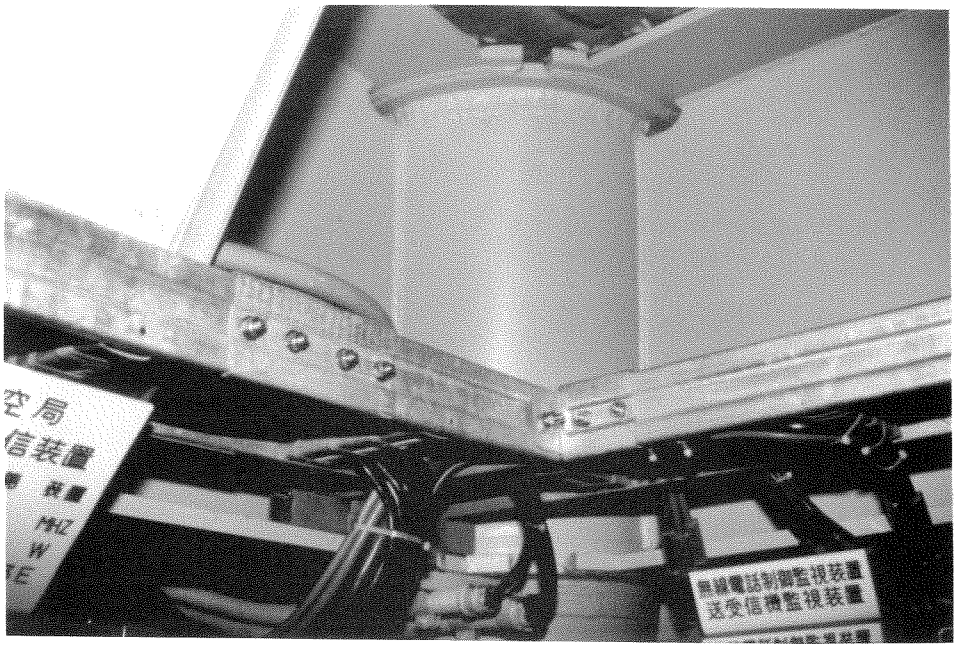


Figure 7-16 Communications Cable Tray with Bolted Connections Above Cab

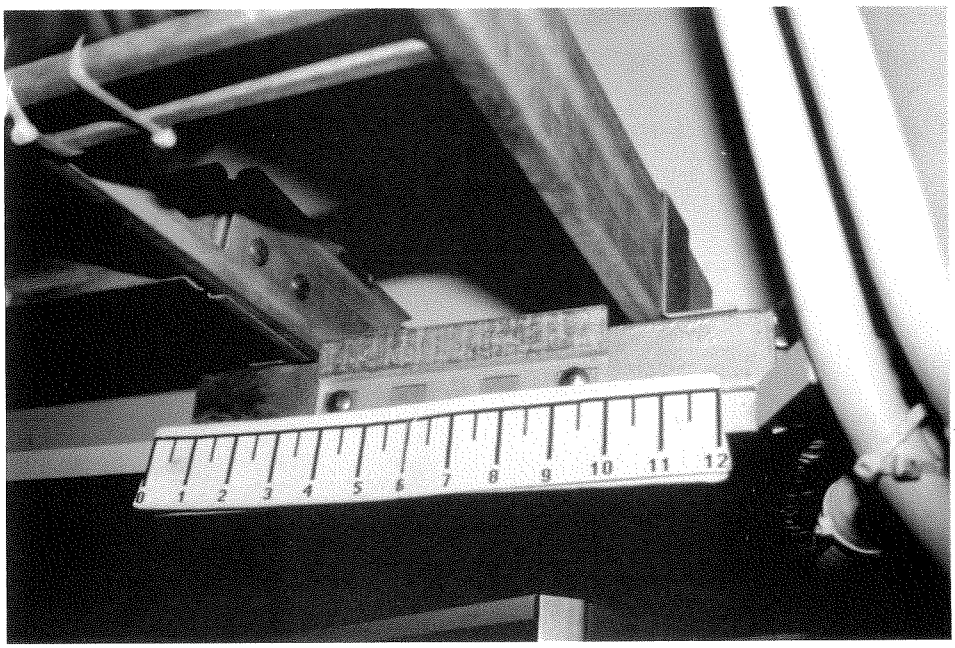


Figure 7-17 Communications Cable Tray Secured with Friction Clips

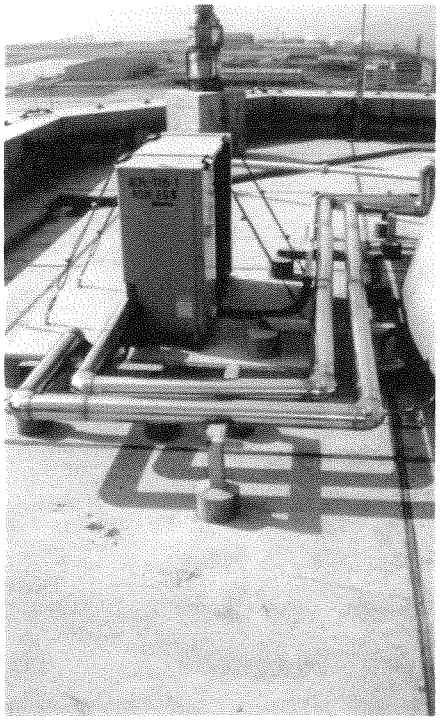


Figure 7-18 Roof-Mounted Heat Exchanger Braced with Cables

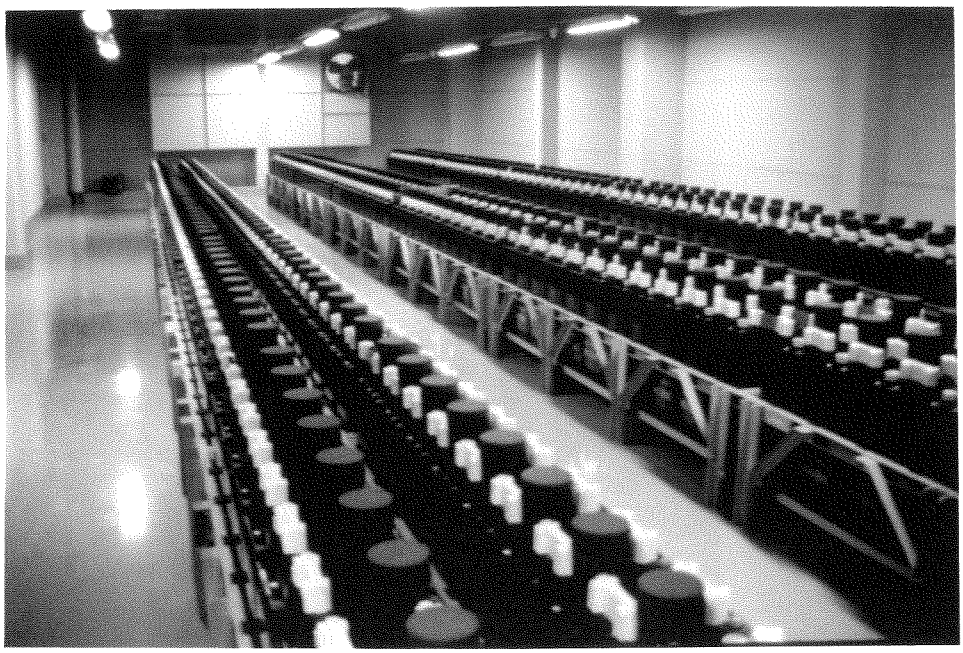


Figure 7-19 Very Long Battery String on Low Slung Battery Racks Provides Emergency Power

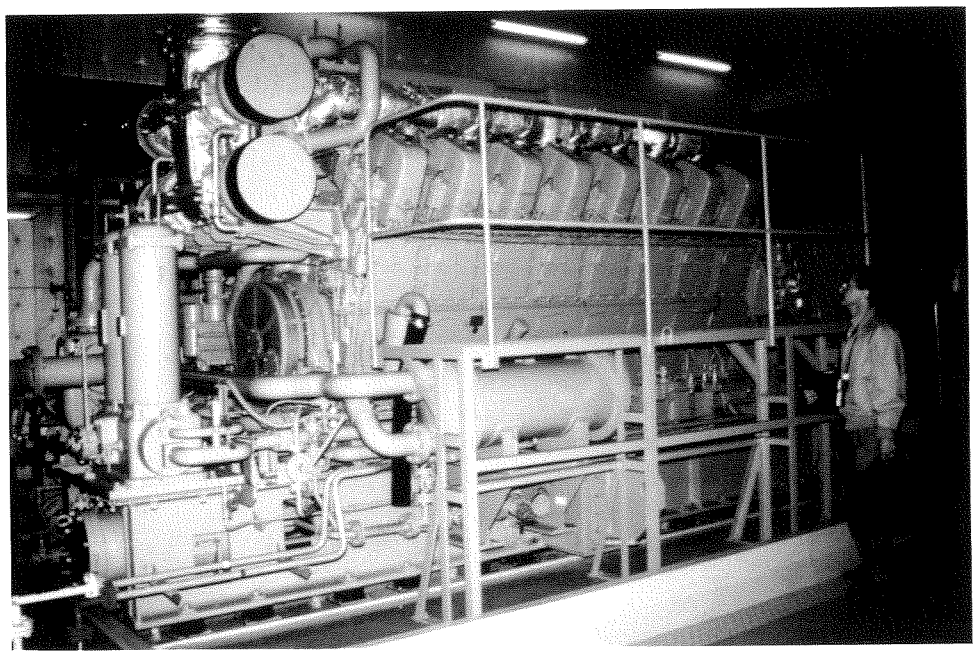


Figure 7-20 Large Diesel Engine-Generator on Vibration Isolators Typically Found in Japan

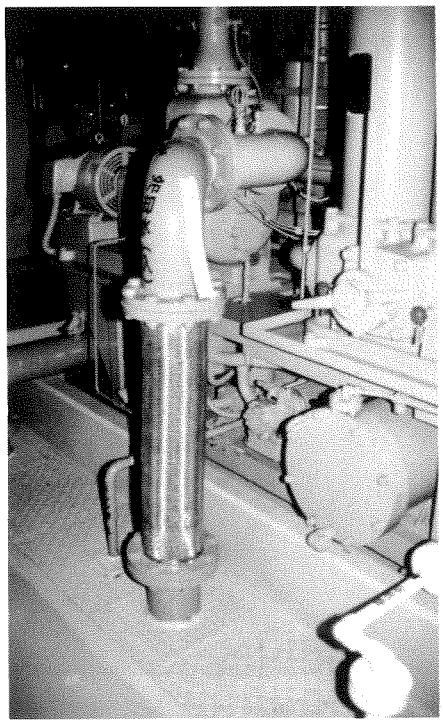


Figure 7-21 Flexible Coupling in Water Cooling Line to Diesel Engine-Generator

15 m by 2 m (see Figure 7-22), so that emergency power could continue to operate for a long time even if the external water supply was disrupted.

7.1.1.2 Osaka Airport

Osaka Airport is located 28 km east-northeast of Kobe Japan Railroad Station and 12 km north-northwest of downtown Osaka. It is located about 43 km east-northeast of the epicenter. The control tower was the only part of the airport that was visited.

The control tower at the Osaka Airport was constructed in 1969. It is on the top of an eight story reinforced concrete administration building. The concrete frame includes shear walls in the short direction. The cab is octagonal in plan and the roof and windows are supported by 16 window mullions. Equipment was generally well anchored, although there were some heat exchanges on the roof that were supported on unsecured concrete blocks (see Figure 7-23), or had anchorage of questionable strength.

The window size is 2 m wide and 2-1/4 m high. They are rectangular except for the corner panes. What appeared to be double paned glass was secured in the mullions by inserting its sides about 2 cm, the bottom about 2.5 cm and top about 2 cm, but it is difficult to make these estimates accurately.

The emergency power was located in a separate building that was closed on the weekend, and the communications facility was off the airport site and was not visited.

7.1.2 Description of Damage to Airport Facilities

7.1.2.1 Kansai Airport

An array of 19 strong-motion instruments recorded the earthquake at Kansai Airport facilities (Werner, 1995). Figure 7-3 provides a schematic layout of airport facilities, and a section view of the access bridge. It also indicates the location of four instruments on runways with letters W, C, S1 and S2. The location of instruments on the access bridge are also indicated. Figure 7-24 and the accompanying Table 7-I indicate the location of strong motion instruments in the main terminal building - 10 instruments at the first, fourth and roof levels, one instrument at the Automated Guideway Transit (AGT) System Control Center, one down-hole instrument, two instruments on the access bridge, and one instrument at the ground surface in the railway station. Table 7-II lists the peak acceleration, in gals, recorded by each instrument. Figure 7-25 shows the largest horizontal component recorded at location W on one of the runways. The duration of strong shaking was about 12 seconds with most of the peaks below 110 gal. Thus, the ground motion at the site, even though it was recorded on land fill, was very low. The records give no indication of liquefaction. An air traffic controller in the Kansai tower at the time of the earthquake said it "shook like a snake," however, it was dark at the time of the earthquake and from the control tower, the deformation of the tower could not be observed. It was assumed that this refers to vibration rather than mode shape.

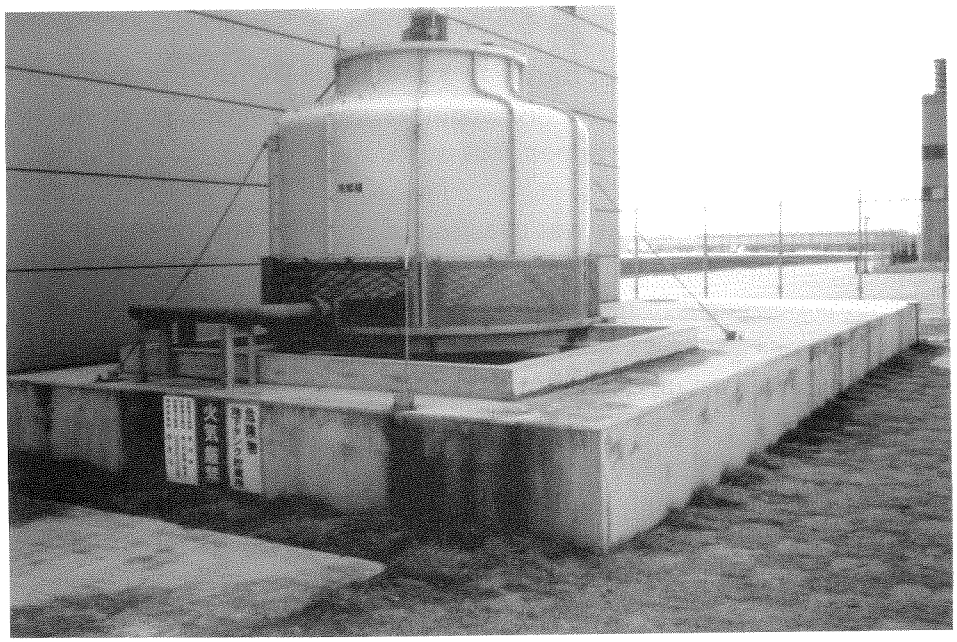


Figure 7-22 Cooling Tower and Water Tank for Emergency Engine-Generator

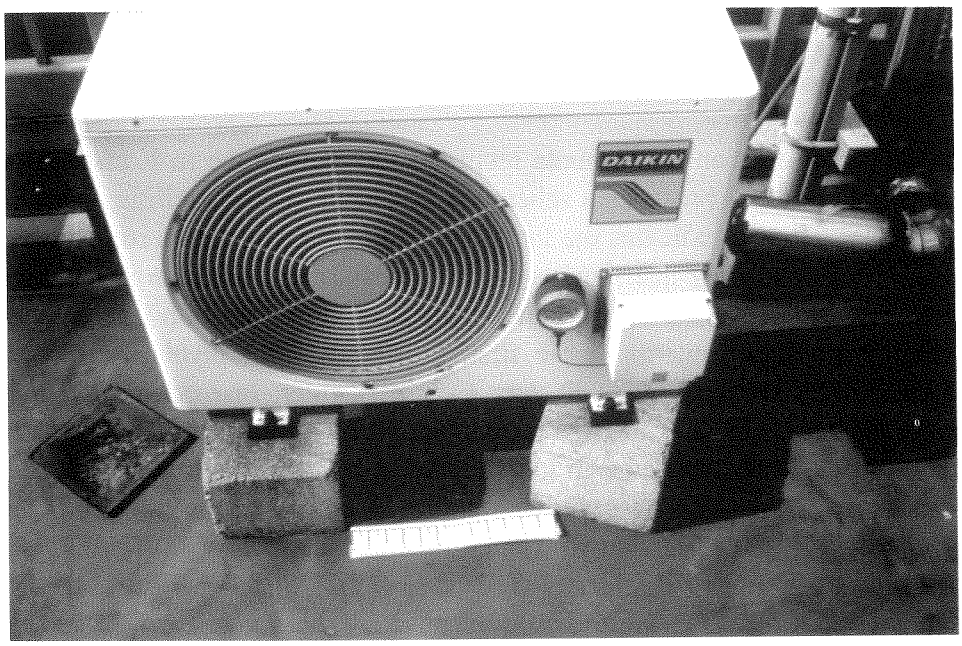
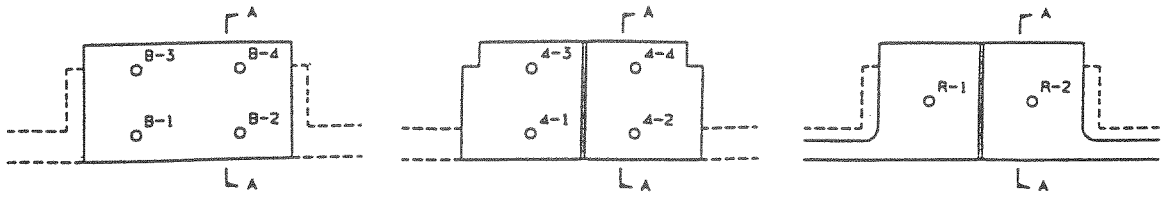
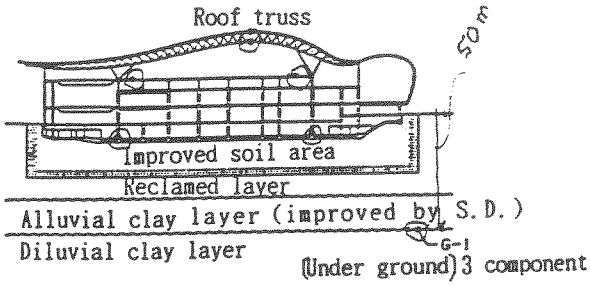


Figure 7-23 Heat Exchanger on Roof Near Control Tower Cab is Rare Example of Poorly Anchored Equipment

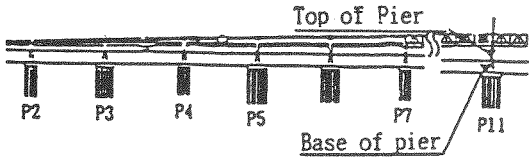


First Floor Plan View Fourth Floor Plan View Roof Plan View

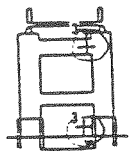


Profile of Terminal Building (Section A-A)

Airport Terminal Building



Access Bridge - Profile



Detail Instrument Location

Access Bridge

Figure 7-24 Strong-Motion Instrument Locations at Kansai Airport

Table 7-I Instrument Locations at Kansai Airport

Facilities		Nos.	Measurement Position
R / W	Runway and Common Duct	4	W, C, S1, S2 (1m under ground)
P	Main Terminal	10	Fig. 7-24 (R-1~B-4)
T	Outside of Building (50 m under ground)	1	Fig. 7-24 (G-1)
B	A G T	1	A G T Control Center
Access Bridge	Top & base of pier	2	Fig. 7-24
Railway Substation		1	Ground Surface

A G T: Automated Guideway Transit System

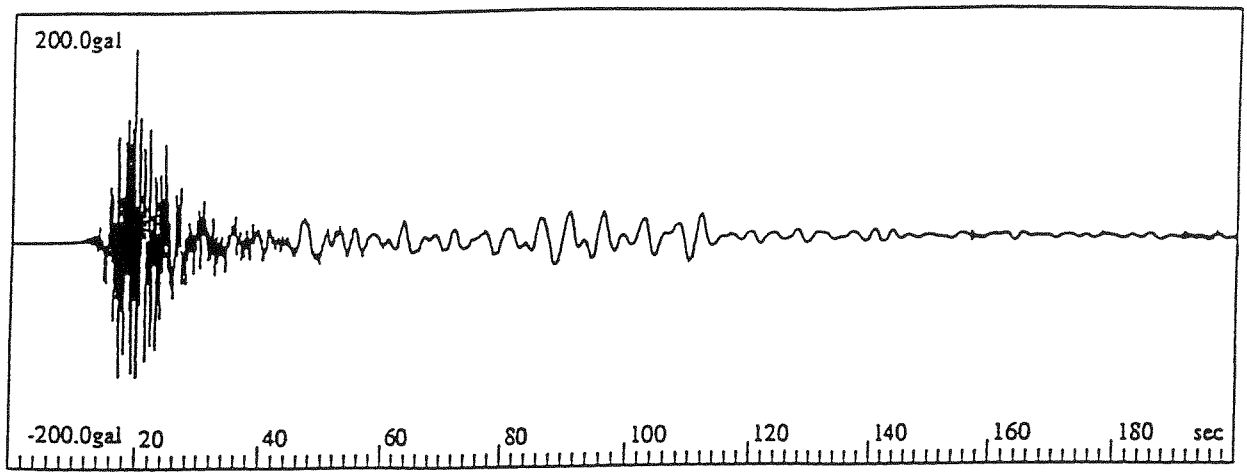


Figure 7-25 Strong-Motion Record from Kansai Airport Runway - Position W

No damage was reported to the tower or its contents. The connections of the cross walks that span the control tower and the administrative building, a location of potential damage due to interaction between the buildings, were inspected for signs of damage from within the cross walk, and none was observed. The area around column footings that support roadways were carefully inspected for signs of differential settlement and none was found. The only indication of damage was to a walkway in front of the main terminal building between the roadway and building foundation. Repairs were being made, but there appeared to be a strip about 3 m wide running the length of the terminal that subsided about 7 cm (see Fig. 7-26). This was the only observed settlement and the strip, which lies between the terminal foundation and roadway, may not have been adequately compacted. It was reported that there was no subsidence or lateral spreading around the boundaries of the island.

Table 7-II Peak Accelerations Recorded at Kansai Airport
(> Indicates input exceeds instrument range)

Airport Facilities			Measurement Position	Maximum Acceleration (gal)		
				① Component	② Component	③ Component
			Fig. 7-3	Horizontal (X)	Horizontal (Y)	Vertical (Z)
Runway		A Common duct	W	168.5	103.9	247.1
		Northern end of Runway	C	147.4	118.0	204.5
		B Common duct	S1	97.1	105.9	154.5
		Southern end of Runway	S2	88.4	70.7	142.9
Access Bridge			Fig. 7-24	Horizontal (X)	Horizontal (Y)	Vertical (Z)
		Top and base of pier	Top	272.4	178.7	83.6
			Base	133.8	93.9	70.6
			Fig. 7-24	Horizontal (N-S)	Horizontal (E-W)	Vertical
	Outside of Building (50 m underground)		G-1	74.8	101.1	103.5
P T B	Main Terminal Building	South Side of B1F	B-1	36.4	36.0	> 102.4
		North Side of B1F	B-2	37.8	32.4	> 102.4
		South Side of B1F	B-3	?	35.1	> 102.4
		North Side of B1F	B-4	33.5	31.8	> 102.4
		South Side of 4F	4-1	95.8	95.8	—
		North Side of 4F	4-2	93.9	79.0	—
		South Side of 4F	4-3	96.3	82.7	—
		North Side of 4F	4-4	86.7	80.1	—
		South Side of Roof	R-1	347.6	276.1	534.6
		North Side of Roof	R-2	310.6	321.9	451.2
		AGT Control Center	31.0 (Horizontal)			
Railway Substation			131.0			

Impact on Operations

At the time of the earthquake, there was a flight on approach. The captain was told to hold until runways could be checked, and then cleared for landing. There are normally about 240 operations per day. Note that a landing and departure are two operations. At the time of the earthquake, a maximum of 23 operations per hour were possible, but this was about to increase to 26 per hour. As a result of the earthquake, there was a drop in tourist traffic, but since east-west

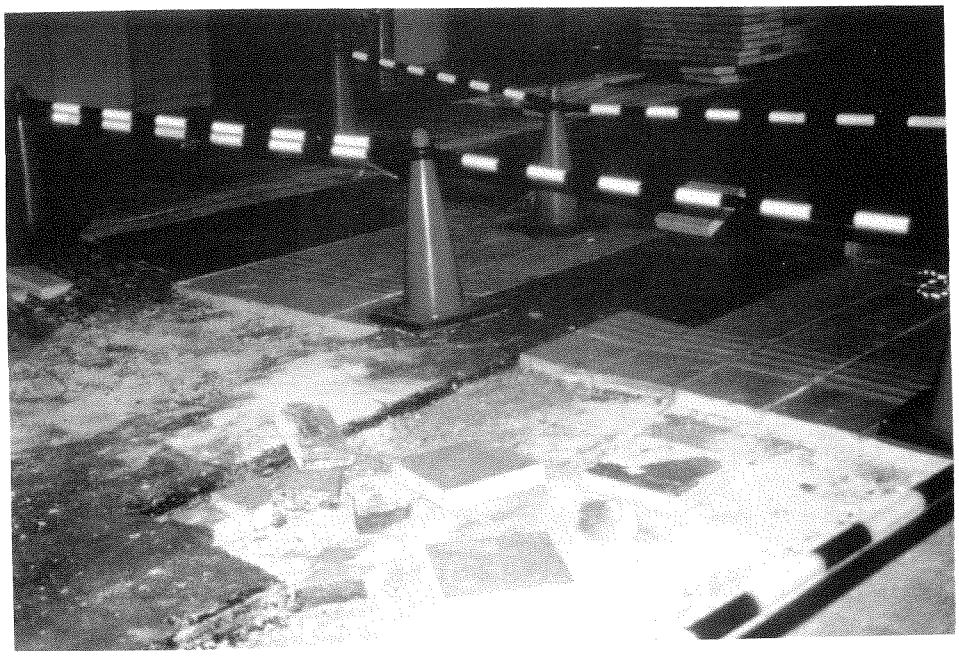


Figure 7-26 Subsidence in Sidewalk and Repaired Sidewalk Outside the Kansai Terminal Building

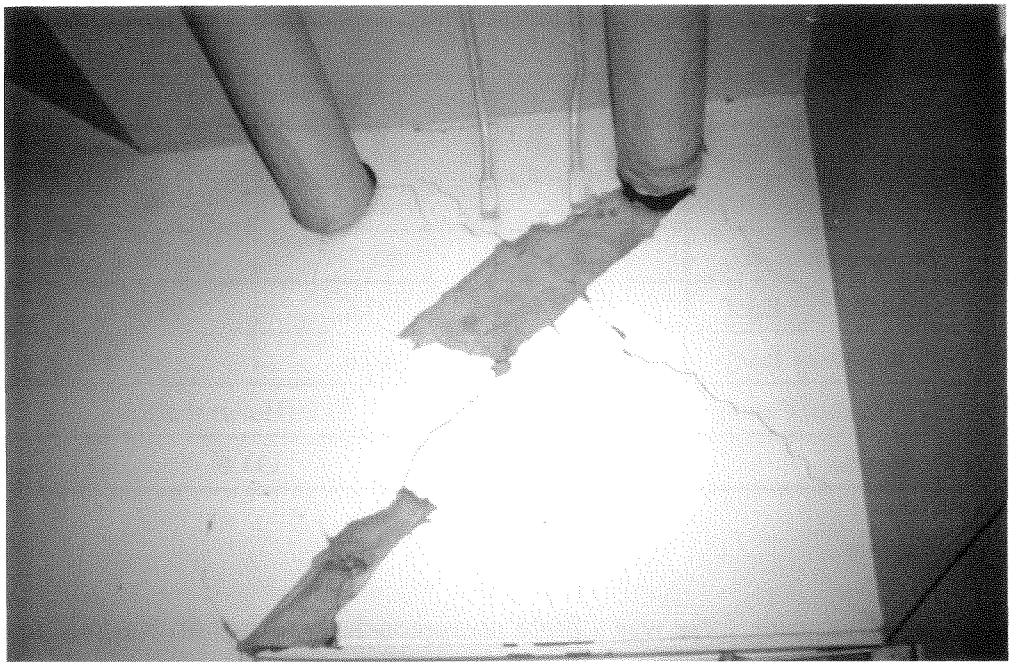


Figure 7-27 Cracks in the Stairwell Shear Walls of the Osaka Airport Administration Building

road and rail links were blocked at Kobe, there was an increase in domestic flights to and from western Japan. These flights were routed through Kansai because of the difficulty in getting to Osaka Airport and to reduce its load, as most relief traffic went to Osaka. As a result, there was little net change in traffic at Kansai Airport.

7.1.2.2 Osaka Airport

The ground motion at the airport is not known, but an air traffic controller on duty at the time of the earthquake indicated that the shaking was very severe, that it was difficult to stand, that things fell off desks, and that it seemed to last one or two minutes.

Numerous diagonal shear cracks were found in shear walls in the stair well and above windows. The largest crack was about 6 mm wide and located at the floor level just above the roof of the main building that adjoins the control tower. Other cracks were about 3 mm wide or less and decreased in size with the height at higher floor levels. The abrupt change in lateral stiffness at the floor above the roof of the main building and the reduction of shear loads with elevation explains the observations. The stairwell shear walls may have attracted large lateral loads because of relatively high stiffness in the short direction of the building. Figure 7-27 shows an example of this damage.

As noted above, this tower, like those in the U.S., has its roofs supported by the mullions. One window had a crack emanating from a lower corner that continued to lengthen as the days passed.

Both elevators serving the control tower were damaged and out of service following the earthquake. One elevator was restored to service in just one day, but the other was out for four or five days.

The earthquake caused a crack perpendicular and through the runway at the Osaka Airport, but it did not disrupt operations.

Impact on Operations

Osaka Airport is a restricted airport, that is, there is no general aviation, however, police, fire, rescue, and press use of helicopters was allowed. Normally there are about 20 Visual Flight Rule (VRF) operations per day. But after the earthquake, the Japan Self Defense Force and the U.S. forces had helicopters and there were about 300 operations a day. These operations were used to deliver emergency supplies and to move emergency personnel in and out.

7.1.3 Lessons from Damage to Airport Facilities

The braced frame structural system in the Kansai control tower appears to have been an effective seismic design. The leveling system provided in the basement of this building appears to be an innovative approach to provide for the possible uneven ground settlement that may be caused by

liquefaction or consolidation. The use of interior columns to support the roof of the cab in the Kansai control tower did not appear to be a significant visual impediment and should reduce earthquake window damage frequently observed in the U.S. Future construction in the U.S. should consider this design feature in structures that might be subjected to seismic loads.

7.1.4 Summary

Two members of the reconnaissance team inspected the control towers at the Kansai and Osaka airports. They found the Kansai tower to be well constructed with an innovative method of leveling the tower should it be subjected to differential settlement. This tower also had columns in the interior of the cab to support the roof and resist lateral motion of the cab, thus protecting the windows. The columns appeared to cause little visual interference. The cooling system for the emergency generator was provided with a large local water supply. This tower sustained no damage from the low level ground motion in this earthquake.

The administration building and control tower at the Osaka airport both sustained some damage in this earthquake. Damage included a crack in a window in the cab of the tower, minor damage to shear walls in the administration building and temporary loss of use of the elevators.

7.1.5 References

Werner, Stu, (1995), Strong-Motion data, provided by Dames and Moore, San Francisco.

7.2 Highways and Bridges

7.2.1 Overview of Highways and Bridges

The Hanshin region comprises parts of the Hyogo, Kyoto and Osaka Prefectures to the north and east of Osaka Bay. The population of 12.5 million people living and working in the region is served by a complex network of freeways and highways built in the last thirty years (since the early 1960's). These major transportation routes generally run parallel to the shoreline of Osaka Bay with major links to the east to Nara, to the northeast to Kyoto, and to the west to Himeji. As the mountains behind Kobe approach the Bay shoreline, the east-west routes are forced into a narrow corridor which is barely 3 km wide in some parts and which must be shared with three major rail lines. Soil conditions vary throughout the region but most of the highway structures are founded on sand-gravel terraces (alluvial deposits) which overlie gravel-sand-mud deposits at depths of less than 10 m. Liquefiable soils are present along the shoreline and in most ports and channels. As a consequence, piled foundations are used extensively and caisson foundations are common for those large bridges that are in port areas or cross shipping channels.

Responsibility for the design, construction and maintenance of these highway routes is divided between the Ministry of Construction and two Public Expressway Corporations. Highways under the jurisdiction of the Ministry of Construction are free for public use whereas those owned by an

Expressway Corporation are toll roads and road user fees are collected. These latter corporations are independent authorities but are nevertheless subject to government control and regulation.

The Ministry of Construction (MOC), through the Naniwa National Highway Work Office, has oversight for the National Highways (NH) in the region. These include Routes R-2 and R-43 which join Osaka with Kobe, as well as several other trunk roads such as Routes R-428 (Kobe to Chugoku Expressway), and R-171 (Nishinomiya to Kyoto and Route R-1). These arterial highways are generally surface routes but with some notable elevated sections. These include the Route 2 Hamate Bypass on the Kobe waterfront, the Port Island Connector and the 6.6 km-long, Airport Access Highway to the new Kansai International Airport in Osaka Bay.

One of the two Expressway Corporations noted above is the Japan Highway Public Corporation (JHPC) which is responsible for at least three major freeways (expressways) in the region. These are the Meishin Expressway (the first such expressway in Japan) and the Chugoku and Kinki Expressways. The Meishin runs in a northeasterly direction from Osaka Bay (at Nishinomiya) to Kyoto. Both the Chugoku and Kinki Expressways start from Suita City, just to the north of Osaka City, and run west and south, respectively.

The second Expressway Corporation noted earlier, is the Hanshin Expressway Public Corporation (HEPC). It is one of the largest such Corporations in Japan and is, today, responsible for approximately 200 km of freeway-standard highway throughout the Hanshin region. Opened in 1964 with an initial length of 2.3 km in Osaka, it has grown in both size and capacity during the intervening 30 years. Almost a million vehicles per day used the system in 1994 with the highest traffic counts (131,500 per day) being recorded on the four lane, loop expressway in the center of Osaka City. For the fiscal year 1993, the average income from tolls was ¥340 million per day (approximately $3.4 million). More than 90% of the system is elevated, supported on about 8,500 spans. Of these, 83% are steel and 17% are concrete spans (Hanshin Expressway Public Corporation, 1994). Most substructures are single column concrete bents but single and multi-column steel bents are also used to a significant degree.

Major routes under the jurisdiction of the HEPC are Route 3 (Osaka - Kobe Route) and Routes 4 and 5 (Wangan Route). The Kobe Route was constructed from Nishinomiya to Kobe from 1965 to 1970. The link to Osaka was constructed from 1981 to 1985. The Wangan (Bayshore) Route, which links Kansai Airport in the south (Route 4) to Rokko Island in the east (Route 5), was completed in 1994 although parts of Route 4 had been completed as early as 1990. Both routes were major technical accomplishments at the time of their construction. Average peak weekday traffic volumes in 1994 were 63,000 and 18,500 for Routes 3 and 5, respectively.

Route 3 is elevated over its entire length and runs above NH 43 from Osaka to Kobe. It is generally supported on single column bents, except at interchanges where ramps and adjoining structures demand additional width and the use of multi-column bents. At the time of its construction it was highly regarded for both its engineering achievement and its aesthetic appeal.

The Wangan Route is also elevated over much of its length but its most remarkable feature is the number of world-class, long span bridges included in its construction. Some of the more notable

bridges include: (1) the Minato Gerber truss bridge (510 m center span, the third longest truss span in the world); (2) three cable-stayed bridges including the Higashi-Kobe bridge (485 m center span, the eighth longest cable-stayed span in the world); (3) two Nielsen-Lohse tied-arches including the Nishinomiya-ko bridge (252 m span); and (4) two Lohse tied-arches including the Rokko Island bridge (217 m span).

The HEPC has an active maintenance program and currently spends about ¥30 billion per year (approximately $300 million) in this area (Hanshin Expressway Public Corporation, 1994). It also has an ongoing seismic retrofit program and has for many years used earthquake couplers to restrain the free ends of simply supported girders. The corporation has recently begun to investigate the use of steel jackets for improving the performance of concrete columns and has installed some trial jackets on single column bents at the west end of Route 3.

Seismic design criteria for new structures meet or exceed those required by the Japan Road Association (Japan Road Association, 1990; Iwasaki et al., 1990). Furthermore, the HEPC has been proactive in the use of energy dissipators in bridges and, as early as 1981, completed the Yoshino-Tamagawa Viaduct on Route 3 in Osaka, using viscous shearing dampers. More recently, the HEPC has constructed two menshin (base isolated) bridges on Route 4 (the Wangan Route near the new Kansai Airport). These are the 4-span, Matsunohama bridge (1994) and the 6-span, Izumisano bridge (1994); both use lead-rubber (LRB) isolators. The Matsunohama bridge is instrumented for strong ground shaking with nine accelerometers and a 23-channel data acquisition system.

7.2.2 Description of Damage to Highways and Bridges

A large number of bridges were damaged in this earthquake and one estimate of the affected number is of the order of 60% of the total inventory. An exact number is difficult to count because of the use of long elevated sections that are tens of kilometers in length and the line where one bridge (or segment) ends and another begins is difficult to determine. Furthermore, several structures at the same interchange may be identified, in some damage reports, as one "bridge". Accepting these limitations, the number of highway "bridges" that sustained major damage (including collapsed spans) is of the order of 27. Many more suffered moderate-to-minor damage such as pounding, spalling of cover concrete and settlement of approach fills.

The 27 structures that were severely damaged by this earthquake are listed by route number in Table 7-III and by name in Table 7-IV. Figure 7-28 shows the location of 16 of these structures. These sites were visited by the UJNR team from February 13-17, 1995.

It is seen in Table 7-III that the HEPC suffered the largest loss, most probably because it has the largest inventory of elevated structures of any agency in the Hanshin region. The HEPC estimate for the direct cost of this damage is ¥460 billion (approximately $4.6 billion). Average traffic counts fell from 920,000 to 500,000 vehicles per day leading to a loss in toll revenue of ¥200 million per day. According to the Hyogo Prefectural Police, 16 persons died in vehicles on the Hanshin Expressway and 280 vehicles were abandoned by their owners. The number of piers sustaining moderate-to-large scale damage on Route 3 has been estimated to be 637.

Corresponding numbers for spans and bearings are 552 and 679, respectively. If all categories of damage are included, the HEPC estimates that the number of damaged spans on Route 3 is in excess of 1,300 (Hanshin Expressway Public Corporation, 1995).

Despite the extent of this damage, Route 5 is expected to be reopened by Golden Week (the first week in May), except for access to Rokko Island. Route 3 will be open by the fall of 1995. Of the two routes, Route 3 is the oldest by about 30 years and this probably accounts for the higher damage rate compared to that on the newer Route 5. Approximately 700 columns on Route 3 will be temporarily repaired and about 50 spans will be replaced before it is opened to traffic in the fall. Eventually, about 200 of these 700 columns will be replaced and the remainder will be strengthened to meet new seismic design criteria. By contrast, Route 5 did considerably better despite poorer soils and difficult foundation conditions. The most likely reason is the improvement in the seismic codes during the intervening 30 years and the fact that a major revision was completed to the design specification in 1990 (Japan Road Association, 1990; Iwasaki et al., 1990). This revision was in effect during the design of some, but not all, of the structures on this route.

Typical damage sustained by these structures includes shear and flexural failures in nonductile concrete columns, flexural and buckling failures in steel columns, steel bearing failures under lateral load, and foundation failures due to liquefaction. In addition, there was pounding between spans, failure of several earthquake couplers and settlement of many approach fills. Not so typical was the failure of a skewed bridge on pin-ended columns and the fracture of a set of holding down bolts in a wind shoe of a cable-stayed bridge which then led to the failure of the seismic energy dissipators and other hardware at this location. This performance is described in the following sections.

Table 7-III: Location of Bridges with Major Damage

Route No./Expressway		Owner/Agency	Number of Bridges (Major Damage)
2	(NH)	MOC	3
3	(Hanshin)	HEPC	11
5	(Hanshin)	HEPC	4
43	(NH)	MOC	1
171	(NH)	MOC	2
	Meishin	JHPC	4
	Chugoku	JHPC	2

Notes:
MOC Ministry of Construction
HEPC Hanshin Expressway Public Corporation
JHPC Japan Highway Public Corporation
NH National Highway

Table 7-IV List of Highway Bridges with Major Damage

Highway (Route)	Name	Type
Hanshin (3)	Takashio District Overpass	steel girders/concrete columns
	Futaba District Overpass	steel box girders/steel columns
	Tateishi District Overpass	steel box girders/steel columns
	Hirata-Fukae Overpass[1,2]	concrete girders/concrete columns
	Fukae District Overpass	steel box girders/concrete columns
	Mikage District Overpass	steel box girders/concrete columns
	Uozaki Ramps[1]	steel girders/concrete columns
	Kaigan-dori-Benten Overpass	concrete and steel girders/concrete cols.
	Hyogo-Nagata District Overpass[1,3]	steel girders/steel and concrete columns
	Minatogawa Ramps[1]	steel girders/concrete columns
	Sanyo Rail Line Overpass[1]	steel box girders/concrete columns
Hanshin (5)	Nishinomiya-ko Bridge[1]	Nielsen-Lohse tied arch/steel columns
	Shukugawa Bridge[1]	steel box girders/concrete multicol. bent
	Higashi Kobe Bridge[1]	cable stayed deck/steel columns
	Rokko Island Bridge[1]	Lohse tied arch/steel columns
Meishin	Moribe Viaduct[1]	concrete box girders/concrete pier walls
	Mukogawa Bridge[1]	steel girders/concrete columns
	Kawaraginishi Bridge[1]	concrete box girders/pin-ended concrete multi-column bent
	Nishinomiya Interchange	
Chugoku	Takarazuka Viaduct[1]	concrete box girder/concrete multi-column bent
	Toyonaka Overpass	
National Highway (NH 2)	Hamate Bypass[1]	steel box girders/steel columns
	Kobe-Port Island Ohashi[1]	steel box girders/concrete dual level 2-column bent
	Shioya Overpass	
National Highway (NH 43)	Iwaya Overpass	concrete girders/concrete columns
National Highway (NH 171)	Mondo Overpass	concrete girders/concrete columns
	Ikeda Overpass	

Notes:
1. Sites visited by UJNR Reconnaissance Team Feb. 12-17, 1995
2. Includes Higashi-Nada Viaduct
3. Includes Meiji District Ramps

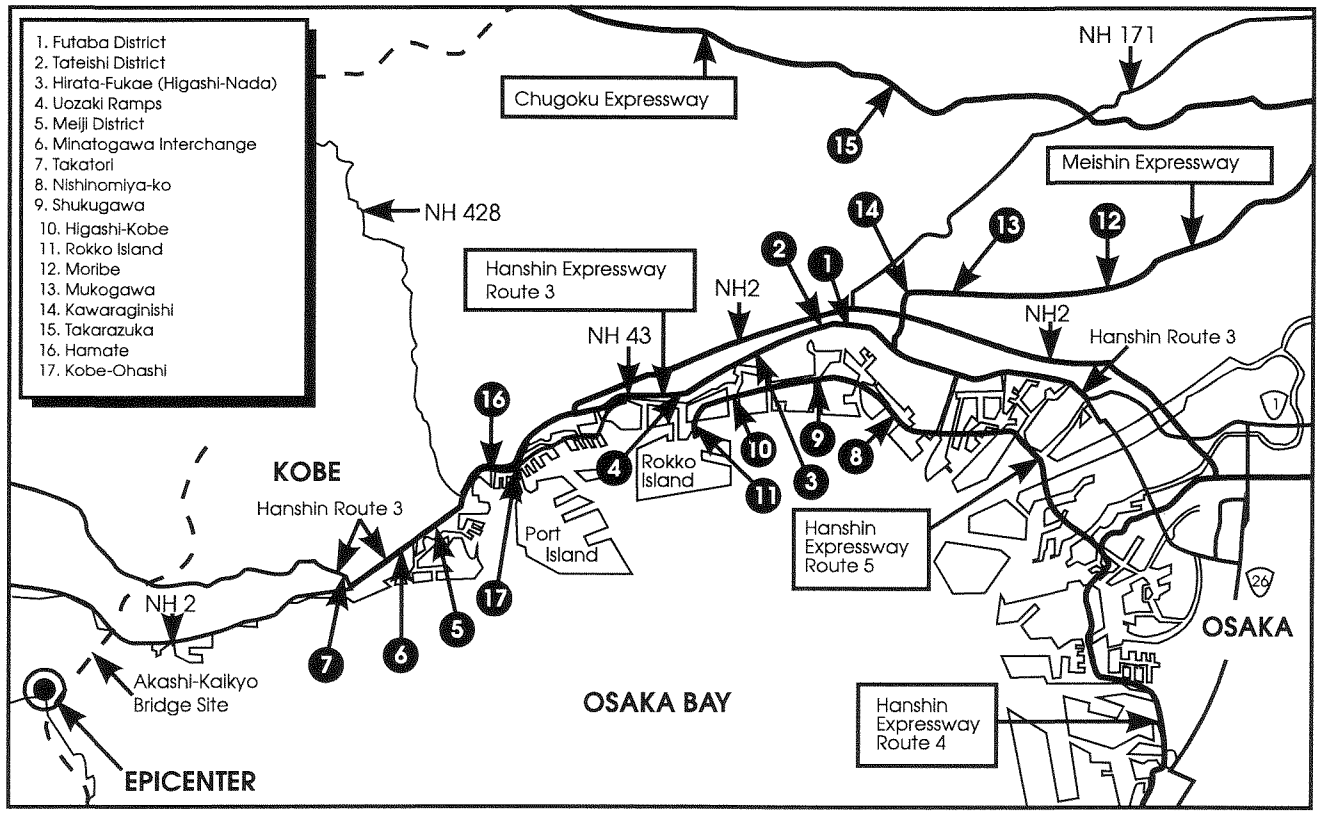


Figure 7-28 Bridge Sites Visited by UJNR Reconnaisssance Team, February 12-17, 1995

7.2.2.1 Damage to Superstructures Due to Bearing Failures

Many bridge bearings were damaged during this earthquake and in general these failures can be grouped into three categories:

(a) *primary* bearing failures which caused member distress elsewhere in the bridge and, in extreme cases, triggered collapse.
(b) *secondary* bearing failures which were the result of structural failures elsewhere in the bridge and caused by the redistribution of load for which the bearings were not designed and which led, in extreme cases, to collapse; and
(c) *fuse-like* bearing failures of either the primary or secondary kind that relieved the supporting substructures of load, protecting them from major damage and preventing collapse.

This section presents examples of Type (a) damage, i.e. examples of bearing failures which appear to have been the primary reason for bridge damage and/or collapse. These four examples are the Nishinomiya-ko, Rokko Island, Mukogawa and Hamate Bypass bridges. Other sections in this report note secondary failures (Type(b)) and Section 7.2.2.3 presents an example of Type (c) behavior.

The **Nishinomiya-ko bridge (8)**[1] carries Route 5 over one of the shipping entrances to the port of Nishinomiya (Figure 7-29a). It is one of the longest Nielsen-Lohse Arch bridges in the world with a main span of 252 m and a rise of 42 m. Constructed in 1993, this all-steel tied-arch weighs approximately 8,000 tonnes and is supported on four bearings: two fixed bearings at the west end (Pier 110) and two expansion bearings at the east end (Pier 111). Both Pier 110 and 111 are steel towers that are approximately 25 m high from top of foundation to bearing level. Each foundation is a concrete caisson extending to depth of about 23 m below ground level. Soils include reclaimed gravels on alternating layers of saturated clays, sands and gravels. N-values range from 2 to 20 over the first 20 m.

At the east end, the first two approach spans (Piers 111-112 and Piers 112-113) are simply supported steel girders on steel piers and are 54 m and 62 m long, respectively. The next three spans (Piers 113 to 116) are a continuous steel box girder of total length 183.5 m; they are also supported on steel piers that are about 23 m high. Support conditions for these piers are given in Table 7-V. Earthquake couplers are provided in the longitudinal direction at all movement joints. In general, these are a pair of 25 mm steel plates that have either one or two slotted holes to accommodate up to ±300 mm before engagement. Plate sizes vary but are of the order of 950 x 250 mm.

[1] Numbers in parentheses refer to bridge sites shown in Figure 7-28.

Table 7-V Support Fixity Conditions for the Nishinomiya-ko Bridge

Pier No.	110	Arch Span	111	112	113	114	115	116	
Fixity	E-F			E-F	E-E	F-E	F	F	E-E

Notes E: Expansion bearing (rotation and longitudinal movement permitted)
F: Fixed bearing (rotation only permitted)

Damage sustained during the earthquake included failure of one of the fixed bearings under the arch span at Pier 110 and collapse of the first span on the eastern approach (Figure 7-29b). This simply supported span fell from its support at Pier 111 but retained its seating on Pier 112. Ground movements measured after the event showed permanent offsets in the position of several piers probably due to lateral spreading of the soils during liquefaction. Secondary damage included anchorage failure in one of the cables between the arch rib and tie beam; failure of all of the restrainers at Pier 111; and failure of the bearings, couplers and expansion joints at Pier 112 and Pier 113 (Figure 7-30).

It seems likely that the collapse began with the failure of one of the fixed bearings at the western end of the arch span (i.e., at Pier 110). These bearings have a gravity load rating of 4,500 tonnes each. Their lateral load capacity is 2,800 tonnes in the longitudinal direction and 1,400 tonnes in the transverse direction. Since the weight of the span is in excess of 8,000 tonnes, the longitudinal capacity of the pair of fixed bearings is about 70% of the weight. Given the high ground accelerations in the area, and the probable uneven distribution of load between the pair of bearings, it is quite possible that the capacity of one of the pair was exceeded, leading to its failure. If this occurred during a half cycle of loading towards the west, then substantial longitudinal loads would have been transferred to the opposite end of the arch, tearing the restrainers out of the webs of the girders in the approach span (Figure 7-31). At the same time, the fixed bearings at this pier (Pier 111) would have been heavily overloaded and failure would follow immediately. In subsequent cycles, the reversed motion of the arch and the lateral movement of Pier 111 towards the center of the channel led to the unseating of the approach span and its collapse from Pier 111.

The **Rokko Island bridge (11)** at the west end of Route 5, was completed in 1992 and gives access to Rokko Island in Osaka Bay. This single span, steel, tied-arch spans 217 m and rises 36 m above its springings (Figure 7-32). It varies in width from 16.25 m at the south end (Rokko Island) to 26.5 m at the north end (Ashiya City) to accommodate on ramps to the expressway. It follows that the ribs of the arch, although vertical, are not parallel to each other. They are held in this position by transverse floor beams at the deck level and by crossbracing members in the plane of the rib. The arch is supported at each end on two multi-column steel bents which are about 26 m high. All major structural members (arch ribs, tie beams and bent columns) are boxed, single cell, steel members fabricated from 50 mm plate and stiffened internally.



Figure 7-29a General View of Nishinomiya-ko Bridge, Route 5



Figure 7-29b Collapsed Approach Span Between Piers 111 and 112, Nishinomiya-ko Bridge

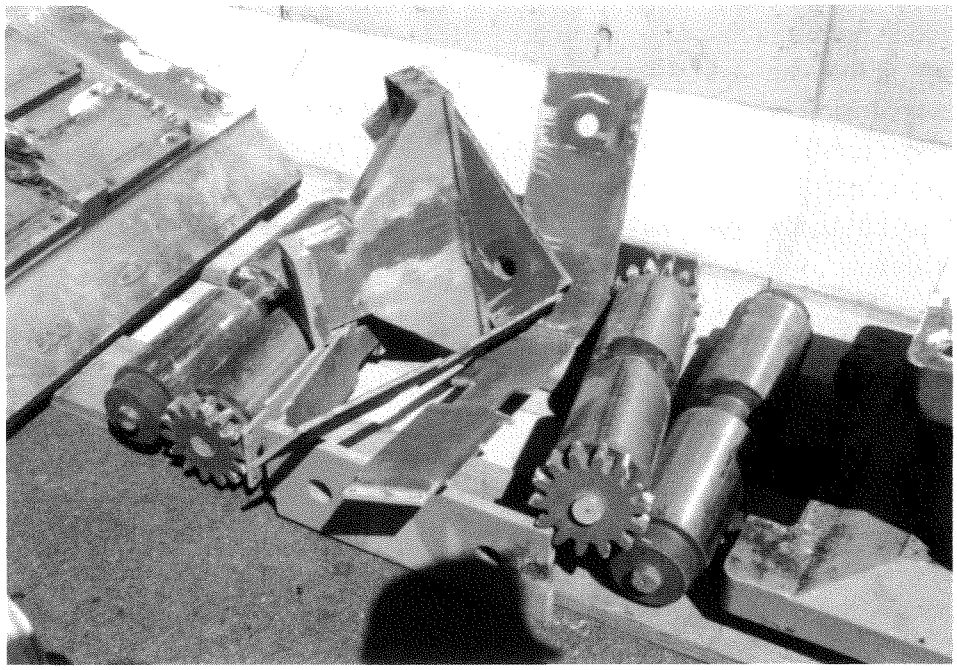


Figure 7-30 Damaged Expansion Bearings from Under Approach Spans, Nishinomiya-ko Bridge, Showing Nested Rollers and Guide Rails

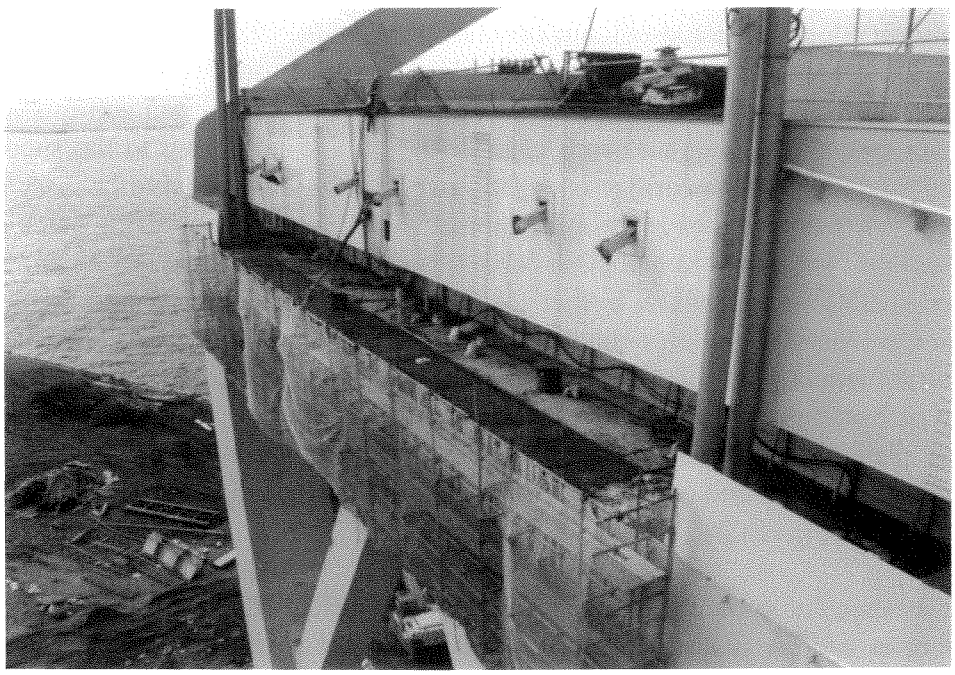


Figure 7-31 Cap Beam of Pier 111, Nishinomiya-ko Bridge, Showing Cross-Girder of Arch and Failed Restrainers

The arch weighs 6,450 tonnes and is supported on four steel bearings, two at each end of the span. The fixed bearings are at the northern end (the wide end); the expansion bearings are at the southern end (the narrow end). Reaction loads are greater at the fixed end because of its greater width. Rotation is permitted but translation prevented (both transversely and longitudinally) at all bearings except at the south end where the expansion bearings permit longitudinal movements to occur. These expansion bearings use nested rollers to accommodate movement in this direction and guide rails to prevent movement normal to the span. The guide rails are expected to transfer wind and seismic loads that are normal to the span of the arch. Normal practice is to design these restraints to resist a seismic load equal to 1.5 times the product of the seismic coefficient and the dead load reaction.

During the earthquake, the guide rails at the expansion bearings failed under transverse loading, allowing the south end of the truss to displace laterally a distance of about 3 m to the east across the bent cap (Figure 7-33). The arch came to rest with the east rib overhanging the end of the cap beam and as a consequence, twisted the superstructure about its longitudinal axis (Figure 7-34). The racking of the superstructure caused buckling in the crossbracing in the plane of the ribs particularly in those panels just to the south of the midspan cross-member (Figure 7-35).

When constructed three years ago, this bridge was prefabricated in a shipyard to the west of Akashi-Kaikyo, transported by barge to the site and lifted into place by six floating cranes. Repair is also expected to involve floating cranes and the lifting of the south end off the damaged bearings, followed by realignment on the supporting bent. Replacement of the buckled crossbracing and the damaged expansion joints will then be possible.

The **Mukogawa bridge (13)** on the Meishin Expressway is a dual carriageway, six-span steel girder structure on concrete, single-column bents (Figure 7-36). Built in 1963, each carriageway is an independent structure and comprises three, 2 m deep, plate girders with concrete deck slab and diagonal crossbracing in the plane of the lower flange. Two three-span continuous segments make up the six spans. The length of each span is 46.5 m and is skewed to the support line by about 30°. The total length of the bridge is slightly over 280 m with an overall carriageway width of about 10 m. All substructures are single, circular, concrete columns with hammerhead cap beams. Each column is tapered to a depth of about 7 m, at which point it is founded on a single large-diameter shaft that extends a further 24 m to stable gravel beds and stiff clays. The abutments are also founded on large-diameter shafts. The columns for Piers 1 and 5 are almost completely buried leaving only the hammerheads above ground level. All girders are supported on steel pin-type bearings, with and without sliding plates to provide for expansion as necessary. Where sliding plates are installed beneath the pin assembly, guide bars are also provided to prevent lateral movement and restrain uplift (Figure 7-37). The location of the fixed and expansion bearings are given in Table 7-VI.

Longitudinal earthquake couplers were installed in the bridge between 1985 and 1990 as a retrofit measure to address inadequate seat widths in the span-wise direction. These steel plate restrainers are located at the abutments and connect the web of each girder directly to the adjacent back wall of the abutment. They are intended to be effective in the longitudinal direction



Figure 7-32 General View of Rokko Island Bridge, Route 5

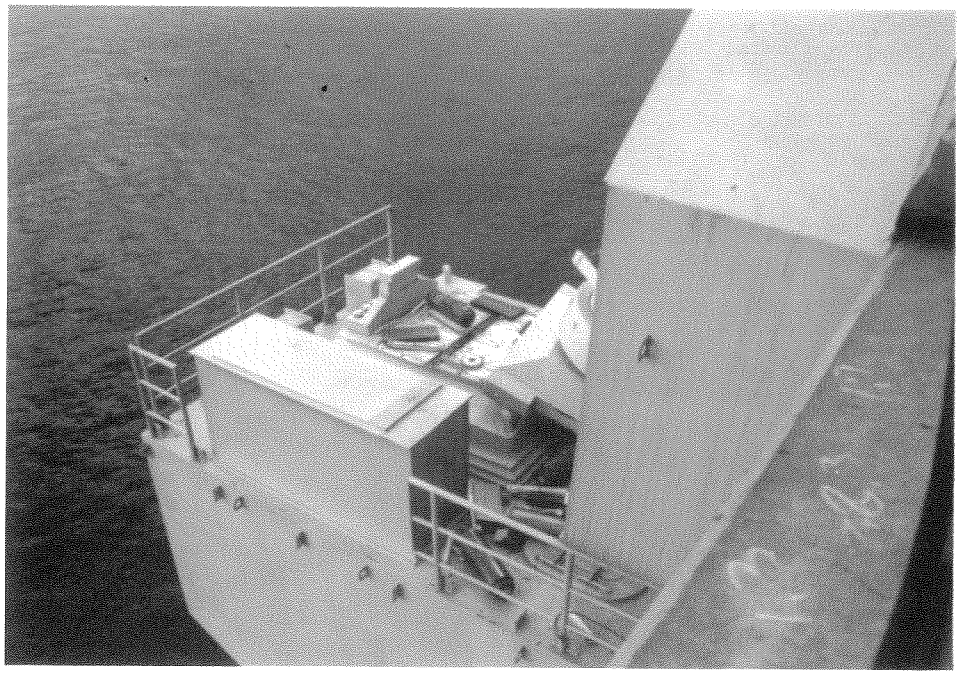


Figure 7-33 Damaged Expansion Bearing and Lateral Offset at West Face of South Pier, Rokko Island Bridge



Figure 7-34 Lateral Offset at East Face of South Pier, Rokko Island Bridge

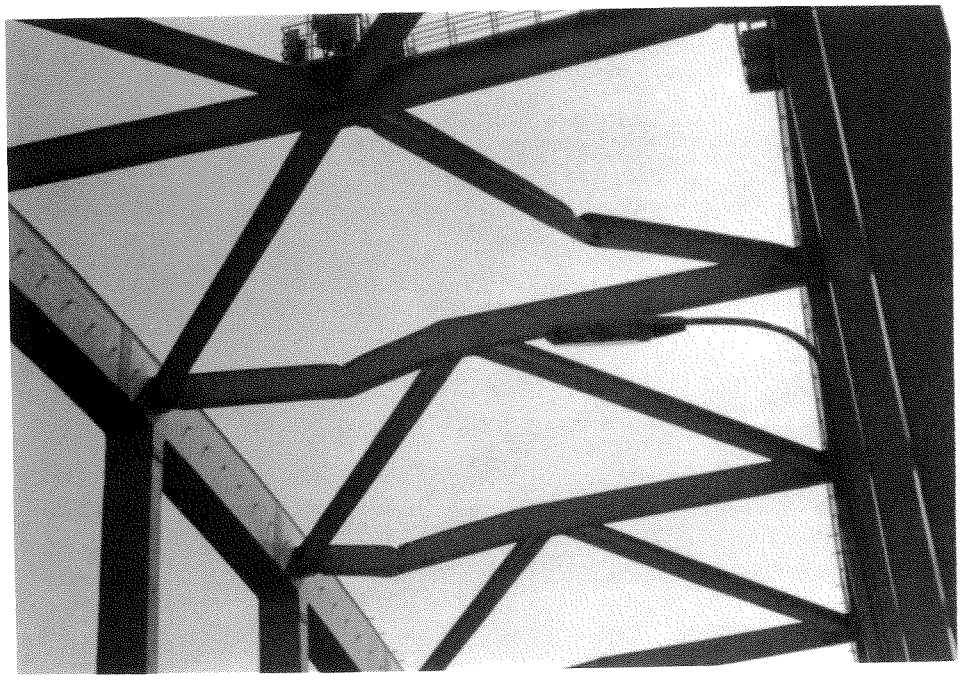


Figure 7-35 Buckled Cross-Members in Upper Chord, Rokko Island Bridge



Figure 7-36 General View of Mukogawa Bridge, Meishin Expressway



Figure 7-37 Bearing and Restrainer Damage at Abutment A1, Mukogawa Bridge, Showing Distorted Guide Rails and Uncoupled Restrainer from Abutment Backwall

Table 7-VI Support Fixity Conditions for the Mukogawa Bridge

Pier	A1	P1	P2	P3	P4	P5	A2
Fixity	E	E	F	E-E	F	E	E

Notes
A1,A2: West and east abutments
P1-P5: Intermediate piers
E: Expansion bearing (rotation and longitudinal movement permitted)
F: Fixed bearing (rotation permitted)

only (the unrestrained expansion direction) and offer no restraint transversely; the bearing guide bars are expected to resist loads in this direction.

During the earthquake, the bearings at the west abutment (A1) failed in transverse loading due to a combination of anchorage pull-out and guide bar distortion. Transverse loads were then transferred to the earthquake couplers which also failed, since they were now loaded in an unintended direction. Several were stripped from the abutment back wall while at the same time bending the webs of the deck girders about their weak vertical axis and imposing severe plastic distortion in these sections (Figure 7-38).

The loss of restraint at the abutment led to a redistribution of load to the intermediate piers and the overload of Piers 1 and 3. It was observed that Pier 1 was almost completely buried over its full height and this may have been the reason it received a disproportionately high share of the seismic load after the abutment released its load. Once excavated, both columns at this location show flexural distress in the upper third of their height, which, because of the taper, is the section of least strength in flexure and shear (Figure 7-39). These non-ductile columns have inadequate transverse steel for confinement and shear reinforcement to satisfy current performance criteria.

Some damage is therefore to be expected during strong ground shaking. In this earthquake, there appeared to be no residual misalignment in the columns and thus repair (to the columns) should be a straightforward exercise.

The **Hamate Bypass (16)** is a two level elevated viaduct carrying Route 2 along the Kobe waterfront. Longer spans are continuous steel box girders supported on steel bents constructed from single cell, internally stiffened, box sections. These dual-column bents support the upper and lower decks at about 22 m and 10 m above the ground, respectively. Overall widths at the carriageway levels are about 15 m except where ramps and emergency stopping shoulders are accommodated. Column cross sections are about 2.8 x 2.2 m. All girders are supported by either fixed or expansion steel bearings at these bents. Transverse restraint is provided by the bearings at all locations.

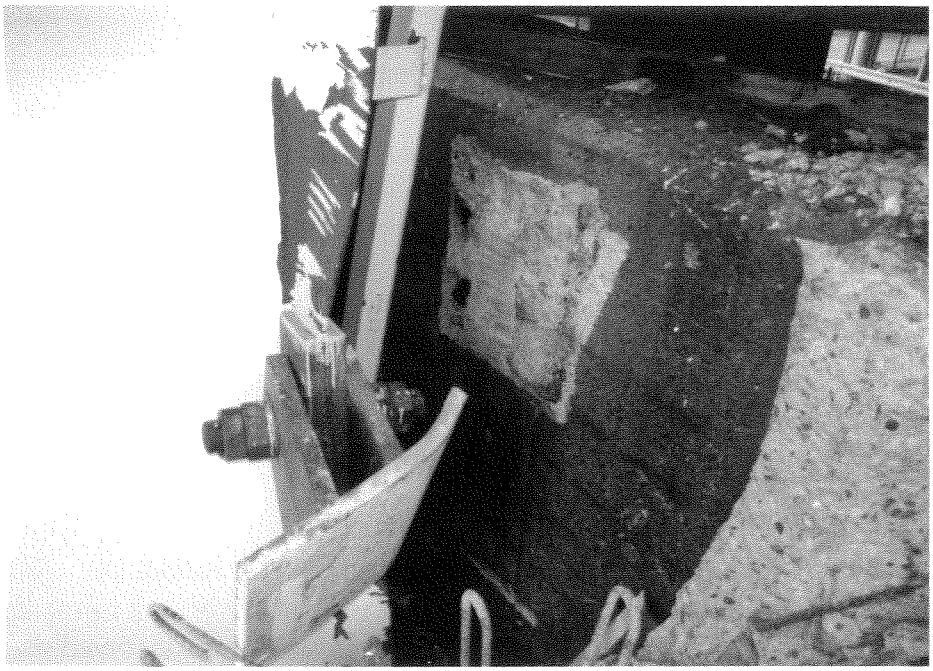


Figure 7-38 Damaged Restrainer at Abutment A1, Mukogawa Bridge Showing Failure of Anchor Bolts and Distortion of Web of Main Girder



Figure 7-39 Failure at Top of Buried Column, Pier P1, Mukogawa Bridge

Several sections of this elevated structure were damaged during the earthquake and the section from Pier 34 to Pier 38 suffered bearing damage with large lateral offsets at Pier 36 (Figure 7-40). This four span section is comprised of two, 2-span, continuous box girders of approximately equal length. All bearings at all five bents under the upper deck appear to have failed. The lack of transverse restraint then led to rotation of the upper level girders about a vertical axis. Both segments appear to have rotated clockwise about their respective end supports at Piers 34 and 38. This then imposed a large lateral displacement (estimated to be of the order of 3-4 m) at the opposite end of each segment (i.e. at Pier 36). Since these displacements are of opposite sign, the relative displacement, parallel to the expansion joint, at this pier is of the order of 6-8 m. A generous cap width in the transverse direction prevented collapse and limited the damage to the bearings, expansion joints and appurtenances (guardrails, down-pipes and the like). It is possible that this is an example of Type (c) bearing behavior, where failure of the transverse restraints at Piers 34 through 38 has relieved these piers of seismic load, protecting them from major damage.

7.2.2.2 Damage to Concrete Substructures

Although several hundred concrete piers were damaged in this earthquake, almost all were designed and constructed in the 1960's and early 1970's without the benefit of modern codes and recent developments in seismology and ductile design. Typical damage involved shear failures in shorter, under-reinforced columns. Flexural failures were also evident in taller columns that lacked adequate confining steel or terminated vertical steel in areas of high moment. Splice failures in this reinforcement were also common, especially those splices that had been butt welded in regions of high moment.

This section presents examples of these failures by summarizing the damage sustained to two sections of the Hanshin Expressway Route 3 (Higashi-Nada Viaduct and Pier 240), the Takarazuka Viaduct on the Chugoku Expressway, and the Moribe Viaduct on the Meishin Expressway. Reference is also made to the damage sustained by the Kobe-ohashi distribution structure and the Route 3 structures at Minatogawa and Takatori (Pier 688).

Constructed in 1969, the **Higashi-Nada viaduct (3)**, also known as the Hirata-Fukae viaduct, is an 18 span segment of the Hanshin Expressway on Route 3. It is the only segment of this Route which has both a concrete superstructure and concrete substructures. The superstructure is a series of 35 m prestressed concrete spans with a total length of 635 m (13 spans are 35 m long and 5 spans are 36 m long). Each span consists of two 6.5 m cantilevers that are monolithic with the columns, one at each end of the span, and a 22 m drop-in girder - a form of construction that was popular in Europe in the 1960's and given the name "piltz" construction from the German word for "mushroom". The overall width of the superstructure is 20.25 m with an effective carriageway width of 15.5 m.

The substructures are single column bents that are 3.3 m in diameter and vary in height from about 10.5 m to 12.5 m, measured from the top of the piled footings to the underside of the cap beam. Vertical reinforcement at the bottom of a typical column comprises 180, 35 mm diameter bars arranged in three equal concentric layers. The inner layer is terminated at 3.5 m above the footing; the remaining two layers extend over the full height of the column and into the cap

beam. Transverse steel comprises three circular hoops of 16 mm bars (one around each layer of vertical steel) at a vertical spacing of 300 mm in the central third of the column height and 200 mm in the end zones.

All foundations are piled footings that vary in size from 10.5 x 9.5 m to 13.8 x 11.5 m with a minimum thickness of 2 m. The number of 1 m diameter concrete piles supporting each footing varies from 16 to 20, with lengths that range from 11 m to 15.5 m.

All 17 single-column bents of this viaduct, from Piers 126 to 142, collapsed on their side during the earthquake (Figures 7-41 through 7-43). The failure mode appears to have been a flexural failure at the base of each column under strong transverse loading. The termination of one-third of the column vertical steel at one-third of the column height meant that this steel was largely ineffective in the potential plastic hinge zone and the section lacked the capacity (and probably the confining steel) to develop a stable plastic hinge. Collapse was due to uncontrolled (irreversible) inelastic rotation at the base of each column.

It is estimated that about 700 columns along Route 3 were damaged to some extent and of these 700 columns, about 200 will need replacement. Typical of this damage is the section from **Piers 238 to 241 of Route 3 near Uozaki (4)**. This 3-span segment is a continuous, steel, twin-spine superstructure supported on single column bents and piled footings (Figure 7-44). Each spine is a 3 m deep single-cell box girder with spans of 55 m, 87 m and 55 m. All piers have hammerhead cap beams that measure 16.2 m in overall length. Their width is constant at 3 m, but their depth varies from 1.5 m at the free end to 3.3 m over the column. Two pairs of steel bearings support the two box girders over each cap beam. These restrain lateral movement and uplift while permitting rotation and longitudinal movement at all locations except at Pier 240 where the bearings are also fixed against longitudinal expansion (See Table 7-VII). Principal dimensions for the columns, footings and piles are also given in Table 7-VII.

During the earthquake, Pier 240 failed catastrophically in longitudinal shear despite the fact that it was clearly designed to resist large lateral loads (Figures 7-45 and 7-46). As the only fixed pier in this 3-span segment, all longitudinal load was attracted to this pier and it is clear from the relative sizes of the four substructures supporting this segment (Table 7-VII) that this was anticipated by the designers. Nevertheless, inadequate transverse steel was provided in this pier to allow ductile flexural hinging to occur before the onset of a brittle failure in shear. Once this column split along a diagonal line from upper right corner to lower left (when looking north at the pier) the column shortened in height and vertical support for the box girder was lost. The girder then sagged over Pier 240 and attempted to rotate about Pier 239. Since it was held down at Pier 238 by a bearing of type S0-36 (Table 7-VII), large compressive forces were generated in the lower flanges of the box girders in the end span from Pier 238 to Pier 239. These forces exceeded the elastic limit and compressive buckling occurred in the lower flanges and webs of these girders (Figure 7-47). Pier 241 also sustained structural damage but not as severe or as catastrophic as its neighbor, Pier 240. The difference in support fixity between these two piers is probably the reason for this difference in damage level.

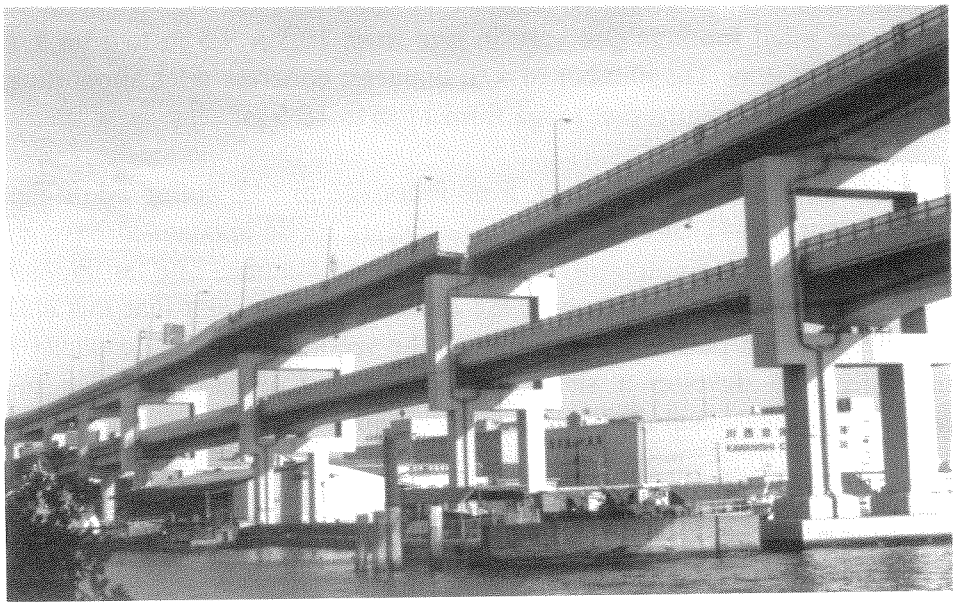


Figure 7-40 Lateral Offset at Pier 36 in Upper Level of Hamate By-Pass Due to Bearing Failures at Piers 34 Through 38



Figure 7-41 View of the Collapsed Higashi-Nada Viaduct Looking West from Pier 125 (Photo courtesy of Andy Taylor)



Figure 7-42 Higashi-Nada Viaduct, Pier 126 (Photo courtesy of Andy Taylor)



Figure 7-43 Higashi-Nada Viaduct, Pier 134 (Photo courtesy of Andy Taylor)



Figure 7-44 General View of Hanshin Expressway (Route 3) Near Uozaki Showing Collapse of Section Over Pier 240 in Middle Distance

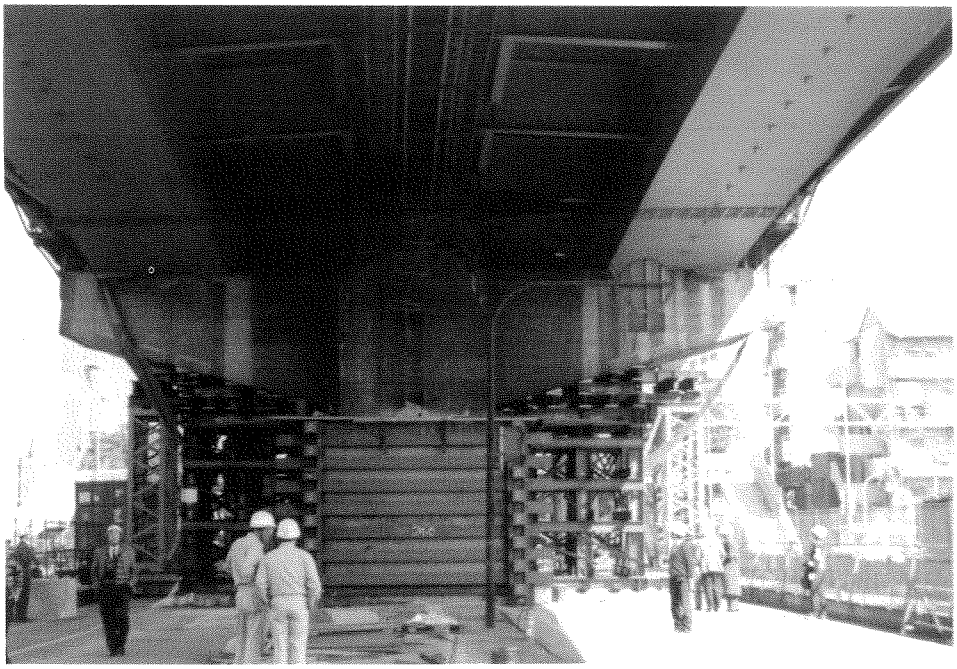


Figure 7-45 Pier 240 of Hanshin Expressway Showing Temporary Repair to This Single Column Bent



Figure 7-46 Shear Failure in Pier 240 of Hanshin Expressway Showing Temporary Repair to Column to Prevent Total Collapse

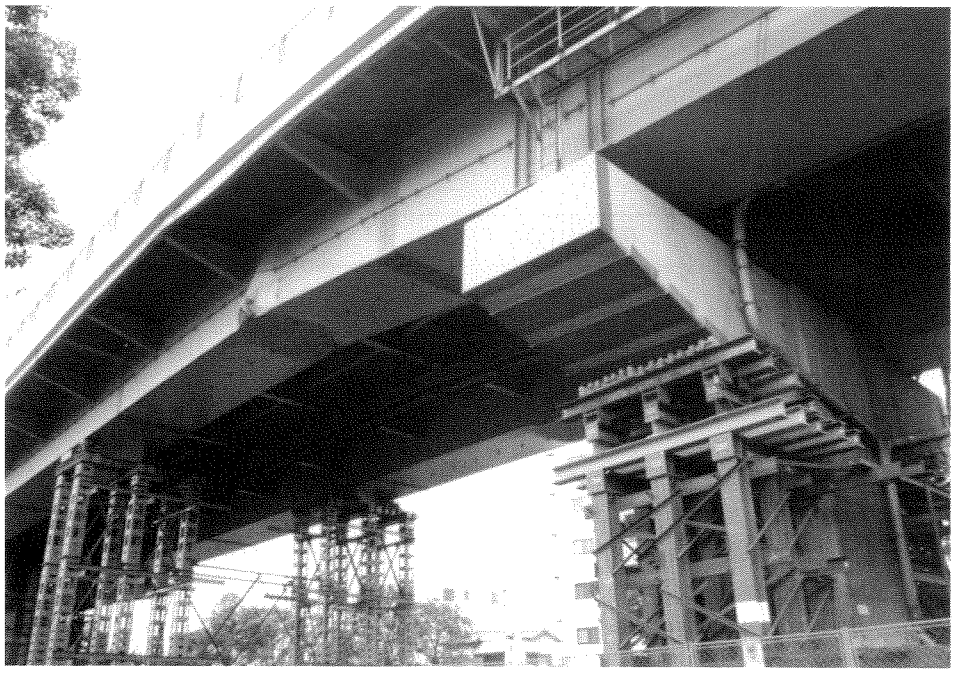


Figure 7-47 Compressive Failure in Lower Flange of Steel Box Girder Between Piers 238 and 239 of Hanshin Expressway

Table 7-VII Substructure Details for Piers 238 to 241, Route 3 Near Uozaki

Pier	P241	P240	P239	P238
Bearing Fixity	E-E	F	E	E-F
Bearing Type	S0-36	S0-37	S0-38	S0-36
Column Size	3.3m dia.	3.6 x 3.3m	3.3m sq.	3.3m dia.
Footing Size	11x11x2.5m	15.5x12x2.5m	12x12x2.5m	10x10x2.5m
Pile Size (LxD)	14 x 1m dia	15 x 1m dia	18.5 x 1m dia	14 x 1m dia
No. of Piles	17	28	25	16

Notes E: Expansion bearing (rotation and longitudinal movement permitted)
F: Fixed bearing (rotation only permitted)
S0-36: Pin and roller bearing with uplift restraint
S0-37: Pin bearing
S0-38: Pin and roller bearing without uplift restraint

The **Takarazuka viaduct (15)** is located on the Chugoku Expressway about 30 km northeast from Kobe (Figure 7-48). Constructed in 1970, it is a 10 span viaduct of total length 172 m.

Two carriageways are carried on two independent structures. Each superstructure is a continuous hollow concrete slab and is supported on concrete multi-column bents. Steel bearings connect the superstructure to the free-standing columns; there is no cap beam below the bearings. The superstructure is comprised of two 5-span segments from the west abutment to Pier 5 and from Pier 5 to Pier 10. A separate elevated structure extends east from Pier 10. All spans are 17.2 m in length; support fixity is given in Table 7-VIII.

Table 7-VIII Support Fixity Conditions for the Takarazuka Viaduct

Pier	A1	P1	P2	P3	P4	P5	P6	P7	P8	P9	P10
Fixity	E	E	F	F	E	E-E	E	F	F	E	E-E

Notes E: Expansion bearing (rotation and longitudinal movement permitted)
F: Fixed bearing (rotation only permitted)

Each multi-column bent consists of three rectangular columns and all are founded on piled footings. Piers 2 and 3 are approximately 4.5 m high from top of footing to top of column and Piers 7 and 8 are about 9 m high over the same distance. The footings under the fixed piers (Piers 2, 3, 7 and 8) are supported on 23 piles of uncertain diameter and length. Those under the expansion piers are supported on either six or eight piles depending on location. Individual columns are about 2.4 x 1.2 m in size and oriented so that the strong direction is transverse to the span. They are typically reinforced with 36 vertical bars that are 35 mm in diameter. Footings for the fixed and expansion piers are approximately 9.5 x 11.5 m and 4.25 x 10.5 m, respectively.

Damage sustained during the earthquake implies strong ground shaking in the longitudinal direction. Piers 2 and 3 failed catastrophically in longitudinal shear under both carriageways (Figure 7-49). Major distress to all six columns under the eastbound carriageway, shortened the overall height of these two piers and allowed this superstructure to sag a distance of 300 mm at Pier 2 and 450 mm at Pier 3. Residual longitudinal displacements of 300 mm and 160 mm at Piers 2 and 3, respectively, were also observed - both in the same easterly direction. Similar distress was observed for the westbound carriageway. Since these piers are the fixed piers for this segment of the bridge, high longitudinal loads are attracted to them. Judging by the size of the substructures at these locations, this effect was clearly anticipated by the designers. However, insufficient transverse steel was provided to force ductile flexural hinging to occur before the onset of a brittle failure in shear. This is a similar situation to that described above for Pier 240 on the Route 3 Expressway. In this case, however, the situation was aggravated by the relatively short height of Piers 2 and 3 which increases the shear demand in proportion to the reduction in height.

By contrast, Piers 7 and 8 were relatively free from damage. These are the fixed piers for the second segment and it is reasonable to expect them to have seen the same ground motion as those in the previous segment. Light flexural cracking was observed at the bottom of almost all the columns in these piers but it was not severe and did not appear to be affecting the gravity load capacity in any way. As noted above, these columns are twice the height of Piers 2 and 3 and the extra height, for the same transverse reinforcement, is favoring a flexural mode of failure.

However, Piers 6 and 9 in this segment were significantly damaged and this is a surprise in view of the expansion bearings carried by these piers. Flexural cracks were observed at the base of several columns in these piers and Pier 9 appeared to be leaning in a westerly direction which is the opposite direction to the residual shear displacements in Piers 2 and 3. It seems likely that the expansion bearings are not free in the longitudinal direction as assumed and some longitudinal shear is being transferred to these piers.

It also seems likely that the two segments are responding as if they were two very different structures. The columns in the first segment have an average height of about 5 m; those in the second segment average about 9 m. This difference in height leads to an almost six-fold difference in lateral stiffness which in turn means that the fundamental period of the second segment is about 2.5 times that of the first segment. This difference in period means that the seismic response of the two segments will be unrelated and quite possibly out-of-phase. Pounding between the two segments at Pier 5 is quite possible.

The **Moribe viaduct (12)** on the Meishin Expressway was completed in 1964 and is located between the Nishinomiya interchange and the Amagaski interchange. It carries east- and westbound traffic on two independent but parallel concrete bridges that are supported on concrete pier walls. The viaduct consists of a series of 5-span segments; each segment is 85 m long and comprises a continuous hollow concrete slab superstructure supported on six piers. All piers are approximately 5 m long and 7 m high and are supported on piled footings. Pier widths vary according to the fixity at the superstructure level. A single footing is used to support the two piers at each support under the parallel structures. Footings that support fixed piers are about 6 m



Figure 7-48 General View of Takarazuka Viaduct, Chugoku Expressway



Figure 7-49 Shear Failures in 3-Column Bent at Pier 3, Takarazuka Viaduct

wide and 18 m long and are founded on a double row of piles of unknown depth. Footings under expansion piers are about 3 m wide and use a single row of piles.

Five segments of this viaduct were damaged in this earthquake. The most common cause of distress was shear failures in those wall piers that were fixed in the longitudinal direction. Typical of this behavior is the performance of the segment from Pier 26 to Pier 31. Of the six piers supporting this section, two have fixed bearings and four have expansion bearings as shown in Table 7-IX. All bearings permit rotation by using rubber pads. At the fixed connections, restraint is provided by extending the vertical reinforcing steel near the neutral axis of the pier across the joint at 45° and anchoring it in the superstructure.

In this segment, Pier 30 of the eastbound bridge and Pier 29 of the westbound bridge failed catastrophically in shear (Figures 7-50 and 7-51). Both are fixed piers and reinforced with two layers of 32 mm diameter bar in the longitudinal direction. Transverse steel is 16 mm bar at 250 mm spacing and placed between the two layers of vertical steel. The width of each pier is about 850 mm. The collapse of Pier 30 reduced the height of the pier and allowed the superstructure to sag about 600 mm; Pier 29 was not as severely affected.

Of interest is the fact that Pier 30 of the westbound bridge and Pier 29 of the eastbound bridge did not suffer the same distress. Both are also fixed piers and detailed in like manner to those piers that did fail at these locations. This might be explained if it is assumed that both fixed piers under the same bridge sustained the same, or almost the same, elastic shears but one had a slightly lower shear capacity than the other and failed first (in a brittle manner). This sudden reduction in stiffness would then have lengthened the natural period of the segment and perhaps unloaded the second pier to safe level for the remainder of the earthquake. Close examination of the westbound Pier 30 did show fine diagonal hairline cracks which indicate that this pier was indeed heavily loaded and perhaps on the brink of a massive shear failure when it was saved by the rupture of the adjacent pier (the westbound Pier 29).

The **Kobe-ohashi (17)** near Port Island is a dual level connector between the Harbor Highway, the Route 2 Bypass at Kobe, and Route 3 of the Hanshin Expressway (Figure 7-52). The steel superstructure is comprised of a series of simple plate girders and 2- and 3-span continuous box girders. The substructures are concrete and steel, multi-column, framed bents that support both the upper and lower carriageways. These bents differ from pier to pier but in general they are two-column bents of increasing height from south (Pier 23) to north (Pier 26). However, Pier 23 has three columns at the lower level and a steel cap beam at the upper level which is not monolithic with the concrete columns. Instead this cap beam, which is also the diaphragm for the box girder that is supported at this level, is connected to the two columns of the bent by fixed bearings. Support fixity for this section of the connector is summarized in Table 7-X. Spans are approximately 25 m in length.

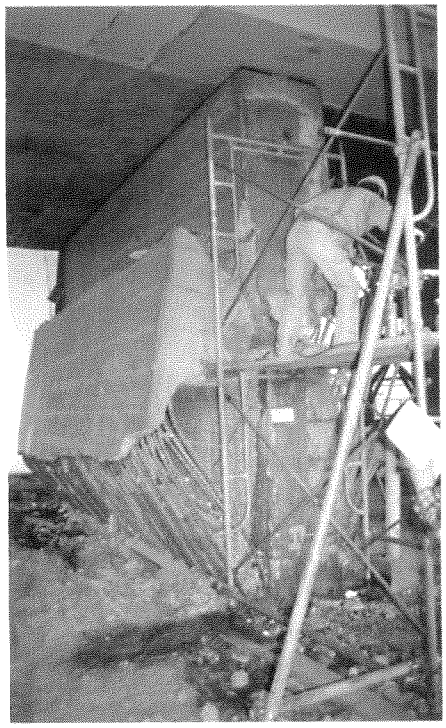


Figure 7-50 Shear Failure in Wall Pier (West Face), Moribe Viaduct

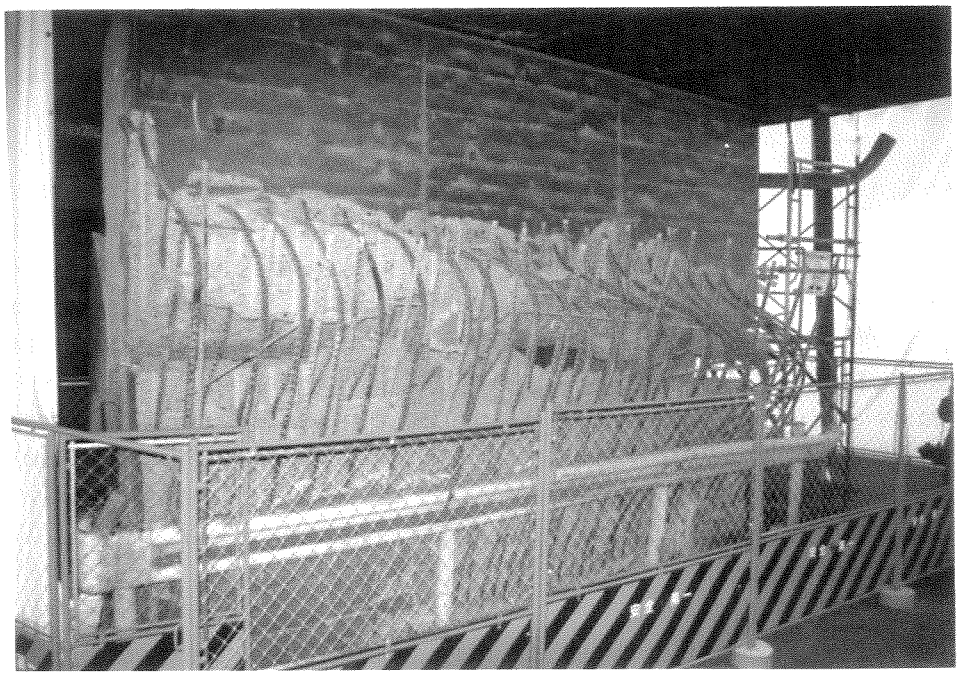


Figure 7-51 Shear Failure in Wall Pier (East Face), Moribe Viaduct

Table 7-IX Support Fixity Conditions for Piers 26 to 31, Moribe Viaduct

Pier	26	27	28	29	30	31
Fixity	E-E	E	E	F	F	E-E

Notes E: Expansion bearing (rotation and longitudinal movement permitted)
F: Fixed bearing (rotation only permitted)

Table 7-X Support Fixity Conditions for Piers 23 to 26, Kobe-Ohashi

Pier	23	24	25	26
Fixity	F	E-F	E-F	E-E

Notes E: Expansion bearing (rotation and longitudinal movement permitted)
F: Fixed bearing (rotation only permitted)

During the earthquake, Piers 23 to 26 were damaged to varying degrees. Flexural hinges formed in the columns of all four piers due to longitudinal loading and bending about the weak axis (the transverse axis) of each bent (Figure 7-53). These hinges were well-developed in the shorter bents (Piers 23 and 24) and less well-developed in the taller frames (Piers 25 and 26). For example, the longitudinal reinforcement was buckled on both faces of the hinge zones and some welded splices failed in the inner steel layers in Pier 23 but only cover concrete was lost in Pier 26. Hinge locations also varied from the mid-height of the lower level columns in Pier 23 to just below the lower cap beam in Pier 26. These variations in the extent and location of the hinging may be due to the difference in column heights and the consequential variations in the amount and detailing of the longitudinal reinforcement. It is also expected that the shorter columns attracted a larger share of the base shear than the taller columns, because of their greater stiffness while in the elastic range.

In addition to the column hinging, other damage sustained by this structure included several connection failures and pounding against adjacent ramp structures and buildings. In particular, the connection between the steel cap beam at the upper level of Pier 23 appears to have failed at one of the columns allowing the girder to slide on that column and develop a permanent offset of about 150 mm. The resulting asymmetric load on the bent may have been sufficient to cause the diagonal cracking that was observed in both the lower cap beam and adjacent column of this bent.

The **Minatogawa interchange (6)** comprises four, highly curved ramp structures that provide access to Route 3 of the Hanshin Expressway between Piers 605 and 611. Each ramp is either a 3- or 4-span structure comprising steel girders on single column concrete bents with large hammerhead cap beams. The 90° curvature in each ramp is largely provided by a 2-span curved



Figure 7-52 General View of Kobe-Ohashi Connector Near Port Island Showing Formation of Flexural Hinges in Lower Level Columns

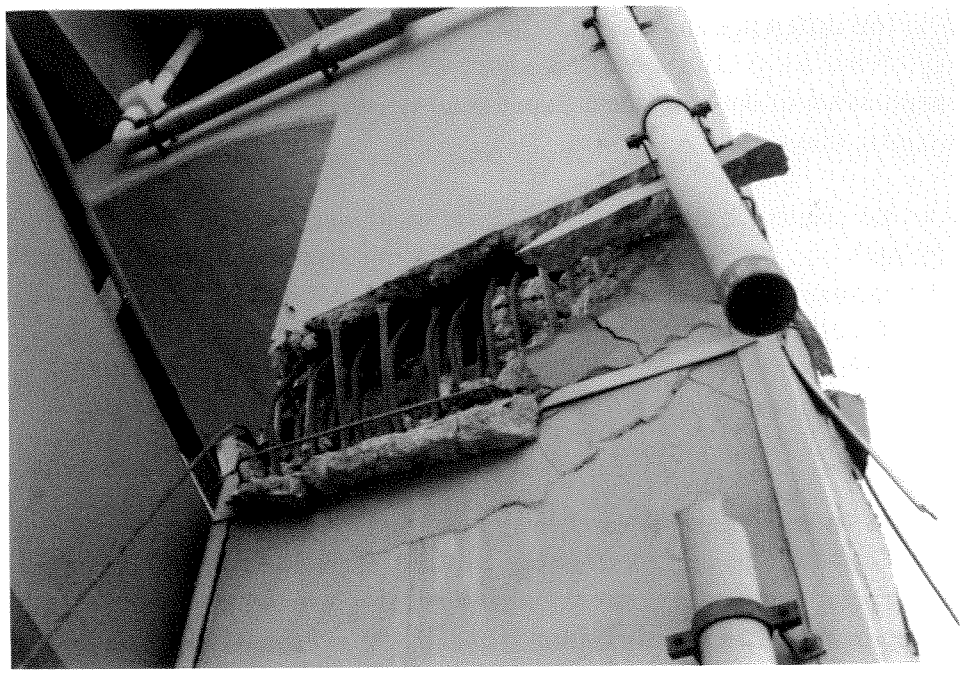


Figure 7-53 Hinge Formation in East Column of Pier 23, Kobe-Ohashi

continuous box girder which is fixed at its center pier but free to expand tangentially at both ends. The span(s) that makes up the remaining length of each ramp is a simply supported span. Since the Expressway is an east-west route, these ramps connect to a north-south highway and the four ramps can be identified by the compass quadrant, i.e. NE, SE, SW and NW. Two of the four footings for both the NE and SE ramps are piled footings whereas all of the bents for the NW and SW ramps are on spread footings. Further, both the NE and SE structures are 4-span ramps whereas the NW and SW ramps are 3-span ramps. These and other details are summarized in Table 7-XI.

It is seen from Table 7-XI that although the NE and SE ramps are superficially similar to the NW and SW ramps, they are in fact different in a number of important details. In general, the structures are longer, the columns are taller and the foundations are softer in the eastern half of the interchange compared to the western half.

Table 7-XI Structure Data for the Minatogawa Ramps, Route 3

Ramp	NE	SE	SW	NW
Number of spans	4	4	3	3
Length of curved spans	42.4/44.0m	40.0/42.5m	30.1/29.2m	39.3/40.4m
Column size[1]	2.5 x 3.75m oval	2.5 x 3.75m oval	2.5m dia. circular	2.5m dia. circular
Clear Column height[1,2]	6.1m	8.4m	5.7m	2.6m
Footing size[1]	8 x 9.5m	8 x 9.5m	8 x 10m	8 x 10m
Number of piled footings	2	2	0	0
Pile data[1]	12, 1m dia. 16m long[3]	12,1m dia 16m long	N.A.	N.A.

Notes 1. Substructure data is given for central pier under curved 2-span segment.
2. Clear height is distance between top of footing and bottom of hammerhead.
3. Estimated.

During the earthquake, the northern-most span of the NE ramp and the southern-most span of the SE ramp collapsed due to loss of support at the expansion ends of these two ramps (Figures 7-54 through 7-56). No span collapsed in either the NW or SW structure. The most probable explanation for this behavior is the greater flexibility of the eastern ramps and thus the greater displacement demands on the available seat width.

In addition to the unseating of these two spans, the central piers under each of the curved, 2-span segments suffered damage to varying degrees. These are the fixed piers for these continuous segments and are required to resist the lateral load from about 80 m of tributary superstructure weight. In the shorter columns, the failure was principally by shear whereas in the taller columns, shear and flexural distress were both evident. Of interest in these columns was the flexural cracking directly under the hammerheads where the bending moments are expected to be small (Figure 7-57). The distress at these locations implies that the superstructure provided significant



Figure 7-54 Collapse of Southeast Ramp at the Minatogawa Interchange



Figure 7-55 Collapse of Northeast Ramp at the Minatogawa Interchange

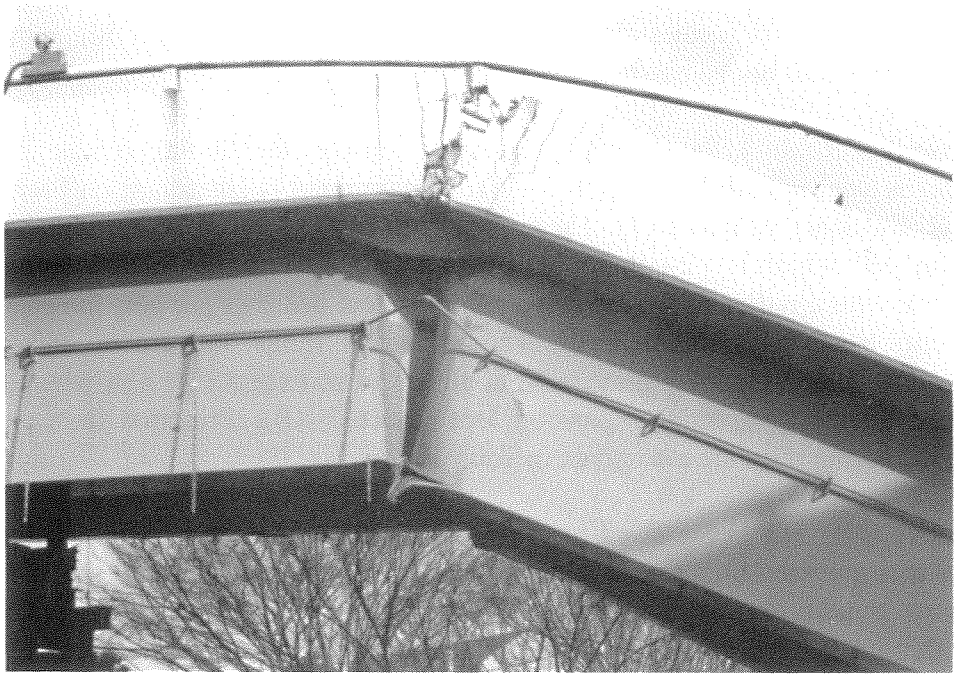


Figure 7-56 Girder Web Failure Due to Unseating of the Southeast Ramp at Minatogawa Interchange

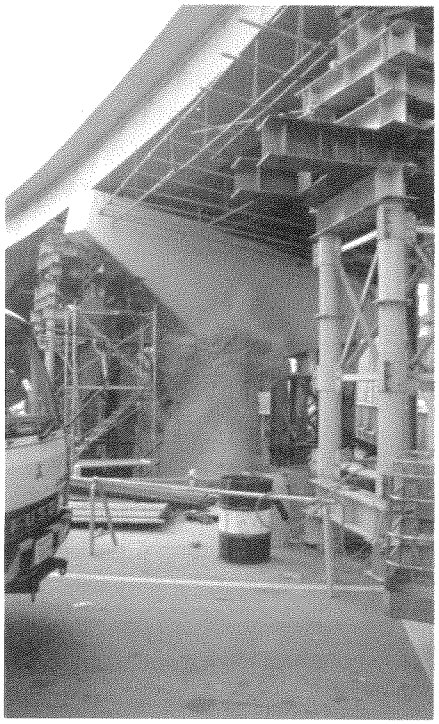


Figure 7-57 Column Failure in Southwest Ramp at Minatogawa Interchange

rotational restraint to these columns which is not unreasonable in view of the high curvature, the high flexural and torsional stiffness of the box girders, and the fixity of the bearings above this pier. Presumably there was similar distress to the columns just above the footings but these were below ground and could not be easily inspected.

At the west end of Route 3, the Hanshin Expressway crosses the JR Sanyo Line on a pair of 3-span continuous steel box girders (Figure 7-58). This segment is supported on **Piers 687 to 690 near the JR Takatori railyard (7)**. These piers are single column bents with hammerheads, except for Pier 688 which is a 2-column bent with a haunched cap beam. The bridge has a mild left-hand curve with a radius of 291 m. Two pairs of steel bearings support the two box girders over each cap beam and hammerhead. These restrain radial movement and uplift while permitting rotation and tangential movement at all locations except Pier 688 where the bearings are also fixed against tangential expansion (see Table 7-XII). Principal dimensions for the columns, footings and piles are also given in Table 7-XII.

As noted above, Pier 688 is the fixed pier for this segment of Route 3 and it has clearly been designed for this purpose. Substantial additional strength has been given to this pier, especially when compared to adjacent substructures (see Table 7-XII). However, during the earthquake both columns in this bent failed catastrophically in shear in the span-wise direction (Figure 7-59). It seems likely that the additional stiffness, which was included with the additional strength, attracted unexpectedly high loads to the bent and the shear capacity was quickly exceeded. The fact that the cap beam was only 2.5 m wide and therefore narrower than the column, meant that not all of the vertical steel was well confined by the cap beam. During the failure, much of the vertical steel on the north face of the cap pulled out of the cap further contributing to severity of the failure. It appears that the gross shear deformation in the vertical direction shortened the height of the bent by about a meter. The superstructure came to rest on the overhead electric supply lines for the JR Line causing closure, not only of the Expressway but also of the rail line.

Table 7-XII Substructure Details for Piers 687 to 690, Route 3 near Takatori

Pier	P690	P689	P688	P687
Bearing Fixity	E-E	E	F	E-F
Column Size	3.2m dia.	3.6m dia.	2.x 3.5 dia.	3.2m dia.
Clear Column Ht	5.3m	4.0m	6.1m	7.4m
Footing Size	8x9.5x2.5m	9.5x12x3.0m	12.5x17x3.0m	9.5x10x2.5m
Pile Size (LxD)	21 x 1m dia.	22.6 x 1m dia.	22.6 x 1m dia.	12.1 x 1m dia.
No. of Piles	11	18	28	10

Notes E: Expansion bearing (rotation and longitudinal movement permitted)
F: Fixed bearing (rotation only permitted)



Figure 7-58 General View of Route 3 Crossing JR Sanyo Line Near Takatori

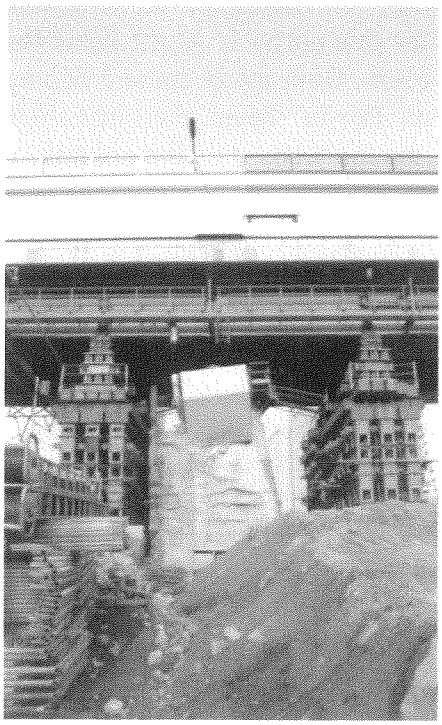


Figure 7-59 Side View of Shear Failure in Pier 688 of Route 3 Near JR Sanyo Line

7.2.2.3 Damage to Steel Substructures

Steel substructures for bridges are used quite frequently in Japan, in contrast to U.S. practice. Although not as common as concrete columns, circular and boxed steel columns are to be found throughout Japan and their performance during this earthquake is of particular interest. Damage was sustained by both older and newer construction and included flexural hinging with local buckling and, in one case, section rupture.

This section presents examples of these failures by summarizing the damage sustained by two sections of the Hanshin Expressway Route 3 (Piers 55 to 58 near Tateishi and Piers 581 to 586 near Meiji) and the Route 2 Bypass at Hamate (Piers 41 to 49). Buckling of the cross-bracing in the Rokko Island tied arch and local buckling in the end piers and approach spans of the Higashi-Kobe cable-stayed bridge are described in Sections 7.2.2.1 and 7.2.2.4, respectively.

The 2-span section of Route 3 from **Pier 54 to Pier 56 near Tateishi (2)** varies in width to accommodate on- and off-ramps that join the elevated expressway here at Tateishi. Of the three bents supporting these two spans, two are steel box columns and one is reinforced concrete. All spans are simply supported steel girders with spans of 70 and 45 m from Piers 54-55 and from Piers 55-56 respectively. The average clear height of these columns is about 8 m measured from the top of the footing to the bottom of the hammerhead cap beam. Foundations are piled footings. Principal dimensions for the columns, footings and piles are summarized in Table 7-XIII.

The excessive width and unusual shape of Pier 55 is the result of subsequent widening to accommodate the later addition of new access ramps. Originally 20 m long, the steel cap beam was doubled in length to 44 m for this purpose. At the same time, concrete columns were added to support the free ends of the beam. Both the beam and column are constructed from internally stiffened single cell box sections. For the beam, the plate thicknesses are 28 mm for the upper and lower flanges and 24 mm for the webs. For the column, the plate thicknesses are 19 mm. Both the beam and column were pre-fabricated in sections using shop welds and assembled on site using bolted splices. High strength, 20 mm diameter bolts were generally used for these connections.

During the earthquake, the steel box column at Pier 55 split open along the welds that run the full height of the four corners of the box, allowing the column to collapse in compression, while the concrete outrigger columns remained upright (Figures 7-60 and 7-61). Without the support of the central column, the extended cap beam failed in flexure on both sides of the main girder as it attempted to span between the two external columns. The articulation in the superstructure allowed this gross deformation to occur without the superstructure being unseated. Other steel box columns in adjacent piers also showed evidence of incipient failures in the corner welds.

In the **Meiji district (5)**, to the west of central Kobe, Route 3 separates into two independent east- and west-bound structures (Figure 7-62). These structures are supported on single steel columns that are in turn supported on hollow concrete shafts. The largest of these circular columns (Piers 583 and 584) have diameters of 2.2 m and clear heights, from foundation to under side of hammerhead, of about 14 m. The foundation shafts under these columns are 4 m in

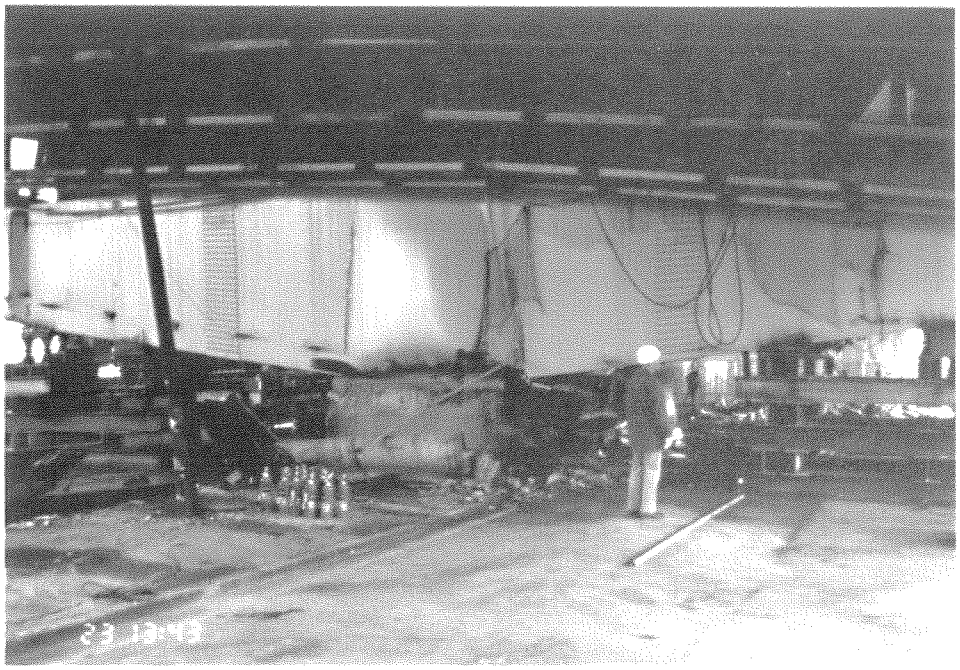


Figure 7-60 Pier 55, Route 3 Near Tateishi (Photo courtesy of Andy Taylor)

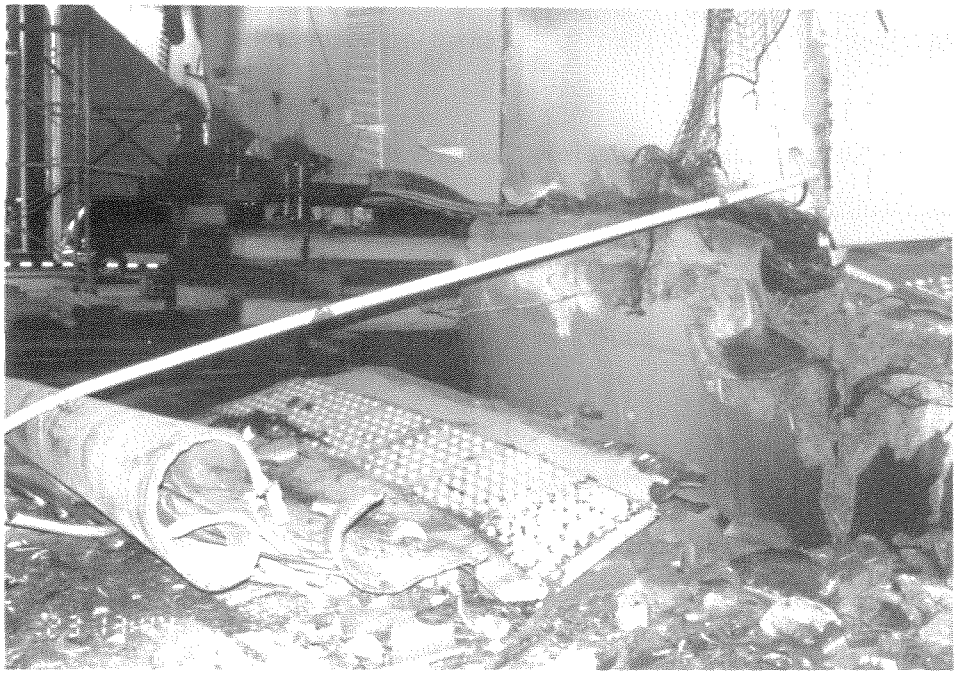


Figure 7-61 Pier 55, Route 3 Near Tateishi Showing Buckled Steel Plate on Ground
(Photo courtesy of Andy Taylor)

Table 7-XIII Substructure Details for Piers 54 to 56, Route 3 near Tateishi

Pier	56	55	54
Bearing Fixity[1]	E-F	E-F	E-F
Column Type	steel box	steel box[2]	concrete
Column Size	3.0x3.3m	2.8x3.0m[2]	3.5m dia.
Clear Column Ht[3]	6.96m	8.23m	9.07m
Cap Beam Length	30.8m	44.3m	19.5m
Footing Size	12x12x3.5m	12x12x3.5m[2]	10x12x2.7m
Pile Size (LxD)	12.5 x 1m dia.	11 x 1m dia.[2]	16 x 1m dia.
No. of Piles	23	212	17

Notes
1. E: Expansion bearing (rotation and longitudinal movement permitted)
   F: Fixed bearing (rotation only permitted)
2. Pier 55 has 2 additional concrete columns that support each end of the cap beam; these columns are 1.2 x 2.7 m in plan by 9.2 m high; footing sizes are 6.5x13x2.5m and supported by nine 11 x 1m dia. piles.
3. Clear height is distance between top of the footing and bottom of cap beam.

diameter and about 23 m deep. The superstructure is also steel and includes a series of simply supported plate girder spans (35 to 50 m spans) and a 3-span continuous box girder segment with spans of 55, 78 and 55 m, respectively. The total length of the 8-span section from Pier 580 to Pier 588, which includes all of the single steel column bents, is approximately 415 m. Principal dimensions for these columns and their foundations on the westbound structure are given in Table 7-XIV.

Table 7-XIV Substructure Details for Piers 581 to 586, Westbound Route 3, Meiji

Pier	586	585	584	583	582	581
Bearing Fixity	F	E-F	E-E	F-E	F-E	F-E
Column Size (dia)	1.8m	1.8m	2.2m	2.2m	1.8m	1.8m
Clear Column Ht.	10.3m	12.4m	14.1m	14.1m	13.4m	12.4m
Shaft Size (dia)	3.5m	3.5m	4.0m	4.0m	3.5m	3.5m
Shaft Depth	24.6m	23.8m	23.2m	23.4m	16.2m	17.4m

Notes E: Expansion bearing (rotation and longitudinal movement permitted)
F: Fixed bearing (rotation only permitted)

During the earthquake, many of the columns in the westbound structure were damaged but the extent of this damage varied according to location. All columns appeared to have been heavily loaded in the transverse direction and in the cases of Piers 584 and 585, the columns suffered permanent transverse displacements. In many columns, plastic hinges attempted to form somewhere in the central one third of the column height, rather than at the base. Changes in the

plate thickness with column height probably accounts for these higher locations. However, fully developed hinges did not occur due to local buckling, tensile ruptures and section buckling caused most probably by column out-of-roundness.

Pier 584 is one of the two largest piers in this section but it failed by section rupture within a potential plastic hinge zone at about mid-height (Figure 7-63). The hinge began to form immediately above a change in plate thickness but the associated weld probably initiated the crack which propagated around the circumference of the column during the reversed loading imposed by the earthquake. The column was completely fractured at this level and it came to rest with a permanent lean to the north of about 10° (Figure 7-64). Pier 585 also sustained permanent displacement but in this case the column did not rupture. Instead, a plastic hinge began to develop about 2 m above the ground line but the section buckled, possibly due to section out-of-roundness, which prevented the full moment capacity from being reached. This column also tilted to the north by rotating about the failed plastic hinge.

As noted in Table 7-XIV, Pier 586 is almost two-thirds of the height of Piers 584 and 585. Despite its smaller diameter, this shorter height implies that it is about 25% stiffer than the adjacent piers. It therefore attracted a higher share of the lateral loads during the earthquake and it should have performed in a similar manner to Piers 584 and 585. In fact, the pier showed no visible signs of distress and the reason for this behavior appears to be the failed connection at the top of the pier (Figures 7-62 and 7-65). Inspection of the bearings at Pier 586 showed that the transverse restraint provided by these bearings had failed in lateral shear and the girder displaced across the pier cap a distance of about one meter. The release of load due to this bearing failure is another example of fuse-like behavior in superstructure-to-substructure connections. The consequential reduction in column shear almost certainly protected the column from the distress suffered by its neighbors. (The bearings on Piers 585 and 584 did not fail in transverse shear).

As noted in Section 7.2.2.1, the **Hamate Bypass (16)** is a two level elevated viaduct carrying Route 2 along the Kobe waterfront. Longer spans are continuous steel box girders supported on multi-column steel bents constructed from single cell, internally stiffened, box sections. In all piers, the upper level roadway is supported by two columns from the lower level cap beam. This lower cap is then supported from the ground, in some cases by two columns, as in Pier 41, and in other cases by a single column (tennis racket-style) as in Pier 49.

In Pier 41, the upper and lower decks are supported at about 22 m and 10 m above the ground, respectively. The overall width of the pier at the carriageway levels is about 15 m. Column cross sections are 2.2 x 2.8 m. This is a fixed pier for the superstructure and it appears that during the earthquake the longitudinal forces attracted to the pier were sufficient to cause one-half cycle of inelastic flexure about 3 m up from the base (Figure 7-66). On the compression face, local buckling occurred between the stiffened panels of both columns whereas on the tension side horizontal striations in the paint were consistent with significant post-yield tensile strain. However, no obvious offset or misalignment was observed in the pier and it was assumed to have returned to its original position. More detailed surveys may show, however, that some residual deformation was sustained.



Figure 7-62 General View of Westbound Elevated Section of Route 3 Near Meiji Looking from Pier 586 Towards Pier 585

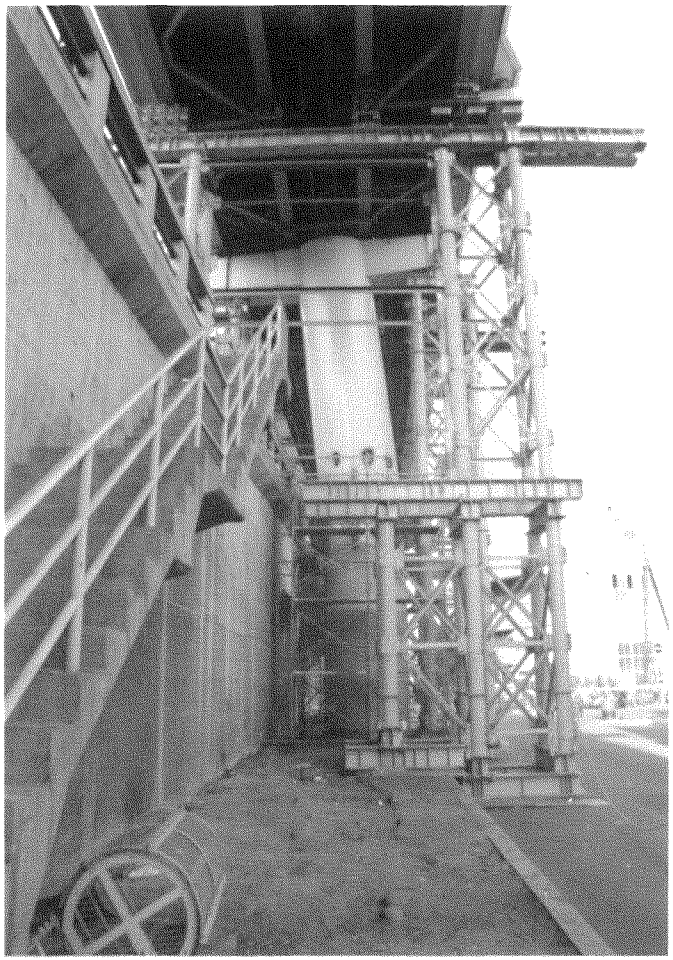


Figure 7-63 Pier 584 of Westbound Route 3 Near Meiji



Figure 7-64 Fracture at Mid-Height of Pier 584 of Westbound Route 3

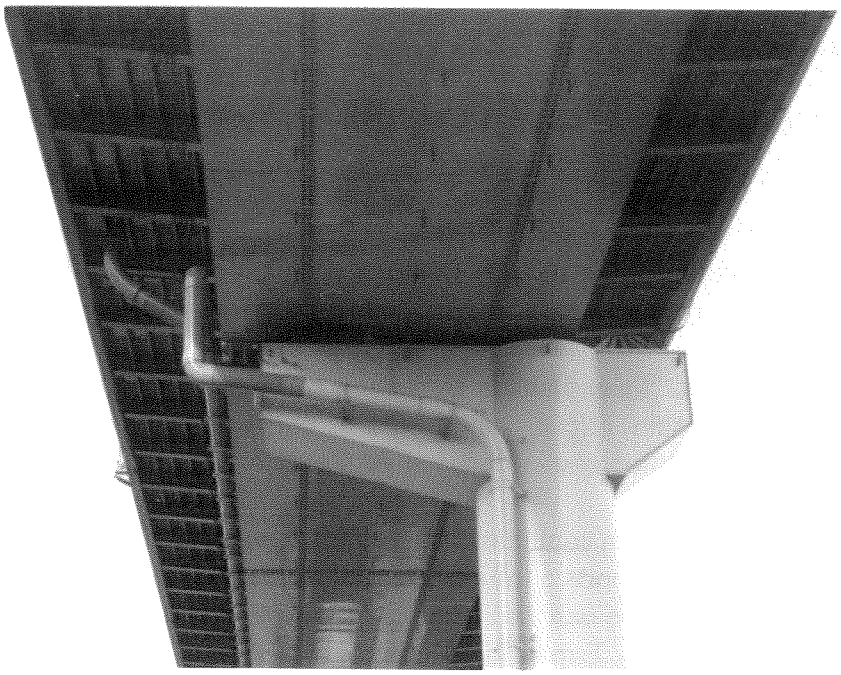


Figure 7-65 Failed Bearings and Lateral Offset at Top of Pier 586 of Westbound Route 3

As noted above, Pier 49 has a single column supporting the first level of traffic from which a two column bent extends upwards to support the second level. This single column is 3.2 m in diameter and is supported on a piled concrete footing that measures 10.0 by 12.6 m. The clear height of this column, from top of footing to bottom of the first cap beam, is 12.1 m. The steel box sections, that comprise the members of the upper level bent, are generally 1.5 x 1.6 m in size. Attention has been drawn by others to the distinctive shape of this bent and its striking similarity to a tennis racket that is standing upright.

This pier is another fixed point for both levels of the superstructure and during the earthquake, sufficient lateral load was attracted to this bent to trigger section buckling (Figure 7-67). Section out-of-roundness and high gravity loads were pre-existing conditions that, when combined with the seismic overturning moment, precipitated a uniform buckling failure across the whole section at the mid-height of the column.

Factors which tend to confirm a failure in compression rather than one in flexure or shear include the location (unusually high for a flexural hinge), the uniform deformation around the circumference and the absence of residual translation over the height of the column. Furthermore, an access ladder runs the full height of this column and is attached to it at about 1.5 m intervals. It was also deformed into a bulge (by bending about its weak axis) but exhibited no horizontal offset between the upper and lower sections that might be indicative of permanent flexural or shear deformation in the column.

The shape of the buckle in the column may be compared to an elephant's foot failure, which occur in large diameter storage tanks during earthquakes. In this case, however, the buckle is half way up the leg of the pier and the damage to Pier 49 might therefore be likened to an elephant's knee failure in the handle of a tennis racket.

7.2.2.4 Damage to Structures Due to Special Conditions (Liquefaction, Skew, Protective Systems)

In addition to the damage to various concrete and steel bridges, there was damage due to causes other than bearings and columns. These include foundation failure, adverse effects of skewed geometry and failure of special connections associated with protective systems.

This section presents examples of these failures by summarizing the damage sustained by the Shukugawa bridge on the Hanshin Expressway Route 5, the Kawaraginishi bridge on the Meishin Expressway and the Higashi-Kobe bridge, also on Route 5.

The **Shukugawa bridge (9)** is a 3-span continuous box girder bridge carrying Route 5 across the Shukugawa (Figure 7-68). It also supports a toll plaza at the west end (Pier 134) and is therefore about twice the width here than at the east end (Pier 131). The girder is supported on concrete multi-column bents and piled footings. Expansion bearings are provided at Piers 131 and 134 and fixed bearings located over Piers 132 and 133.



Figure 7-66 Local Buckling in Steel Box Columns at Pier 41 of the Hamate Bypass Viaduct



Figure 7-67 Buckling in Steel Column at Pier 49 of the Hamate Bypass Viaduct

During the earthquake, liquefaction was widespread in the general area of the bridge and lateral spreading was evident at many locations. Both banks of the Shukugawa were subject to large soil deformations and moved towards the center of the river (Figure 7-69). Piers 131 and 134 were displaced with the soil and in the process dislodged the bearings under the main girders as well as the approach spans. At Pier 134, the movement was of the order of one meter to the east, while at Pier 131, the movement was less (about 0.5m) to the west. In addition to bearing damage, the expansion joints were also dislodged and twisted out of alignment by large vertical (up to 600 mm) and horizontal offsets imposed by the piers (Figure 7-70).

At Pier 134, the one meter movement of the pier almost caused the collapse of the approach span due to insufficient seat width at the cap. The remaining overlap between girder and seat was of the order of 100 mm or less but collapse was apparently prevented by the earthquake couplers (Figure 7-71). Preliminary results from excavations behind the footing under Pier 134 indicate that some piles failed during the lateral spreading and that replacements will be necessary around the perimeter of an expanded footing.

The 3-span **Kawaraginishi Bridge (14)** comprises two independent structures that carry east and westbound traffic on the Meishin Expressway (Figure 7-72). Both structures have continuous, reinforced concrete hollow slab superstructures supported on wall piers at each end (Piers 24 and 27) and by two multi-column bents (Piers 25 and 26). Two special features are of interest with this bridge. The first is that the bridge is skewed 35° to the line of the support and fixed at the east end only (Pier 27); all other bearings permit longitudinal movements. The second feature is that each intermediate bent comprises three pin-ended columns and therefore has no lateral stiffness or resistance to lateral load.

During the earthquake, the transverse restraint at the west end (Pier 24) of the eastbound bridge failed and in the absence of any restraint from the intermediate piers, the superstructure was free to rotate about the fixed end (Pier 27) in a clockwise direction. Once support was lost at Pier 24, collapse of one or more spans and the associated intermediate bent (Pier 25) followed almost immediately. In addition, the high shear forces and twisting moments placed on Pier 27, as the superstructure rotated, exceeded the capacity of this wall and it failed in shear (Figure 7-73).

Since the westbound bridge shares the same features, it is surprising that it did not also collapse. It is of course possible that the eastbound bridge prevented the westbound structure from losing support at Pier 24 moments before the eastbound bridge lost its own support. It follows that an earthquake with a longer duration might have caused the collapse of both bridges.

The **Higashi-Kobe bridge (10)** is a 3-span cable-stayed bridge with a total length of 885 m (Figure 7-74). The main girder weighs 14,100 tonnes and is totally supported by 48 cables arranged in a harp pattern from the two towers. It is restrained against transverse wind and seismic loads by six wind shoes, one at each tower and one at each of the two piers in both end spans. These shoes are only effective in the transverse direction and offer no restraint to the girder against longitudinal loads. A pair of viscous, vane-type dampers are therefore provided at both ends of the main girder to control longitudinal seismic loads. These dampers permit up to 900 mm of span-wise movement, and each can develop a peak force of 108 tonnes at a velocity

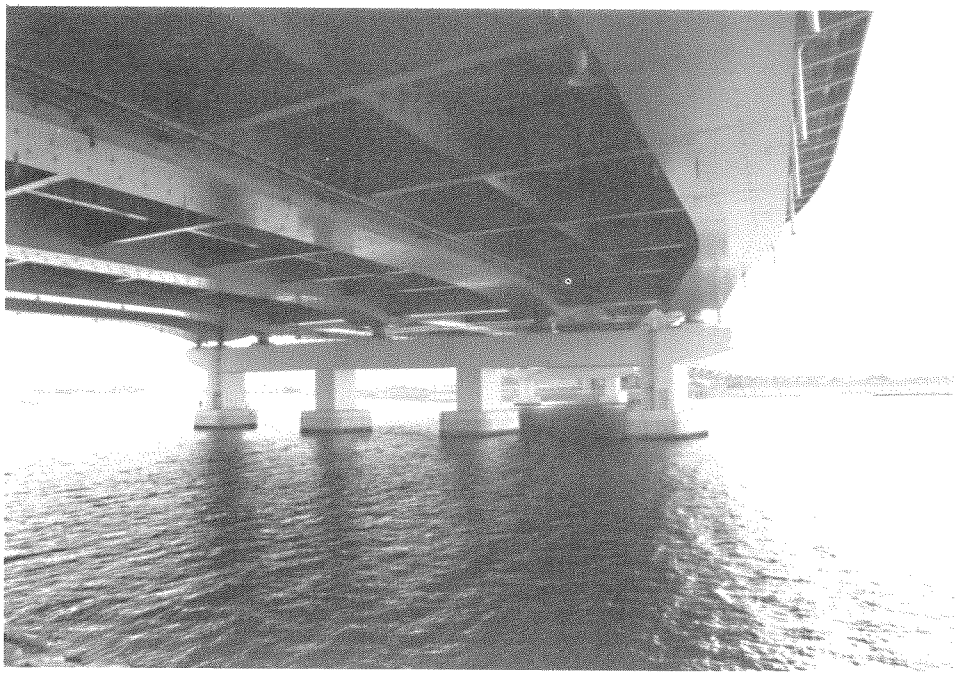


Figure 7-68 General View of the Shukugawa Bridge on Route 5



Figure 7-69 Distant View of the Shukugawa Bridge Showing Lateral Deformation of the Foundation Soils and Spreading to the Right (to the center of the channel)

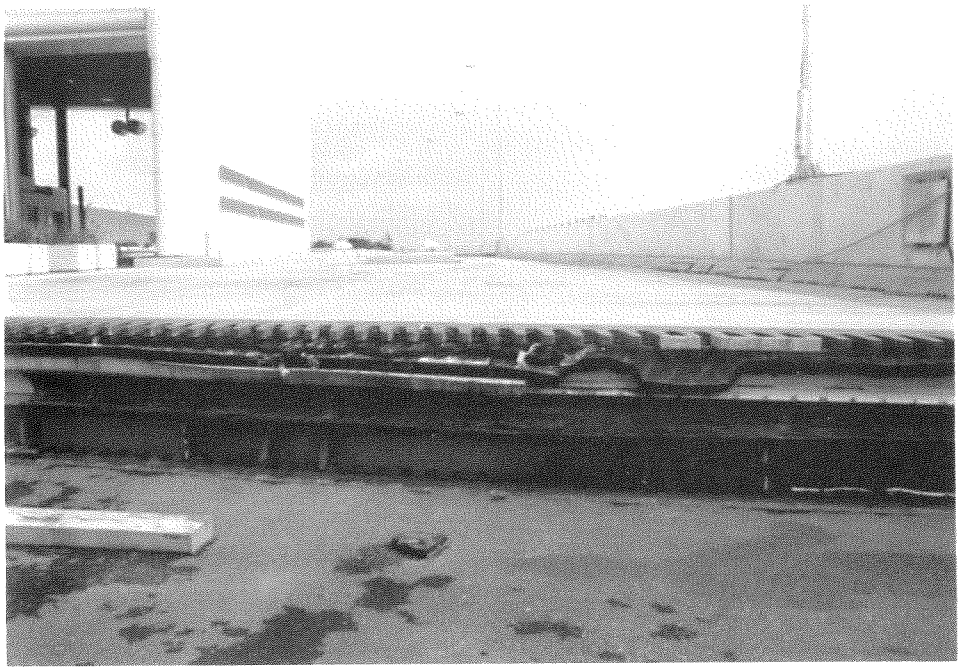


Figure 7-70 Vertical Offset in the Expansion Joints Above Pier 134 of the Shukugawa Bridge Due to Bearing Failure on the Bent Cap Below



Figure 7-71 Approach Span at Edge of Seat at Pier 134 of Shukugawa Bridge Due to Lateral Movement of the Pier Towards the Center of the Channel by About 1 m



Figure 7-72 General View of Kawaraginishi Bridge After Removal of Collapsed Eastbound Bridge Showing Skew and Pin-Ended Columns Under Westbound Bridge

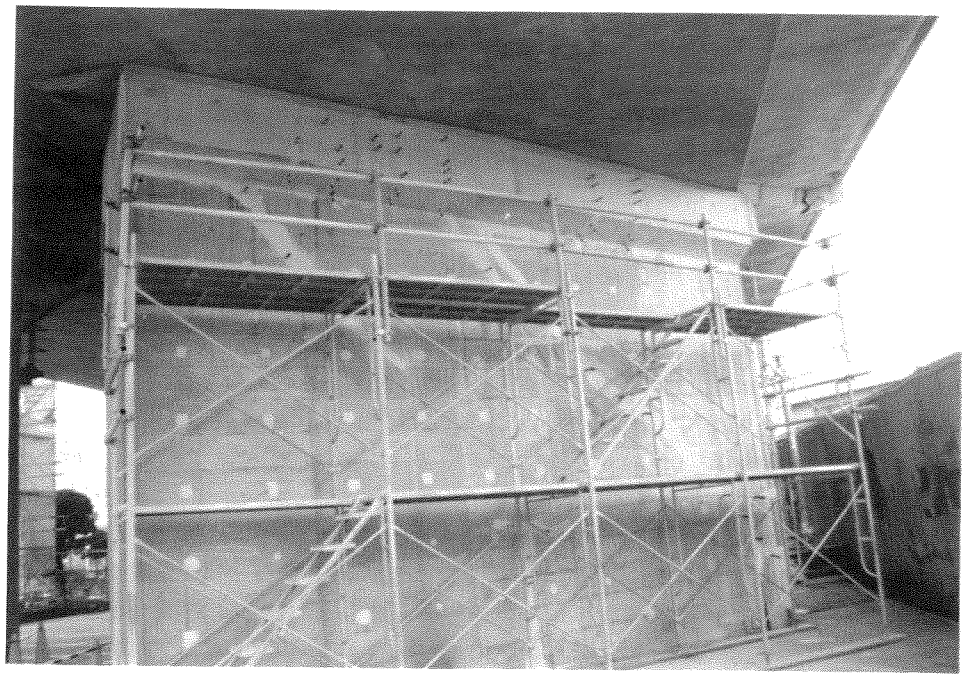


Figure 7-73 Pier 27 of the Westbound Kawaraginishi Bridge Showing Shear Cracking and Repair by Injection Grouting

of 750 mm/sec. In addition, a pair of vertical eye-bars is provided to counteract the uplift in the main girder due to an imbalance in dead load.

During the earthquake, the anchor bolts for the wind shoe at the west end of the main girder failed and the transverse restraint for the girder at this end was lost (Figure 7-75). The redistribution of load to the dampers and eye-bars (for which they were not designed) triggered failure in these devices also, and the end of the girder, which was now free of all restraint, rose upwards about one meter (Figures 7-76 and 7-77). Records from strong motion instruments in the east tower show that the input ground accelerations in the transverse direction were about 0.4g. These records also show considerable amplification up the height of the tower: to 0.8g at deck level and to greater than 1g at the top of the tower. These are very high in-structure accelerations and significantly larger than those assumed in design (the 2% damped, design spectrum has a peak value of 0.4g from 0.6 to 2.0 s).

It is therefore not surprising that the structure suffered some distress, including not only the failure of the protective systems, but also local buckling in the box steel bents that support the western end of the main girder and the adjacent approach spans.

The above observation, regarding the design accelerations for the Higashi-Kobe bridge, also applies to the other structures described earlier. The design seismic coefficient for the Hanshin region is 0.3 and the minimum connection forces are 1.5 times the product of this coefficient and the tributary weight. These values were clearly exceeded during this earthquake and most probably by very wide margins.

7.2.2.5 Performance of Other Highway Bridge Structures

When completed in 1997, the Akashi-Kaikyo suspension bridge will have the world's longest span at 1,990 m. Currently under construction between the main island of Honshu and Awaji island immediately to the west and south of Kobe, the epicenter for the earthquake was directly under the bridge and the causative fault passes obliquely between the two towers. The right lateral movement on this strike-slip fault was of the order of a meter which has lengthened the distance between the towers by about 0.8 m and created an offset of about 0.6 m. At the time of the earthquake, the towers had been completed and the main cables were in place. Erection of the suspenders and the stiffening trusses had not begun. No significant structural damage to the bridge has been reported but detailed inspection and redesign of the stiffening trusses to accommodate the new geometry is expected to add a 10-month delay to the completion of the structure.

Many bridge spans had been seismically retrofitted with couplers before the earthquake and at least two structures on Route 4 are menshin-designed bridges fitted with seismic isolators. As noted above, some earthquake couplers failed during the earthquake, but in many other instances they performed well and are believed to have prevented further collapses of simply supported spans. Furthermore, those few concrete columns that had been retrofitted with steel jackets at the west end of Route 3, also appeared to have performed well during ground motion that caused shear failures in adjacent (unretrofitted) columns. There was likewise good performance of the

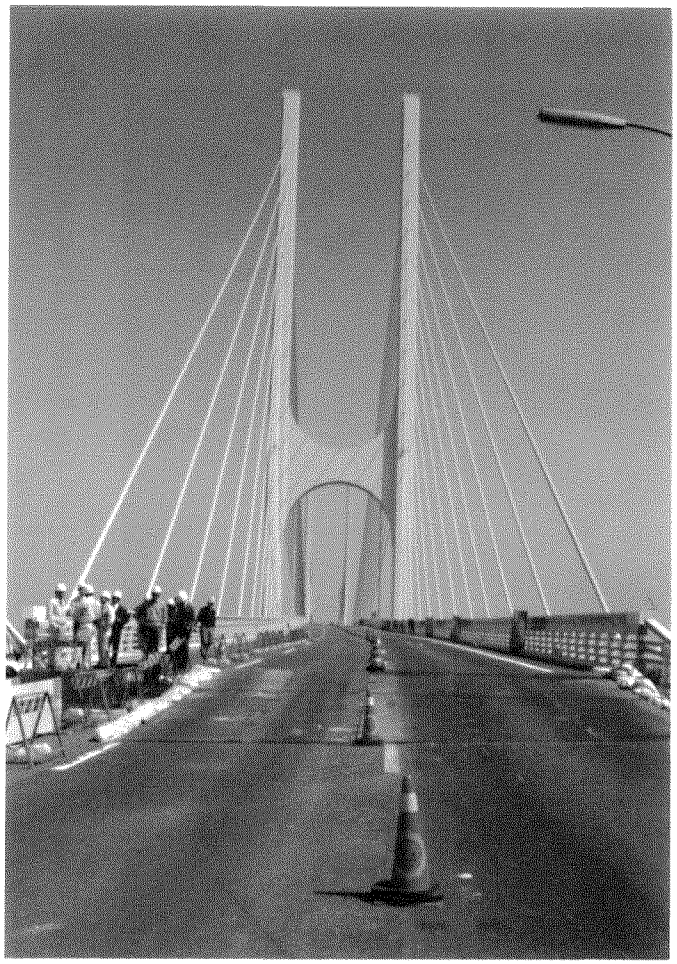


Figure 7-74 General View of the Higashi-Kobe Bridge on Route 5

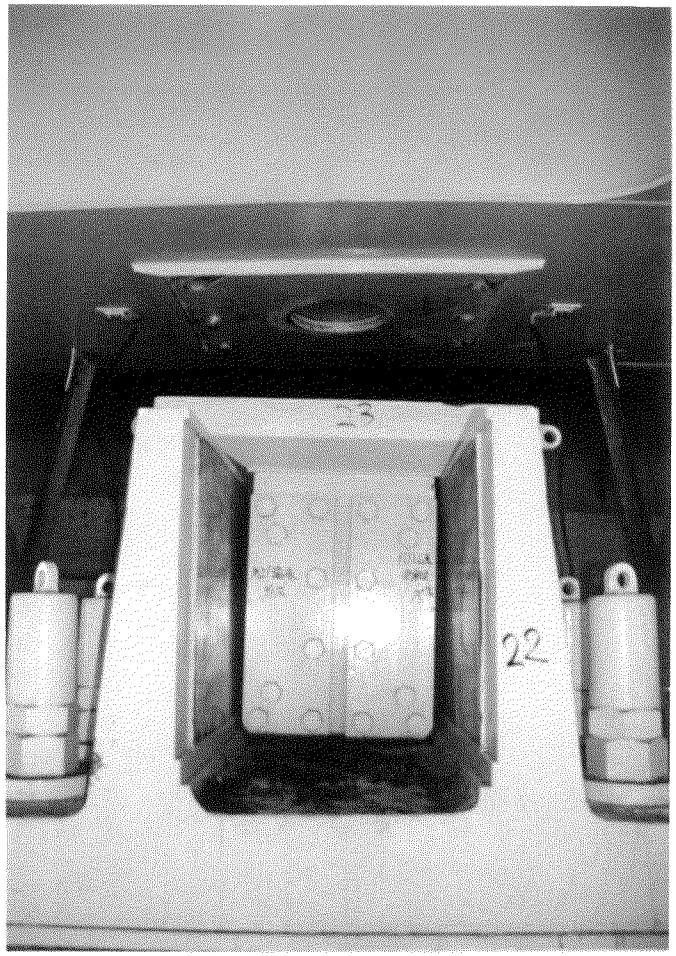


Figure 7-75 Failed Wind Shoe at Pier 187 of the Higashi-Kobe Bridge

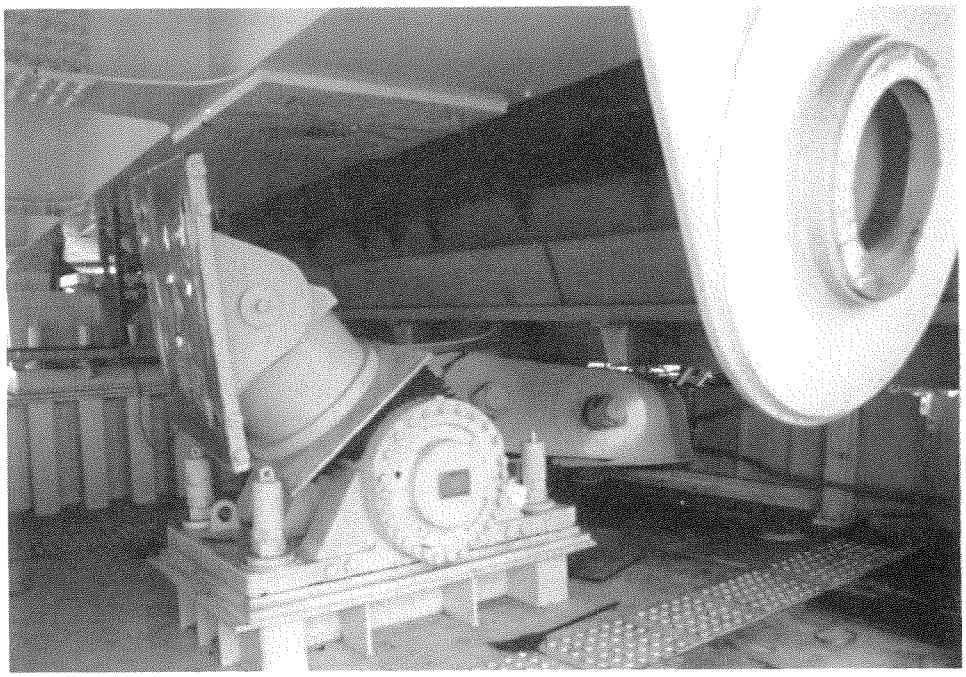


Figure 7-76 Failed Connection of Vane-Type Energy Dissipator and (at upper right) Part of Failed Dead Load Tie-down at Pier 187 of the Higashi-Kobe Bridge



Figure 7-77 Uplift at the West End (Pier 187) of the Main Girder of the Higashi-Kobe Bridge Due to Failure of the Dead Load

two menshin bridges. No damage was sustained in either one but at 45 km from the epicenter, the input motion was less than 0.15g and the performance of adjacent conventional bridges was also damage-free. Nevertheless, the records obtained from the Matsunohama bridge confirm the expected performance of a menshin-designed bridge during low-to-moderate ground motion i.e. slight amplification in the isolated (span-wise) direction and strong amplification in the fixed (transverse) direction.

7.2.3 Lessons from Damage to Highways and Bridges

To bridge engineers and owners in the central and eastern United States, this particular earthquake is perhaps of greater significance than recent earthquakes in California (e.g., Loma Prieta, 1989 and Northridge, 1994). One reason for this opinion is that the predominant type of bridge in Japan is the steel girder superstructure (simple and/or continuous spans) supported by bearings on concrete columns and foundations. This class of bridge is also found throughout the central and eastern U.S., whereas bridges in California tend to be concrete box girders with monolithic bents and integral abutments especially in shorter bridges. It follows that bridges in the central and eastern U.S. are more like those in Japan than those in California and the performance of Japanese bridges is thus of particular relevance to states east of the Sierra Nevada mountains.

A second reason is that an earthquake of this size was considered to be a rare event for this part of Japan. Although bridges in this region are designed for seismic loads, the design coefficients are considerably lower than those recorded during this earthquake. The possibility of an earthquake larger than the design earthquake was considered to be unlikely and only nominal attention had been given to the problem, and then only for structures designed since 1990. This difference, between the maximum credible earthquake and the design earthquake, is clearly very large for this region of Japan - a situation that is also considered to exist in the U.S., but to a greater degree in the eastern and central states than in the west.

It follows that the eastern and central U.S. may have more to learn from this earthquake in Japan, than from California. Some of these lessons are as follows:

(1) Large earthquakes can be very destructive in terms of lives lost, injuries sustained, business losses, reconstruction costs and societal disruption. The closure of arterial highways and bridges affects emergency relief and business recovery and can have a major economic impact on a region and its ability to survive such a disaster.

(2) Large damaging earthquakes can occur in areas that are considered to have, on average, only a moderate exposure to seismic hazards.

(3) Capacity design procedures, ductile details and generous seat widths are necessary to prevent catastrophic collapse during large earthquakes.

(4) Minimum connection forces need to be enforced for all seismic zones unless such connections can be shown to be fully protected by acceptable yielding of the substructures. Redundancy in connection detailing is particularly important for essential structures. Alternative load paths are necessary if the primary load path fails due to unforeseen circumstances.

(5) Critically important structures must be designed to a higher level of performance than that provided by current specifications, if full service is to be maintained after a large earthquake. Multi-level performance criteria and corresponding design strategies are necessary for important bridges.

(6) Retrofit measures reduce damage but inappropriate use and/or installation can defeat their purpose and perhaps even trigger collapse. This observation is made with particular reference to couplers (restrainers).

(7) Lateral spreading due to liquefaction can lead to span collapse even in modern structures with massive foundations (caissons) and well-engineered fills.

(8) Premature failure of some bearings appear to have reduced the seismic loads in their supporting substructures by uncoupling the superstructure from its supports. This fuse-like action may have saved a number of spans from collapse and columns from failure in shear and flexure.

(9) Accelerations in isolated superstructures are less than in conventional structures.

(10) Skewed bridges are susceptible to in-plane rotation leading to large displacements at their supports and possible unseating of girders in the acute corners.

7.2.4 Summary

Damage to highway bridges was both widespread and catastrophic. Typical damage included shear and flexural failures in nonductile concrete columns, flexural and buckling failures in steel columns, unseated girders due to bearing failures, and gross foundation movements due to liquefaction. In addition, pounding between spans occurred and approach fills behind abutment walls settled. Some special structures also suffered atypical damage such as the excessive rotation of a skew bridge on pin-ended columns and the loss of seismic energy dissipators in a cable-stayed bridge due to the failure of a wind shoe.

Most of this distress was confined to older structures built more than 30 years ago and before the introduction of modern seismic codes. The poor performance of these older bridges and elevated expressways confirms previous lessons learned in California and elsewhere, about the pressing need to retrofit the existing inventory of deficient bridges.

However some new bridges also suffered serious damage which implies a need to re-evaluate the design loads and procedures in the current design specifications. As noted above, the peak ground accelerations due to this "rare" earthquake were considerably higher than the seismic coefficients used in design and this is an example of a low-probability but high-consequence event causing serious distress to modern construction. From an owner's viewpoint, these circumstances might be best addressed through multiple-level performance criteria. In the US, dual-level criteria have only recently been developed, and then only for critically important, long-span structures and a privately-owned transportation corridor. They should perhaps be extended to a wider range of bridge types and in doing so clearly state the expected performance under both small and large, rare and frequent earthquakes and identify design strategies that will satisfy these criteria.

The closure of three major expressways in the Hanshin region has had a major societal and economic impact on the region. The estimated total repair cost for the Hanshin Expressway Public Corporation is $4.6 billion. Even though this is only about 4% of the total direct costs for the earthquake (estimated at $130 billion on 17 Feb 1995), it is still a significant sum. Furthermore, it does not include the loss of toll revenue while the network is down (estimated at $2 million per day) nor does it include the indirect losses which are expected to exceed the repair costs by the time the system is fully operational, sometime in the fall of 1995. The simultaneous closure of the other transportation routes in the region, principally the rail lines, further aggravated the situation and paralyzed the region as emergency access and relief teams were forced to use surface streets. The interdependency of these lifelines, especially when collocated in narrow corridors, deserves further study.

7.2.5 References

Hanshin Expressway Public Corporation, (1994), "Techno Gallery: Structures and Technologies of the Hanshin Expressway," Osaka, 88 pp.

Japan Road Association, (1990), "Design Specifications of Road Bridges; Part V: Seismic Design."

Iwasaki, T., Kawashima, K. and Hasegawa, K., (1990), "New Seismic Design Specifications of Highway Bridges in Japan," Proceedings of the 22nd Joint Meeting of the US-Japan Panel on Wind and Seismic Effects, UJNR, Gaithersburg, MD.

Hanshin Expressway Public Corporation, (1995), "Report on Damage to the Hanshin Expressways by the Great Hanshin Earthquake and its Restoration," Osaka.

7.3 Underground Rapid Transit Systems

7.3.1 Overview of Underground Rapid Transit Systems

The Kobe Rapid Transit Railway, or Kobe Kosoku, is owned and operated by the Kobe Rapid Transit Railway Company, Ltd. As shown in Figure 7-78, the Kobe Rapid Transit Railway (KRTR) provides a rail system which interconnects the Hankyu and Hansin Railways in the east with the Sanyo Electric Railway in the west and the Kobe Electric Railway in the north. The KRTR is owned jointly by the City of Kobe, the four railway companies whose lines it interconnects, and local business investors.

A schematic of the KRTR is provided in Figure 7-79. The east-west routes are 7.2 km long in total, and the north-south line is 0.4 km long. About 6.6 km of the system are underground, with the remaining sections at grade or carried by elevated structures. The system was constructed between 1962 and 1968. Underground sections were built by means of cut-and-cover tunneling techniques. Running tunnels are reinforced concrete box structures with center column support, generally having about 4.5 to 6 m of cover between street surface and top of box. With the exception of the Shin Kaichi Station, the stations are reinforced concrete box structures with center column support.

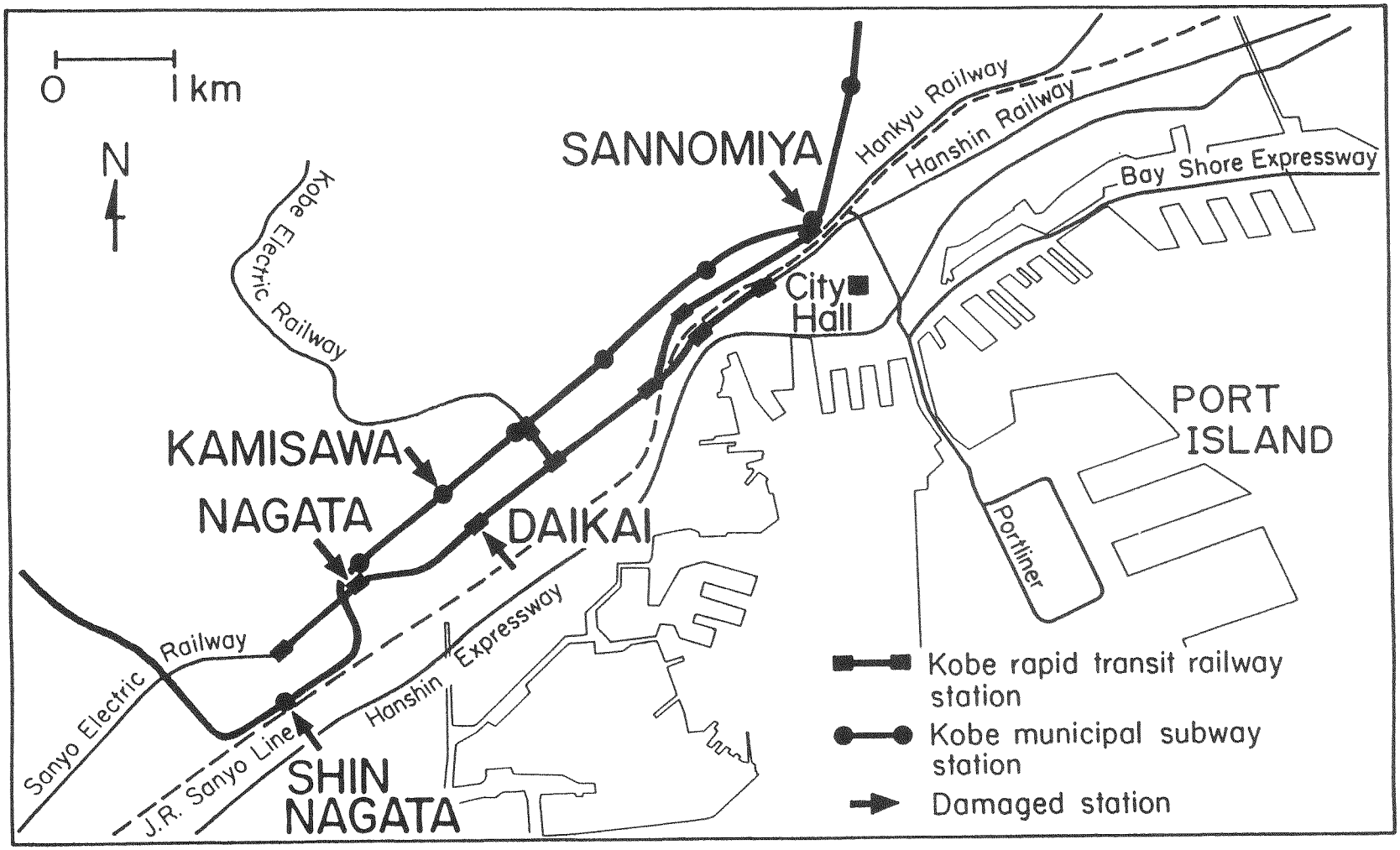


Figure 7-78 Map of Kobe Underground Rapid Transit Systems Showing Locations of Earthquake Damaged Stations

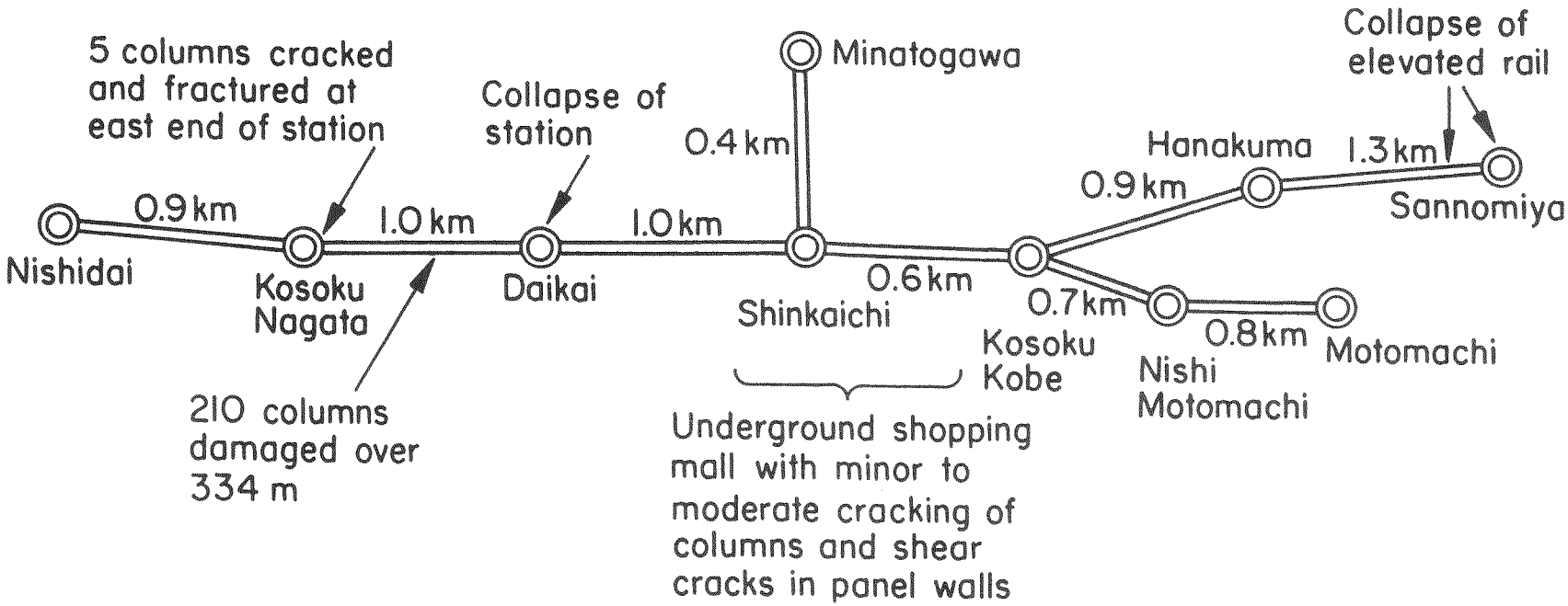


Figure 7-79 Schematic of the Kobe Rapid Transit Railway Showing Locations of Earthquake Damage

The Shin Kaichi Station is a steel frame structure with Vierendeel trusses and a mezzanine level. Depth of cover at the stations is approximately 4 to 5 m.

The Kobe Municipal Subway, or Metro, is operated by the City of Kobe and is composed of 22.7 km of elevated, surface, and underground railway. Underground construction between Shin Nagata and Sannomiya Stations was performed by cut-and-cover techniques prior to 1977. Soil shield tunneling and rock tunneling were used for portions of the system northwest of the Shin Nagata Station. Cut-and-cover sections of the Metro are similar to those of the KRTR. Both stations and running tunnels are reinforced concrete box structures with center columns separating inbound and outbound tracks. Depth of cover from street surface to top of box is typically 4.5 to 7.0 m.

7.3.2 Description of Damage to Underground Rapid Transit Systems

As shown in Figure 7-78, damage was sustained at the Daikai and Nagata Stations of the KRTR and at the Sannomiya, Kamisawa, and Shin Nagata Stations of the Metro. Damage to the Metro was less severe than that to the KRTR, and was primarily in the form of cracked and deformed reinforced concrete center columns. Metro transit service was restored one month after the earthquake, although the Sannomiya Station remained closed because of damage to the center columns. The KRTR, where more severe damage occurred, was not expected to resume service for over a year.

Figure 7-79 shows the locations of damage in the KRTR. Although the most serious damage in the system was the collapse of the Daikai Station, significant distress and failure were evident at other locations. There was structural damage in five reinforced concrete columns at the eastern end of the Nagata Station. Between the Daikai and Nagata Stations, 210 reinforced concrete columns were cracked and deformed in the running tunnel. Minor to moderate cracking of reinforced concrete columns and panel walls was observed in an underground shopping mall adjacent to the KRTR near Shin Kaichi Station. Figures 7-80 and 7-81 show typical damage within the shopping mall. There was severe damage of the elevated rail structure near Sannomiya Station.

Soil conditions adjacent to the Daikai Station and connecting running tunnels are shown in Figure 7-82 by means of boring records obtained by the Kobe Rapid Transit Railway Company, Ltd. at the eastern and western ends of the station. The soil profile consists of relatively loose silty sand to a depth of about 3 to 4 m, with the water table at 3 m depth. The percentage of fines in the upper silty sand layer generally exceeds 20% by weight. Because the silty and clayey sands and organic silty clay have relatively high percentages of fines with considerable plasticity, they are not considered to be susceptible to liquefaction. Uncorrected standard penetration test (SPT) values are plotted for each boring. The locally high values are associated with the presence of gravel, and thus do not provide a reliable representation of in-situ density.

Using the criteria for liquefaction susceptibility set forth by Seed, et al. (1985) and assuming a peak acceleration of 0.7 to 0.8 g, the silty sand and sand between 3.5 and 6 m deep appear to be susceptible to liquefaction. The cyclic stress ratios and corrected blow counts for sands 4.5 to 6.0 m deep plot very close to the empirical threshold for liquefaction proposed by Seed, et al., and thus may be marginal regarding their tendency to liquefy.

The cut-and-cover construction for Daikai Station involved a braced excavation supported by steel sheetpiles. The sheetpiles were left in place, and the concrete walls of the station were cast-in-place. A gap, approximately 300-mm wide, was left between the reinforced concrete walls and sheetpiles. Because the narrow separation did not allow for compaction, sandy fill was mainly loose-dumped between the station walls and existing sheetpiles.

Figure 7-83 presents plan and profile views of the collapsed Daikai Station. Cross-sections at select locations along the station and running tunnel are shown in Figure 7-84. The station and running tunnel are reinforced concrete box structures with 4.8 to 5.2 m of soil cover. The eastern end of the station contains a second structural level which apparently provided sufficient strength and stiffness to restrict roof collapse to the single level box structure. The collapsed box structure was approximately 100 m long, 7.2 m high, and 17.0 m wide. The central reinforced concrete columns of the station failed, apparently by a combination of shear and vertical loading. There was only nominal confining steel (9 mm diameter on 180 mm spacing) for the 20 mm diameter longitudinal rebar on 140 mm centers in the concrete. Collapse of the columns caused subsidence at the street surface of a maximum 2.5 m, with substantial settlement over an area of 100 m by 20 m. Apart from the structural collapse-induced movement, there was no clear evidence of permanent ground deformation at the site induced by other causes, such as liquefaction.

Figures 7-85 and 7-86 show the interior portions of the collapsed station. Compressive failure of the columns in Figure 7-86 occurred in the form of bird caging of longitudinal steel and shear rupture of concrete. It appears that compressive failure occurred at the mid-height of the columns. Figure 7-87 shows subsidence at the street surface over the station. Many pipelines and conduits in the street failed, although some were able to survive the large deformation. An NTT fiber optic cable, for example, continued to provide a suitable signal despite the substantial deformation imposed on it. A medium pressure A-line operated by Osaka Gas (see Section 4 for gas system description) was deformed severely by the differential settlement, but did not leak at this location.

Because of severe distortion in the station walls, roof, and columns related to the roof collapse, clear evidence of structural response at incipient failure could not be found at the station. Nevertheless, observations provided by Professor M. Hamada of Waseda University in the running tunnel between Daikai and Nagata Stations do provide clues about the seismic response of the reinforced box at the onset of structural failure. He observed shear distortion of the box, with flexural failure of the reinforced concrete wall at a construction joint connecting the wall and base slab. He also observed bending failure where the center columns connect with the base slab. Cracks were observed at the street surface roughly parallel to and directly over the running tunnel walls.

Deformation consistent with reconnaissance observations is illustrated at an exaggerated scale in Figure 7-88. The deformed running tunnel structure is shown relative to idealized soil conditions inferred from Borings 6 and 7 presented in Figure 7-82. The approximate locations of the sheetpiles used for temporary support during construction are also shown. Shear distortion of the box structure is the result of transient shear deformation in the soil. This type of deformation leads to the formation of plastic hinges where columns and walls connect with the roof and base slab. Hinge formation and associated eccentric loading, in combination with increased loads from



Figure 7-80 Cracked Reinforced Concrete Column at Underground Shopping Mall Near Shin Kaichi Station



Figure 7-81 Cracked Reinforced Concrete Column and Concrete Panel Wall at Underground Shopping Mall Near Shin Kaichi Station

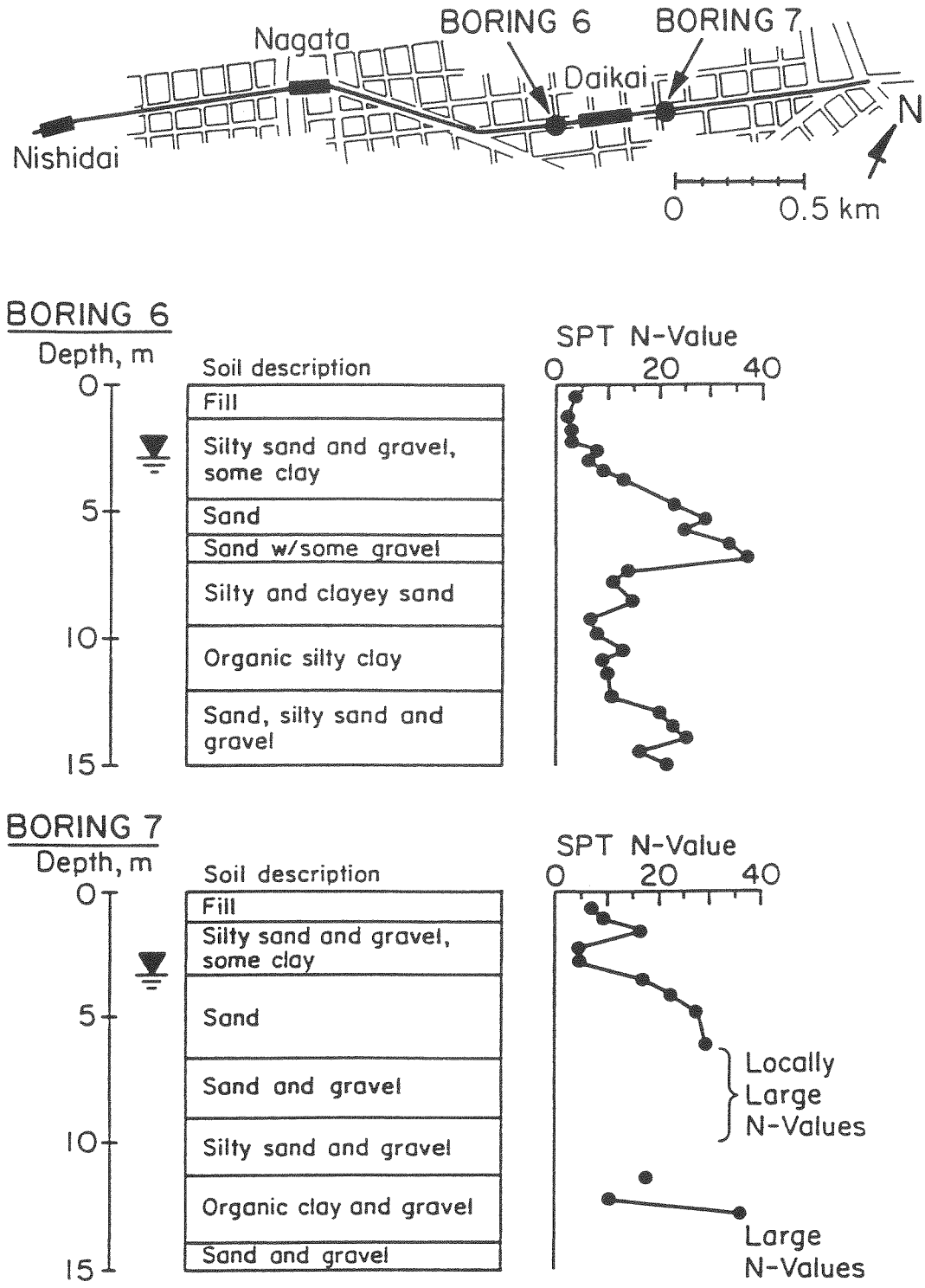


Figure 7-82 Soil Boring Records Near Daikai Station

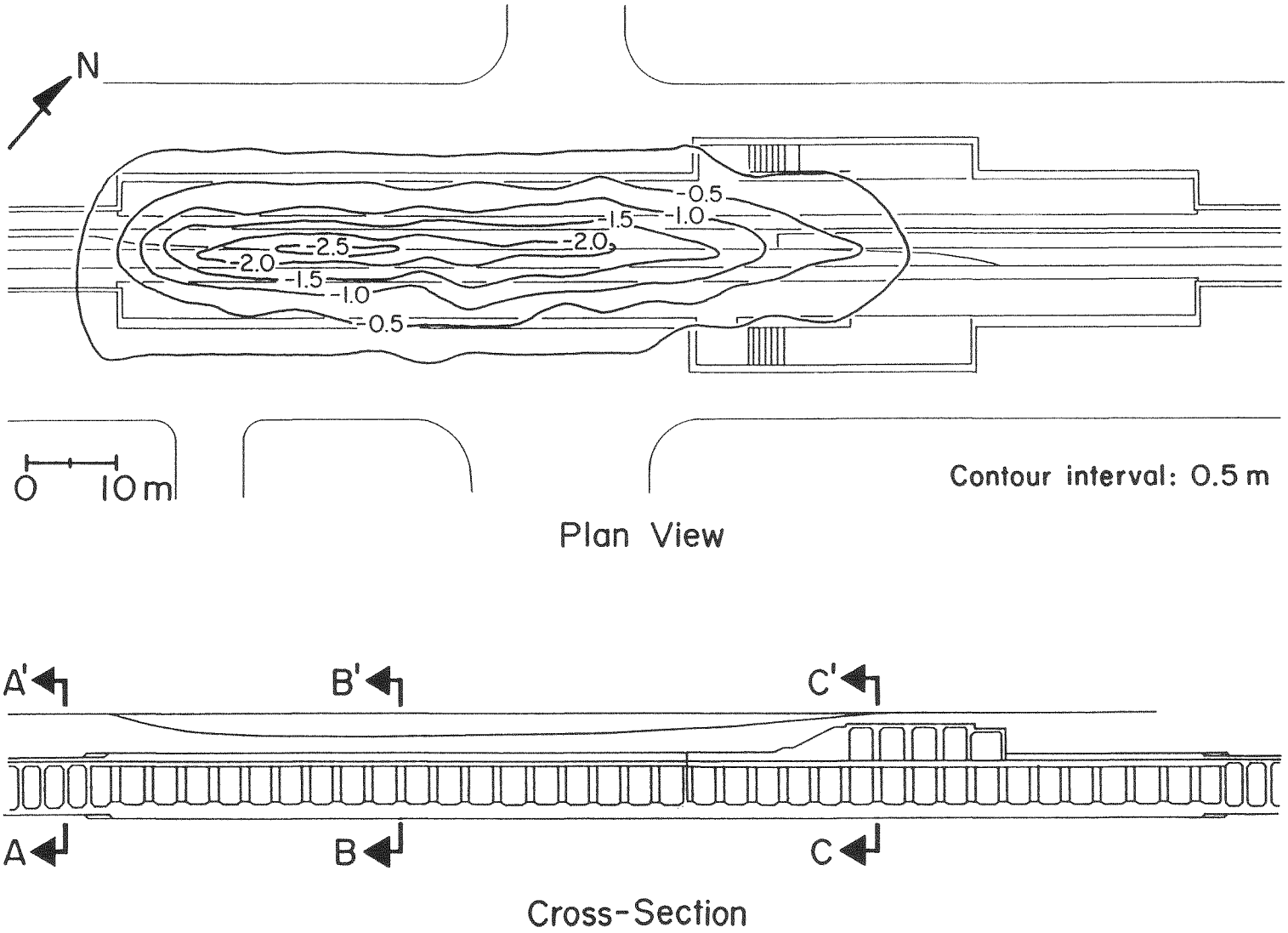


Figure 7-83 Plan and Profile Views of Daikai Station Collapse

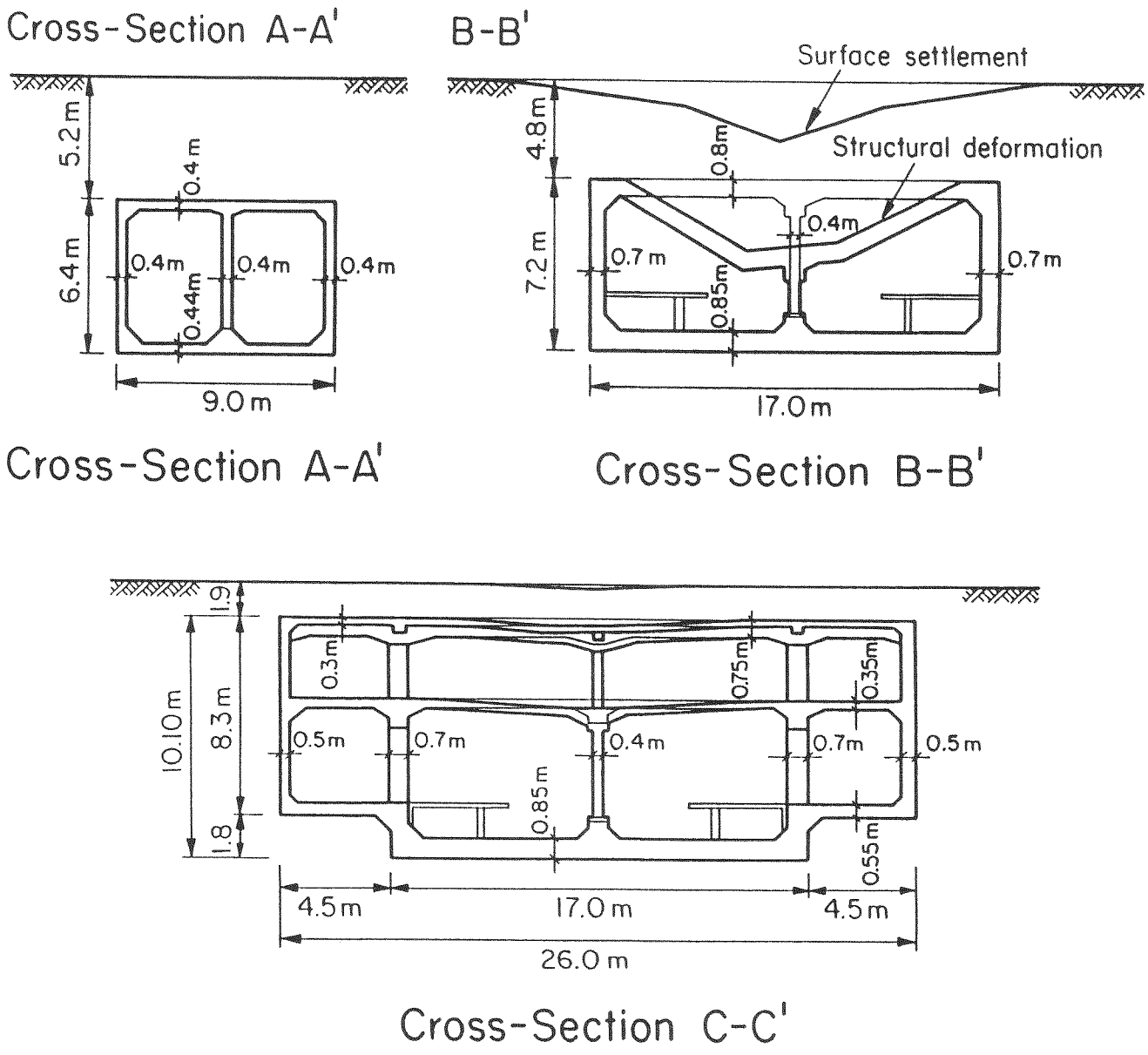


Figure 7-84 Cross-Sections of Reinforced Concrete Station and Running Tunnel Structures at Daikai Station



Figure 7-85 Roof Collapse Viewed from the Station Platform at Daikai Station



Figure 7-86 Compressive Failure of Center Columns at Daikai Station



Figure 7-87 Subsidence of Street Surface Over the Collapsed Daikai Station

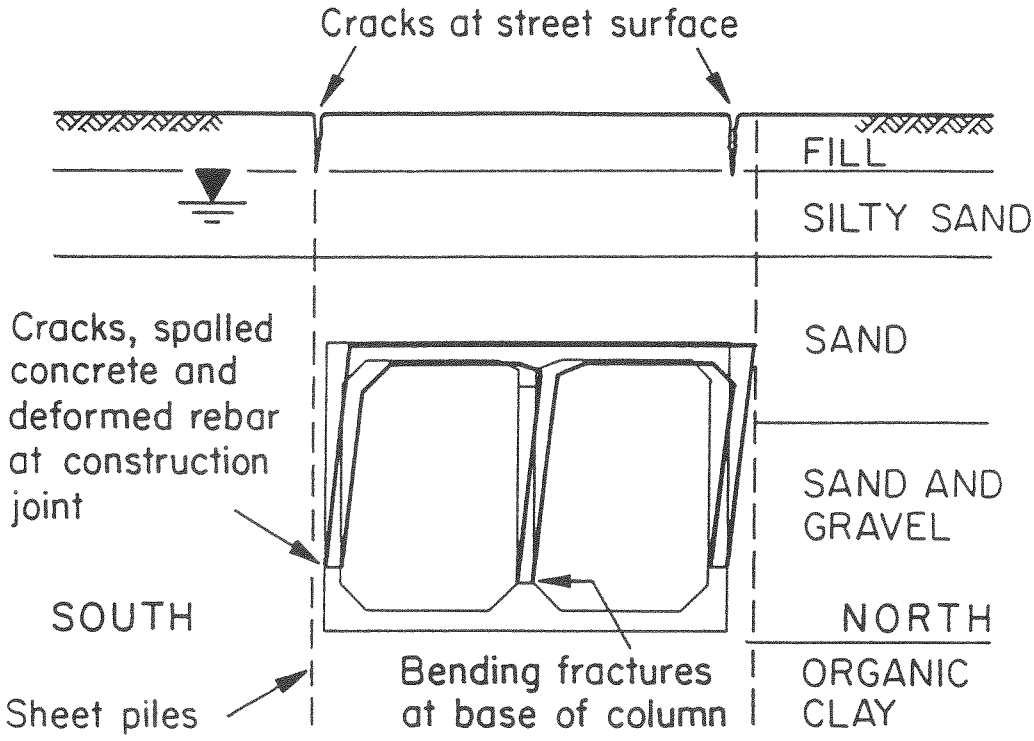


Figure 7-88 Earthquake Deformation of Running Tunnel at an Exaggerated Scale as Inferred from Reconnaissance Observations

vertical accelerations and geometric distortion, appear to have caused compressive failure of the columns at Daikai Station. The greater width of the station relative to running tunnel would have contributed to higher vertical forces at the station center columns. Moreover, loose sandy fill between the station walls and excavation sheetpiles would have been subject to liquefaction and softening during dynamic loading, thereby reducing the shear stiffness and lateral support from adjacent soil.

The deformed shape of the running tunnel is consistent with assumptions about earthquake-induced deformation which are part of current design practices. For example, design criteria for the Southern California Rapid Transit District (SCRTD) Metro Rail Project (Merritt, et al., 1985) call for the evaluation of shear deformation in reinforced concrete boxes by assuming it is equal to shear deformation in the surrounding soil as determined by one-dimensional wave propagation analyses using equivalent linear soil models (Schnabel, et al., 1972). If certain joints are strained into the plastic range, the structure is checked and redesigned to assure that no plastic hinge combination capable of leading to a collapse mechanism can be formed. The effect of the potential shear distortions evaluated during design has been to increase the reinforcing steel at some joints by 5 to 10% of that required for static loads. In addition, vertical loads for maximum earthquake conditions are taken as 40% larger than gravity loads under static conditions to account for vertical accelerations.

Seismic design for underground rapid transit structures was introduced in the U.S. during the planning and construction of the Bay Area Rapid Transit (BART) system during the 1960s. The design practices for BART were based on an assumed equivalence of soil and structural shear deformation and the introduction of additional reinforcing steel to prevent plastic hinge formation under the design transient shear deformation (Kuesel, 1969).

The KRTR followed design procedures which were derived from those of the Japan Railway and Tokyo Metropolitan Subway Corporation. In the KRTR design, dynamic earth pressures were considered, using the Mononobe Okabe analysis which has been discussed extensively in the technical literature (Seed and Whitman, 1970; Whitman, 1990). A horizontal seismic coefficient of 0.1 to 0.15 was taken into consideration, but vertical acceleration was not accounted for. When hydrostatic pressures are included in the analysis, the increase in total lateral pressure associated with horizontal seismic coefficients of 0.1 to 0.15 is small, typically less than 5 to 10% of the lateral forces under static loads.

7.3.3 Lessons from Damage to Underground Rapid Transit Systems

The failure of the Daikai Station is highly significant because it is the first instance of catastrophic earthquake damage to a modern tunnel for reasons other than fault displacement and instability near the portal. The failure appears to have resulted from earthquake-induced transverse shear distortion in combination with loads enhanced by vertical accelerations. Shear distortion promotes plastic hinge formation which, in combination with enhanced vertical loads, can result in a collapse mechanism. Shear distortion and vertical accelerations apparently led to collapse of the center reinforced concrete columns at the Daikai Station. There was evidence of hinge formation and associated shear distortion in the running tunnel of the KRTR between Daikai and Nagata Stations.

Elsewhere in an underground shopping mall near Shin Kaichi Station and at stations of the Kobe Municipal Subway, cracking and deformation of center columns provided evidence of high vertical loads and shear distortion in the cut-and-cover structures.

Current design practices, which account for transient shear deformation and vertical accelerations, are consistent with the failure mechanisms inferred from observations of damaged sections of the Kobe underground rapid transit systems. Failure of the central columns at Daikai Station emphasize the importance of designing to prevent plastic hinge formation leading to a collapse mechanism. The lack of significant confining steel at failed reinforced concrete columns suggests that attention to confinement and ductility can play an important role in strengthening underground structures against earthquake effects. Attention also needs to be focused on the density and stiffness of backfill adjacent to structures built by cut-and-cover methods.

For design purposes, large shear distortions have been considered primarily in deep deposits of soft clay, where significant amplification of bedrock ground motion can occur. Because a rapid transit box structure tends to be relatively rigid with respect to adjacent soft clay, the shear deformation sustained by the embedded structure is considerably less than that of the surrounding ground (Wang, 1993). Strong motion records from the Kobe and Northridge earthquakes, however, show that large transient shear distortions can be generated in relatively dense and stiff soils at locations close to fault rupture. Because an underground box structure may not be relatively rigid in a stiff soil, large shear distortions may be conveyed to the embedded structure under conditions of near source ground motion. This condition should be considered for underground structures located close to a seismic source.

7.3.4 References

Kuesel, T.R., (1969), "Earthquake Design Criteria for Subways," Journal of the Structural Division, ASCE, Vol. ST6, pp. 1213-1231.

Merritt, J.L., J.E. Monsees, and A.J. Hendron, (1985), "Seismic Design of Underground Structures," Proceedings, Rapid Excavation and Tunneling Conference, C.D. Mann and M.N. Kelly, Eds., AIMMPE, New York, NY, pp. 104-131.

Schnabel, P.B., J. Lysmer, and H.B. Seed, (1972), "SHAKE: A Computer Program for Earthquake Response Analysis of Horizontally Layered Sites," Report No. EERC 72-12, University of California, Berkeley, CA.

Seed, H.B. and R.V. Whitman, (1970), "Design of Earth Retaining Structures for Dynamic Loads," Proceedings, Lateral Stresses and Earth Retaining Structures Specialty Conference, ASCE, New York, NY, pp. 103-147.

Seed, H.B., K. Tokimatsu, M. Harder, and R.M. Chung, (1985), "Influence of SPT Procedures in Soil Liquefaction Resistance Evaluations," Journal of Geotechnical Engineering, Vol. 111, No. 12, pp. 1425-1445.

Wang, Jaw-Nan (Joe), (1993), "Seismic Design of Tunnels: A Simple State-of-the-Art Design Approach", 1991 William Barclay Parsons Fellowship, Monograph 7, Parsons Brinckerhoff, Inc., New York.

Whitman, R.V., (1970), "Seismic Design and Behavior of Gravity Walls," Design and Performance of Earth Retaining Structures, Geotechnical Special Publication No. 25, P.C. Lambe and L.A. Hansen, Eds., ASCE, New York, NY, pp. 817-842.

SECTION 8
WATER AND WASTEWATER

This section describes the City of Kobe water system, and the Hanshin Water Authority Water Purification Plant that provides water to the cities of Kobe, Ashiya, Nishinomiya, and Amagasaki. In addition, damage to the Kobe wastewater system is described. No information has been gathered for cities east of Kobe.

The City of Kyoto's water system had no pipeline damage, and suffered only minor window glass and small diameter buried pipeline damage at one of their purification plants.

8.1 Overview of the Water System

The City of Kobe water system serves 608,844 households, including 1.5 million people. The system was started in 1900, and is the seventh modern water system in Japan. The City area is 547 square km of which 245 square km has water service. The balance of the City is undeveloped, and has no water service. The Kobe Water Department has over 1,000 employees. The Kobe Water system includes the following inventory:

3,963 km pipe
239 reservoirs at 119 sites
46 pump stations w/ 231 pumps
64 km transmission tunnels (including Sengari Aqueduct (16 km))

Figure 8-1 shows a schematic of the system and Figure 8-2 shows a more detailed map of the system serving the urban area.

The Water Department began actively using computers in 1987, and input water pipe drawings and boring log data for 4,000 bores in 1988.

The system is divided by Mt. Rokko into two service areas, Hokushin and Shigaichi. The Hokushin area is served by the Sengari Reservoir located in the north of the area. The mountainous area makes up less than 10 percent of the water demand, and has been developed primarily since the 1960's.

The Shigaichi area, the Kobe urban and western parts, is served by the Yodogawa River. The area is approximately 30 km long, east to west, and 1.5 to 6 km wide, running between the shoreline and the mountains. Over 90 percent of the water demand is from this region. Water to this area is supplied from the east; it takes up to 12 hours for the water to traverse the distance from east to west.

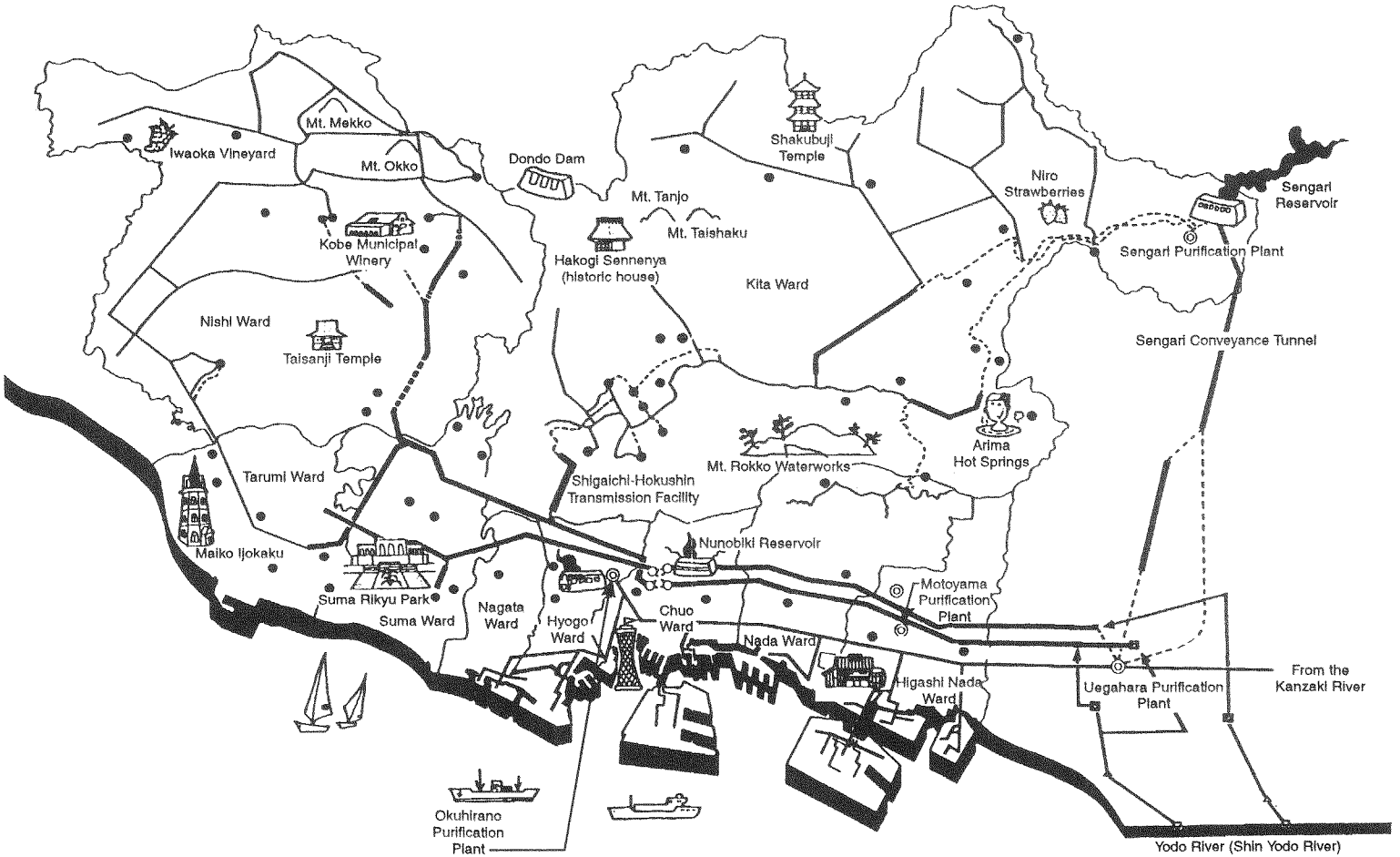


Figure 8-1 Schematic of Kobe Water System

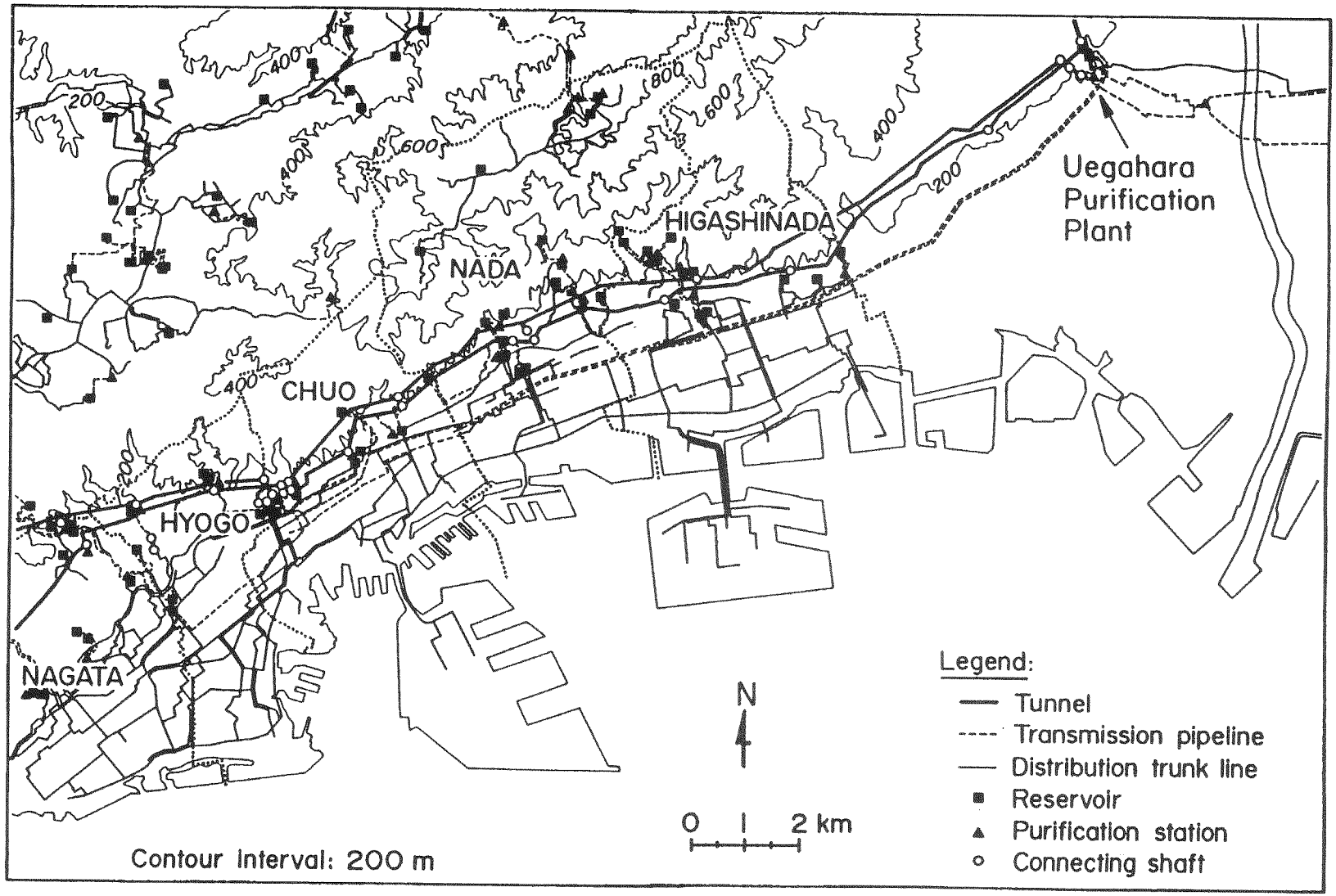


Figure 8-2 Kobe Water System, Urban Area

Water for the area is pumped to the water purification plants, and runs by gravity to the west at an elevation starting at 90 m above sea level through Kobe's tunnel system. The tunnel system operates in the open channel flow or low pressure regime. The first tunnel, 1.8-meter diameter, was built in the 1930's and is constructed in rock with an unreinforced concrete lining. The second tunnel, 2.5-meter diameter, was built in the 1950's and lined with reinforced concrete. There is apparently no concern about water quality degradation in the tunnel even though it is open channel flow. Water used at an elevation above 90 meters (approximately 15 percent of the demand) is pumped from the tunnel system. Figure 8-3 presents a schematic of the system profile.

The Kobe potable water system is designed to provide both water for drinking and fire protection. There is no dedicated water system for fire suppression, although one was under consideration in 1993. Firefighting is the responsibility of the fire department.

There are a number of cisterns located throughout the City for use for fire suppression (see Figure 8-4). The urban area is laid out on a 400 x 400 meter grid. Three quadrants of the grid each have a fire hydrant, and the fourth quadrant has a cistern.

There is one special radio system for communication between the water and fire departments during emergency response situations.

8.1.1 Supplies

Nearly all Kobe's water comes from surface water supplies. Nearly three-quarters of Kobe's water supply comes from the east with primary sources including Lake Biwa and the Yodogawa River. Table 8-I summarizes these sources. Figure 8-1 shows where many of these sources are located.

Table 8-I Kobe Water Supplies

Source and Comments	Percent of Total Supply	Supply in 1000 m^3/day
Lake Biwa/Yodogawa River - includes Hanshin Water Supply Authority (Yodogawa River 30 km east of Kobe).	73.9	606
Sengari Reservoir (constructed in 1919)	13.8	113
Karasuhara Reservoir (constructed in 1905)	4.4	36
Rivers in City - Sumiyoshi, Sanyo Shinkansen Tunnel	3.8	31
Nunobiki Reservoir, 420,000 m^3 capacity constructed in 1900; oldest gravity concrete dam in Japan)	2.4	20
Dondo Dam	1.7	14
Total	**100**	**820**

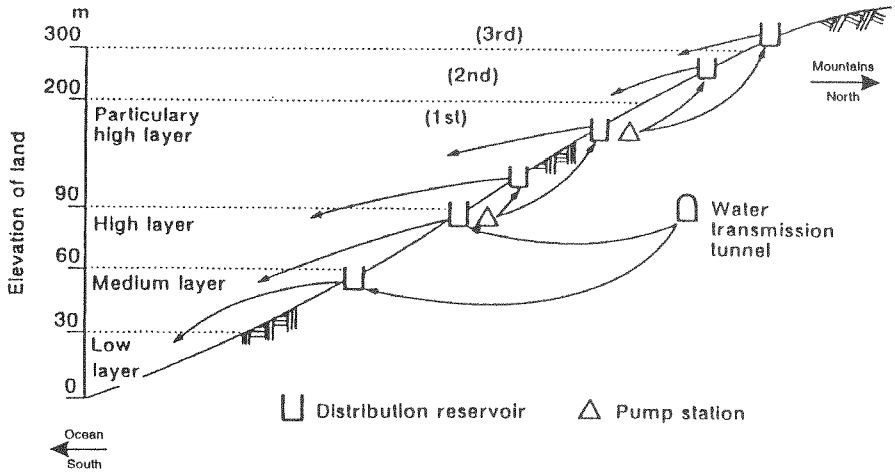


Figure 8-3 Schematic Profile of Kobe Water Delivery System

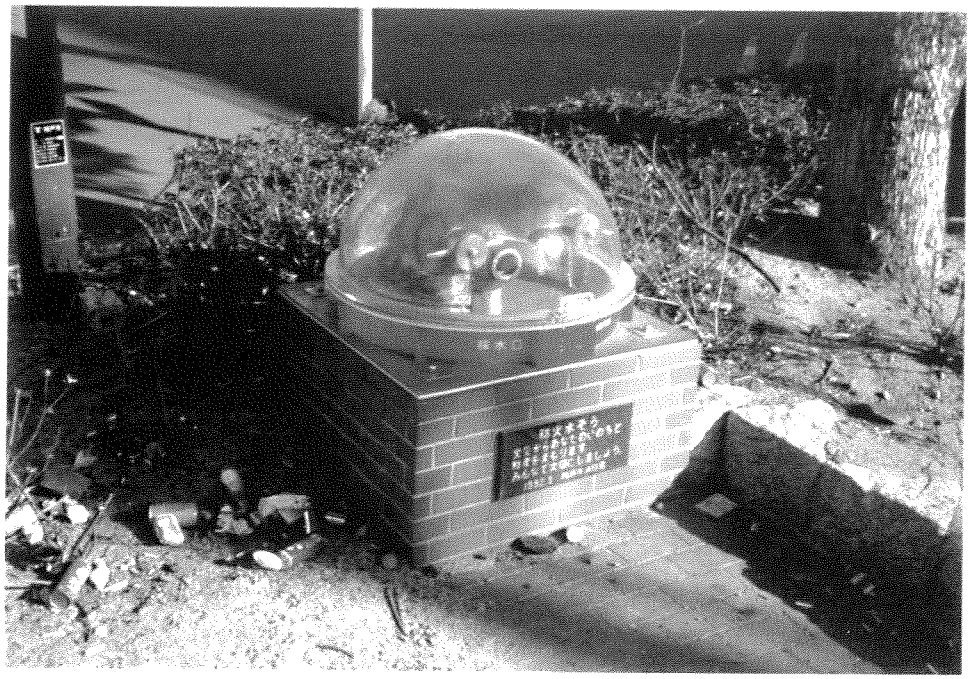


Figure 8-4 Cistern for Water for Fire Protection in Kobe

8.1.2 Water Treatment Plants

All Kobe's water is treated before it is distributed. There are eight water purification plants treating potable water for Kobe, and one treating water for industrial use. The three largest plants are Uegahara, Hanshin, and Sengari. The Uegahara and Hanshin Kabutoyama plants are immediately adjacent to one another, and are located to the east of the City. The Sengari plant is located north/northeast of the City. Table 8-II summarizes information regarding the water treatment plants.

Table 8-II Water Treatment Plants Serving Kobe

Filter Plant		Han-shin Kabuto-yama[1]	Urban Area							
			Uegahara (potable)[2]	Uegahara (indus.)	Okuhirano[3]	Moto-yama	Sumi-yoshi	Sengari	Arima	Mt. Rokko
Date Constructed			1917	1964	1900			1967		
Source		Yodo-gawa River	Sengari Reserv.	Yodogawa River	Nonobiki, Karasuhara Reservoirs	Sumi-yoshi River		Sengari Reserv.		
Number of Filter Basins	slow		8		-	-	-	-	1	-
	rapid		8		4	4	5	8[4]	-	1
Capacity per day (1000 m^3)		144	128	150	60	8[5]	6	108	0.3	1

Notes:
1. Municipal corporation including Kobe, Ashiya, Nishinomiya, and Amagasaki. Also owns Inagawa and Amagasaki Plants.
2. The Hanshin Water Authority Kabutoyama Water Treatment Plant is immediately adjacent to the Uegahara Water Purification Plant. Uegahara uses sodium hypochlorite for disinfection.
3. Also houses control center.
4. Granular activated carbon media.
5. Usually runs at 6000 m^3, including 1000 m^3 to Sake plant in summer and 2000 m^3 in winter.

Figures 8-5 and 8-6 show schematics of two of the purification plants that were damaged in the earthquake, Uegahara and Motoyama.

8.1.3 Distribution

Kobe has an aggressive pipeline replacement program which began in 1964. As a result of the program, 90 percent of the system is now constructed of steel or ductile iron pipe. The pipe inventory is summarized in Table 8-III. Tables 8-IV and 8-V summarize the replacement program, covering both general renewal and earthquake specific upgrades.

Table 8-III Pipe in Place as of April, 1994

Pipe Material		Length (km)	Remarks
Ductile Iron Pipe	Earthquake Resistant Joint (S, SII)	237.3 (6.0%)	All trunk mains >400 mm diameter; =>300 mm for reclaimed land and landslide areas.
	Mechanical Joint	3,180.2 (80.2%)	300 mm (sub main)
	Tyton Joint		75 mm-200 mm (distribution pipe)
Steel Pipe	Welded Joint	103.3 (2.6%)	high pressure pipe (>100 psi)
Cast Iron Pipe	Mechanical Joint	308.9 (7.7%)	Replacement in progress
	Leaded Joint	7.0 (0.2%)	
Polyvinyl Chloride Pipe	Bell & Spigot Joint	126.4 (3.1%)	Replacement in progress
Asbestos Cement Pipe		0	Replacement completed in 1987
Total		**3963.1 (100%)**	

Table 8-IV Rehabilitation and Renewal Project -1978

Year	Cost (million yen)	Diameter (mm)	Length Replaced (km)
1982-86	10,480	700-100	139
86-88	4000	800-150	20
89-91	4000	800-150	27

Table 8-V Strengthening/Earthquake Proofing Pipelines - 1991

	Cast Iron Pipe	Polyvinyl Chloride Pipe	High-Pressure Pipe Network	Total
Length Replaced (km)	84	3	20	107
Cost (billion yen)	9.1	0.2	2.2	11.5

The results of Kobe's pipeline replacement program were evident in a leakage survey of the system undertaken in 1990. The Kobe system had 93.5 percent effective use of the water compared to Tokyo, which had 87.8 percent, and Osaka, which had 92.7 percent. Effective use was calculated by dividing the amount of water delivered to customers (through meters) by the amount of water taken from the source. Meter accuracy and system leakage are the two elements that can dramatically affect the effective use evaluation results.

Approximately six percent of the piping employs special seismic joints as depicted in Figures 8-7 and 8-8. These joints, Japan Water Works Association (JWWA) Standard G 113 and 114, are specially designed to allow longitudinal extension and compression but are restrained before they separate. The ductile iron pipe with S joints is manufactured by both Kubota and Kurimoto, and is estimated to cost 30 percent more than pipe without seismic joints. All new pipelines greater

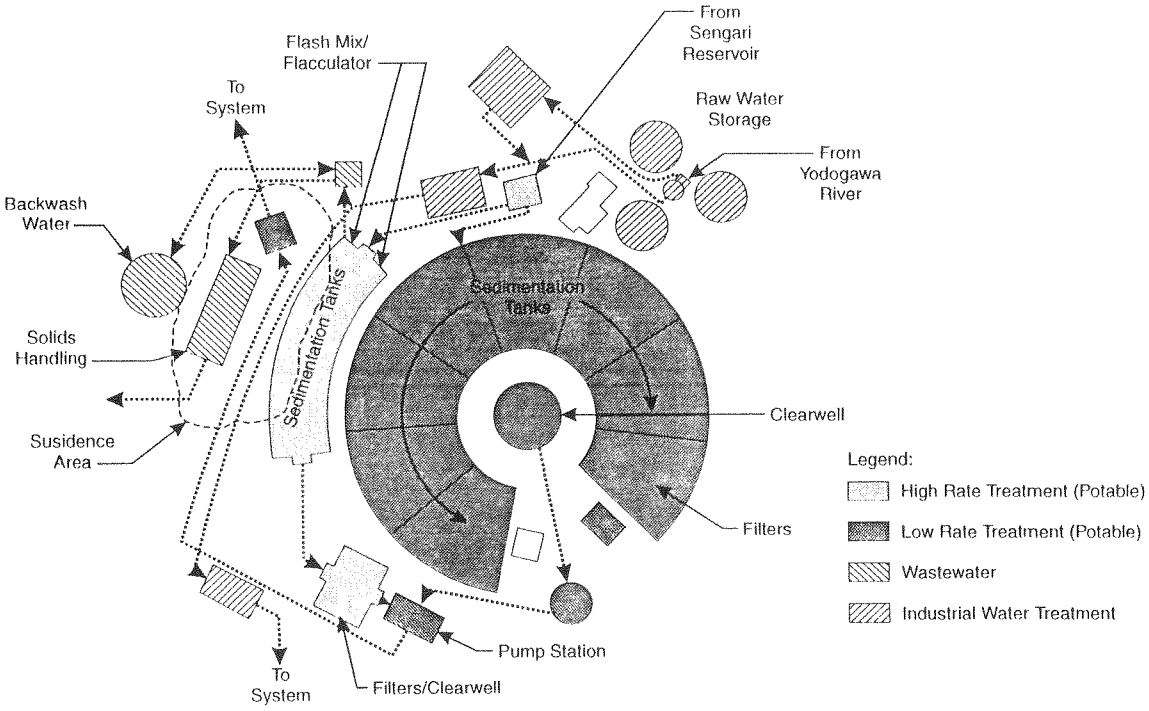


Figure 8-5 Schematic of Uegahara Water Purification Plant

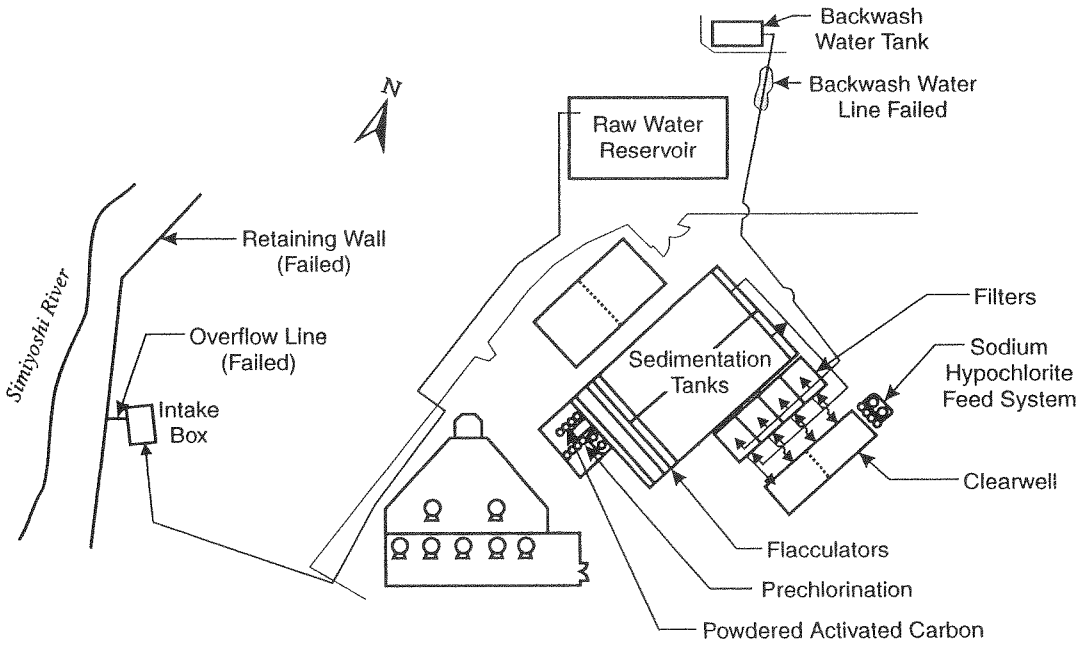


Figure 8-6 Schematic of Motoyama Water Treatment Plant

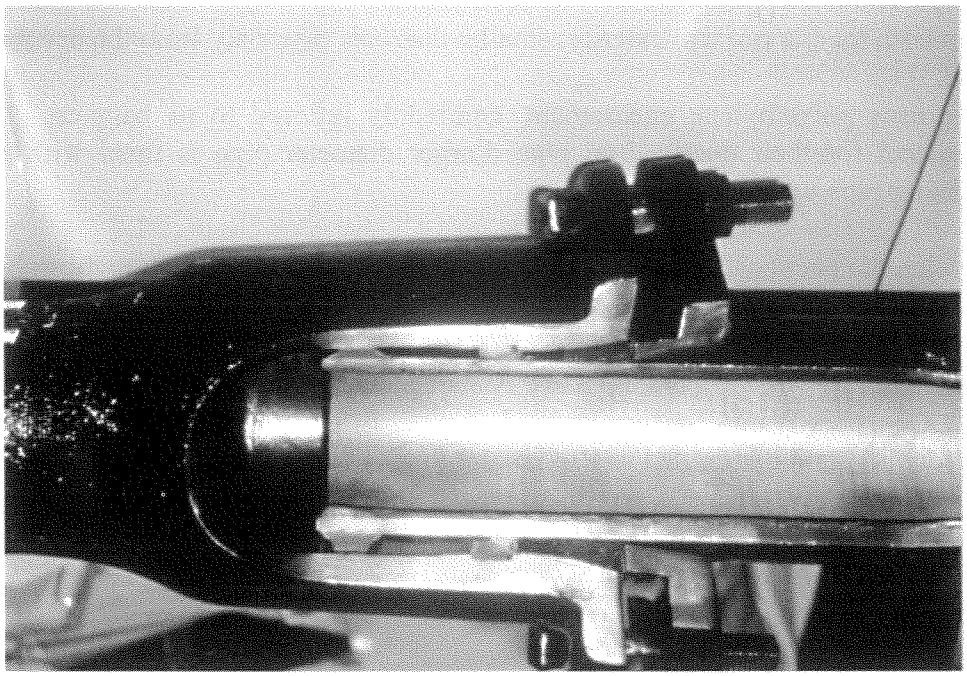
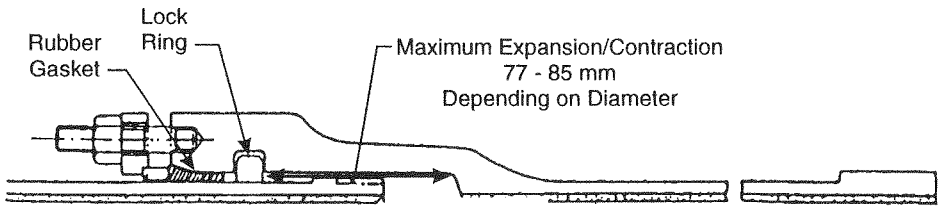
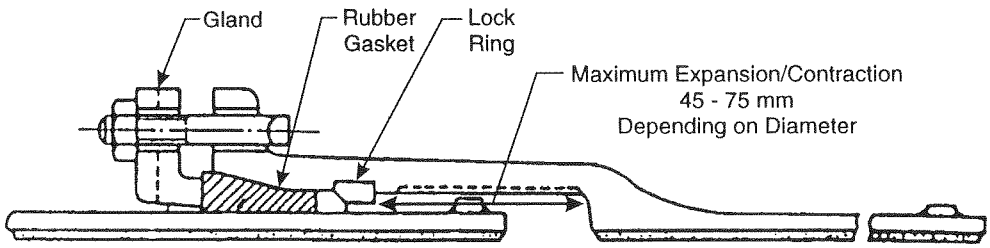


Figure 8-7 Type SII (Seismic) Joint



"S" Joint (500 - 2600 mm Diameter)



"SII" Joint (100 - 450 mm Diameter)

Figure 8-8 Seismic Joints (S and SII)

than 400 mm in diameter and all pipelines in reclaimed and landslide areas are required to be constructed with this seismic resistant joint. All major pipelines on Rokko Island are constructed with this special seismic resistant joint.

The steel pipe Kobe uses employs butt welded joints. Pipe larger than 600 mm diameter is welded from both the interior and exterior; smaller diameter pipe only from the exterior.

Kobe Water uses polyethylene encasement, commonly referred to as baggies, for external corrosion control for their ductile iron pipe. Larger diameter pipe is lined with mortar, and smaller diameter pipe with epoxy.

For new service connections, High Impact Vinyl Pipe is used, which is thought to be similar to PVC used in the United States.

In addition to potable water pipelines, Kobe has an industrial water pipeline system. Water is treated at the Uegahara Water Purification Plant in a separate treatment system delivering a lower grade water quality, and distributed to Rokko and Port Islands, and to industrial areas along the shoreline. That system includes 21 km of conveyance pipe, 13 km of transmission pipe, and 62 km of distribution pipe.

8.1.4 Distribution Reservoirs and Pump Stations

The Kobe Water Department has an inventory of 240 service reservoirs at 119 sites. These include cast-in-place concrete (approximately 80 percent), and precast concrete and welded steel (approximately 20 percent combined), and range in capacity from 40 to 20,000 m^3. Table 8-VI summarizes the location of these reservoirs by elevation, and Table 8-VII by area.

Table 8-VI Summary of Service Reservoirs by Elevation

Layer	Altitude Above Sea Level	Blocks	Water Consumption (%)	Reservoir Sites
1	0-30 m	10	53	10
2	31-60 m	10	20	13
3	61-90 m	14	13	19
4	91-180 m	31	11	77 (includes layers 5,6)
5	181-280	8	3	included in layer 4
6	Over 280	1	< 1	included in layer 4
Total		**74**	**100**	**119**

Table 8-VII Reservoir Distribution by Area

Block Name		Urban	Western	Northern	Total
Distribution Reservoirs	Sites	71	8	30	109[1]
	Reservoirs	147	14	54	215[1]
Pumps	Sites	25	5	12	42
	Pumps	132	18	50	200
	Discharge Lines	50	9	17	76
Population (1,000's)		1117	103	174	1394
Population Served (1,000's)		1116	86	174	1377

Notes 1. Total numbers of distribution reservoirs differ from Table 8-VI. Information source is different and presumed to be from several years earlier.

Nearly all the reservoirs are constructed with two at each site. This provides redundancy for post-earthquake function and allows removing one from service for cleaning without impacting service.

Kobe does not use pressure reducing valves between pressure zones as are commonly used in the United States. Rather, they use control tanks, with flow from the upper pressure zone into the tank controlled by an altitude valve.

Kobe Water has a program to advance the design of reservoirs to meet a wide range of requirements including general structural performance, earthquake performance and corrosion resistance. At the Okuhirano Water Purification Plant site, two reservoirs were constructed at about the same time, one using welded steel and the other using precast/post-tensioned concrete. The objective was to be able to evaluate the relative long-term performance of both designs. Figure 8-9 shows a section of the steel reservoir. It is specially designed to accommodate radial expansion during filling, similar to U.S. precast/post-tensioned concrete tank designs. Inherent in the design is damping of compressive earthquake loading on the steel shell. Figure 8-10 shows the steel and concrete water storage tanks, which are both less than seven years old.

All of Kobe's pump stations either have diesel generators on site (10 sites), or have a dual source of power from alternate substations.

8.1.5 Control System

The Kobe Water Control Center is located at the Okuhirano Purification Plant. It was built in 1977. It is a Fujitsu 400 MHz UHF-multidirectional multiplex broadcasting system. It monitors over 2,000 points including reservoir level; tunnel level; tunnel, transmission, and distribution flow; pump status; and access alarms. It controls 469 components including pump on/off, rate-of-flow controllers, valve controls, and control selection.

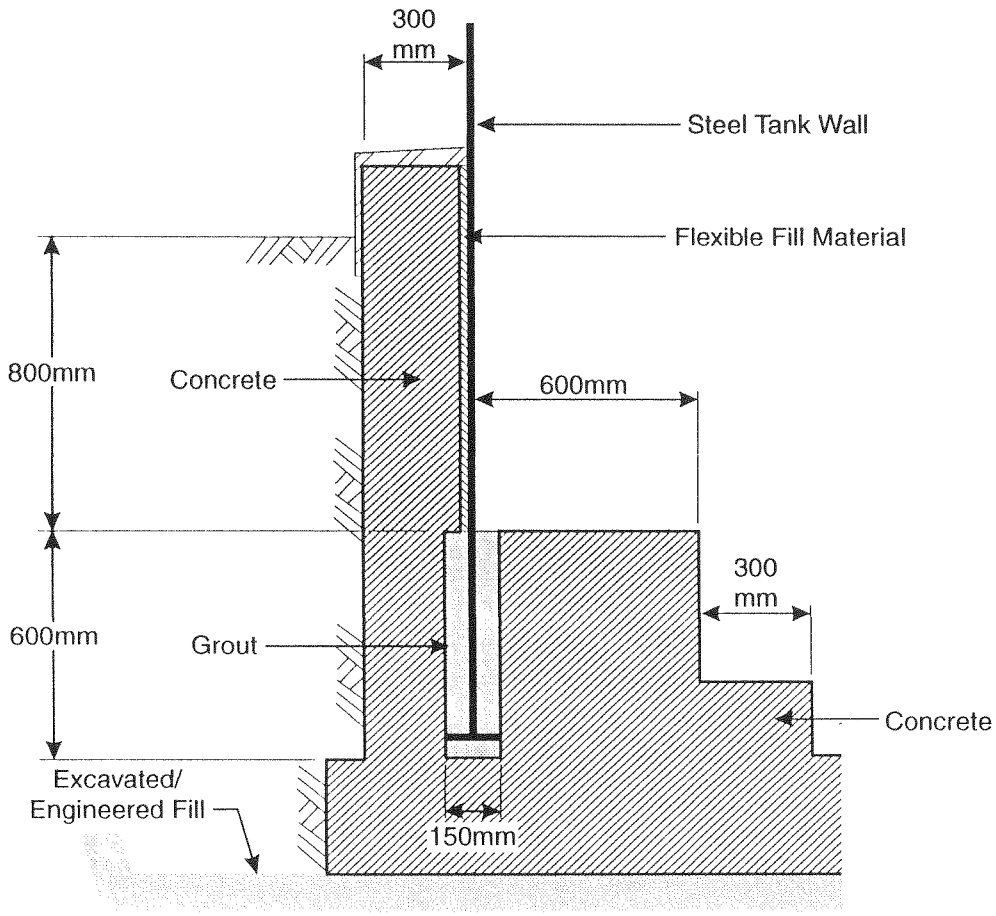


Figure 8-9 Steel Tank Section at Okuhirano Purification Plant



Figure 8-10 (Top) Steel and (Bottom) Concrete Water Storage Tanks at Okuhirano Purification Plant

The Control Center communicates with distributed facilities through a repeater station on the International Trade Center Building. That repeater serves much of the urban area and the Uegahara Water Purification Plant directly and also transmits secondary repeaters at:

Mt. Rokko (serving Northern Service Area; Sengari Water Purification Plant)
Mt. Takao (serving Western area)

Figure 8-11 presents a schematic of the communication/repeater system.

8.1.6 Earthquake Monitoring and Control

Kobe Water has an earthquake monitoring and control system in place to isolate water in selected reservoirs from the system to maintain it for drinking following an earthquake. Without this system in place, the typical scenario is that pipe damage in the system would result in quickly draining the service reservoirs. The system is not designed to maintain water for fire suppression. There is no system to isolate major lines crossing vulnerable areas, such as lines to the reclaimed land areas.

The system consists of earthquake ground motion monitoring at the Okuhirano Control Center, a control panel, telemetry (as described above), and reservoirs with earthquake isolation valves at 21 locations, and planned for 29 locations (see Figures 8-12 and 8-13). The earthquake valves are motor operated with backup batteries.

The seismograph at the Control Center measures ground motion, and provides input into the earthquake control system. The earthquake control system allows both automated and manual control of isolation valves on service reservoirs. The decision logic is as follows:

Peak Ground Acceleration Control Thresholds

1. 40 gal - manual alarm (980 gal = 1 x gravity)
2. 80 gal - automatic shut down when combined with excessive rate of change of flow
3. 250 gal - automatic shut down

Figure 8-14 shows a schematic of the control system.

There are dual reservoirs at 21 sites; one has an isolation valve to be controlled following an earthquake, and one does not. Planning was underway for the addition of isolation valves to eight additional reservoirs at the time of the earthquake. This concept allows shutdown of one reservoir while maintaining service should an inadvertent shutdown signal be received. If the system can keep up with leakage, the isolated reservoir can be put back on line from the Control Center. If the system cannot keep up with the demand, the reservoir remains isolated.

Emergency planners based the number of locations of isolated reservoirs on serving the population 3 liters/day drinking water for seven days. Planners estimated that it would take up to

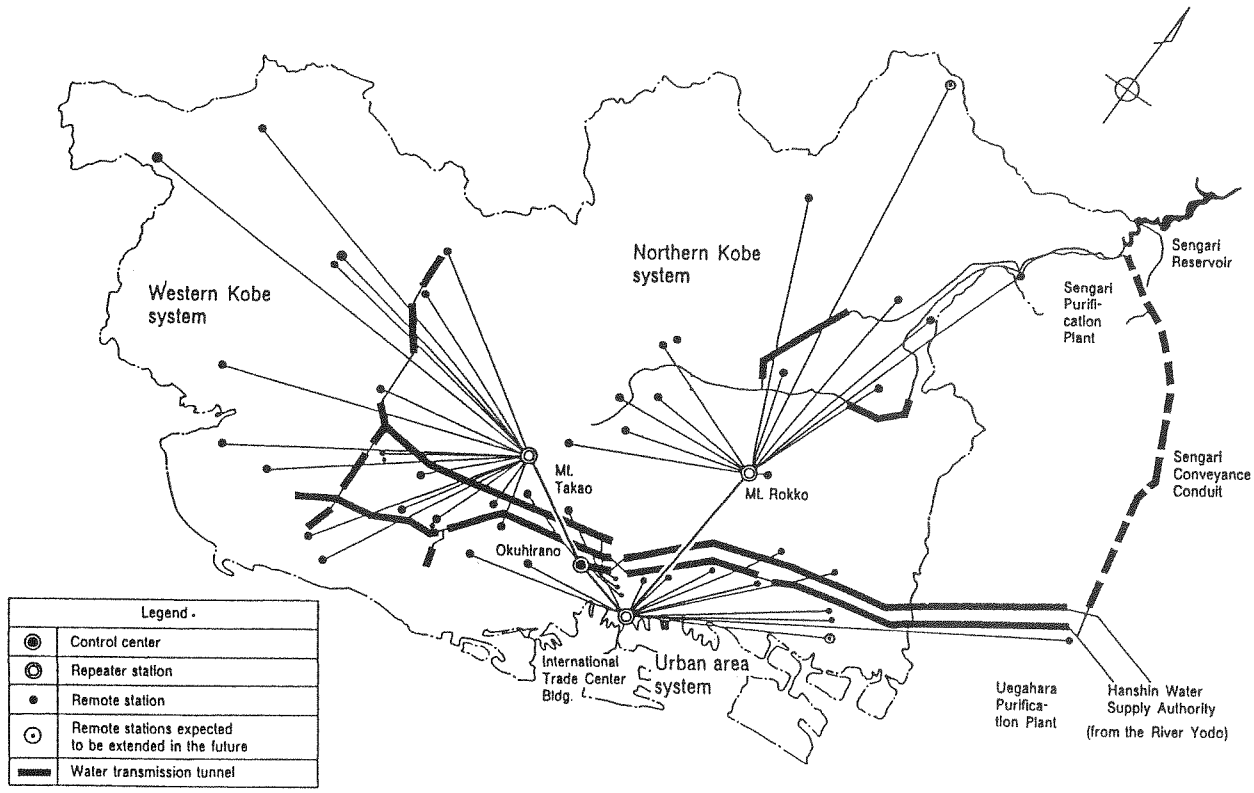


Figure 8-11 Schematic of Communication/Repeater System

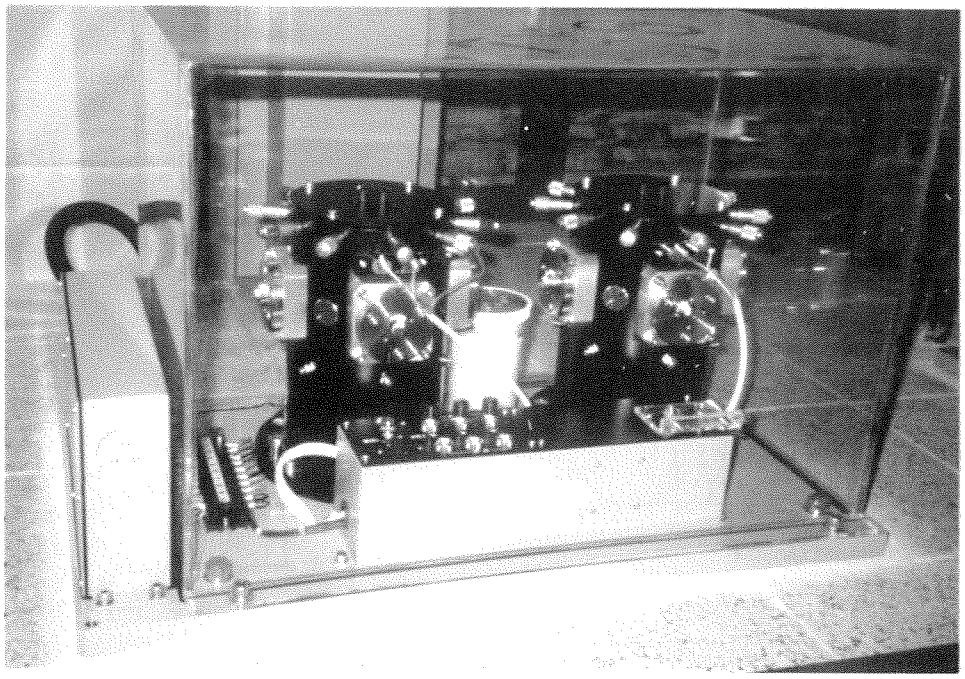


Figure 8-12 Seismograph at Okuhirano Control Center used for Control of Earthquake Valves on Reservoirs

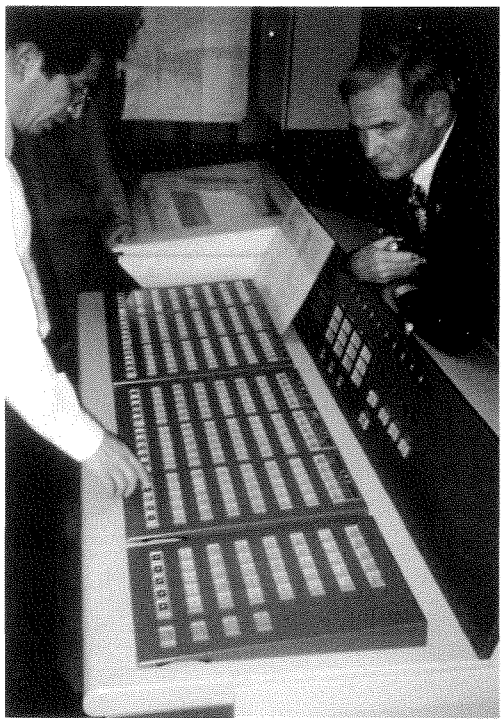


Figure 8-13 Control Panel for Earthquake Valves to Provide Flexibility to Control Automatically or by Operations Staff in Okuhirano Control Center

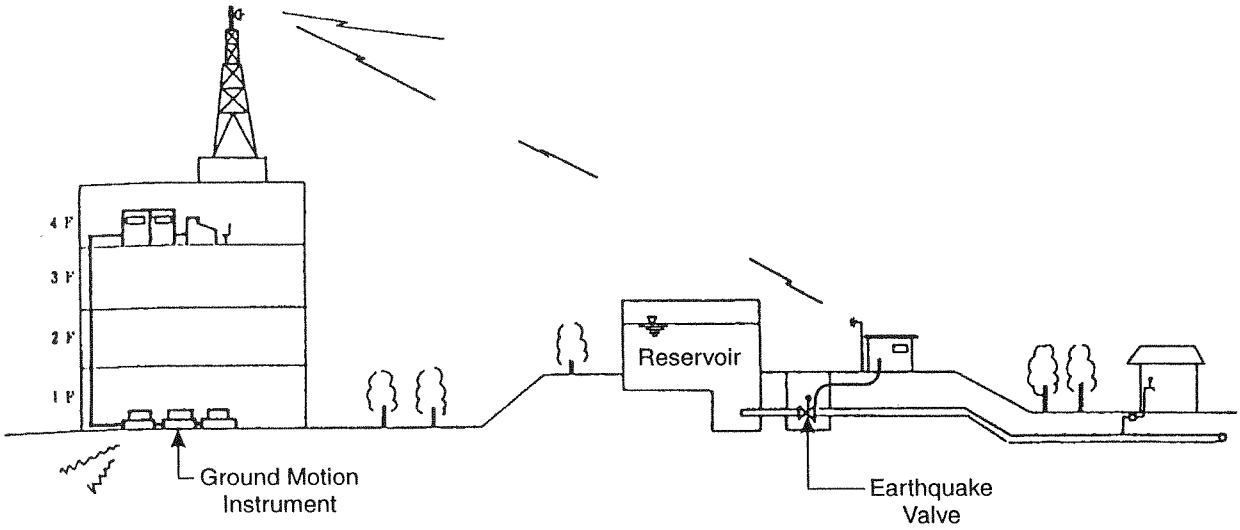


Figure 8-14 Schematic of Typical Communication from Ground Motion Instrument, Through Radio Communication, to the Earthquake Valve

seven days to repair the system. Figure 8-15 shows the locations of the reservoirs within the system. Isolated tanks were selected so that each would serve an area approximately 4 km in diameter. Figure 8-16 shows a schematic of the local post-earthquake water distribution system at each reservoir.

8.2 Description of Damage to the Water System

8.2.1 Conditions Following the Earthquake

Earthquake valves closed on 18 of 21 service reservoirs following the earthquake, storing 33,800 m^3 of water. Storage before the earthquake (1/17 - 5:05 a.m.) was 338,455 m^3. The earthquake occurred at 5:46 a.m. Minimum storage after the earthquake (1/18 - 6:01 a.m.) was 94,908 m^3.

The 86 distribution reservoirs serving the urban area without earthquake valves quickly emptied, as shown in Figure 8-17. This resulted in inadequate water available for fire suppression.

Water carried by the Hanshin system dropped from 6,000 to 1,000 m^3/hr immediately following the earthquake. This was caused by loss of power to the Yodogawa River Pump Stations for 15 hours following the earthquake as well as transmission main breaks.

When service was resumed, the chlorine feed rate at the purification plant was increased but no boil water notice was issued. When leaks were repaired, lines were flushed, but not disinfected.

Emergency supply using water tank trucks was initiated on the evening of January 17. Later, water supply aid came from other cities and from the Self Defense Forces. Regular water supply points were established and increased in numbers as time went on (see Figures 8-18 and 8-19).

Starting January 18, water restoration began. Leaks were identified and repaired with the following priorities:

1. Damaged areas, medical facilities, areas with large populations
2. Broken pipes, minor leakage areas (that is, fix areas that first that could be easily restored)
3. Broken pipes, major leakage areas
4. Shelters and areas in danger of landslides

Water Department crews worked from the outside in. Mutual aid was provided by 37 agencies including an estimated 1,000 people.

Figure 8-20 shows the status of the emergency water supply in the days following the earthquake in terms of truck loads of water, distribution points, and relief workers working on water distribution. It is not clear what the correlation is between trucking in water and use of the service reservoirs that had been isolated for local distribution for drinking.

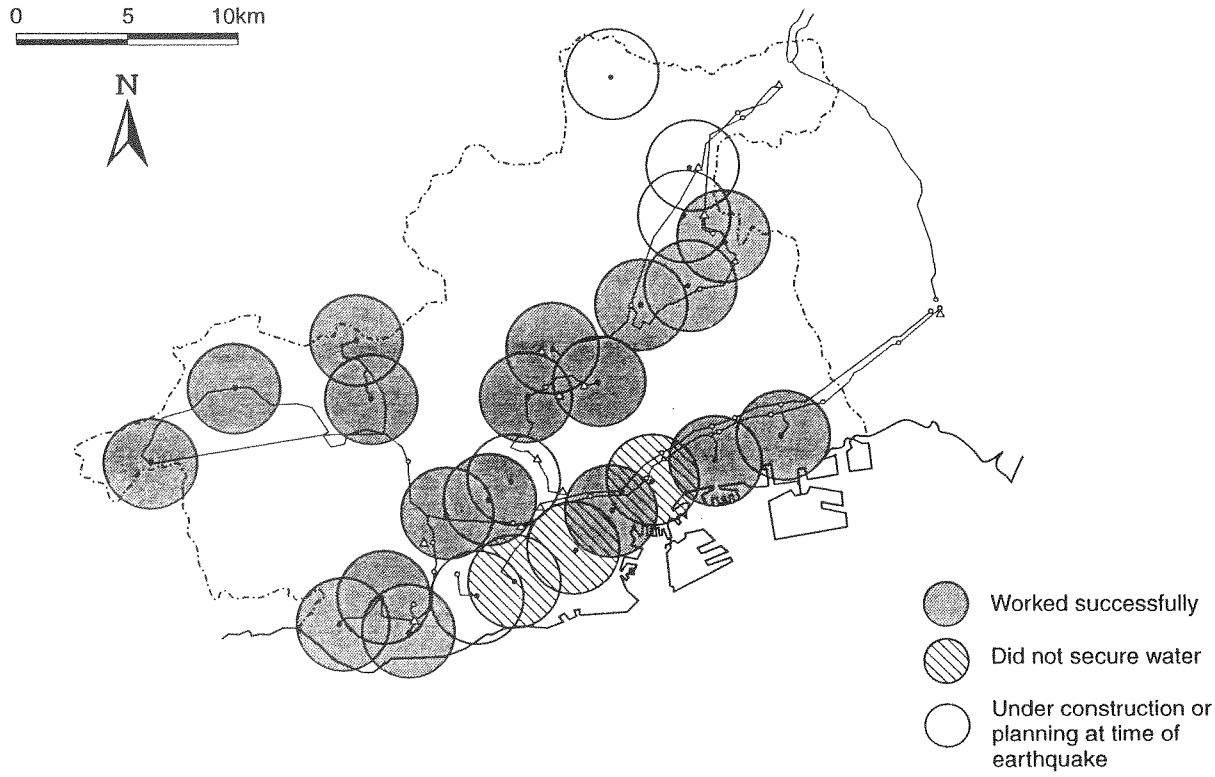


Figure 8-15 Map of Kobe Water Service Area Showing Reservoirs with Earthquake Valves and Their Respective Service Area

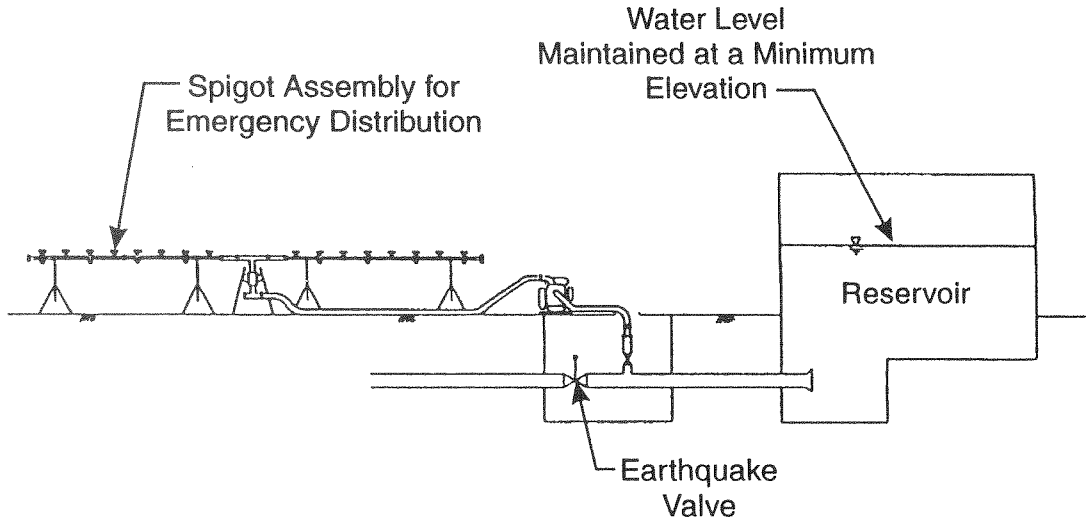


Figure 8-16 Schematic of Water Distribution from Tank with Earthquake Valve

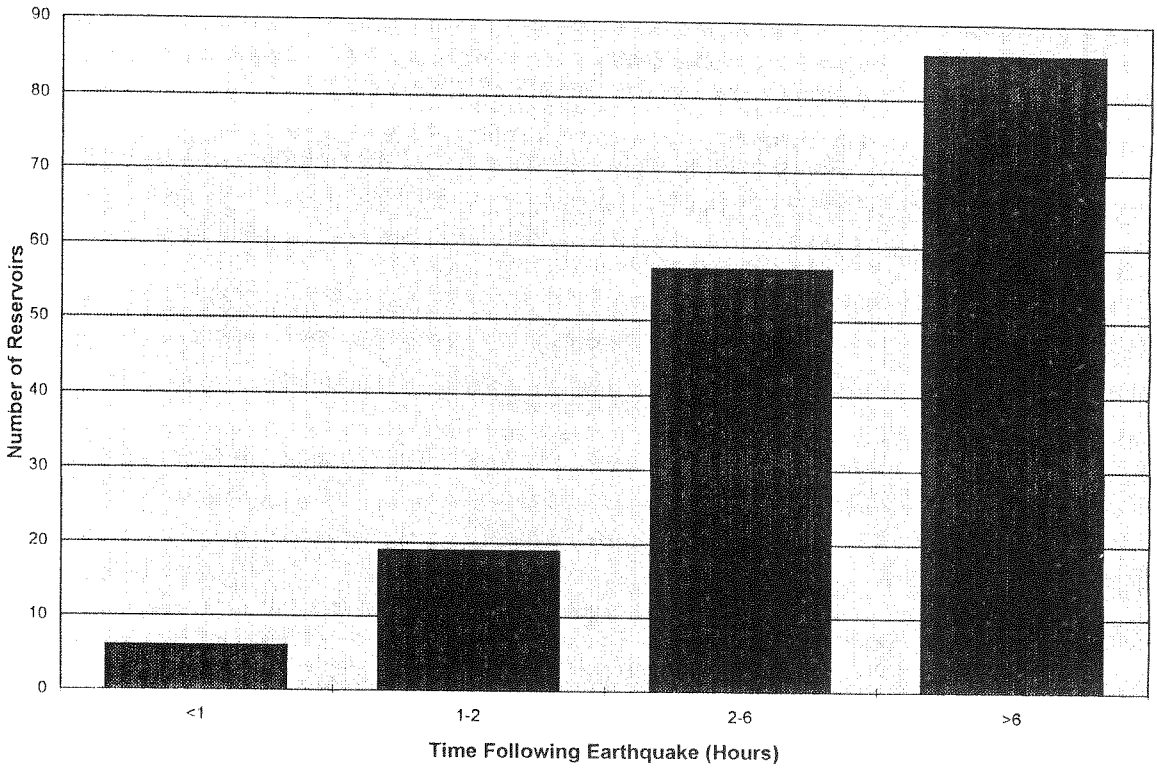


Figure 8-17 Water Loss from Reservoirs After Kobe Earthquake



Figure 8-18 Person Collecting Water from Central Water Distribution Point Near the Collapsed Daikai Subway Station



Figure 8-19 Emergency Water Supply Delivered in Tank Trailer

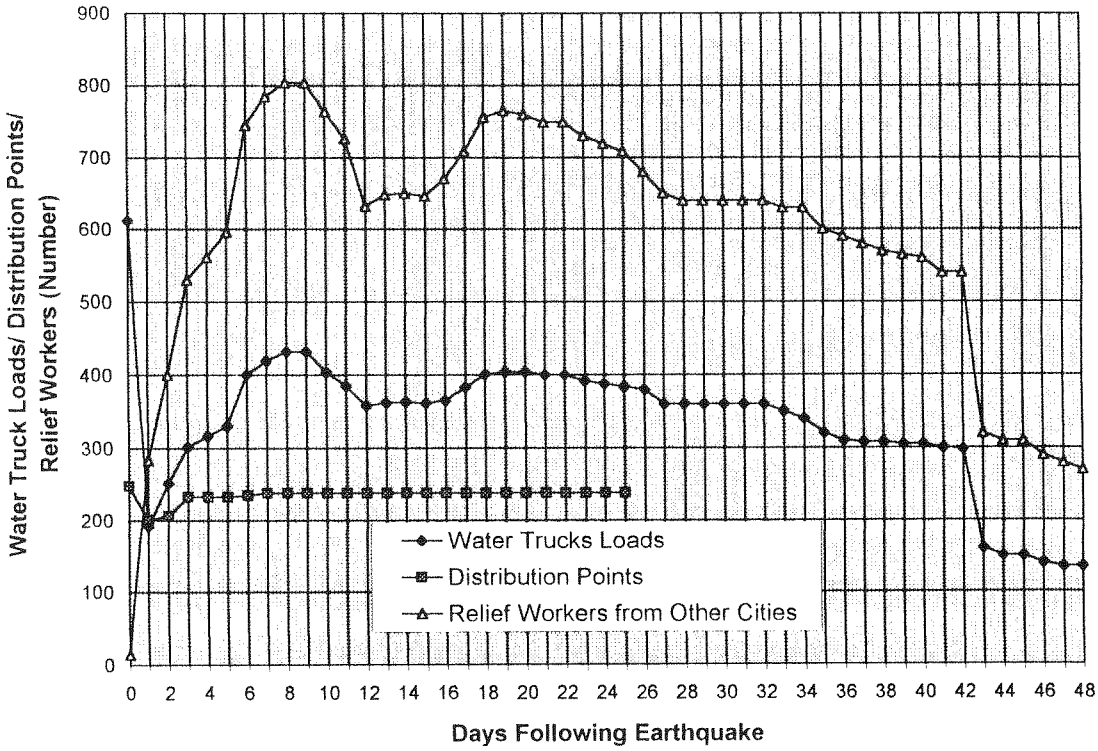


Figure 8-20 Status of Emergency Water Supply

Figures 8-21 and 8-22 show the numbers of emergency response workers from other cities assisting in restoration of the distribution system and purification and pump station equipment, respectively, by ward. Based on the information provided by the Kobe Water Department in these figures, it appears that it took approximately one week to gather mutual aid. Areas of the system noted on these tables can be identified in Figures 8-1 and 8-2.

Figure 8-23 shows the status of water system restoration by ward, through February 13. Based on the information in this figure, approximately three-quarters of this system was initially without service. The western area of the system was the most severely impacted, while the northern part of the system had the least damage. Other parts of the system appear to be equally hard hit. Water was restored to 99 percent of customers by March 29. It took 35 days to restore water to Port Island.

Figure 8-24 shows restoration (filling) of distribution reservoirs and water mains. The Hokushin and Rokko Mountain reservoirs were restored within about four days, after which the total reservoir and Shigaichi reservoir curves are parallel. Distribution main restoration lags behind restoration of the reservoirs, as expected.

8.2.2 Damage to Water Facilities

This section describes damage to specific system components.

8.2.2.1 Supply Reservoirs

Damage to two supply reservoirs can be described as follows:

- Nunobiki Reservoir - cracked hand rail in walkway on dike. Damage to foot of service bridge requiring major repairs.
- Karasuhara Reservoir - vertical crack at one location on back of dike.

8.2.2.2 Water Purification Plants

This section describes damage to the Uegahara, Hanshin and Motoyama water purification plants. The Sengari, Okuhirano, and Sumiyoshi water purification plants had little damage. Information is not available on the other two small plants, Arima and Mt. Rokko.

Uegahara Water Purification Plant

An aerial view of the Uegahara Water Purification Plant is shown in Figure 8-25. In the photograph, the landslide that undercut the Hanshin Kabutoyama Plant's solids handling building is evident. In addition, referring to Figure 8-25, the area at about 10:00 o'clock outside the circular basin settled approximately 30 cm, separating joints on three 1.2 meter diameter pipelines over a length of approximately 100 meters, and damaging the solids handling building. The plant was rendered inoperable following the earthquake. On the west side of the plant, fill

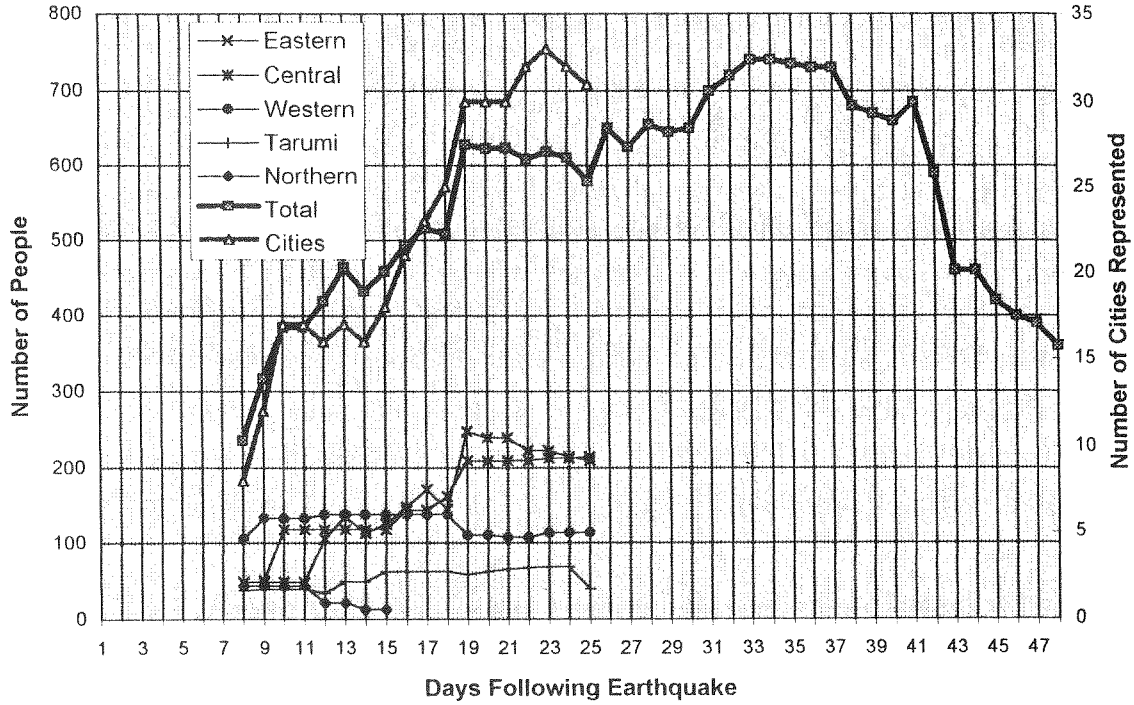


Figure 8-21 Mutual Aid from Other Cities Repairing the Water Distribution System

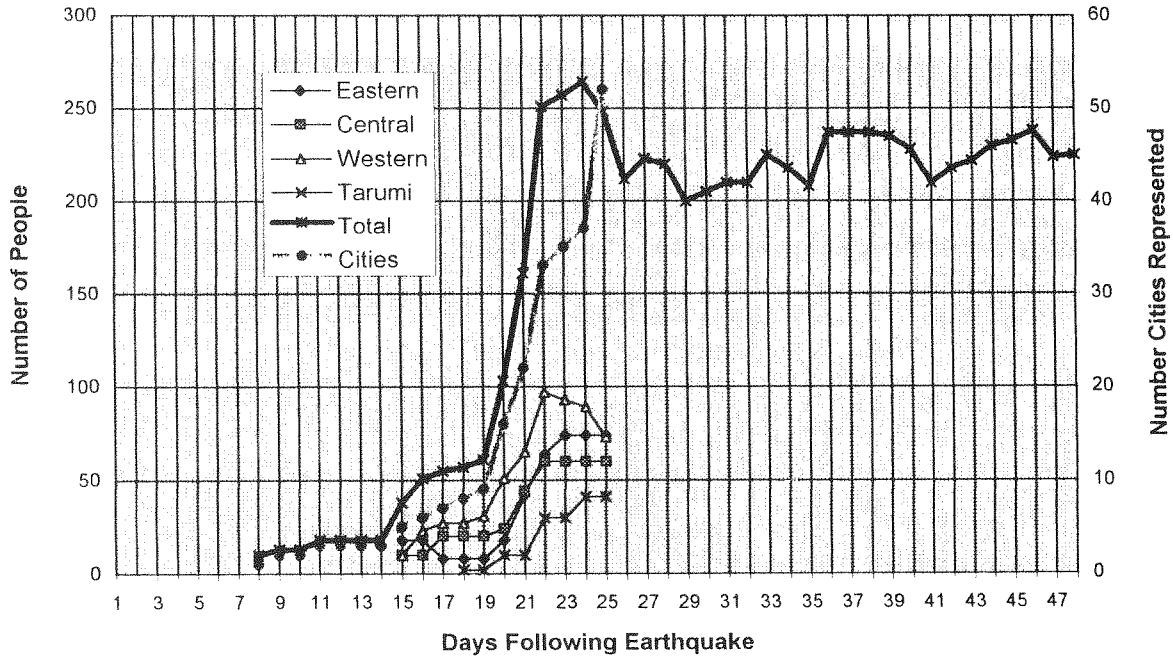


Figure 8-22 Mutual Aid from Other Cities Repairing the Water Supply Equipment (Purification Plants, Pump Stations, and Tanks)

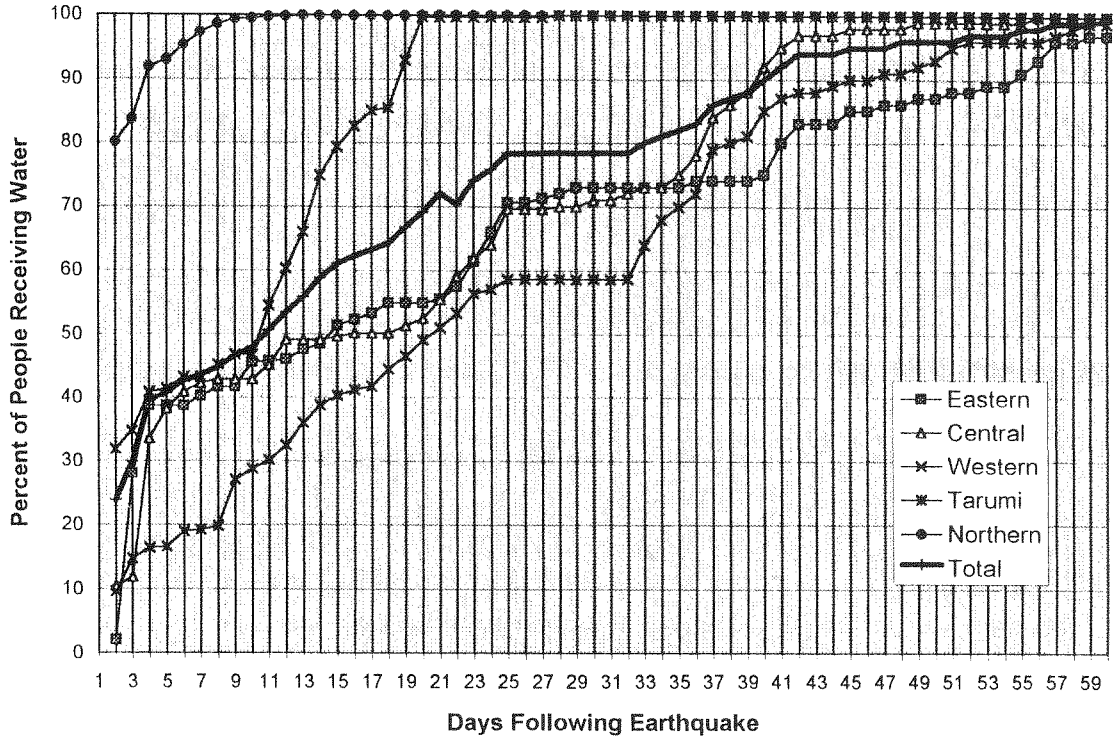


Figure 8-23 Percent of People in Kobe Without Water Following Earthquake

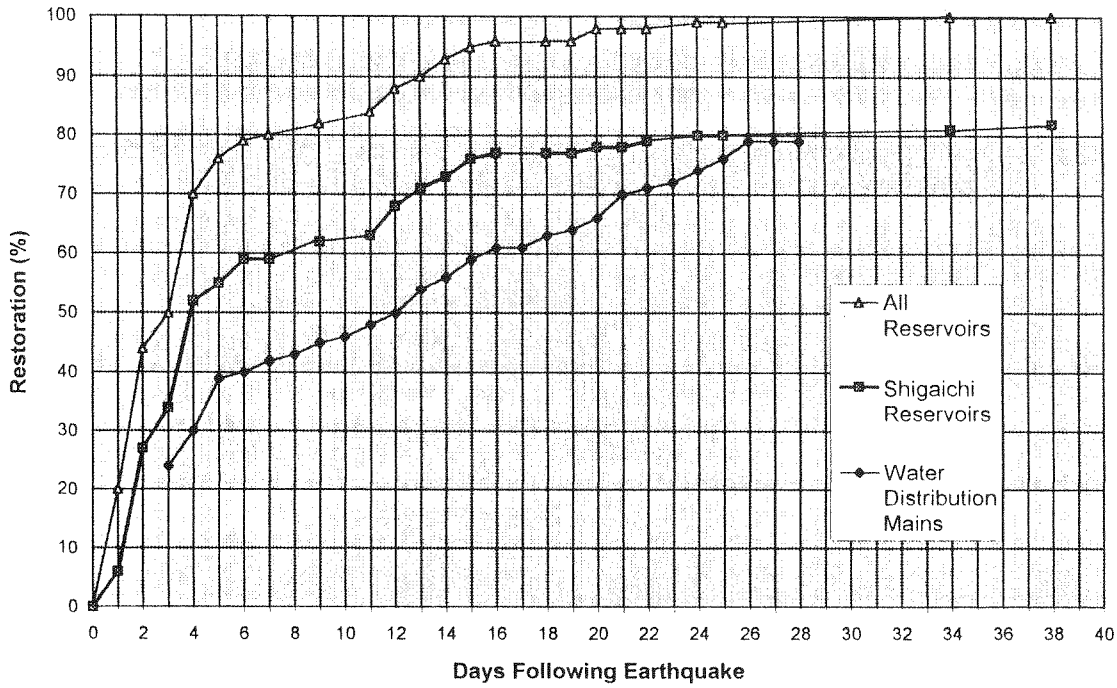


Figure 8-24 Restoration of Distribution Reservoirs and Water Mains

behind a retaining wall subsided when the retaining wall moved outward, resulting in pipeline joints separating on three treated water lines, each 1.2 m diameter reinforced concrete (see Figure 8-26). The lines were 1) Uegahara potable water, 2) Uegahara industrial water, and 3) Hanshin potable pipelines. The Hanshin line was operating as of February 11.

Some subsidence occurred under the sludge thickener building. The floor settled differentially. There was subsidence around the pile supported foundation of sludge hoppers (see Figure 8-27). Unanchored electrical equipment toppled in the sludge thickener building. Apparently, the building and adjacent sludge hoppers were pile supported, so the cross section of the slope/retaining/fill is unclear. This same subsidence also probably led to the following damage:

- Muddy water and increased water volume in water passages (pipe galleries?)
- Clarifiers - damage to expansion joints; water leakage
- Process Tanks - some leakage
- Sludge thickening equipment - extensive damage to piping and equipment
- High Rate Filter Piping - bent and disconnected
- Other - damage to pipe, mechanical, and electrical equipment.

Steel baffles in the clarifiers were damaged from impulsive hydraulic forces.

Hanshin Water Authority Kabutoyama Water Purification Plant

The Hanshin Water Authority Water Purification Plant was not damaged and was operating at 3000 m^3/hr as of February 12. There was a major landslide in back (NE) of the treatment plant (see Figure 8-28), undercutting the wastewater treatment building which was pile supported, and destroying a tennis court and a sludge drying bed. The slide killed 36 people in a housing development below, and dammed the Nigawa River. The slide is the responsibility of Hyogo Prefecture. The original slope was 18 degrees, much less than the 30 degrees where the code requires mitigation. Plastic covering was placed in the area above the slide to keep rain off, slope monitoring was in place, and borings had been started to further investigate the slide. This is the largest slide in the urban area which occurred as a result of the Kobe earthquake. Damage to buildings in the area appeared to be light, and consisted primarily of roof damage.

Motoyama Water Purification Plant

The Motoyama Water Purification Plant had damage to two segments of pipelines and minor cracking in a process tank. Pipelines to and from the backwash water tank failed as a result of slope failure as shown in Figure 8-29.

The retaining wall alongside the Simiyoshi River moved, breaking the intake box overflow line (see Figure 8-30). Water is fed to the intake box through a pipeline connected to a small diversion structure in the river bed. This facility is located upstream of the plant. There was a concern that the cast iron raw water line running from the intake box to the treatment plant may have been damaged as a result of the retaining wall movement, and should be checked before it is

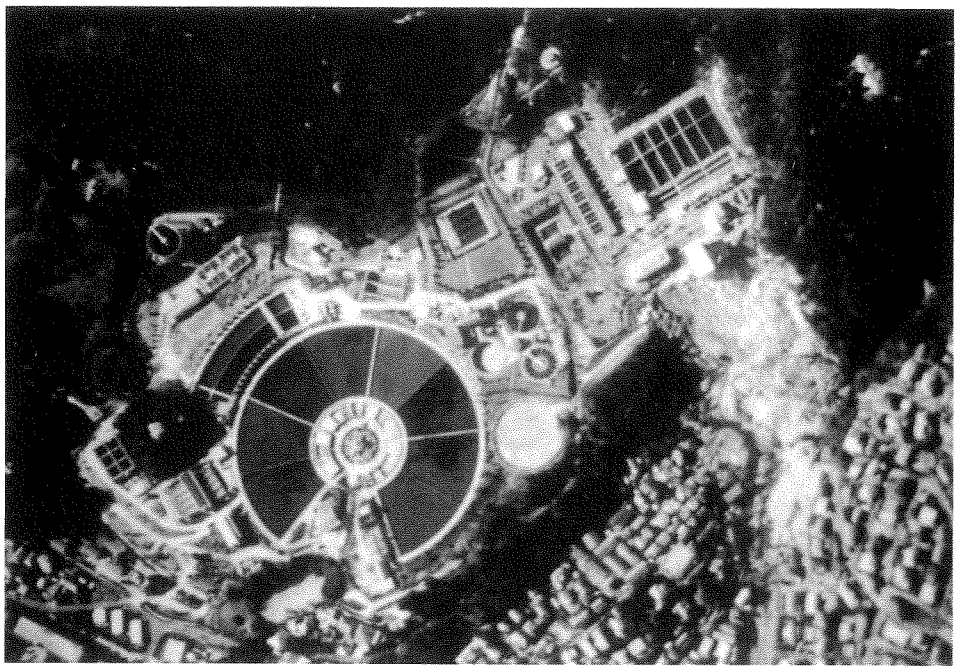


Figure 8-25 Aerial view of Kobe's Uegahara Water Purification Plant (lower left) with the Hanshin Water Purification Plant Immediately Adjacent (upper right)



Figure 8-26 Repair of One of Three 1.2 Meter Treated Water Lines Leaving the Uegahara/Hanshin Plants Site

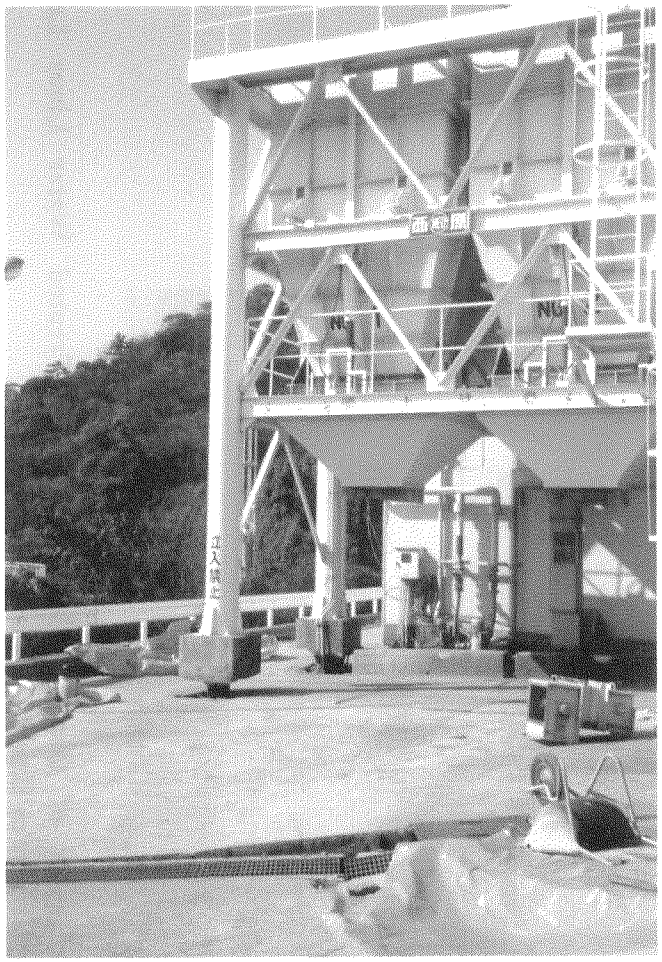


Figure 8-27 Subsidence (Approximately 30 cm) Around Pile-Supported Sludge Hoppers at Uegahara Plant



Figure 8-28 Landslide; Undermined Solids Handling Building



Figure 8-29 Broken Lines to/from Backwash Tank at the Motoyama Water Purification Plant



Figure 8-30 The Retaining Wall (on the left) Cracked, Damaging the Overflow Line from the Motoyama Plant's Intake Box

put into operation. The property owners, just above the suspect raw water line are uneasy. If the water line broke, it could undermine the house foundation. Blue tarps (as can be seen in Figure 8-30) were in place to prevent further slope failure from rain.

8.2.2.3 Intake, Pump Stations, and Transmission Pipelines

The intakes in and pump stations near the Yodogawa River were not damaged. Two major lines from the Yodogawa River were broken in 10 locations. One ductile iron line had a split 30 cm long and 5 cm wide. One 100 meter section had to be replaced. It took 12 days to repair the raw water lines serving the plant. Transmission pipe materials may have included both ductile iron and/or prestressed concrete.

The tunnel transmitting water from the Sengari Reservoir to the Uegahara Treatment Plant, and the Mt. Rokko tunnels, carrying water from the Uegahara and Hanshin Kabutoyama plants west to be distributed, had damaged concrete lining.

Pumps in Karasuhara mine (spring) were destroyed and put out of service. However, this was only a minor supply. Other pump stations were undamaged. Damage to air release valves was reported.

8.2.2.4 Distribution Reservoirs (Tanks)

Of the 119 reservoirs throughout the City, there was damage to one pre-World-War-II cast-in-place partially buried concrete tank, where there was a crack on the bottom and side.

At the Egeyama Reservoir, there was leakage in the pipe connecting the reservoir and the adjoining well, and a vertical crack in the expansion joint. A 500 mm diameter transmission main to Egeyama Reservoir 10 meters long was replaced.

8.2.2.5 Distribution Pipes

Distribution pipeline damage was reported as follows:

Distribution pipes (75-300 mm)	1,800
Service Lines (<75 mm)	10,000
Total	11,800

An early survey of the 328 distribution pipe failures is shown below:

	Failures	Percent
Pipe Breaks	53	16
Pipe joint damage (ramming and pull out)	136	41
Equipment (fire hydrants, air release valves, etc.)	69	21
Other	70	22
Total	328	100%

Table 8-VIII shows Kobe Water pipeline damage data as of March 29, including the type of damage. Only 964 of the 1,800 repairs identified at that time are shown on the table. Pipe material is not identified in the table.

Table 8-VIII Kobe Water Pipeline Damage as of March 29, 1995

Diameter (mm)	Inventory (m)	Repairs	Repairs/km	Broken Pipe	Pulled Joint	Damaged Fitting
50	63,143	15	0.24	6	9	0
75	165,051	40	0.24	7	30	3
100	790,329	197	0.25	43	127	27
150	1,455,137	301	0.21	55	206	40
200	744,689	138	0.19	23	104	11
250	39,706	6	0.15	3	3	0
300	386,606	139	0.36	20	96	23
350	18,195	5	0.27	0	4	1
400	79,700	30	0.38	4	17	9
450	3,082	0	0	0	0	0
500	88,450	24	0.27	2	7	15
600	45,224	13	0.29	2	3	8
700	46,857	24	0.51	1	7	16
800	10,264	9	0.88	3	5	1
900	26,131	21	0.80	1	6	14
1,000	498	2	4.02	0	0	2
Total	**3,963,062**	**964**	**0.24**	**170**	**624**	**170**

Approximately 80 percent of the pipe in the system was ductile iron. Ductile iron pipe has performed well in previous earthquakes. The three predominant types of service line failures were 1) house collapse, 2) joint separation, and 3) failure where the line passed below the concrete stormwater gutter. Service line repairs were being accomplished at a rate of two per day with a crew of five to six workers.

It is estimated that indoor and outdoor supply pipe leakage sites will number 50,000, out of a total city water supply region of 650,000 homes.

There was significant pipeline damage on Kobe's Port Island where Tyton-type and/or mechanical joints were deployed. In contrast, there was very little water pipeline damage on Rokko Island where the great majority of mains were ductile iron pipe with S-type joints. Only one failure of the S-type joint was reported.

As the distribution system repair was nearing completion, water demand was more than 30 percent greater than pre-earthquake use. There was concern that there were still many leaks that had not been identified.

There were two major issues identified that had delayed system restoration:

- No water pressure was available to check the repairs as the tunnels were drained.
- Access was limited by collapsed buildings and traffic congestion.

There were adequate repair materials.

Pipelines hung on the Kobe, Rokko, Mikage, and Fukae bridges were damaged, and in some cases disrupted service to these islands (see Figure 8-31). Figure 8-32 shows the repair of a 700-mm welded steel pipeline which ruptured at a weld on the north side of Port Island in an area affected by liquefaction induced lateral spread. This line carried the entire potable water supply for Port Island.

Figure 8-33 shows ground cracking from lateral spread in fill area along a waterway. As can be seen in the figure, immediately behind the crack, a pipeline emerges out of the ground to be supported on the bridge. The 300 mm pipe joint can be seen in the bottom of the crack (Figure 8-34) where the bell was separated from the spigot.

Figure 8-35 shows a pipe repair on approach to the bridge to the island where the wastewater plant is located. The pipe failure was probably caused by settlement and slight lateral movement (see concrete wall on right in the figure). The Kyoto Water Department truck and crew making the repair shown in Figure 8-35 is shown in Figure 8-36. The crew indicated that they were directed to make the repairs as quickly as possible, even though they might be temporary. They said the materials they used in Kyoto (and had with them) were completely different than those used by Kobe Water.



Figure 8-31 Pipe Hanging from Bridge to Rokko Island (Just to the Right of Crane Cab)

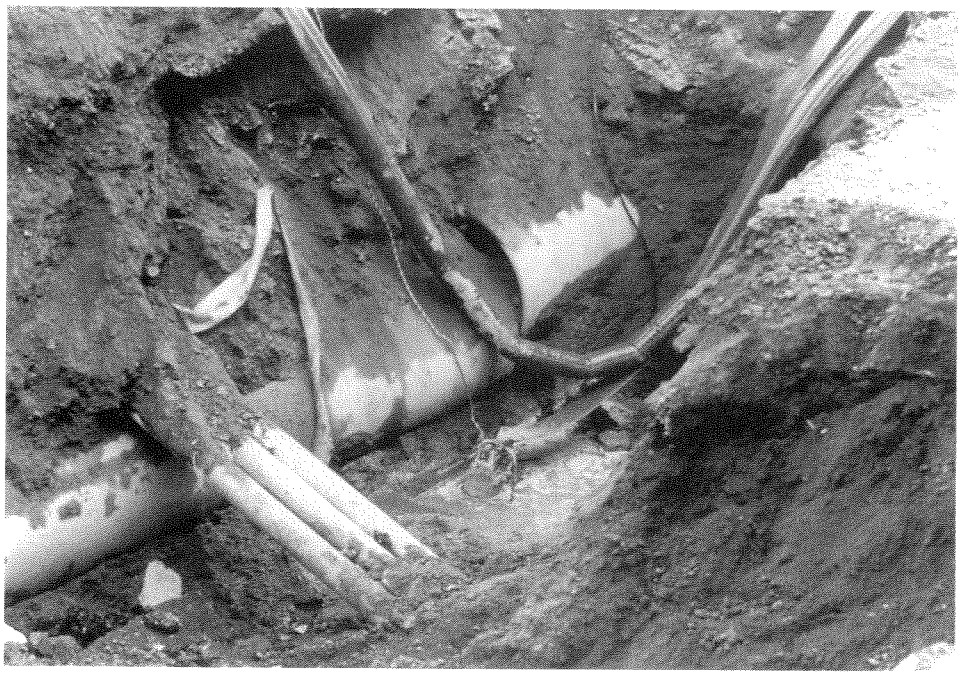


Figure 8-32 Repair of 700 mm Welded Steel Pipeline



Figure 8-33 Ground Cracking from Lateral Spread in Fill Area Along Waterway



Figure 8-34 Pipe Joint in Bottom of Crack, where the Bell (to the right) was Separated from the Spigot (under foot)



Figure 8-35 Pipe Repair on Approach to Bridge to Island where Wastewater Plant is Located



Figure 8-36 Kyoto Water Department Crew Making Repairs to Pipe Shown in Figure 8-35

Figure 8-37 shows differential settlement of a building located on mid-Rokko Island. Most modern buildings on the island were pile supported and were not damaged. Differential settlement required repair of utility connections as shown in Figure 8-38. Figure 8-39 shows utility connections that were left hanging due to differential settlement of approximately 1 meter along the front of the pile supported ferry terminal on Port Island which connects Kobe to Kansai Airport.

8.2.2.6 Water Department Buildings

The Water Department Main Office, including administration and engineering, was located on the sixth floor of the Old City Hall Building (City Hall Annex). The sixth floor of the eight story concrete frame building pancaked as shown in Figure 8-40. Because of the early morning hour, only one employee was inside, and was killed. Distribution system maps, facility drawings, etc. were not available during the initial restoration phase. Later in the restoration, some records were being pulled out of the collapsed floor. There are no definite plans for restoration at present. During this investigator's post-earthquake visit to Kobe, a television news reporter was shown on evening television squeezing his way between the fifth and seventh floor of the building.

The Water Department maintained distribution and maintenance buildings in five areas throughout the City. The upper three floors of the eight story Water Department Eastern Center partially collapsed. The Western Center partially burned. The unburned section was being used. The combined damage of these three facilities made emergency response and restoration very difficult. The Central, North, and Tarumi Centers were not damaged.

8.2.2.7 Monitoring and Control System

The control system designed to isolate 21 reservoirs for drinking worked in 18 of the 21 cases, and water was saved for drinking. Two of the failures were electrical or mechanical related, and one, hydraulic related. Three repeater stations and telemetry systems were undamaged.

8.3 Description of Damage to the Wastewater System

The Kobe sewer system serves 1.46 million people. The collection area of 157 km^2 is 97.4 percent sewered.

Kobe has eight wastewater treatment plants, three of which were damaged in the earthquake, as shown in Table 8-IX. The sludge is barged to Rokko Island where it is incinerated. The remaining 15 tons of ash are land filled.

In the future, Kobe officials are considering constructing a transmission line between the Higashinada and Tarumi wastewater treatment plants to provide operational flexibility.

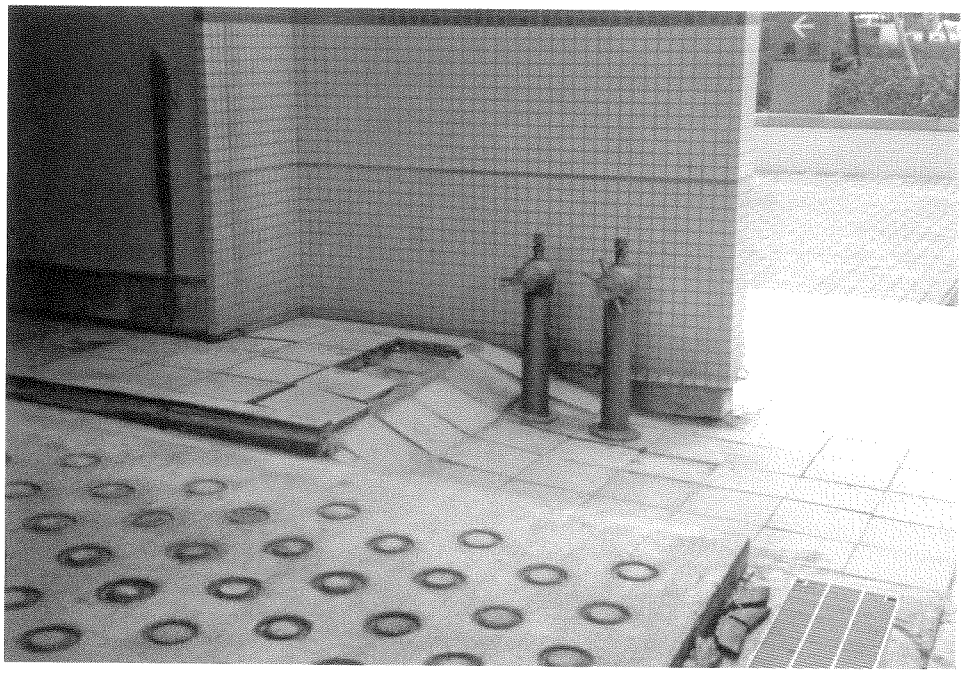


Figure 8-37 Differential Settlement of Building on mid-Rokko Island



Figure 8-38 Utility Connections Required Repair Due to Differential Settlement

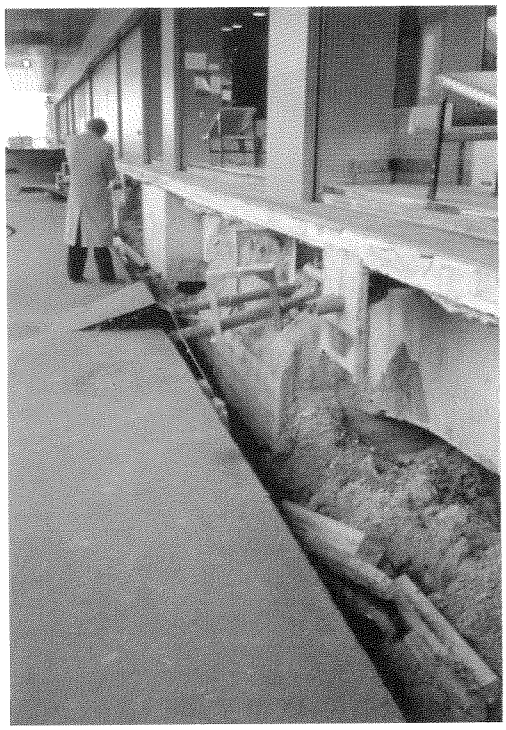


Figure 8-39 Utility Connections are Hanging Due to Differential Settlement Along Front of Pile Supported Ferry Terminal on Port Island



Figure 8-40 Pancaked Sixth Floor of City Hall Annex

Table 8-IX Kobe Wastewater Treatment Plants

Wastewater Treatment Plant	Capacity (1000 m^3/day)	Location	Post-Earthquake Status
Higashinada	225.0	Shoreline	Heavily damaged; detailed damage description in text.
Seibu	161.5	Shoreline	Secondary plant with two process trains. Concrete yard piping was damaged; pump station settled and flooded. Repaired within one week.
Tarumi	133.9	Shoreline	No damage to treatment function.
Chubu	77.9	Shoreline	Plant suffered cracks in the sedimentation tank and the dislodged chain drive. Operating within one day.
Tamatsu	75.0	1 km inland	No damage to treatment function.
Suzurandi	43.8	10 km inland	No damage to treatment function.
Port Island	20.3	Port Island	No damage to treatment function.
Myodani	12.0	10 km inland	No damage to treatment function.
Total	749.4		
Tobu Sludge Center	150 tons/day	Rokko Island	Damaged

There are 23 pump stations; 20 were damaged/inoperable from power loss, building structure damage, and 1.5 m caisson damage. Most were operable when power was restored.

The collection system pipe is 70% concrete, 20% PVC, and 10% VCP. Fiber Reinforced Plastic is used for large diameter pipe and PVC is used for smaller diameter pipe in liquefaction-susceptible areas. The length of sewers by sewage treatment plant service area is shown in Table 8-X.

Table 8-X Kobe Wastewater System Pipe

Treatment Plant Area	Sanitary Sewer Length (km)	Storm Sewer Length (km)
Chubu + Seibu	790	109
Higashinada	719	76
Tarumi	619	108
Tamatsu	570	103
Inland Areas	406	49
Suzurandi	186	33
Port Island	28	4
Total	**3318**	**482**

While we were told that some of the sewers were combined sewers, it is unclear whether the storm sewers shown in Table 8-X drain into the respective treatment plant.

Three pipelines in the Daikai area were relocated where the subway station collapsed. Otherwise, only one sewer collapsed. Flows in manholes were being checked, and 60 km of sewers were being TVed with 30 to 40 crews in operation. There was only one public health incident where sewerage was backed up. Figure 8-41 shows a manhole that floated due to liquefaction near the Higashinada Plant. Figure 8-42 shows a sewer that was buoyed as a result of liquefaction on Port Island. The estimated cost of sewer repair is 12 billion yen ($120 million).

An estimated 400 people were assisting in the restoration effort and 50 people were involved in planning and design restoration efforts.

Higashinada Wastewater Treatment Plant

The Higashinada Wastewater Treatment Plant is the City of Kobe's largest plant, providing one-third of the city's treatment capacity. An aerial view is shown in Figure 8-43. It is an activated sludge plant. It is located on Uozaki Hama Machi (Island), just east of the bridge to Rokko Island as shown in Figure 8-44.

The plant has an average daily flow of 162,000 m^3/day of which 23% is industrial. Some sewage is from a combined sanitary/storm collection system. The plant capacity is 225,000 m^3/day, and is being expanded to 350,000 m^3/day. The oldest portion of the plant was constructed in 1962, shortly after placement of the fill for the island was completed.

The facility was heavily damaged when the seawall wall along the north side of the plant adjacent to the channel moved as much as 3 m towards the water as a result of liquefaction (Figures 8-45 and 8-46). As a result of the movement, the entire site settled an average of one meter. The seawall on the north moved up to 1 m south. Liquefaction-induced lateral spread and settlement were most severe within a distance of 100 m south of the seawall along the southern margin of the channel. Horizontal displacements of 3 m and settlements as large as 2 m were observed within the plant site. Figure 8-47 shows the plant layout and notes damage locations.

Lateral displacement and settlement ruptured the inverted siphon at the plant through which raw sewage was conveyed to the plant on the other side of the channel for treatment. Because of the loss of the siphon, sewage was being dumped directly into the channel.

Figure 8-47 presents a soil profile for the borings located on Figure 8-48. The soils consist of about 6 to 8 m of artificial fill, primarily granitic sands and gravels, underlain by approximately 3 to 5 m of alluvial sand. The fill and alluvial sands are loose, as evidenced by the low uncorrected blow counts between 5 and 15. The sands are underlain by soft to medium soft alluvial clay approximately 8 m thick, which overlie deep deposits of dense granular soils and stiff clays. The water table is about 2 m below ground surface.

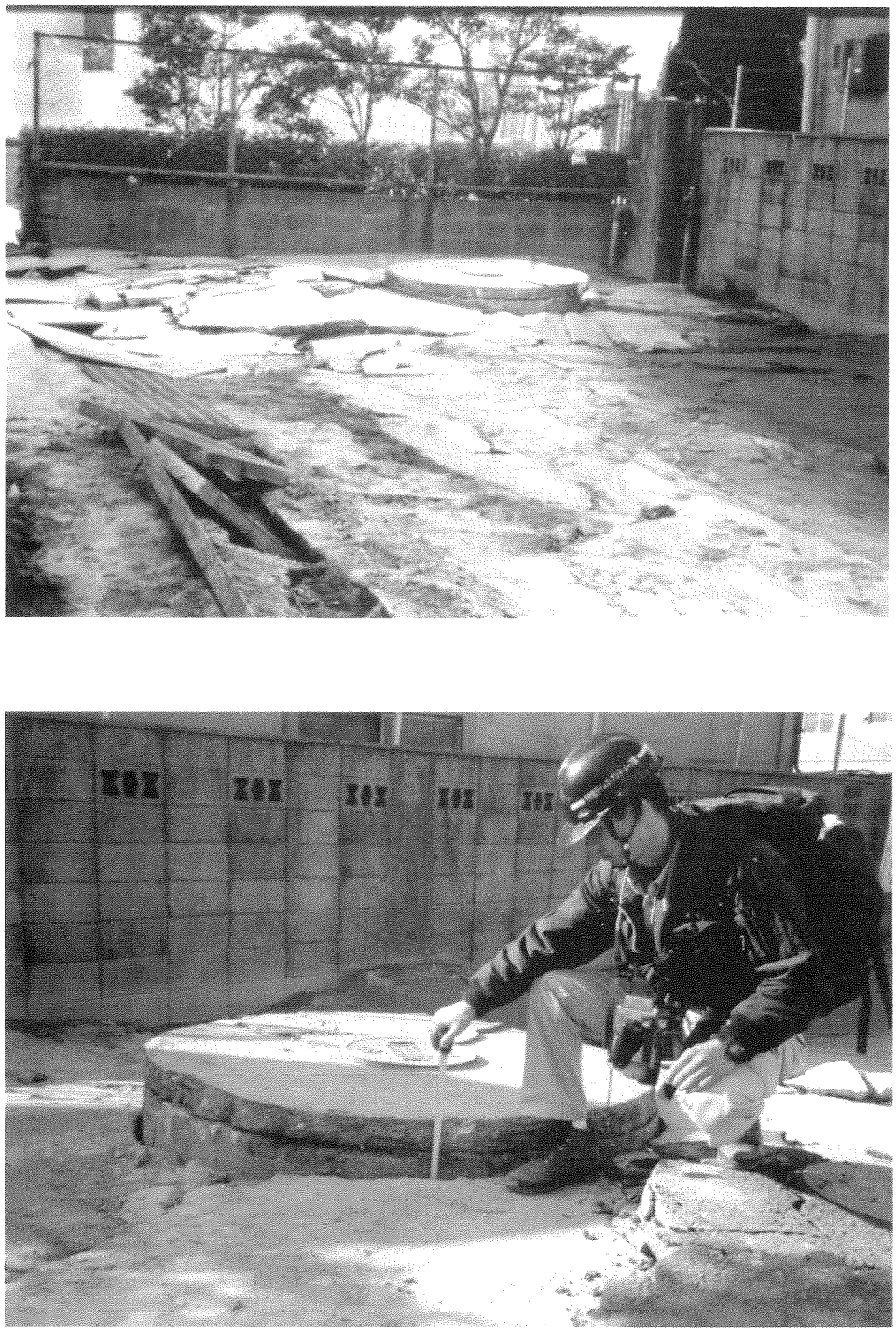


Figure 8-41 Manhole Floated as a Result of Liquefaction Near the Wastewater Treatment Plant



Figure 8-42 500 mm Diameter Sewer Floated Upward on Port Island, Resulting in the Upheaval of Ground



Figure 8-43 Aerial View of Higashinada Wastewater Treatment Plant

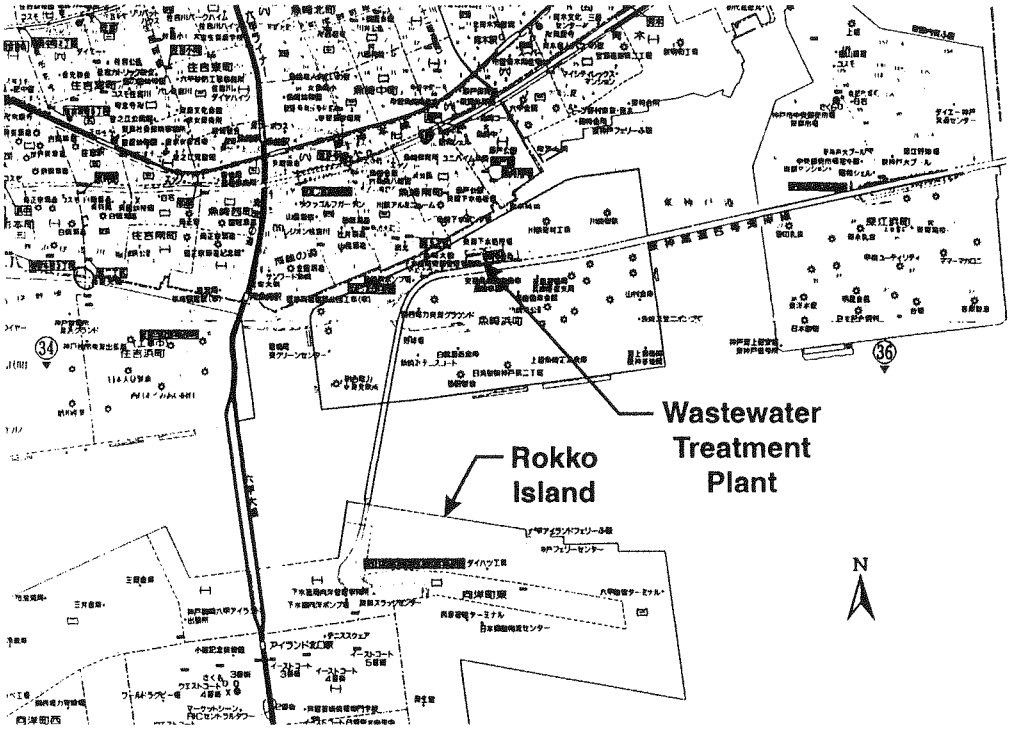


Figure 8-44 Location Map for Higashinada Wastewater Plant

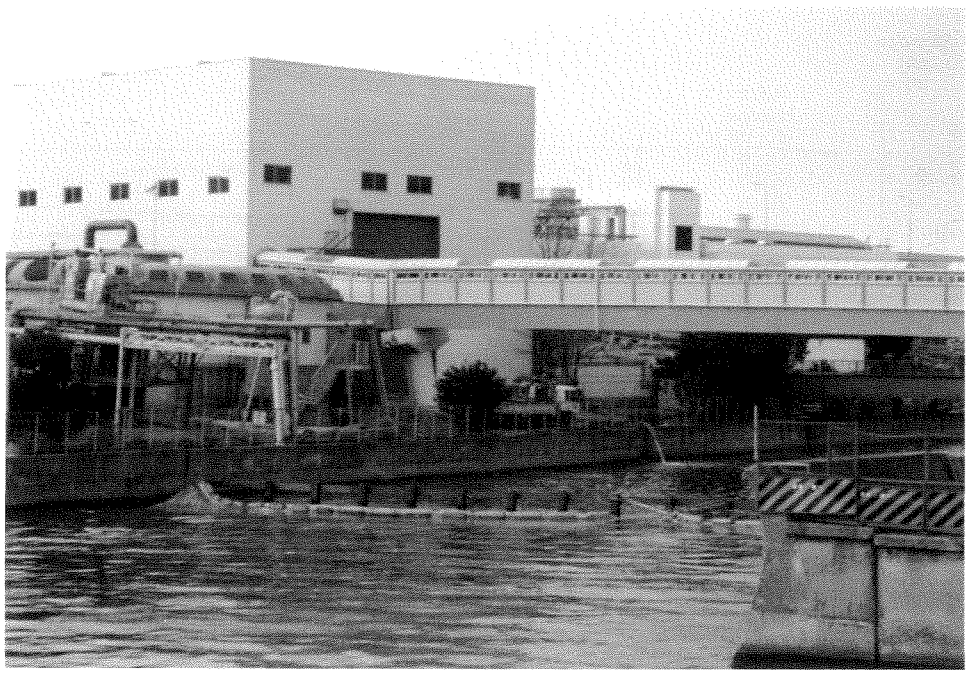


Figure 8-45 Retaining Wall Along the Inlet Between the Island and Mainland Moved Towards the Water (north) 2 to 3 Meters

Lateral deformation caused severe damage to underground structures and facilities founded on spread footings. The effluent channel separated in four places (Figure 8-49). The pipe rack distorted from foundation settlement (Figure 8-50).

Primary and secondary clarifiers, and aeration basins were pile supported. The primary clarifiers were 8 m deep so the pile length subjected to liquefied sand was relatively small. Secondary clarifiers and aeration basins were only 4 m deep which subjected a longer pipe length to liquefaction and lateral movement resulting in some damage. Aeration tank joint separation is shown in Figures 8-51 and 8-52. Sludge scrapper chains came off sprockets, as shown in Figure 8-53.

Concrete piles supporting digester tanks closest to the channel cracked at their tops. Sludge digester connecting piping broke (Figures 8-54 and 8-55).

Differential settlement of approximately 600 mm relative to the pile supported filter building occurred as shown in Figure 8-56. The control building and sludge thickener room moved north 60 cm walls (Figure 8-57). The return activated the sludge pump room and the backup blower room flooded.

Equipment and piping on mat foundations near the south edge of the channel was damaged due to ground movement (Figures 8-58 and 8-59).

It is expected to take two to three years to repair the plant at a cost of 25 billion yen ($250 million). This estimate seems low for the extensive damage observed.

As of February 10, the Higashinada Wastewater Treatment Plant was providing primary treatment with chlorination. This was accomplished by an innovative use of the channel between the mainland and island. The channel was blocked off at either end with a row of piles and covered with a filter membrane making a temporary sedimentation basin. Temporary baffles were placed in the sedimentation basin to keep solids away from the membrane filter, and to keep sewage from short circuiting to the filter membranes on each end. As raw sewage enters the pump station, chlorine and a chemical coagulant are added. The sewage enters into the temporary sedimentation basin. The sewage solids settle to the bottom of the basin, and the liquid passes through the filter membrane. The solids are dredged from the bottom and pumped to a barge located outside the sedimentation basin where they are thickened. Solids are then dewatered and taken to a landfill.

8.4 Lessons from Damage to Water and Wastewater Systems

There do not appear to be any significant technical surprises from this earthquake applicable to the U.S., but there are a number of reoccurrences of many situations that should help to clarify earthquake planning and design.

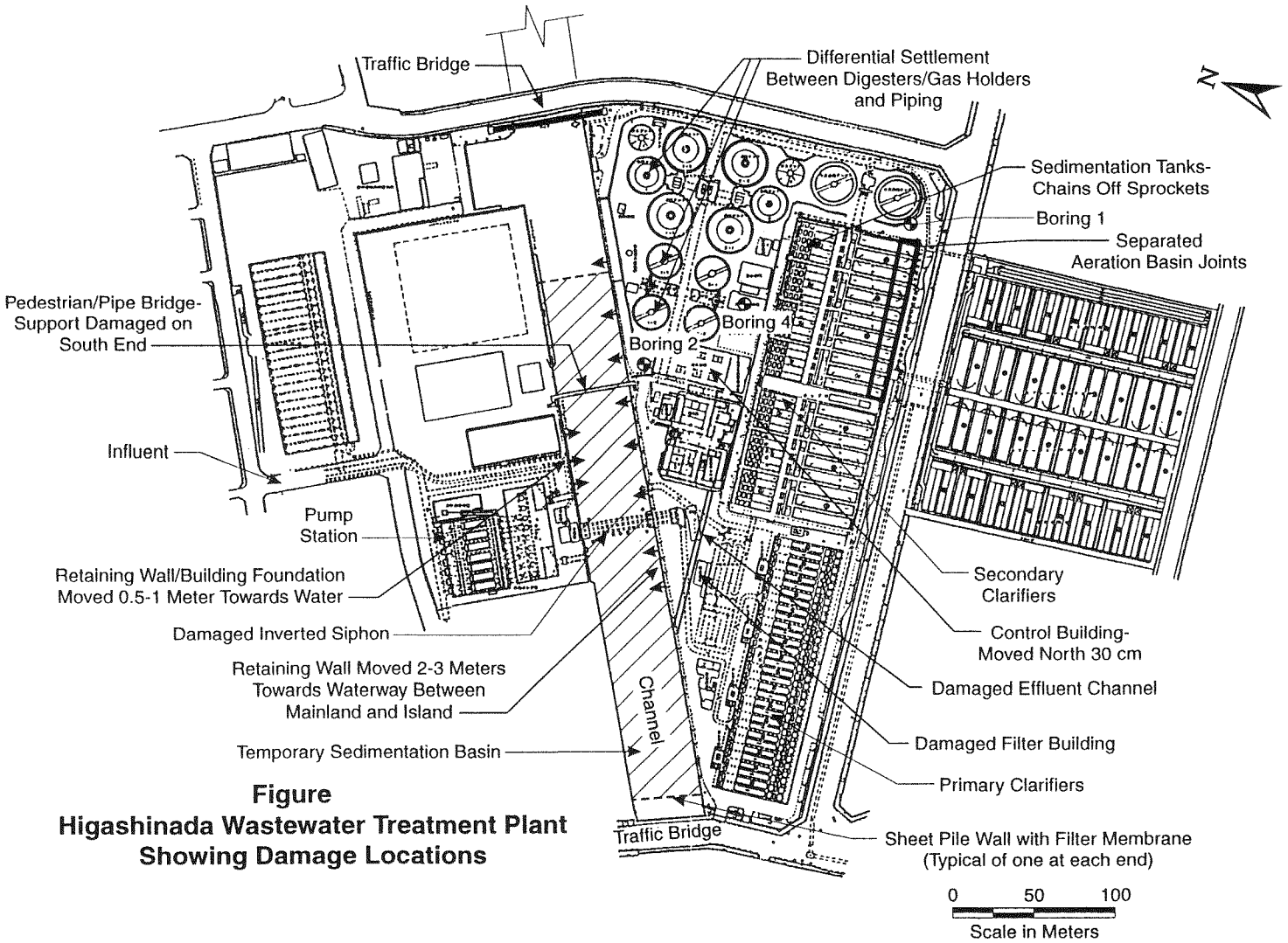


Figure
Higashinada Wastewater Treatment Plant
Showing Damage Locations

Figure 8-48 Higashinada Wastewater Treatment Plant Site Plan Showing Damage Locations



Figure 8-49 Effluent Channel, Approximately 2 Meters Square, Offset Nearly 1 Meter From Lateral Spreading

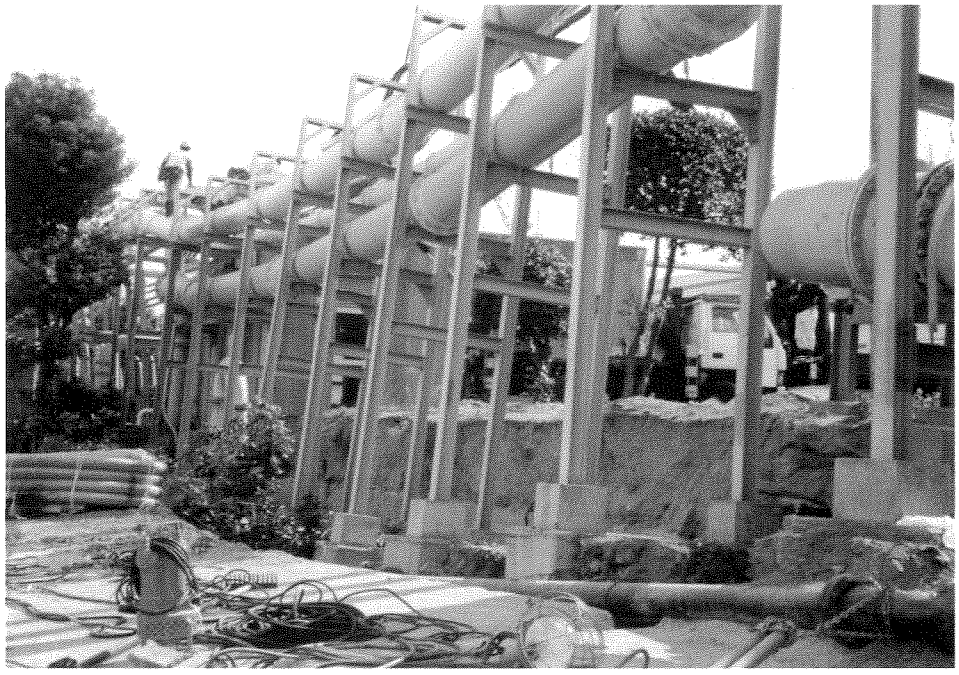


Figure 8-50 Pipe Rack Foundations Adjacent to Channel Settled Approximately 1 Meter Distorting Piping

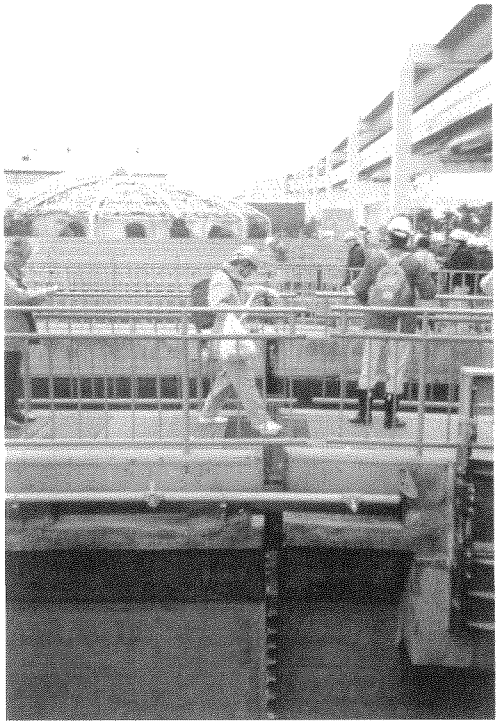


Figure 8-51 Aeration Tanks Construction Joint Separated Down the Entire Bank of Tankage as a Result of Settlement

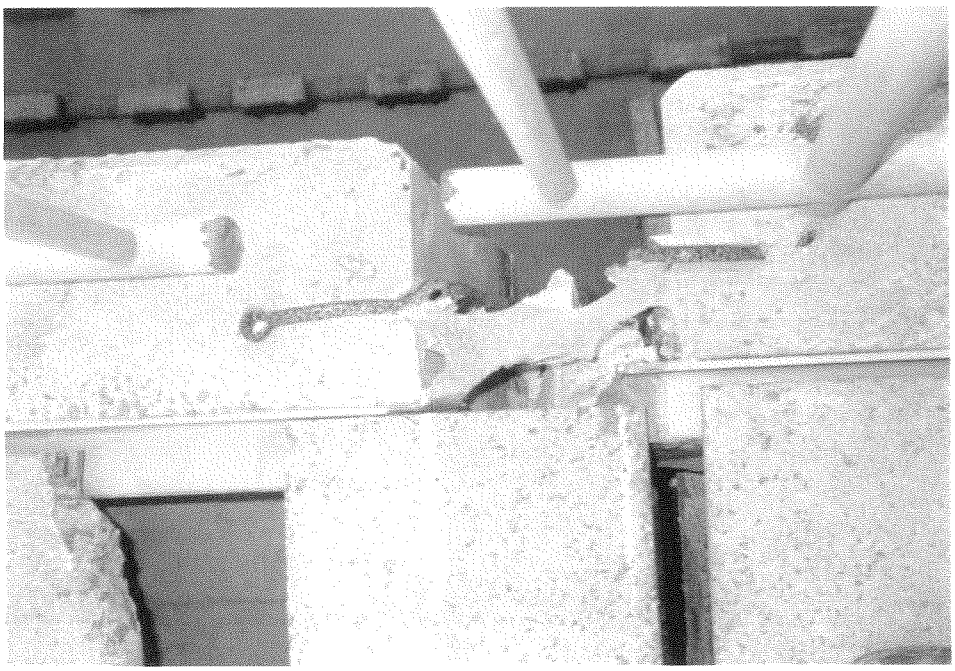


Figure 8-52 Close up of Torn Dumbbell Rubber Water Stop in Aeration Tank

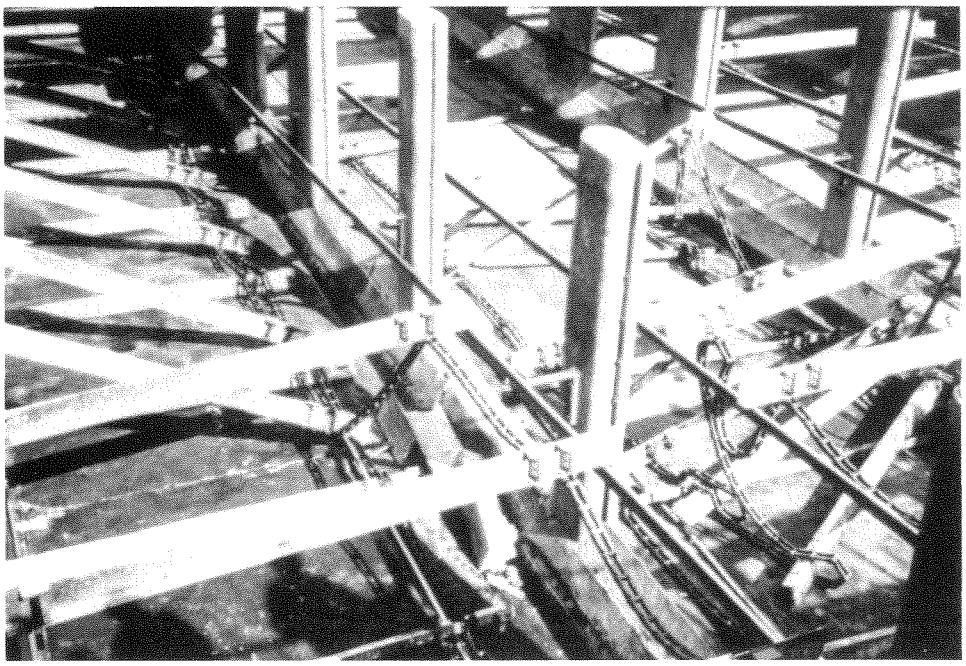


Figure 8-53 Sludge Scraper Chain Came off Sprockets in Sedimentation Tanks

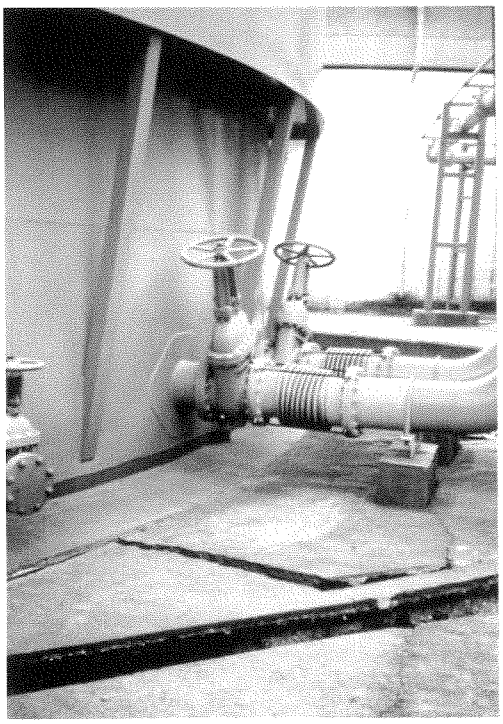


Figure 8-54 Differential Movement from Settlement Between Pile Supported Tanks and Non-pile Supported Pipe Caused Flexible Joint to Distort



Figure 8-55 Differential Settlement Between Pipe and Non-pile Supported Structures Damaged Piping Throughout the Plant



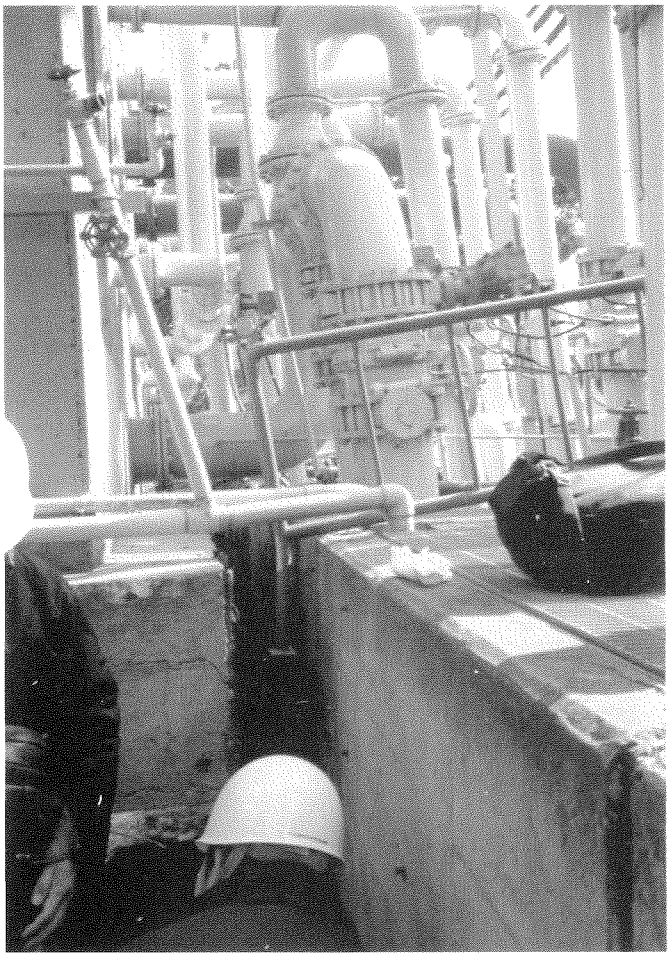


Figure 8-56 (Top) Filter Building Support Pipes Failed Allowing the Building to Move and Settle Differentially; (Bottom) Piping Distorted as a Result of the Building Movement

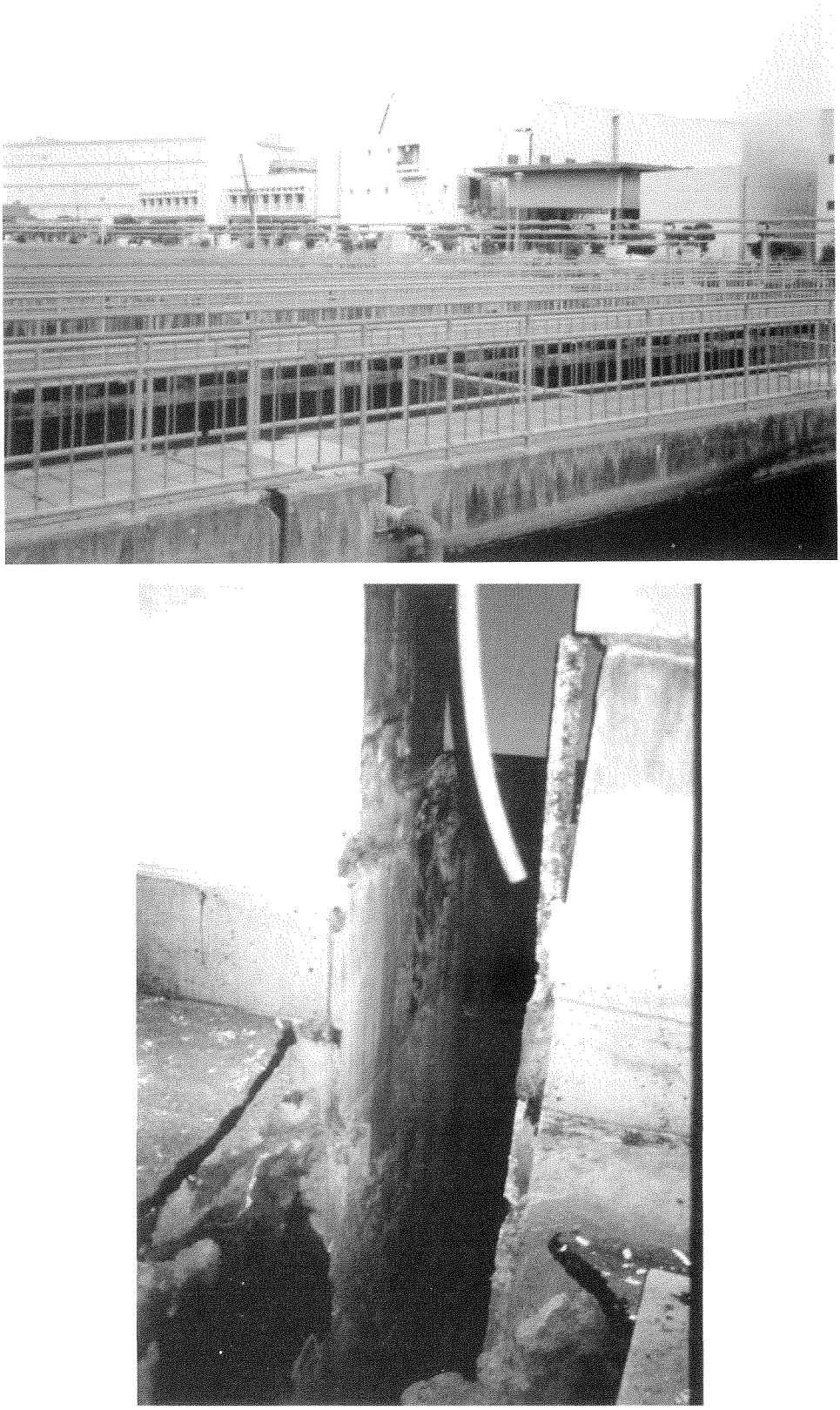


Figure 8-57 (Top) Control Building (upper right) Pile Supported Building Moved Towards Inlet Approximately 30 cm, Moving Away from Adjacent Building that had a Basement; (Bottom) Gap Between Buildings

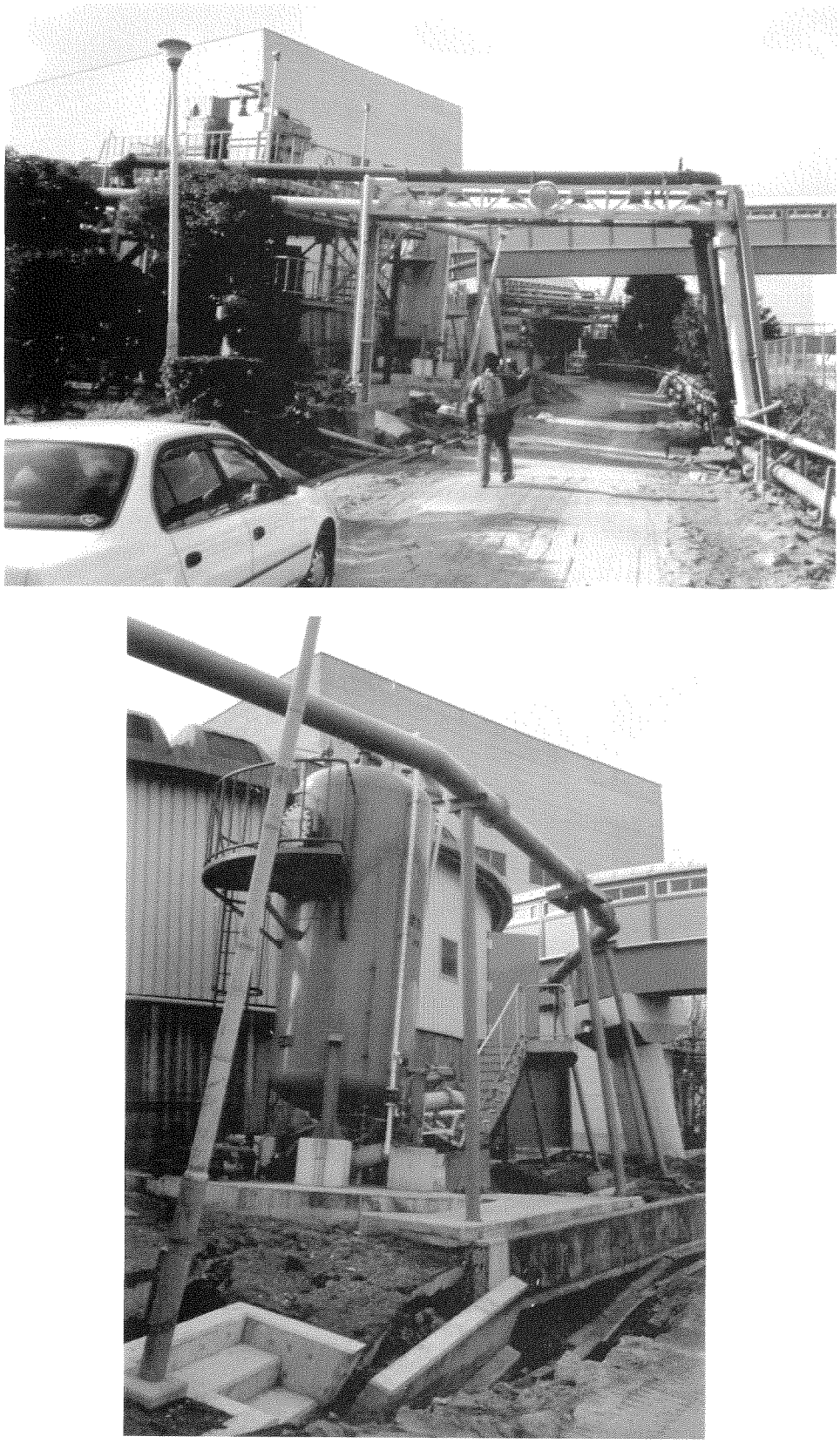


Figure 8-58 Damage to Equipment on Mat Foundations; (Top) Piping Distorted as a Result of Movement; (Bottom) Piping and Equipment Distorted as a Result of Subsidence at Foundation

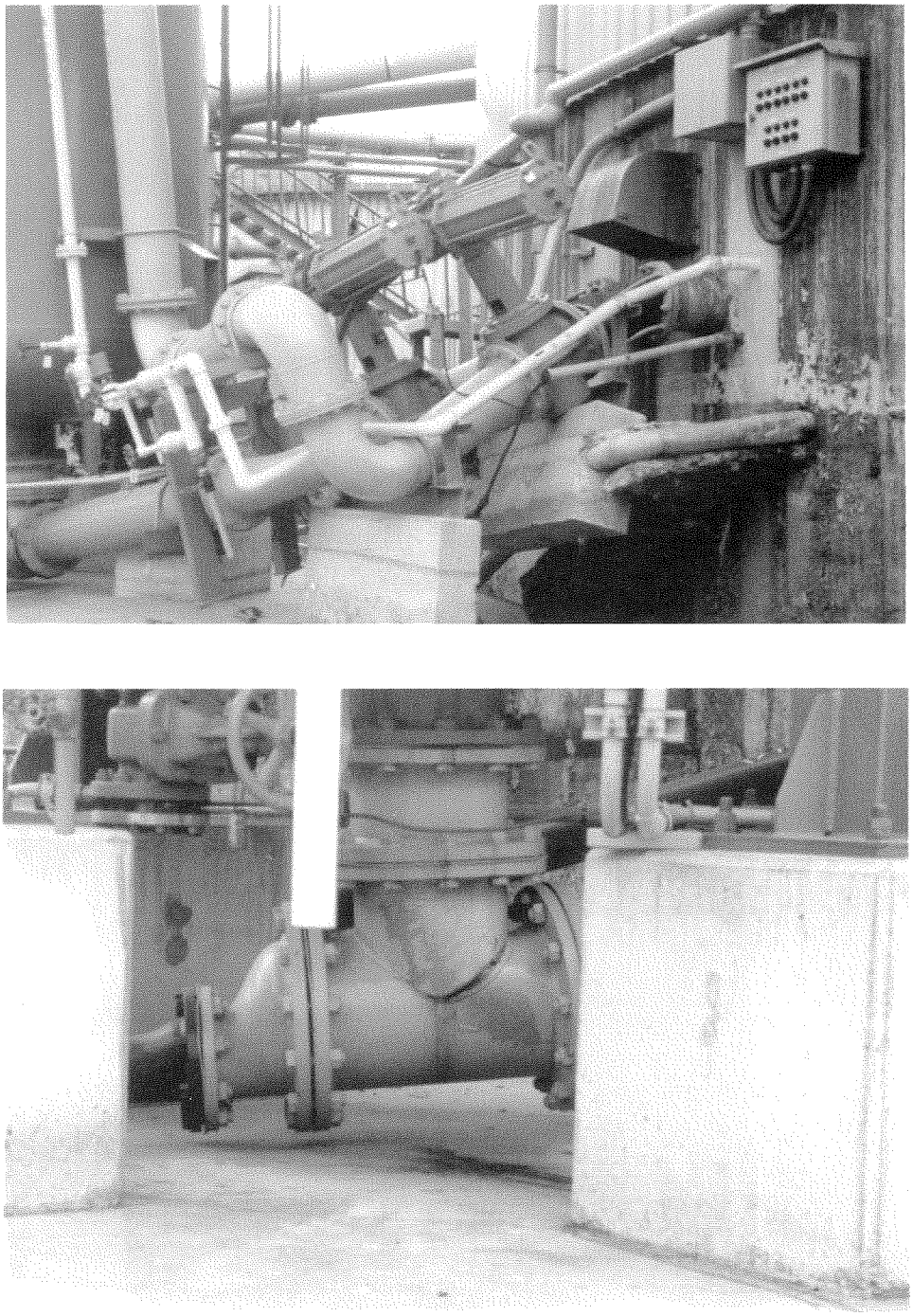


Figure 8-58 Damage to Equipment on Mat Foundations (cont'd); (Top) Piping and Equipment Distorted as a Result of Subsidence at Foundation; (Bottom) Welded Steel Tee, Approximately 300 mm in Diameter, Cracked at Weld Between the Leg and Run



Figure 8-59 Welded Steel Pipe; Approximately 200 mm in Diameter Folded When the Foot/Pipe Bridge Support was Distorted from Lateral Spread

8.4.1 Overwhelming Conditions

We need to always be aware of the potential magnitude of earthquake consequences. This was the largest earthquake to directly impact an urban area in a country with facilities comparable to the United States. The results were overwhelming in terms of loss of life and property damage, as well as poor performance of utility systems.

From an emergency response perspective, there is always discussion about what might occur following a large earthquake located in a densely populated area. It is beyond comprehension for most people outside California that such an event will happen, and therefore they do not truly consider the consequences. One of the biggest issues in the Kobe event was transportation; being able to get to where one needed to go. Every major transportation route had failed, and surface roads were blocked by fallen buildings. The resulting congestion made walking the fastest form of transportation. The result was that emergency response slowed to a crawl.

The same situation was true for response of utility personnel. For moderate earthquakes, there is an emergency response plan to enable effective data acquisition and response. Utility decision makers need to be thinking in terms of consequences similar in magnitude to the Kobe event. For example, what happens when there are no records, that is, all utility buildings are destroyed. What happens if the plan is to dispatch crews to isolate critical pipelines to save water or shut off natural gas, and the fastest way to get there is to walk?

8.4.2 Fire Following Earthquake

The issue of fire following earthquakes needs to be refocused. While there was no fire storm, there were 380 ignitions, and in many cases no water to suppress them. Water purveyors and fire departments should relook at the vulnerability of water supplies. Recent earthquakes have shown that there is a low probability of maintaining a water system following an earthquake. Consideration should be given to identifying and developing alternate supplies.

Similarly, the use of monitoring and control systems should be considered and/or reconsidered to enable timely control of a water system following an earthquake to increase the probability of delivering water to suppress fires.

Water purveyors and fire departments should use permanent ground deformation mapping to identify areas where pipelines will likely fail so that plans can be made to isolate damaged areas and/or use alternative water supplies.

8.4.3 Geotechnical Issues

Many lifeline system owners are lulled into an earthquake program that includes nonstructural upgrades, and minor building strengthening. Geotechnical hazards are considered, and the potentially dramatic consequences of failures are identified, but dropped when mitigation costs are developed.

In Kobe, geotechnical failures governed the poor performance of the water system. Landslides, consolidation, and liquefaction/lateral spread stopped the flow of water from the source, damaged two major water, and one smaller water treatment plant, and tore the distribution system apart. In general, the structural aspects of the "steel" transmission pipelines matched current designs used in the U.S. The treatment plant structures performed reasonably well except that they were on soils that failed. An aggressive pipeline replacement program apparently only marginally helped mitigate geotechnical failure-related damage to the pipeline distribution system.

8.4.4 Design

In general, water treatment plants and service reservoirs performed well. The Japanese design approaches for these facilities should be studied. As discussed above, their tank designs are somewhat different than those used in the U.S., and apparently had no damage when subjected to high peak ground accelerations.

Pipelines were heavily damaged. Preliminary information on the performance of the S joint pipe is that it appears that it had no or few failures. If it is confirmed that it performed well in areas of significant permanent ground deformation, they should be introduced in the U.S. If it did not perform well, researchers should find out why, and improve U.S. pipe designs based on those findings.

An estimated 65 percent of the pipeline failures were pulled joints. As 80 percent of the pipe inventory in Kobe was ductile iron pipe with Tyton or mechanical joints without restraint, the U.S. should not become complacent with use of non-restrained joints in areas expecting significant permanent ground deformation.

8.4.5 Recovery

The three Kobe Water buildings storing records were destroyed. The probability of this occurring is very low. In the U.S., resources should be distributed so that loss of any one facility will not substantially impact the ability to respond to an earthquake.

8.5 Summary

The earthquake left one million households without water following the event, with only 70 percent restoration in three weeks. Water for fire suppression was substantially exhausted after six hours.

The two large diameter transmission lines carrying water from the Yodogawa River to the Uegahara and Hanshin Kabutoyama water purification plants failed in ten locations. This source constitutes nearly three-quarters of Kobe's supply. The Uegahara and Hanshin plants are Kobe's largest. In addition to supplies being disrupted, soil failures at the plants resulted in failure of the major treated water lines, as well as moderate damage at the plants themselves.

The tunnels carrying water from the plants west to Kobe remained intact.

Kobe Water had an aggressive earthquake design program for at least some service reservoirs. There were no tank failures reported for 239 tanks at 119 sites. There was some connecting piping failure at one tank.

Nearly 90 percent of Kobe's water distribution system was made up of either welded steel or ductile iron pipe, both thought to be resistant to earthquakes. This unusually high percentage of pipe resulted from an aggressive pipeline replacement program initiated in the mid-1960's. Even with this in place, an estimated 2,000 pipeline failures occurred in distribution piping, on the order of two times as many as in the Northridge earthquake. It was speculated that much of this damage was associated with joint separation due to liquefaction/lateral spread. Details are not yet available.

Kobe had implemented a monitoring and control system designed to isolate reservoirs following an earthquake to be used for drinking. The system worked as designed, however, an analysis needs to be performed to determine if it would have been better to focus mitigation efforts on water for fire suppression. In other words, was the water saved for drinking critical in meeting that demand, or was drinking water available from other sources? No system focused on the post-earthquake performance of the water system to provide water for fire suppression, and no water was available to put out many of the 380 ignitions.

The Higashinada Wastewater Treatment Plant provides one-third of Kobe's treatment capacity. Liquefaction/lateral spreading failures resulting in movement of a retaining wall 2 to 3 meters towards a waterway caused the entire site to drop an average of one meter. The results were devastating. A two-meter square effluent channel separated in four places. The control and filter buildings moved, and equipment and piping settled as the soil moved away from under them. More attention must be paid to geotechnical failures.

The lifeline earthquake community in the U.S. should learn from both the successes and failures observed in Kobe. Successes include the monitoring and control system, performance of water treatment plants (except geotechnical) and tankage, and possibly seismic joint pipe. Failures include lack of adequate water supply for fire suppression (including alternate supplies), and inadequate focus on geotechnical failures.

8.6 Acknowledgments

Mr. Ballantyne would like to thank Professor Takada at Kobe University and Mr. Matsushita at the Kobe Water Department for providing information on the Kobe water system both before the earthquake (October, 1993), and following the earthquake. Input and review is also gratefully acknowledged from Professor Tom O'Rourke, Cornell University, and Messrs. John Eidinger and LeVal Lund who provided information gathered on the ASCE Technical Council on Lifeline Earthquake Engineering (TCLEE) reconnaissance trip to Kobe. The assistance of Dr. Ian Austin, Mr. Fumihiro Kujihara and Mr. Ken Sasaki from Chiyoda-Dames and Moore in Tokyo in making local arrangements, providing translation, and traveling with Mr. Ballantyne in Kobe is greatly appreciated.

NATIONAL CENTER FOR EARTHQUAKE ENGINEERING RESEARCH
LIST OF TECHNICAL REPORTS

The National Center for Earthquake Engineering Research (NCEER) publishes technical reports on a variety of subjects related to earthquake engineering written by authors funded through NCEER. These reports are available from both NCEER's Publications Department and the National Technical Information Service (NTIS). Requests for reports should be directed to the Publications Department, National Center for Earthquake Engineering Research, State University of New York at Buffalo, Red Jacket Quadrangle, Buffalo, New York 14261. Reports can also be requested through NTIS, 5285 Port Royal Road, Springfield, Virginia 22161. NTIS accession numbers are shown in parenthesis, if available.

NCEER-87-0001 "First-Year Program in Research, Education and Technology Transfer," 3/5/87, (PB88-134275).

NCEER-87-0002 "Experimental Evaluation of Instantaneous Optimal Algorithms for Structural Control," by R.C. Lin, T.T. Soong and A.M. Reinhorn, 4/20/87, (PB88-134341).

NCEER-87-0003 "Experimentation Using the Earthquake Simulation Facilities at University at Buffalo," by A.M. Reinhorn and R.L. Ketter, to be published.

NCEER-87-0004 "The System Characteristics and Performance of a Shaking Table," by J.S. Hwang, K.C. Chang and G.C. Lee, 6/1/87, (PB88-134259). This report is available only through NTIS (see address given above).

NCEER-87-0005 "A Finite Element Formulation for Nonlinear Viscoplastic Material Using a Q Model," by O. Gyebi and G. Dasgupta, 11/2/87, (PB88-213764).

NCEER-87-0006 "Symbolic Manipulation Program (SMP) - Algebraic Codes for Two and Three Dimensional Finite Element Formulations," by X. Lee and G. Dasgupta, 11/9/87, (PB88-218522).

NCEER-87-0007 "Instantaneous Optimal Control Laws for Tall Buildings Under Seismic Excitations," by J.N. Yang, A. Akbarpour and P. Ghaemmaghami, 6/10/87, (PB88-134333). This report is only available through NTIS (see address given above).

NCEER-87-0008 "IDARC: Inelastic Damage Analysis of Reinforced Concrete Frame - Shear-Wall Structures," by Y.J. Park, A.M. Reinhorn and S.K. Kunnath, 7/20/87, (PB88-134325).

NCEER-87-0009 "Liquefaction Potential for New York State: A Preliminary Report on Sites in Manhattan and Buffalo," by M. Budhu, V. Vijayakumar, R.F. Giese and L. Baumgras, 8/31/87, (PB88-163704). This report is available only through NTIS (see address given above).

NCEER-87-0010 "Vertical and Torsional Vibration of Foundations in Inhomogeneous Media," by A.S. Veletsos and K.W. Dotson, 6/1/87, (PB88-134291).

NCEER-87-0011 "Seismic Probabilistic Risk Assessment and Seismic Margins Studies for Nuclear Power Plants," by Howard H.M. Hwang, 6/15/87, (PB88-134267).

NCEER-87-0012 "Parametric Studies of Frequency Response of Secondary Systems Under Ground-Acceleration Excitations," by Y. Yong and Y.K. Lin, 6/10/87, (PB88-134309).

NCEER-87-0013 "Frequency Response of Secondary Systems Under Seismic Excitation," by J.A. HoLung, J. Cai and Y.K. Lin, 7/31/87, (PB88-134317).

NCEER-87-0014 "Modelling Earthquake Ground Motions in Seismically Active Regions Using Parametric Time Series Methods," by G.W. Ellis and A.S. Cakmak, 8/25/87, (PB88-134283).

NCEER-87-0015 "Detection and Assessment of Seismic Structural Damage," by E. DiPasquale and A.S. Cakmak, 8/25/87, (PB88-163712).

NCEER-87-0016 "Pipeline Experiment at Parkfield, California," by J. Isenberg and E. Richardson, 9/15/87, (PB88-163720). This report is available only through NTIS (see address given above).

NCEER-87-0017 "Digital Simulation of Seismic Ground Motion," by M. Shinozuka, G. Deodatis and T. Harada, 8/31/87, (PB88-155197). This report is available only through NTIS (see address given above).

NCEER-87-0018 "Practical Considerations for Structural Control: System Uncertainty, System Time Delay and Truncation of Small Control Forces," J.N. Yang and A. Akbarpour, 8/10/87, (PB88-163738).

NCEER-87-0019 "Modal Analysis of Nonclassically Damped Structural Systems Using Canonical Transformation," by J.N. Yang, S. Sarkani and F.X. Long, 9/27/87, (PB88-187851).

NCEER-87-0020 "A Nonstationary Solution in Random Vibration Theory," by J.R. Red-Horse and P.D. Spanos, 11/3/87, (PB88-163746).

NCEER-87-0021 "Horizontal Impedances for Radially Inhomogeneous Viscoelastic Soil Layers," by A.S. Veletsos and K.W. Dotson, 10/15/87, (PB88-150859).

NCEER-87-0022 "Seismic Damage Assessment of Reinforced Concrete Members," by Y.S. Chung, C. Meyer and M. Shinozuka, 10/9/87, (PB88-150867). This report is available only through NTIS (see address given above).

NCEER-87-0023 "Active Structural Control in Civil Engineering," by T.T. Soong, 11/11/87, (PB88-187778).

NCEER-87-0024 "Vertical and Torsional Impedances for Radially Inhomogeneous Viscoelastic Soil Layers," by K.W. Dotson and A.S. Veletsos, 12/87, (PB88-187786).

NCEER-87-0025 "Proceedings from the Symposium on Seismic Hazards, Ground Motions, Soil-Liquefaction and Engineering Practice in Eastern North America," October 20-22, 1987, edited by K.H. Jacob, 12/87, (PB88-188115).

NCEER-87-0026 "Report on the Whittier-Narrows, California, Earthquake of October 1, 1987," by J. Pantelic and A. Reinhorn, 11/87, (PB88-187752). This report is available only through NTIS (see address given above).

NCEER-87-0027 "Design of a Modular Program for Transient Nonlinear Analysis of Large 3-D Building Structures," by S. Srivastav and J.F. Abel, 12/30/87, (PB88-187950).

NCEER-87-0028 "Second-Year Program in Research, Education and Technology Transfer," 3/8/88, (PB88-219480).

NCEER-88-0001 "Workshop on Seismic Computer Analysis and Design of Buildings With Interactive Graphics," by W. McGuire, J.F. Abel and C.H. Conley, 1/18/88, (PB88-187760).

NCEER-88-0002 "Optimal Control of Nonlinear Flexible Structures," by J.N. Yang, F.X. Long and D. Wong, 1/22/88, (PB88-213772).

NCEER-88-0003 "Substructuring Techniques in the Time Domain for Primary-Secondary Structural Systems," by G.D. Manolis and G. Juhn, 2/10/88, (PB88-213780).

NCEER-88-0004 "Iterative Seismic Analysis of Primary-Secondary Systems," by A. Singhal, L.D. Lutes and P.D. Spanos, 2/23/88, (PB88-213798).

NCEER-88-0005 "Stochastic Finite Element Expansion for Random Media," by P.D. Spanos and R. Ghanem, 3/14/88, (PB88-213806).

NCEER-88-0006 "Combining Structural Optimization and Structural Control," by F.Y. Cheng and C.P. Pantelides, 1/10/88, (PB88-213814).

NCEER-88-0007 "Seismic Performance Assessment of Code-Designed Structures," by H.H-M. Hwang, J-W. Jaw and H-J. Shau, 3/20/88, (PB88-219423).

NCEER-88-0008 "Reliability Analysis of Code-Designed Structures Under Natural Hazards," by H.H-M. Hwang, H. Ushiba and M. Shinozuka, 2/29/88, (PB88-229471).

NCEER-88-0009 "Seismic Fragility Analysis of Shear Wall Structures," by J-W Jaw and H.H-M. Hwang, 4/30/88, (PB89-102867).

NCEER-88-0010 "Base Isolation of a Multi-Story Building Under a Harmonic Ground Motion - A Comparison of Performances of Various Systems," by F-G Fan, G. Ahmadi and I.G. Tadjbakhsh, 5/18/88, (PB89-122238).

NCEER-88-0011 "Seismic Floor Response Spectra for a Combined System by Green's Functions," by F.M. Lavelle, L.A. Bergman and P.D. Spanos, 5/1/88, (PB89-102875).

NCEER-88-0012 "A New Solution Technique for Randomly Excited Hysteretic Structures," by G.Q. Cai and Y.K. Lin, 5/16/88, (PB89-102883).

NCEER-88-0013 "A Study of Radiation Damping and Soil-Structure Interaction Effects in the Centrifuge," by K. Weissman, supervised by J.H. Prevost, 5/24/88, (PB89-144703).

NCEER-88-0014 "Parameter Identification and Implementation of a Kinematic Plasticity Model for Frictional Soils," by J.H. Prevost and D.V. Griffiths, to be published.

NCEER-88-0015 "Two- and Three- Dimensional Dynamic Finite Element Analyses of the Long Valley Dam," by D.V. Griffiths and J.H. Prevost, 6/17/88, (PB89-144711).

NCEER-88-0016 "Damage Assessment of Reinforced Concrete Structures in Eastern United States," by A.M. Reinhorn, M.J. Seidel, S.K. Kunnath and Y.J. Park, 6/15/88, (PB89-122220).

NCEER-88-0017 "Dynamic Compliance of Vertically Loaded Strip Foundations in Multilayered Viscoelastic Soils," by S. Ahmad and A.S.M. Israil, 6/17/88, (PB89-102891).

NCEER-88-0018 "An Experimental Study of Seismic Structural Response With Added Viscoelastic Dampers," by R.C. Lin, Z. Liang, T.T. Soong and R.H. Zhang, 6/30/88, (PB89-122212). This report is available only through NTIS (see address given above).

NCEER-88-0019 "Experimental Investigation of Primary - Secondary System Interaction," by G.D. Manolis, G. Juhn and A.M. Reinhorn, 5/27/88, (PB89-122204).

NCEER-88-0020 "A Response Spectrum Approach For Analysis of Nonclassically Damped Structures," by J.N. Yang, S. Sarkani and F.X. Long, 4/22/88, (PB89-102909).

NCEER-88-0021 "Seismic Interaction of Structures and Soils: Stochastic Approach," by A.S. Veletsos and A.M. Prasad, 7/21/88, (PB89-122196).

NCEER-88-0022 "Identification of the Serviceability Limit State and Detection of Seismic Structural Damage," by E. DiPasquale and A.S. Cakmak, 6/15/88, (PB89-122188). This report is available only through NTIS (see address given above).

NCEER-88-0023 "Multi-Hazard Risk Analysis: Case of a Simple Offshore Structure," by B.K. Bhartia and E.H. Vanmarcke, 7/21/88, (PB89-145213).

NCEER-88-0024 "Automated Seismic Design of Reinforced Concrete Buildings," by Y.S. Chung, C. Meyer and M. Shinozuka, 7/5/88, (PB89-122170). This report is available only through NTIS (see address given above).

NCEER-88-0025 "Experimental Study of Active Control of MDOF Structures Under Seismic Excitations," by L.L. Chung, R.C. Lin, T.T. Soong and A.M. Reinhorn, 7/10/88, (PB89-122600).

NCEER-88-0026 "Earthquake Simulation Tests of a Low-Rise Metal Structure," by J.S. Hwang, K.C. Chang, G.C. Lee and R.L. Ketter, 8/1/88, (PB89-102917).

NCEER-88-0027 "Systems Study of Urban Response and Reconstruction Due to Catastrophic Earthquakes," by F. Kozin and H.K. Zhou, 9/22/88, (PB90-162348).

NCEER-88-0028 "Seismic Fragility Analysis of Plane Frame Structures," by H.H-M. Hwang and Y.K. Low, 7/31/88, (PB89-131445).

NCEER-88-0029 "Response Analysis of Stochastic Structures," by A. Kardara, C. Bucher and M. Shinozuka, 9/22/88, (PB89-174429).

NCEER-88-0030 "Nonnormal Accelerations Due to Yielding in a Primary Structure," by D.C.K. Chen and L.D. Lutes, 9/19/88, (PB89-131437).

NCEER-88-0031 "Design Approaches for Soil-Structure Interaction," by A.S. Veletsos, A.M. Prasad and Y. Tang, 12/30/88, (PB89-174437). This report is available only through NTIS (see address given above).

NCEER-88-0032 "A Re-evaluation of Design Spectra for Seismic Damage Control," by C.J. Turkstra and A.G. Tallin, 11/7/88, (PB89-145221).

NCEER-88-0033 "The Behavior and Design of Noncontact Lap Splices Subjected to Repeated Inelastic Tensile Loading," by V.E. Sagan, P. Gergely and R.N. White, 12/8/88, (PB89-163737).

NCEER-88-0034 "Seismic Response of Pile Foundations," by S.M. Mamoon, P.K. Banerjee and S. Ahmad, 11/1/88, (PB89-145239).

NCEER-88-0035 "Modeling of R/C Building Structures With Flexible Floor Diaphragms (IDARC2)," by A.M. Reinhorn, S.K. Kunnath and N. Panahshahi, 9/7/88, (PB89-207153).

NCEER-88-0036 "Solution of the Dam-Reservoir Interaction Problem Using a Combination of FEM, BEM with Particular Integrals, Modal Analysis, and Substructuring," by C-S. Tsai, G.C. Lee and R.L. Ketter, 12/31/88, (PB89-207146).

NCEER-88-0037 "Optimal Placement of Actuators for Structural Control," by F.Y. Cheng and C.P. Pantelides, 8/15/88, (PB89-162846).

NCEER-88-0038 "Teflon Bearings in Aseismic Base Isolation: Experimental Studies and Mathematical Modeling," by A. Mokha, M.C. Constantinou and A.M. Reinhorn, 12/5/88, (PB89-218457). This report is available only through NTIS (see address given above).

NCEER-88-0039 "Seismic Behavior of Flat Slab High-Rise Buildings in the New York City Area," by P. Weidlinger and M. Ettouney, 10/15/88, (PB90-145681).

NCEER-88-0040 "Evaluation of the Earthquake Resistance of Existing Buildings in New York City," by P. Weidlinger and M. Ettouney, 10/15/88, to be published.

NCEER-88-0041 "Small-Scale Modeling Techniques for Reinforced Concrete Structures Subjected to Seismic Loads," by W. Kim, A. El-Attar and R.N. White, 11/22/88, (PB89-189625).

NCEER-88-0042 "Modeling Strong Ground Motion from Multiple Event Earthquakes," by G.W. Ellis and A.S. Cakmak, 10/15/88, (PB89-174445).

NCEER-88-0043 "Nonstationary Models of Seismic Ground Acceleration," by M. Grigoriu, S.E. Ruiz and E. Rosenblueth, 7/15/88, (PB89-189617).

NCEER-88-0044 "SARCF User's Guide: Seismic Analysis of Reinforced Concrete Frames," by Y.S. Chung, C. Meyer and M. Shinozuka, 11/9/88, (PB89-174452).

NCEER-88-0045 "First Expert Panel Meeting on Disaster Research and Planning," edited by J. Pantelic and J. Stoyle, 9/15/88, (PB89-174460).

NCEER-88-0046 "Preliminary Studies of the Effect of Degrading Infill Walls on the Nonlinear Seismic Response of Steel Frames," by C.Z. Chrysostomou, P. Gergely and J.F. Abel, 12/19/88, (PB89-208383).

NCEER-88-0047 "Reinforced Concrete Frame Component Testing Facility - Design, Construction, Instrumentation and Operation," by S.P. Pessiki, C. Conley, T. Bond, P. Gergely and R.N. White, 12/16/88, (PB89-174478).

NCEER-89-0001 "Effects of Protective Cushion and Soil Compliancy on the Response of Equipment Within a Seismically Excited Building," by J.A. HoLung, 2/16/89, (PB89-207179).

NCEER-89-0002 "Statistical Evaluation of Response Modification Factors for Reinforced Concrete Structures," by H.H-M. Hwang and J-W. Jaw, 2/17/89, (PB89-207187).

NCEER-89-0003 "Hysteretic Columns Under Random Excitation," by G-Q. Cai and Y.K. Lin, 1/9/89, (PB89-196513).

NCEER-89-0004 "Experimental Study of `Elephant Foot Bulge' Instability of Thin-Walled Metal Tanks," by Z-H. Jia and R.L. Ketter, 2/22/89, (PB89-207195).

NCEER-89-0005 "Experiment on Performance of Buried Pipelines Across San Andreas Fault," by J. Isenberg, E. Richardson and T.D. O'Rourke, 3/10/89, (PB89-218440). This report is available only through NTIS (see address given above).

NCEER-89-0006 "A Knowledge-Based Approach to Structural Design of Earthquake-Resistant Buildings," by M. Subramani, P. Gergely, C.H. Conley, J.F. Abel and A.H. Zaghw, 1/15/89, (PB89-218465).

NCEER-89-0007 "Liquefaction Hazards and Their Effects on Buried Pipelines," by T.D. O'Rourke and P.A. Lane, 2/1/89, (PB89-218481).

NCEER-89-0008 "Fundamentals of System Identification in Structural Dynamics," by H. Imai, C-B. Yun, O. Maruyama and M. Shinozuka, 1/26/89, (PB89-207211).

NCEER-89-0009 "Effects of the 1985 Michoacan Earthquake on Water Systems and Other Buried Lifelines in Mexico," by A.G. Ayala and M.J. O'Rourke, 3/8/89, (PB89-207229).

NCEER-89-R010 "NCEER Bibliography of Earthquake Education Materials," by K.E.K. Ross, Second Revision, 9/1/89, (PB90-125352).

NCEER-89-0011 "Inelastic Three-Dimensional Response Analysis of Reinforced Concrete Building Structures (IDARC-3D), Part I - Modeling," by S.K. Kunnath and A.M. Reinhorn, 4/17/89, (PB90-114612).

NCEER-89-0012 "Recommended Modifications to ATC-14," by C.D. Poland and J.O. Malley, 4/12/89, (PB90-108648).

NCEER-89-0013 "Repair and Strengthening of Beam-to-Column Connections Subjected to Earthquake Loading," by M. Corazao and A.J. Durrani, 2/28/89, (PB90-109885).

NCEER-89-0014 "Program EXKAL2 for Identification of Structural Dynamic Systems," by O. Maruyama, C-B. Yun, M. Hoshiya and M. Shinozuka, 5/19/89, (PB90-109877).

NCEER-89-0015 "Response of Frames With Bolted Semi-Rigid Connections, Part I - Experimental Study and Analytical Predictions," by P.J. DiCorso, A.M. Reinhorn, J.R. Dickerson, J.B. Radziminski and W.L. Harper, 6/1/89, to be published.

NCEER-89-0016 "ARMA Monte Carlo Simulation in Probabilistic Structural Analysis," by P.D. Spanos and M.P. Mignolet, 7/10/89, (PB90-109893).

NCEER-89-P017 "Preliminary Proceedings from the Conference on Disaster Preparedness - The Place of Earthquake Education in Our Schools," Edited by K.E.K. Ross, 6/23/89, (PB90-108606).

NCEER-89-0017 "Proceedings from the Conference on Disaster Preparedness - The Place of Earthquake Education in Our Schools," Edited by K.E.K. Ross, 12/31/89, (PB90-207895). This report is available only through NTIS (see address given above).

NCEER-89-0018 "Multidimensional Models of Hysteretic Material Behavior for Vibration Analysis of Shape Memory Energy Absorbing Devices, by E.J. Graesser and F.A. Cozzarelli, 6/7/89, (PB90-164146).

NCEER-89-0019 "Nonlinear Dynamic Analysis of Three-Dimensional Base Isolated Structures (3D-BASIS)," by S. Nagarajaiah, A.M. Reinhorn and M.C. Constantinou, 8/3/89, (PB90-161936). This report is available only through NTIS (see address given above).

NCEER-89-0020 "Structural Control Considering Time-Rate of Control Forces and Control Rate Constraints," by F.Y. Cheng and C.P. Pantelides, 8/3/89, (PB90-120445).

NCEER-89-0021 "Subsurface Conditions of Memphis and Shelby County," by K.W. Ng, T-S. Chang and H-H.M. Hwang, 7/26/89, (PB90-120437).

NCEER-89-0022 "Seismic Wave Propagation Effects on Straight Jointed Buried Pipelines," by K. Elhmadi and M.J. O'Rourke, 8/24/89, (PB90-162322).

NCEER-89-0023 "Workshop on Serviceability Analysis of Water Delivery Systems," edited by M. Grigoriu, 3/6/89, (PB90-127424).

NCEER-89-0024 "Shaking Table Study of a 1/5 Scale Steel Frame Composed of Tapered Members," by K.C. Chang, J.S. Hwang and G.C. Lee, 9/18/89, (PB90-160169).

NCEER-89-0025 "DYNA1D: A Computer Program for Nonlinear Seismic Site Response. Analysis - Technical Documentation," by Jean H. Prevost, 9/14/89, (PB90-161944). This report is available only through NTIS (see address given above).

NCEER-89-0026 "1:4 Scale Model Studies of Active Tendon Systems and Active Mass Dampers for Aseismic Protection," by A.M. Reinhorn, T.T. Soong, R.C. Lin, Y.P. Yang, Y. Fukao, H. Abe and M. Nakai, 9/15/89, (PB90-173246).

NCEER-89-0027 "Scattering of Waves by Inclusions in a Nonhomogeneous Elastic Half Space Solved by Boundary Element Methods," by P.K. Hadley, A. Askar and A.S. Cakmak, 6/15/89, (PB90-145699).

NCEER-89-0028 "Statistical Evaluation of Deflection Amplification Factors for Reinforced Concrete Structures," by H.H.M. Hwang, J-W. Jaw and A.L. Ch'ng, 8/31/89, (PB90-164633).

NCEER-89-0029 "Bedrock Accelerations in Memphis Area Due to Large New Madrid Earthquakes," by H.H.M. Hwang, C.H.S. Chen and G. Yu, 11/7/89, (PB90-162330).

NCEER-89-0030 "Seismic Behavior and Response Sensitivity of Secondary Structural Systems," by Y.Q. Chen and T.T. Soong, 10/23/89, (PB90-164658).

NCEER-89-0031 "Random Vibration and Reliability Analysis of Primary-Secondary Structural Systems," by Y. Ibrahim, M. Grigoriu and T.T. Soong, 11/10/89, (PB90-161951).

NCEER-89-0032 "Proceedings from the Second U.S. - Japan Workshop on Liquefaction, Large Ground Deformation and Their Effects on Lifelines, September 26-29, 1989," Edited by T.D. O'Rourke and M. Hamada, 12/1/89, (PB90-209388).

NCEER-89-0033 "Deterministic Model for Seismic Damage Evaluation of Reinforced Concrete Structures," by J.M. Bracci, A.M. Reinhorn, J.B. Mander and S.K. Kunnath, 9/27/89.

NCEER-89-0034 "On the Relation Between Local and Global Damage Indices," by E. DiPasquale and A.S. Cakmak, 8/15/89, (PB90-173865).

NCEER-89-0035 "Cyclic Undrained Behavior of Nonplastic and Low Plasticity Silts," by A.J. Walker and H.E. Stewart, 7/26/89, (PB90-183518).

NCEER-89-0036 "Liquefaction Potential of Surficial Deposits in the City of Buffalo, New York," by M. Budhu, R. Giese and L. Baumgrass, 1/17/89, (PB90-208455).

NCEER-89-0037 "A Deterministic Assessment of Effects of Ground Motion Incoherence," by A.S. Veletsos and Y. Tang, 7/15/89, (PB90-164294).

NCEER-89-0038 "Workshop on Ground Motion Parameters for Seismic Hazard Mapping," July 17-18, 1989, edited by R.V. Whitman, 12/1/89, (PB90-173923).

NCEER-89-0039 "Seismic Effects on Elevated Transit Lines of the New York City Transit Authority," by C.J. Costantino, C.A. Miller and E. Heymsfield, 12/26/89, (PB90-207887).

NCEER-89-0040 "Centrifugal Modeling of Dynamic Soil-Structure Interaction," by K. Weissman, Supervised by J.H. Prevost, 5/10/89, (PB90-207879).

NCEER-89-0041 "Linearized Identification of Buildings With Cores for Seismic Vulnerability Assessment," by I-K. Ho and A.E. Aktan, 11/1/89, (PB90-251943).

NCEER-90-0001 "Geotechnical and Lifeline Aspects of the October 17, 1989 Loma Prieta Earthquake in San Francisco," by T.D. O'Rourke, H.E. Stewart, F.T. Blackburn and T.S. Dickerman, 1/90, (PB90-208596).

NCEER-90-0002 "Nonnormal Secondary Response Due to Yielding in a Primary Structure," by D.C.K. Chen and L.D. Lutes, 2/28/90, (PB90-251976).

NCEER-90-0003 "Earthquake Education Materials for Grades K-12," by K.E.K. Ross, 4/16/90, (PB91-251984).

NCEER-90-0004 "Catalog of Strong Motion Stations in Eastern North America," by R.W. Busby, 4/3/90, (PB90-251984).

NCEER-90-0005 "NCEER Strong-Motion Data Base: A User Manual for the GeoBase Release (Version 1.0 for the Sun3)," by P. Friberg and K. Jacob, 3/31/90 (PB90-258062).

NCEER-90-0006 "Seismic Hazard Along a Crude Oil Pipeline in the Event of an 1811-1812 Type New Madrid Earthquake," by H.H.M. Hwang and C-H.S. Chen, 4/16/90(PB90-258054).

NCEER-90-0007 "Site-Specific Response Spectra for Memphis Sheahan Pumping Station," by H.H.M. Hwang and C.S. Lee, 5/15/90, (PB91-108811).

NCEER-90-0008 "Pilot Study on Seismic Vulnerability of Crude Oil Transmission Systems," by T. Ariman, R. Dobry, M. Grigoriu, F. Kozin, M. O'Rourke, T. O'Rourke and M. Shinozuka, 5/25/90, (PB91-108837).

NCEER-90-0009 "A Program to Generate Site Dependent Time Histories: EQGEN," by G.W. Ellis, M. Srinivasan and A.S. Cakmak, 1/30/90, (PB91-108829).

NCEER-90-0010 "Active Isolation for Seismic Protection of Operating Rooms," by M.E. Talbott, Supervised by M. Shinozuka, 6/8/9, (PB91-110205).

NCEER-90-0011 "Program LINEARID for Identification of Linear Structural Dynamic Systems," by C-B. Yun and M. Shinozuka, 6/25/90, (PB91-110312).

NCEER-90-0012 "Two-Dimensional Two-Phase Elasto-Plastic Seismic Response of Earth Dams," by A.N. Yiagos, Supervised by J.H. Prevost, 6/20/90, (PB91-110197).

NCEER-90-0013 "Secondary Systems in Base-Isolated Structures: Experimental Investigation, Stochastic Response and Stochastic Sensitivity," by G.D. Manolis, G. Juhn, M.C. Constantinou and A.M. Reinhorn, 7/1/90, (PB91-110320).

NCEER-90-0014 "Seismic Behavior of Lightly-Reinforced Concrete Column and Beam-Column Joint Details," by S.P. Pessiki, C.H. Conley, P. Gergely and R.N. White, 8/22/90, (PB91-108795).

NCEER-90-0015 "Two Hybrid Control Systems for Building Structures Under Strong Earthquakes," by J.N. Yang and A. Danielians, 6/29/90, (PB91-125393).

NCEER-90-0016 "Instantaneous Optimal Control with Acceleration and Velocity Feedback," by J.N. Yang and Z. Li, 6/29/90, (PB91-125401).

NCEER-90-0017 "Reconnaissance Report on the Northern Iran Earthquake of June 21, 1990," by M. Mehrain, 10/4/90, (PB91-125377).

NCEER-90-0018 "Evaluation of Liquefaction Potential in Memphis and Shelby County," by T.S. Chang, P.S. Tang, C.S. Lee and H. Hwang, 8/10/90, (PB91-125427).

NCEER-90-0019 "Experimental and Analytical Study of a Combined Sliding Disc Bearing and Helical Steel Spring Isolation System," by M.C. Constantinou, A.S. Mokha and A.M. Reinhorn, 10/4/90, (PB91-125385).

NCEER-90-0020 "Experimental Study and Analytical Prediction of Earthquake Response of a Sliding Isolation System with a Spherical Surface," by A.S. Mokha, M.C. Constantinou and A.M. Reinhorn, 10/11/90, (PB91-125419).

NCEER-90-0021 "Dynamic Interaction Factors for Floating Pile Groups," by G. Gazetas, K. Fan, A. Kaynia and E. Kausel, 9/10/90, (PB91-170381).

NCEER-90-0022 "Evaluation of Seismic Damage Indices for Reinforced Concrete Structures," by S. Rodriguez-Gomez and A.S. Cakmak, 9/30/90, PB91-171322).

NCEER-90-0023 "Study of Site Response at a Selected Memphis Site," by H. Desai, S. Ahmad, E.S. Gazetas and M.R. Oh, 10/11/90, (PB91-196857).

NCEER-90-0024 "A User's Guide to Strongmo: Version 1.0 of NCEER's Strong-Motion Data Access Tool for PCs and Terminals," by P.A. Friberg and C.A.T. Susch, 11/15/90, (PB91-171272).

NCEER-90-0025 "A Three-Dimensional Analytical Study of Spatial Variability of Seismic Ground Motions," by L-L. Hong and A.H.-S. Ang, 10/30/90, (PB91-170399).

NCEER-90-0026 "MUMOID User's Guide - A Program for the Identification of Modal Parameters," by S. Rodriguez-Gomez and E. DiPasquale, 9/30/90, (PB91-171298).

NCEER-90-0027 "SARCF-II User's Guide - Seismic Analysis of Reinforced Concrete Frames," by S. Rodriguez-Gomez, Y.S. Chung and C. Meyer, 9/30/90, (PB91-171280).

NCEER-90-0028 "Viscous Dampers: Testing, Modeling and Application in Vibration and Seismic Isolation," by N. Makris and M.C. Constantinou, 12/20/90 (PB91-190561).

NCEER-90-0029 "Soil Effects on Earthquake Ground Motions in the Memphis Area," by H. Hwang, C.S. Lee, K.W. Ng and T.S. Chang, 8/2/90, (PB91-190751).

NCEER-91-0001 "Proceedings from the Third Japan-U.S. Workshop on Earthquake Resistant Design of Lifeline Facilities and Countermeasures for Soil Liquefaction, December 17-19, 1990," edited by T.D. O'Rourke and M. Hamada, 2/1/91, (PB91-179259).

NCEER-91-0002 "Physical Space Solutions of Non-Proportionally Damped Systems," by M. Tong, Z. Liang and G.C. Lee, 1/15/91, (PB91-179242).

NCEER-91-0003 "Seismic Response of Single Piles and Pile Groups," by K. Fan and G. Gazetas, 1/10/91, (PB92-174994).

NCEER-91-0004 "Damping of Structures: Part 1 - Theory of Complex Damping," by Z. Liang and G. Lee, 10/10/91, (PB92-197235).

NCEER-91-0005 "3D-BASIS - Nonlinear Dynamic Analysis of Three Dimensional Base Isolated Structures: Part II," by S. Nagarajaiah, A.M. Reinhorn and M.C. Constantinou, 2/28/91, (PB91-190553).

NCEER-91-0006 "A Multidimensional Hysteretic Model for Plasticity Deforming Metals in Energy Absorbing Devices," by E.J. Graesser and F.A. Cozzarelli, 4/9/91, (PB92-108364).

NCEER-91-0007 "A Framework for Customizable Knowledge-Based Expert Systems with an Application to a KBES for Evaluating the Seismic Resistance of Existing Buildings," by E.G. Ibarra-Anaya and S.J. Fenves, 4/9/91, (PB91-210930).

NCEER-91-0008 "Nonlinear Analysis of Steel Frames with Semi-Rigid Connections Using the Capacity Spectrum Method," by G.G. Deierlein, S-H. Hsieh, Y-J. Shen and J.F. Abel, 7/2/91, (PB92-113828).

NCEER-91-0009 "Earthquake Education Materials for Grades K-12," by K.E.K. Ross, 4/30/91, (PB91-212142).

NCEER-91-0010 "Phase Wave Velocities and Displacement Phase Differences in a Harmonically Oscillating Pile," by N. Makris and G. Gazetas, 7/8/91, (PB92-108356).

NCEER-91-0011 "Dynamic Characteristics of a Full-Size Five-Story Steel Structure and a 2/5 Scale Model," by K.C. Chang, G.C. Yao, G.C. Lee, D.S. Hao and Y.C. Yeh," 7/2/91, (PB93-116648).

NCEER-91-0012 "Seismic Response of a 2/5 Scale Steel Structure with Added Viscoelastic Dampers," by K.C. Chang, T.T. Soong, S-T. Oh and M.L. Lai, 5/17/91, (PB92-110816).

NCEER-91-0013 "Earthquake Response of Retaining Walls; Full-Scale Testing and Computational Modeling," by S. Alampalli and A-W.M. Elgamal, 6/20/91, to be published.

NCEER-91-0014 "3D-BASIS-M: Nonlinear Dynamic Analysis of Multiple Building Base Isolated Structures," by P.C. Tsopelas, S. Nagarajaiah, M.C. Constantinou and A.M. Reinhorn, 5/28/91, (PB92-113885).

NCEER-91-0015 "Evaluation of SEAOC Design Requirements for Sliding Isolated Structures," by D. Theodossiou and M.C. Constantinou, 6/10/91, (PB92-114602).

NCEER-91-0016 "Closed-Loop Modal Testing of a 27-Story Reinforced Concrete Flat Plate-Core Building," by H.R. Somaprasad, T. Toksoy, H. Yoshiyuki and A.E. Aktan, 7/15/91, (PB92-129980).

NCEER-91-0017 "Shake Table Test of a 1/6 Scale Two-Story Lightly Reinforced Concrete Building," by A.G. El-Attar, R.N. White and P. Gergely, 2/28/91, (PB92-222447).

NCEER-91-0018 "Shake Table Test of a 1/8 Scale Three-Story Lightly Reinforced Concrete Building," by A.G. El-Attar, R.N. White and P. Gergely, 2/28/91, (PB93-116630).

NCEER-91-0019 "Transfer Functions for Rigid Rectangular Foundations," by A.S. Veletsos, A.M. Prasad and W.H. Wu, 7/31/91.

NCEER-91-0020 "Hybrid Control of Seismic-Excited Nonlinear and Inelastic Structural Systems," by J.N. Yang, Z. Li and A. Danielians, 8/1/91, (PB92-143171).

NCEER-91-0021 "The NCEER-91 Earthquake Catalog: Improved Intensity-Based Magnitudes and Recurrence Relations for U.S. Earthquakes East of New Madrid," by L. Seeber and J.G. Armbruster, 8/28/91, (PB92-176742).

NCEER-91-0022 "Proceedings from the Implementation of Earthquake Planning and Education in Schools: The Need for Change - The Roles of the Changemakers," by K.E.K. Ross and F. Winslow, 7/23/91, (PB92-129998).

NCEER-91-0023 "A Study of Reliability-Based Criteria for Seismic Design of Reinforced Concrete Frame Buildings," by H.H.M. Hwang and H-M. Hsu, 8/10/91, (PB92-140235).

NCEER-91-0024 "Experimental Verification of a Number of Structural System Identification Algorithms," by R.G. Ghanem, H. Gavin and M. Shinozuka, 9/18/91, (PB92-176577).

NCEER-91-0025 "Probabilistic Evaluation of Liquefaction Potential," by H.H.M. Hwang and C.S. Lee," 11/25/91, (PB92-143429).

NCEER-91-0026 "Instantaneous Optimal Control for Linear, Nonlinear and Hysteretic Structures - Stable Controllers," by J.N. Yang and Z. Li, 11/15/91, (PB92-163807).

NCEER-91-0027 "Experimental and Theoretical Study of a Sliding Isolation System for Bridges," by M.C. Constantinou, A. Kartoum, A.M. Reinhorn and P. Bradford, 11/15/91, (PB92-176973).

NCEER-92-0001 "Case Studies of Liquefaction and Lifeline Performance During Past Earthquakes, Volume 1: Japanese Case Studies," Edited by M. Hamada and T. O'Rourke, 2/17/92, (PB92-197243).

NCEER-92-0002 "Case Studies of Liquefaction and Lifeline Performance During Past Earthquakes, Volume 2: United States Case Studies," Edited by T. O'Rourke and M. Hamada, 2/17/92, (PB92-197250).

NCEER-92-0003 "Issues in Earthquake Education," Edited by K. Ross, 2/3/92, (PB92-222389).

NCEER-92-0004 "Proceedings from the First U.S. - Japan Workshop on Earthquake Protective Systems for Bridges," Edited by I.G. Buckle, 2/4/92, (PB94-142239, A99, MF-A06).

NCEER-92-0005 "Seismic Ground Motion from a Haskell-Type Source in a Multiple-Layered Half-Space," A.P. Theoharis, G. Deodatis and M. Shinozuka, 1/2/92, to be published.

NCEER-92-0006 "Proceedings from the Site Effects Workshop," Edited by R. Whitman, 2/29/92, (PB92-197201).

NCEER-92-0007 "Engineering Evaluation of Permanent Ground Deformations Due to Seismically-Induced Liquefaction," by M.H. Baziar, R. Dobry and A-W.M. Elgamal, 3/24/92, (PB92-222421).

NCEER-92-0008 "A Procedure for the Seismic Evaluation of Buildings in the Central and Eastern United States," by C.D. Poland and J.O. Malley, 4/2/92, (PB92-222439).

NCEER-92-0009 "Experimental and Analytical Study of a Hybrid Isolation System Using Friction Controllable Sliding Bearings," by M.Q. Feng, S. Fujii and M. Shinozuka, 5/15/92, (PB93-150282).

NCEER-92-0010 "Seismic Resistance of Slab-Column Connections in Existing Non-Ductile Flat-Plate Buildings," by A.J. Durrani and Y. Du, 5/18/92.

NCEER-92-0011 "The Hysteretic and Dynamic Behavior of Brick Masonry Walls Upgraded by Ferrocement Coatings Under Cyclic Loading and Strong Simulated Ground Motion," by H. Lee and S.P. Prawel, 5/11/92, to be published.

NCEER-92-0012 "Study of Wire Rope Systems for Seismic Protection of Equipment in Buildings," by G.F. Demetriades, M.C. Constantinou and A.M. Reinhorn, 5/20/92.

NCEER-92-0013 "Shape Memory Structural Dampers: Material Properties, Design and Seismic Testing," by P.R. Witting and F.A. Cozzarelli, 5/26/92.

NCEER-92-0014 "Longitudinal Permanent Ground Deformation Effects on Buried Continuous Pipelines," by M.J. O'Rourke, and C. Nordberg, 6/15/92.

NCEER-92-0015 "A Simulation Method for Stationary Gaussian Random Functions Based on the Sampling Theorem," by M. Grigoriu and S. Balopoulou, 6/11/92, (PB93-127496).

NCEER-92-0016 "Gravity-Load-Designed Reinforced Concrete Buildings: Seismic Evaluation of Existing Construction and Detailing Strategies for Improved Seismic Resistance," by G.W. Hoffmann, S.K. Kunnath, A.M. Reinhorn and J.B. Mander, 7/15/92, (PB94-142007, A08, MF-A02).

NCEER-92-0017 "Observations on Water System and Pipeline Performance in the Limón Area of Costa Rica Due to the April 22, 1991 Earthquake," by M. O'Rourke and D. Ballantyne, 6/30/92, (PB93-126811).

NCEER-92-0018 "Fourth Edition of Earthquake Education Materials for Grades K-12," Edited by K.E.K. Ross, 8/10/92.

NCEER-92-0019 "Proceedings from the Fourth Japan-U.S. Workshop on Earthquake Resistant Design of Lifeline Facilities and Countermeasures for Soil Liquefaction," Edited by M. Hamada and T.D. O'Rourke, 8/12/92, (PB93-163939).

NCEER-92-0020 "Active Bracing System: A Full Scale Implementation of Active Control," by A.M. Reinhorn, T.T. Soong, R.C. Lin, M.A. Riley, Y.P. Wang, S. Aizawa and M. Higashino, 8/14/92, (PB93-127512).

NCEER-92-0021 "Empirical Analysis of Horizontal Ground Displacement Generated by Liquefaction-Induced Lateral Spreads," by S.F. Bartlett and T.L. Youd, 8/17/92, (PB93-188241).

NCEER-92-0022 "IDARC Version 3.0: Inelastic Damage Analysis of Reinforced Concrete Structures," by S.K. Kunnath, A.M. Reinhorn and R.F. Lobo, 8/31/92, (PB93-227502, A07, MF-A02).

NCEER-92-0023 "A Semi-Empirical Analysis of Strong-Motion Peaks in Terms of Seismic Source, Propagation Path and Local Site Conditions, by M. Kamiyama, M.J. O'Rourke and R. Flores-Berrones, 9/9/92, (PB93-150266).

NCEER-92-0024 "Seismic Behavior of Reinforced Concrete Frame Structures with Nonductile Details, Part I: Summary of Experimental Findings of Full Scale Beam-Column Joint Tests," by A. Beres, R.N. White and P. Gergely, 9/30/92, (PB93-227783, A05, MF-A01).

NCEER-92-0025 "Experimental Results of Repaired and Retrofitted Beam-Column Joint Tests in Lightly Reinforced Concrete Frame Buildings," by A. Beres, S. El-Borgi, R.N. White and P. Gergely, 10/29/92, (PB93-227791, A05, MF-A01).

NCEER-92-0026 "A Generalization of Optimal Control Theory: Linear and Nonlinear Structures," by J.N. Yang, Z. Li and S. Vongchavalitkul, 11/2/92, (PB93-188621).

NCEER-92-0027 "Seismic Resistance of Reinforced Concrete Frame Structures Designed Only for Gravity Loads: Part I - Design and Properties of a One-Third Scale Model Structure," by J.M. Bracci, A.M. Reinhorn and J.B. Mander, 12/1/92, (PB94-104502, A08, MF-A02).

NCEER-92-0028 "Seismic Resistance of Reinforced Concrete Frame Structures Designed Only for Gravity Loads: Part II - Experimental Performance of Subassemblages," by L.E. Aycardi, J.B. Mander and A.M. Reinhorn, 12/1/92, (PB94-104510, A08, MF-A02).

NCEER-92-0029 "Seismic Resistance of Reinforced Concrete Frame Structures Designed Only for Gravity Loads: Part III - Experimental Performance and Analytical Study of a Structural Model," by J.M. Bracci, A.M. Reinhorn and J.B. Mander, 12/1/92, (PB93-227528, A09, MF-A01).

NCEER-92-0030 "Evaluation of Seismic Retrofit of Reinforced Concrete Frame Structures: Part I - Experimental Performance of Retrofitted Subassemblages," by D. Choudhuri, J.B. Mander and A.M. Reinhorn, 12/8/92, (PB93-198307, A07, MF-A02).

NCEER-92-0031 "Evaluation of Seismic Retrofit of Reinforced Concrete Frame Structures: Part II - Experimental Performance and Analytical Study of a Retrofitted Structural Model," by J.M. Bracci, A.M. Reinhorn and J.B. Mander, 12/8/92, (PB93-198315, A09, MF-A03).

NCEER-92-0032 "Experimental and Analytical Investigation of Seismic Response of Structures with Supplemental Fluid Viscous Dampers," by M.C. Constantinou and M.D. Symans, 12/21/92, (PB93-191435).

NCEER-92-0033 "Reconnaissance Report on the Cairo, Egypt Earthquake of October 12, 1992," by M. Khater, 12/23/92, (PB93-188621).

NCEER-92-0034 "Low-Level Dynamic Characteristics of Four Tall Flat-Plate Buildings in New York City," by H. Gavin, S. Yuan, J. Grossman, E. Pekelis and K. Jacob, 12/28/92, (PB93-188217).

NCEER-93-0001 "An Experimental Study on the Seismic Performance of Brick-Infilled Steel Frames With and Without Retrofit," by J.B. Mander, B. Nair, K. Wojtkowski and J. Ma, 1/29/93, (PB93-227510, A07, MF-A02).

NCEER-93-0002 "Social Accounting for Disaster Preparedness and Recovery Planning," by S. Cole, E. Pantoja and V. Razak, 2/22/93, (PB94-142114, A12, MF-A03).

NCEER-93-0003 "Assessment of 1991 NEHRP Provisions for Nonstructural Components and Recommended Revisions," by T.T. Soong, G. Chen, Z. Wu, R-H. Zhang and M. Grigoriu, 3/1/93, (PB93-188639).

NCEER-93-0004 "Evaluation of Static and Response Spectrum Analysis Procedures of SEAOC/UBC for Seismic Isolated Structures," by C.W. Winters and M.C. Constantinou, 3/23/93, (PB93-198299).

NCEER-93-0005 "Earthquakes in the Northeast - Are We Ignoring the Hazard? A Workshop on Earthquake Science and Safety for Educators," edited by K.E.K. Ross, 4/2/93, (PB94-103066, A09, MF-A02).

NCEER-93-0006 "Inelastic Response of Reinforced Concrete Structures with Viscoelastic Braces," by R.F. Lobo, J.M. Bracci, K.L. Shen, A.M. Reinhorn and T.T. Soong, 4/5/93, (PB93-227486, A05, MF-A02).

NCEER-93-0007 "Seismic Testing of Installation Methods for Computers and Data Processing Equipment," by K. Kosar, T.T. Soong, K.L. Shen, J.A. HoLung and Y.K. Lin, 4/12/93, (PB93-198299).

NCEER-93-0008 "Retrofit of Reinforced Concrete Frames Using Added Dampers," by A. Reinhorn, M. Constantinou and C. Li, to be published.

NCEER-93-0009 "Seismic Behavior and Design Guidelines for Steel Frame Structures with Added Viscoelastic Dampers," by K.C. Chang, M.L. Lai, T.T. Soong, D.S. Hao and Y.C. Yeh, 5/1/93, (PB94-141959, A07, MF-A02).

NCEER-93-0010 "Seismic Performance of Shear-Critical Reinforced Concrete Bridge Piers," by J.B. Mander, S.M. Waheed, M.T.A. Chaudhary and S.S. Chen, 5/12/93, (PB93-227494, A08, MF-A02).

NCEER-93-0011 "3D-BASIS-TABS: Computer Program for Nonlinear Dynamic Analysis of Three Dimensional Base Isolated Structures," by S. Nagarajaiah, C. Li, A.M. Reinhorn and M.C. Constantinou, 8/2/93, (PB94-141819, A09, MF-A02).

NCEER-93-0012 "Effects of Hydrocarbon Spills from an Oil Pipeline Break on Ground Water," by O.J. Helweg and H.H.M. Hwang, 8/3/93, (PB94-141942, A06, MF-A02).

NCEER-93-0013 "Simplified Procedures for Seismic Design of Nonstructural Components and Assessment of Current Code Provisions," by M.P. Singh, L.E. Suarez, E.E. Matheu and G.O. Maldonado, 8/4/93, (PB94-141827, A09, MF-A02).

NCEER-93-0014 "An Energy Approach to Seismic Analysis and Design of Secondary Systems," by G. Chen and T.T. Soong, 8/6/93, (PB94-142767, A11, MF-A03).

NCEER-93-0015 "Proceedings from School Sites: Becoming Prepared for Earthquakes - Commemorating the Third Anniversary of the Loma Prieta Earthquake," Edited by F.E. Winslow and K.E.K. Ross, 8/16/93.

NCEER-93-0016 "Reconnaissance Report of Damage to Historic Monuments in Cairo, Egypt Following the October 12, 1992 Dahshur Earthquake," by D. Sykora, D. Look, G. Croci, E. Karaesmen and E. Karaesmen, 8/19/93, (PB94-142221, A08, MF-A02).

NCEER-93-0017 "The Island of Guam Earthquake of August 8, 1993," by S.W. Swan and S.K. Harris, 9/30/93, (PB94-141843, A04, MF-A01).

NCEER-93-0018 "Engineering Aspects of the October 12, 1992 Egyptian Earthquake," by A.W. Elgamal, M. Amer, K. Adalier and A. Abul-Fadl, 10/7/93, (PB94-141983, A05, MF-A01).

NCEER-93-0019 "Development of an Earthquake Motion Simulator and its Application in Dynamic Centrifuge Testing," by I. Krstelj, Supervised by J.H. Prevost, 10/23/93, (PB94-181773, A-10, MF-A03).

NCEER-93-0020 "NCEER-Taisei Corporation Research Program on Sliding Seismic Isolation Systems for Bridges: Experimental and Analytical Study of a Friction Pendulum System (FPS)," by M.C. Constantinou, P. Tsopelas, Y-S. Kim and S. Okamoto, 11/1/93, (PB94-142775, A08, MF-A02).

NCEER-93-0021 "Finite Element Modeling of Elastomeric Seismic Isolation Bearings," by L.J. Billings, Supervised by R. Shepherd, 11/8/93, to be published.

NCEER-93-0022 "Seismic Vulnerability of Equipment in Critical Facilities: Life-Safety and Operational Consequences," by K. Porter, G.S. Johnson, M.M. Zadeh, C. Scawthorn and S. Eder, 11/24/93, (PB94-181765, A16, MF-A03).

NCEER-93-0023 "Hokkaido Nansei-oki, Japan Earthquake of July 12, 1993, by P.I. Yanev and C.R. Scawthorn, 12/23/93, (PB94-181500, A07, MF-A01).

NCEER-94-0001 "An Evaluation of Seismic Serviceability of Water Supply Networks with Application to the San Francisco Auxiliary Water Supply System," by I. Markov, Supervised by M. Grigoriu and T. O'Rourke, 1/21/94.

NCEER-94-0002 "NCEER-Taisei Corporation Research Program on Sliding Seismic Isolation Systems for Bridges: Experimental and Analytical Study of Systems Consisting of Sliding Bearings, Rubber Restoring Force Devices and Fluid Dampers," Volumes I and II, by P. Tsopelas, S. Okamoto, M.C. Constantinou, D. Ozaki and S. Fujii, 2/4/94, (PB94-181740, A09, MF-A02 and PB94-181757, A12, MF-A03).

NCEER-94-0003 "A Markov Model for Local and Global Damage Indices in Seismic Analysis," by S. Rahman and M. Grigoriu, 2/18/94.

NCEER-94-0004 "Proceedings from the NCEER Workshop on Seismic Response of Masonry Infills," edited by D.P. Abrams, 3/1/94, (PB94-180783, A07, MF-A02).

NCEER-94-0005 "The Northridge, California Earthquake of January 17, 1994: General Reconnaissance Report," edited by J.D. Goltz, 3/11/94, (PB193943, A10, MF-A03).

NCEER-94-0006 "Seismic Energy Based Fatigue Damage Analysis of Bridge Columns: Part I - Evaluation of Seismic Capacity," by G.A. Chang and J.B. Mander, 3/14/94, (PB94-219185, A11, MF-A03).

NCEER-94-0007 "Seismic Isolation of Multi-Story Frame Structures Using Spherical Sliding Isolation Systems," by T.M. Al-Hussaini, V.A. Zayas and M.C. Constantinou, 3/17/94, (PB193745, A09, MF-A02).

NCEER-94-0008 "The Northridge, California Earthquake of January 17, 1994: Performance of Highway Bridges," edited by I.G. Buckle, 3/24/94, (PB94-193851, A06, MF-A02).

NCEER-94-0009 "Proceedings of the Third U.S.-Japan Workshop on Earthquake Protective Systems for Bridges," edited by I.G. Buckle and I. Friedland, 3/31/94, (PB94-195815, A99, MF-MF).

NCEER-94-0010 "3D-BASIS-ME: Computer Program for Nonlinear Dynamic Analysis of Seismically Isolated Single and Multiple Structures and Liquid Storage Tanks," by P.C. Tsopelas, M.C. Constantinou and A.M. Reinhorn, 4/12/94.

NCEER-94-0011 "The Northridge, California Earthquake of January 17, 1994: Performance of Gas Transmission Pipelines," by T.D. O'Rourke and M.C. Palmer, 5/16/94.

NCEER-94-0012 "Feasibility Study of Replacement Procedures and Earthquake Performance Related to Gas Transmission Pipelines," by T.D. O'Rourke and M.C. Palmer, 5/25/94, (PB94-206638, A09, MF-A02).

NCEER-94-0013 "Seismic Energy Based Fatigue Damage Analysis of Bridge Columns: Part II - Evaluation of Seismic Demand," by G.A. Chang and J.B. Mander, 6/1/94, (PB95-18106, A08, MF-A02).

NCEER-94-0014 "NCEER-Taisei Corporation Research Program on Sliding Seismic Isolation Systems for Bridges: Experimental and Analytical Study of a System Consisting of Sliding Bearings and Fluid Restoring Force/Damping Devices," by P. Tsopelas and M.C. Constantinou, 6/13/94, (PB94-219144, A10, MF-A03).

NCEER-94-0015 "Generation of Hazard-Consistent Fragility Curves for Seismic Loss Estimation Studies," by H. Hwang and J-R. Huo, 6/14/94, (PB95-181996, A09, MF-A02).

NCEER-94-0016 "Seismic Study of Building Frames with Added Energy-Absorbing Devices," by W.S. Pong, C.S. Tsai and G.C. Lee, 6/20/94, (PB94-219136, A10, A03).

NCEER-94-0017 "Sliding Mode Control for Seismic-Excited Linear and Nonlinear Civil Engineering Structures," by J. Yang, J. Wu, A. Agrawal and Z. Li, 6/21/94, (PB95-138483, A06, MF-A02).

NCEER-94-0018 "3D-BASIS-TABS Version 2.0: Computer Program for Nonlinear Dynamic Analysis of Three Dimensional Base Isolated Structures," by A.M. Reinhorn, S. Nagarajaiah, M.C. Constantinou, P. Tsopelas and R. Li, 6/22/94, (PB95-182176, A08, MF-A02).

NCEER-94-0019 "Proceedings of the International Workshop on Civil Infrastructure Systems: Application of Intelligent Systems and Advanced Materials on Bridge Systems," Edited by G.C. Lee and K.C. Chang, 7/18/94, (PB95-252474, A20, MF-A04).

NCEER-94-0020 "Study of Seismic Isolation Systems for Computer Floors," by V. Lambrou and M.C. Constantinou, 7/19/94, (PB95-138533, A10, MF-A03).

NCEER-94-0021 "Proceedings of the U.S.-Italian Workshop on Guidelines for Seismic Evaluation and Rehabilitation of Unreinforced Masonry Buildings," Edited by D.P. Abrams and G.M. Calvi, 7/20/94, (PB95-138749, A13, MF-A03).

NCEER-94-0022 "NCEER-Taisei Corporation Research Program on Sliding Seismic Isolation Systems for Bridges: Experimental and Analytical Study of a System Consisting of Lubricated PTFE Sliding Bearings and Mild Steel Dampers," by P. Tsopelas and M.C. Constantinou, 7/22/94, (PB95-182184, A08, MF-A02).

NCEER-94-0023 "Development of Reliability-Based Design Criteria for Buildings Under Seismic Load," by Y.K. Wen, H. Hwang and M. Shinozuka, 8/1/94, (PB95-211934, A08, MF-A02).

NCEER-94-0024 "Experimental Verification of Acceleration Feedback Control Strategies for an Active Tendon System," by S.J. Dyke, B.F. Spencer, Jr., P. Quast, M.K. Sain, D.C. Kaspari, Jr. and T.T. Soong, 8/29/94, (PB95-212320, A05, MF-A01).

NCEER-94-0025 "Seismic Retrofitting Manual for Highway Bridges," Edited by I.G. Buckle and I.F. Friedland, to be published.

NCEER-94-0026 "Proceedings from the Fifth U.S.-Japan Workshop on Earthquake Resistant Design of Lifeline Facilities and Countermeasures Against Soil Liquefaction," Edited by T.D. O'Rourke and M. Hamada, 11/7/94, (PB95-220802, A99, MF-E08).

NCEER-95-0001 "Experimental and Analytical Investigation of Seismic Retrofit of Structures with Supplemental Damping: Part 1 - Fluid Viscous Damping Devices," by A.M. Reinhorn, C. Li and M.C. Constantinou, 1/3/95, (PB95-266599, A09, MF-A02).

NCEER-95-0002 "Experimental and Analytical Study of Low-Cycle Fatigue Behavior of Semi-Rigid Top-And-Seat Angle Connections," by G. Pekcan, J.B. Mander and S.S. Chen, 1/5/95.

NCEER-95-0003 "NCEER-ATC Joint Study on Fragility of Buildings," by T. Anagnos, C. Rojahn and A.S. Kiremidjian, 1/20/95, (PB95-220026, A06, MF-A02).

NCEER-95-0004 "Nonlinear Control Algorithms for Peak Response Reduction," by Z. Wu, T.T. Soong, V. Gattulli and R.C. Lin, 2/16/95.

NCEER-95-0005 "Pipeline Replacement Feasibility Study: A Methodology for Minimizing Seismic and Corrosion Risks to Underground Natural Gas Pipelines," by R.T. Eguchi, H.A. Seligson and D.G. Honegger, 3/2/95, (PB95-252326, A06, MF-A02).

NCEER-95-0006 "Evaluation of Seismic Performance of an 11-Story Frame Building During the 1994 Northridge Earthquake," by F. Naeim, R. DiSulio, K. Benuska, A. Reinhorn and C. Li, to be published.

NCEER-95-0007 "Prioritization of Bridges for Seismic Retrofitting," by N. Basöz and A.S. Kiremidjian, 4/24/95, (PB95-252300, A08, MF-A02).

NCEER-95-0008 "Method for Developing Motion Damage Relationships for Reinforced Concrete Frames," by A. Singhal and A.S. Kiremidjian, 5/11/95, (PB95-266607, A06, MF-A02).

NCEER-95-0009 "Experimental and Analytical Investigation of Seismic Retrofit of Structures with Supplemental Damping: Part II - Friction Devices," by C. Li and A.M. Reinhorn, 7/6/95.

NCEER-95-0010 "Experimental Performance and Analytical Study of a Non-Ductile Reinforced Concrete Frame Structure Retrofitted with Elastomeric Spring Dampers," by G. Pekcan, J.B. Mander and S.S. Chen, 7/14/95.

NCEER-95-0011 "Development and Experimental Study of Semi-Active Fluid Damping Devices for Seismic Protection of Structures," by M.D. Symans and M.C. Constantinou, 8/3/95.

NCEER-95-0012 "Real-Time Structural Parameter Modification (RSPM): Development of Innervated Structures," by Z. Liang, M. Tong and G.C. Lee, 4/11/95.

NCEER-95-0013 "Experimental and Analytical Investigation of Seismic Retrofit of Structures with Supplemental Damping: Part III - Viscous Damping Walls," by A.M. Reinhorn and C. Lin, 10/1/95, to be published.

NCEER-95-0014 "Seismic Fragility Analysis of Equipment and Structures in a Memphis Electric Substation," by J-R. Huo and H.H.M. Hwang, 8/10/95.

NCEER-95-0015 "The Hanshin-Awaji Earthquake of January 17, 1995: Performance of Lifelines," Edited by M. Shinozuka, 11/3/95.



NATIONAL CENTER FOR EARTHQUAKE ENGINEERING RESEARCH

State University of New York at Buffalo
Red Jacket Quadrangle
Buffalo, New York 14261
Telephone: 716/645-3391
FAX: 716/645-3399

ISSN 1088-3800